



FACULTY OF SCIENCES

Ghent University Faculty of Sciences Department of Plant Biotechnology and Bioinformatics

A multi-angled view on oxidative stress in *A. thaliana* leaves: filling the gaps

Silke Jacques

Thesis submitted in partial fulfillment of requirements for the degree of Doctor (Ph. D.) in Sciences,
Biochemistry-Biotechnology

Academic year: **2014-2015**

Promoter: **Prof. Dr Frank Van Breusegem**

Faculty of Sciences, Department of Plant Biotechnology and Bioinformatics, Ghent University, Belgium
VIB Department of Plant Systems Biology, Oxidative Stress Signaling Group, B-9052 Ghent, Belgium

Co-promoter: **Prof. Dr Kris Gevaert**

Faculty of Medicine, Department of Biochemistry, Ghent University, B-9000 Ghent, Belgium
VIB Department of Medical Protein Research, VIB, B-9000 Ghent, Belgium



EXAM COMMISSION

Prof. Dr Ann Depicker (Chair)

Faculty of Sciences, Department of Plant Biotechnology and Bioinformatics, Ghent University, Belgium

Prof. Dr Frank Van Breusegem (Promoter)

Faculty of Sciences, Department of Plant Biotechnology and Bioinformatics, Ghent University, Belgium

Prof. Dr Kris Gevaert (Co-promoter)

Faculty of Medicine, Department of Medical Protein Research, VIB, B-9000 Ghent, Belgium

Prof. Dr Dieter Deforce*

Faculty of Pharmaceutical Sciences, Department of Pharmaceutics, Ghent University, Belgium

Prof. Dr Dirk Inzé

Faculty of Sciences, Department of Plant Biotechnology and Bioinformatics, Ghent University, Belgium

Prof. Dr Bart Devreese*

Faculty of Sciences, Department of Biochemistry and Microbiology, Ghent University, Belgium

Prof. Dr Geert De Jaeger*

Faculty of Sciences, Department of Plant Biotechnology and Bioinformatics, Ghent University, Belgium

Prof. Dr Yves Guisez

Molecular Plant Physiology and Biotechnology, University Antwerp, Belgium

Prof. Jörg Durner*

Institute of Biochemical Plant Pathology, Munich

Dr Henning Redestig*

Bayer CropScience NV, Ghent, Belgium

*Members of the reading committee

TABLE OF CONTENTS

LIST OF ABBREVIATIONS		13
<hr/>		
CHAPTER 1	Summary	17
<hr/>		
CHAPTER 2	Plants proteins under oxidative attack	23
<hr/>		
CHAPTER 3	Context & Aims	43
<hr/>		
CHAPTER 4	Systems-wide analysis of the oxidative stress response in <i>A. Thaliana</i>	49
<hr/>		
CHAPTER 5	The dynamics of protein-bound methionine oxidation events in <i>A. Thaliana</i> during oxidative stress	111
<hr/>		
CHAPTER 6	Functional implications of methionine oxidation: GST as a case study	143
<hr/>		
CHAPTER 7	Conclusions and perspectives	159
<hr/>		
CHAPTER 8	Samenvatting	167
<hr/>		
CHAPTER 9	Addenda	173
<hr/>		



A SPECIAL THANKS TO...

My 2 bosses:

Kris Gevoert
& Frank Van Breuzegen



My nerdy colleagues @
PSB & Rommelaere!

lots of help! crazy times!

good memories!
loads of fun!

great science!

nice lunches!

listening?

big new stuff!

Those who gave me that little
extra sparkle!

@ PJ & Julie : for the great jokes

@ Laga : for all the Duvel

@ Hans : for the morning coffee &
all your wisdom

@ Chesqui : for all the farts and
awesome science

@ Petra : for helping me out when I
needed it the most

@ Freya : for your sweetness & smile

@ Rebecca: for being my mom
 @ Cezary: for being my duuuude
 @ Veronique: for being my lovely neighbour
 @ Jenny: for being my lovely neighbour
 @ Annelies: for the great coffee breaks
 @ Kim, Stes & Daria: for the GIRL POWER
 @ Alan, Pavel, Robert & Boris: for being you
 @ Mass Spec Ninjas: for your awesomeness

Uni BUDDIES
 TEAM OILSJT
 RUGBY CHICAS
 - Ancient Garde -
 F & F FRIENDS
 Mom & Dad
 100% eternal support
 Sis & Fred
 becoming a godmother is the nicest gift I ever got!
 Fil & Helena
 1/2 the and back
 LAD LARS = ♥



My 2 best mates
-whom I will miss dearly

~ Stat & Wal ~

I don't know where to start but you have been there from the very beginning and hope you will stay till long after... You never failed me (except for some ditching :-)), were always there for me & I forget the countless times you guys put a smile on my face... Now is

a good time to say a BIG

THANK

I hope you can read this too, Hendrik!

YOU

and without you, it would only have been half as fun!!



3 UNCLASSIFIABLE SPECIES

My dearest GG, (& PP!!)
I feel blessed to have met
you! Without you everything
would be a bit less magical

with one T, unlike butt :D



Le Petit Prince



Beufski
zoveloki plezieroki,
zoveelski gelachski,
you ROCKSKI

Mon Petit Prince
het duurde even voor ik het
zag, maar nu hoop ik dat
ons sprookje voor eeuwig en
altijd duzen mag!



★ AND last but definitely NOT least: ★
My Design Wonder Stephanie Shroé



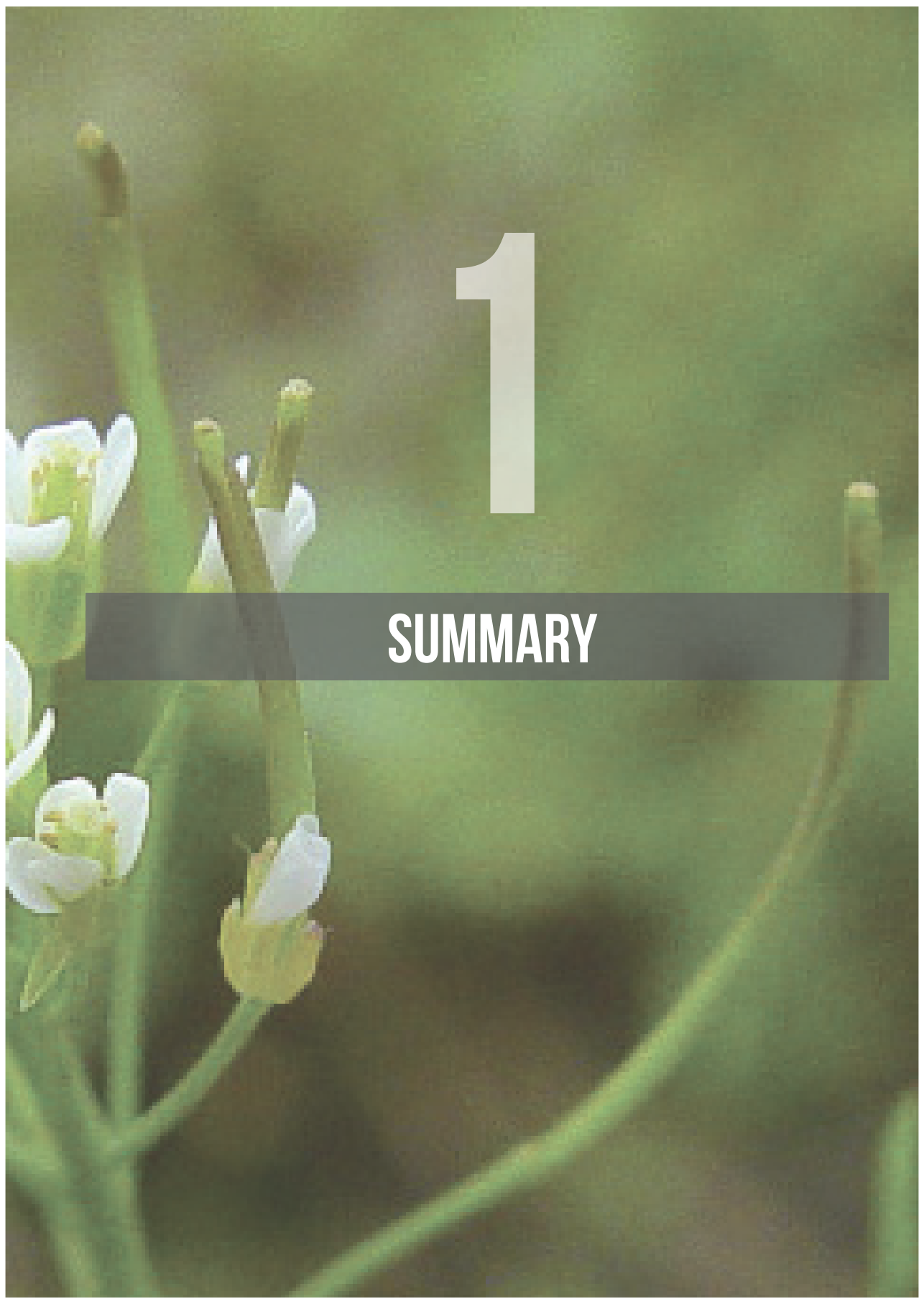


LIST OF ABBREVIATIONS

ABA	abscisic acid
AIM1	The abnormal inflorescence meristem protein
APPD	3R,4S-1-4-aminomethylphenylsulfonyl pyrrolidine-3,4-diol
Avr	avirulent
BY-2	Bright-Yellow 2
CAD	cinnamoyl-CoA reductase
CAT2	catalase 2
CCL	the cinnamoyl-CoA reductase like
CHI	chalcone isomerase
CHS	chalcone synthase
COFRADIC	combined fractional diagonal chromatography
COI1	coronatine insensitive 1
Col-0	ecotype Columbia-0
COR	cold regulated
CYT1	cytokinesis defective 1
DAHPS	3-deoxy-D-arabino-heptulosonate 7-phosphate synthase
DREB	dehydration-responsive element binding
F3H	flavanone-3-hydroxylase
GO	glycolate oxidase
GS	glutamine synthase
HL	high light
INF1	infestin 1
JA	jasmonic acid
JAZ	JASMONATE-ZIM-DOMAIN
KNIME	Konstanz Information Miner
LC-MS	liquid chromatography-mass spectroscopy
LTI	low temperature-induced
MetSO	methionine sulfoxide
Mhb1	Medicago hemoglobin 1

MSR	methionine sulfoxide reductase
MtGS1	Medicago truncatula glutamine synthase 1
Ni-NTA	nickel-nitrilotriacetic acid
OASA	O-acetylserine(thiol)lyase
OPDA	12-oxo-phytodienoic acid
OPR1	12-oxo-phytodienic acid reductase 1
ORFs	open reading frames
P5CS1	DELTA1-PYRROLINE-5-CARBOXYLATE SYNTHASE
PAL1	phenylalanine ammonia lyase 1
PAP1	PRODUCTION OF ANTHOCYANIN PIGMENT 1
RAN	RAS-related nuclear
RNS	reactive nitrogen species
ROS	reactive oxygen species
RP-HPLC	reversed phase-high performance liquid chromatography
SAHH	S-adenosyl-L-homocysteine hydrolase
SAM	statistical analysis of microarrays
SAMH	S-adenosylmethionine synthetase
SATA	N-succinimidyl S-acetylthioacetate
sHSP21	small heat shock protein 21
SIN-1	3-morpholinopyrrolidine
SPAER	solid-phase active ester reagent
TEAB	triethylammonium bicarbonate
WT	wild-type





1

SUMMARY

SUMMARY

In order to survive, plants continuously adapt their developmental program to fluctuating environmental conditions, aiming to increase their fitness [1]. These adaptations involve mechanisms to sense, monitor and transduce a diverse array of environmental stimuli. Perturbation of reactive oxygen species (ROS) homeostasis leads to transient or permanent changes in the cellular redox status and is exploited by plants in different stress signaling mechanisms [2-4]. However, full comprehension of the ROS signal transduction network, leading to the appropriate cellular responses, is lacking.

In this project we generated the necessary additional omics data, essential to grasp the complex, dynamic regulation of the oxidative stress response in *A. thaliana*. For this, next-generation mRNA sequencing, ribosomal profiling and mass spectrometry based proteomics were combined. We focused on the dynamics of early ROS-mediated cellular responses by using *cat2-2* plants as a non-invasive model system for hydrogen peroxide modulation. Upon exposure to photorespiratory inducing conditions such as high light and moderate CO₂ concentrations, the consequences of accumulated hydrogen peroxide levels can be studied. Part of these consequences is described in **chapter 2**, introducing the ROS-sensitive proteome, while **chapter 3** depicts the aims of this thesis.

Chapter 4 describes how we created insights into the complex dynamic interplay of transcriptional and translational regulations that shape the molecular landscape and impact overall protein levels in stressed plants. The dynamics of ROS-responsive proteins was studied by sampling wild-type and *cat2-2* plants at multiple time points during oxidative stress. Based on the isotopic labelling of peptides, a gel-free proteome profiling strategy enabled us to quantify the differences in steady-state protein levels. The generated proteome data were complemented with mRNA- and ribo-seq data, generated by ribosome profiling [5].

We demonstrated that there is a prominent role for protein degradation to initiate a fast stress response together with a general shutdown of translation. Furthermore, translational efficiency was largely affected by enhanced hydrogen peroxide concentrations. This illustrates the need for an integrative systems-wide approach to explore the cellular regulatory mechanisms at play so we can understand how plant leaves globally cope with oxidative stress.

Chapters 5 and 6 focused on methionine oxidation as a reversible posttranslational modification. As it is not yet clear how the majority of stress-related redox stimuli are perceived and transduced, a possible mechanism to sense ROS via modification of proteins on specific methionine residues, was explored here. We made use of the gel-free COFRADIC technology [6] to map the exact sites of methionine oxidation in wild-type and *cat2-2* plants during oxidative stress and were also able to capture the dynamics of oxidation by time-resolved proteome analysis. This resulted in the mapping of 513 oxidation sites in 403 proteins. Taken together, our results support the hypothesis that methionine oxidation is not a random event, but might steer molecular signaling.

A facing challenge is the validation and functional characterization of the identified proteins for their biochemical, functional and structural aspects in order to get extra insights into the ROS signal transduction at the molecular level. The impact of in vivo methionine oxidation on two glutathione S-transferases, phi 9 and tau 23, was performed as a case study (**chapter 6**). This revealed stereospecific methionine oxidation which negatively affects the enzyme activity of both GST phi 9 and tau 23.

This project enabled us to create a multi-angle view of the plant's response to oxidative stress for which transcriptional, translational and even post-translational regulation was explored. This will further help to reveal yet uncharacterized regulatory mechanisms in the oxidative stress response of *A. thaliana* and can contribute to novel applications of engineering plant stress tolerance.

REFERENCES

- [1] Wituszynska, W., Galazka, K., Rusaczonek, A., Vanderauwera, S., et al., Multivariable environmental conditions promote photosynthetic adaptation potential in *Arabidopsis thaliana*. *J Plant Physiol* 2013, 170, 548-559.
- [2] Miller, G., Shulaev, V., Mittler, R., Reactive oxygen signaling and abiotic stress. *Physiologia plantarum* 2008, 133, 481-489.
- [3] Suzuki, N., Koussevitzky, S., Mittler, R., Miller, G., ROS and redox signalling in the response of plants to abiotic stress. *Plant Cell Environ* 2012, 35, 259-270.
- [4] Gilroy, S., Suzuki, N., Miller, G., Choi, W. G., et al., A tidal wave of signals: calcium and ROS at the forefront of rapid systemic signaling. *Trends Plant Sci* 2014, 19, 623-630.
- [5] Ingolia, N. T., Ghaemmaghami, S., Newman, J. R., Weissman, J. S., Genome-wide analysis in vivo of translation with nucleotide resolution using ribosome profiling. *Science* 2009, 324, 218-223.
- [6] Ghesquiere, B., Jonckheere, V., Colaert, N., Van Durme, J., et al., Redox proteomics of protein-bound methionine oxidation. *Mol Cell Proteomics* 2011.



2

PLANT PROTEINS UNDER OXIDATIVE ATTACK

INTRODUCTION

SILKE JACQUES, BART GHESQUIÈRE, FRANK VAN BREUSEGEM, KRIS GEVAERT

A modified version of this chapter was published as a review in “Proteomics”
Silke Jacques wrote the manuscript with corrections by Bart Ghesquière, Frank Van Breusegem
and Kris Gevaert

Silke Jacques contributed to two additional papers, based on her initial extended manuscript elaborating on
cysteine oxidation.

Both articles are accepted for publication in “Journal of Experimental Botany”:

Oxidative post-translational modifications of cysteine residues in plant signal transduction
Cezary Waszczak, Salma Akter, Silke Jacques, Jingjing Huang, Joris Messens and Frank Van Breusegem

Cysteines under ROS attack in plants: a proteomics view
Salma Akter, Cezary Waszczak, Jingjing Huang, Silke Jacques, Kris Gevaert, Frank Van Breusegem and Joris Messens

ABSTRACT

Reactive oxygen and nitrogen species can modify various biomolecules, including proteins. The resulting protein modifications are highly diverse, can be reversible as well as irreversible, and might affect protein structure and function. Besides random modifications, targeted modifications at specific amino acids in surface-accessible protein regions occur. These changes are of particular interest as, e.g. by altering the local protein conformation; they might initiate specific (oxidative) signaling pathways. Here, we focus on two protein modifications that are found under conditions of oxidative stress in plants: oxidation of the sulfur-containing methionine and nitration of tyrosine. We review the functional consequences caused by the oxidation of several plant proteins and line-up those proteomics technologies that are amenable to study these selected modifications.

INTRODUCTION

Abiotic and biotic stress factors (e.g. drought, extreme temperatures and various pathogen attacks) lead to severe crop yield losses worldwide due to their adverse effect on plant growth and development. Recently, the Food and Agricultural Organization of the United Nations has revealed that these detrimental environmental conditions account for up to 37% of the global crop production that is lost before harvest. One common theme of these adverse environmental conditions is the accumulation of ROS and reactive nitrogen species (RNS). At higher concentrations, partially reduced or activated oxygen species, like hydrogen peroxide (H_2O_2), superoxide radical ($\text{O}_2^{\bullet-}$), and singlet oxygen ($^1\text{O}_2$), as well as nitrogen-derived species, such as nitric oxide (NO^\bullet) and peroxynitrite (ONOO^-) can modify different biomolecules, including oligonucleotides, sugars, proteins, and lipids, ultimately leading to oxidative destruction of the cell [1]. However, when tightly regulated, ROS and RNS can also have a signaling role, explaining the term “oxidative signaling” [2].

During the course of evolution, plants have evolved a fine-tuned balance between ROS production and scavenging to gain strict control over ROS toxicity [3]. A plethora of both nonenzymatic (ascorbate, glutathione, tocopherol, flavonoids, alkaloids and carotenoids) and enzymatic antioxidants (including superoxide dismutase, catalase, ascorbate peroxidase, methionine sulfoxide reductases [MSRs], peroxiredoxins and glutathione peroxidase), located in each cellular plant compartment, are present to maintain a cellular redox balance. In *Arabidopsis thaliana*, this balance is governed by a complex network that comprises at least 152 genes encoding both ROS-producing and ROS-scavenging enzymes [4].

Significant progress has been made in the understanding of redox-dependent gene regulation in multiple plant species, albeit mainly based on transcriptome data [5-9]. However, a plausible mechanism for cells to perceive ROS and RNS is through posttranslational modifications (PTMs) given that ROS and RNS directly cause oxidation and nitrosation of amino acids (and peptide bonds ([oxidation])), which may further affect enzymatic activity, intracellular localization, protein–protein interactions and protein stability. Therefore, PTMs are often viewed as cellular switches and potential sensors of the complex redox regulation system [10]. However, in plants only a few examples of PTM-based redox regulation were reported.

The rapidly evolving field of proteomics has greatly contributed to a better understanding and mapping of diverse and complex PTMs in plants, thanks to the application of advanced mass spectrometry [11-14]. To date, the RESID database (release 75.00) contains over 600 possible protein modifications (note however that some of these are a bit redundant (e.g., N-acetylation of N-terminal amino acids)) and this list keeps on growing (<http://pir.georgetown.edu/resid/>). One of the major challenges for the identification of new PTMs resides in the fact that most modifications are present only in substoichiometric amounts in biological samples, making (affinity-based) enrichments often necessary. In addition, many PTMs can be unstable under analytical conditions for proteomics and MS [15].

Identification of the modified residues is obviously key for the understanding of the effect of a specific PTM on a protein function and associated biological processes. Pinpointing this site can only be achieved by identifying the modified peptide and by mapping the modification back to a single amino acid. Another bottleneck in the study of PTMs is that an apparent single protein frequently represents a heterogeneous population of proteins with possibly multiple PTMs at different or similar sites that can be transient in

nature. Sampling at one given time point might thus result in a rather static picture of protein PTMs. This review focuses on two PTMs associated with oxidative stress in plants, namely methionine oxidation and tyrosine nitration, their biological significance and the methodologies used to study these modifications.

METHIONINE OXIDATION

Most ROS are electron-deficient (oxidizing, electrophilic) and, as such, they tend to react most rapidly with electron-rich amino acid side chains, such as those of methionine and cysteine residues. The thioether group (R-S-R') of methionine has a low oxidation potential and, hence, is readily oxidized by a large number of reactive species [16]. The resulting oxidation product is methionine sulfoxide (MetSO) that can be further oxidized to methionine sulfone, albeit to a much lesser extent (**Figure 1**). Methionine sulfoxide comes in two stereoisomers: methionine S- and R-sulfoxide and the enzymatic reduction step back to methionine is stereospecific through two types of methionine sulfoxide reductases, MSRA and MSRB, which specifically reduce the S-MetSO and R-MetSO diastereomers, respectively [17]. For a detailed overview of the MSR families and their physiological roles in photosynthetic organisms, see Tarrogo *et al.* [18]. *Arabidopsis* possesses five MSRA and nine MSRB isoforms, localized in three subcellular locations: the plastids, the endoplasmic reticulum and the cytosol [18-21]. All *Arabidopsis* MSRs contain two redox-active cysteines, with the exception of MSRB1 that has only one. Although no general sequence or structure similarity is observed between the A and B types of MSRs, they have a common reaction mechanism in which the catalytic cysteine attacks the sulfur of MetSO, leading to the formation of a sulfenic acid intermediate (**Figure 2**). This is followed by the formation of an intramolecular disulfide bond due to the nucleophilic attack of the resolving cysteine (except for MSRB1, which, in turn, is reduced by thioredoxins [17, 22-24]. In *Arabidopsis*, the MSR genes display differential expression and activity patterns, with environmental stress strongly controlling the regulation of the MSR activity.

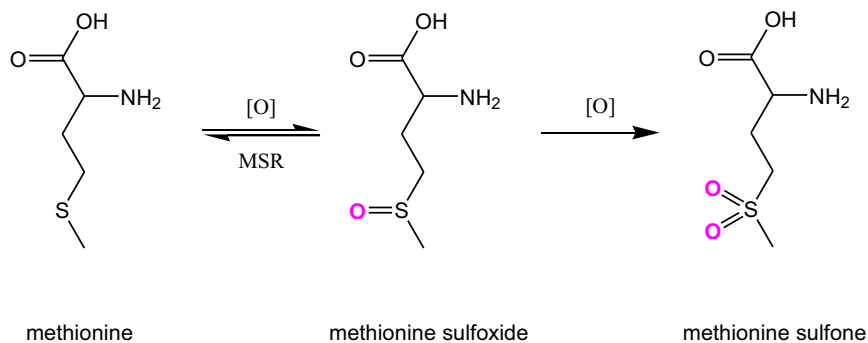


Figure 1: Methionine oxidation states

The sulfur group of methionine is readily oxidized by a range of reactive species to methionine sulfoxide (MetSO). The stereospecific oxidation of methionine results in a mixture of diastereomers (Met-S/R-sulfoxide) that can be reduced by MSRA and MSRB, respectively. MetSO can be further oxidized to the irreversible methionine sulfone, albeit to a much lesser extent.

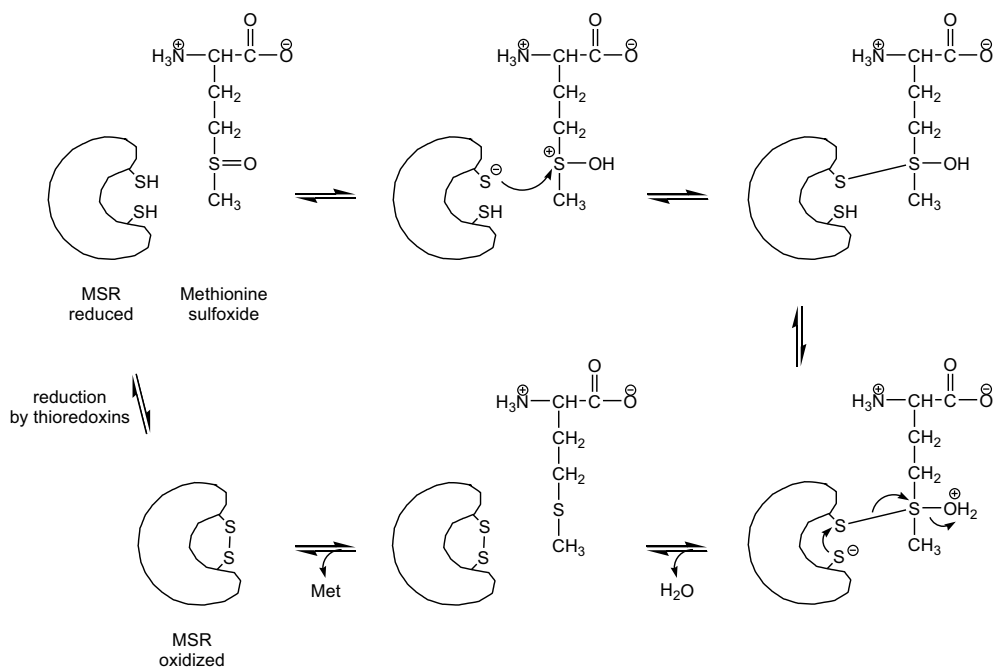


Figure 2: Catalytic mechanism of methionine sulfoxide reductases. The general reaction mechanism of MSR enzymes that contain two redox-active cysteines is presented. The catalytic cysteine from MSR in its reduced state performs a nucleophilic attack on the sulfur atom of methionine sulfoxide, leading to the formation of a sulfenic acid intermediate. An intramolecular disulfide bond is formed by a nucleophilic attack of the second redox-active cysteine on the sulfur atom of sulfenic acid, leading to a subsequent release of water and methionine. MSR is finally reduced back to its original state via thioredoxins. The redox-active cysteines differ along the different *MsrA* and *MsrB* genes as well as between plant species.

Upon oxidation of protein-bound methionines, structural changes can occur which is the case for the chloroplast-located small heat shock protein 21 (sHSP21, AT4G27670). The methionine-rich stretch at its N-terminus forms an amphiphatic α -helix with all methionines exposed to one side [25]. The chaperone-like activity of sHSP21 is explained by binding of this amphiphatic helix to hydrophobic stretches of partially unfolded proteins to protect such proteins from aggregation [26]. Sulfoxidation of four highly conserved methionine residues (Met49, Met52, Met55, and Met59) causes a conformational change in this helix, resulting in a loss of chaperone-like activity [27]. Thus, methionine sulfoxidation can have a major impact on the structural conformation of the sHSP21 protein concomitant with a loss of function. Interestingly, and in this perspective, the myristoylated *MsrA*, compared to its unmodified form, has been hypothesized to interact with proteins (and hence repair them faster) that undergo structural changes upon methionine oxidation [28]. Moreover, a link has been established between methionine oxidation and other protein PTMs, such as phosphorylation. Recombinant soybean (*Glycine max*) calcium-dependent protein kinases (CDPKs) have been found unable to phosphorylate *in vitro* phosphorylation motif-containing synthetic peptides with an oxidized methionine. *In vivo* inhibition of phosphorylation by methionine oxidation was demonstrated by monitoring the phosphorylation status of nitrate reductase in *Arabidopsis*. Phosphorylation of Ser543 decreased significantly when H₂O₂ was added, but increased when a cytosolic MSRA was overexpressed, giving two lines of evidence that the nearby surface-exposed

methionine (Met547) can function as a hydrophobic recognition element within a phosphorylation motif [29].

MetSO is the predominant oxidation marker in *Arabidopsis* leaves [30], in which the oxidative damage was more severe in chloroplast proteins than in proteins residing in other subcellular locations: the total MetSO content is estimated to be 10%, whereas that in chloroplasts is 20–30% of the total methionines [31]. The upregulation of MSRs under oxidative stress conditions [19] further hints to the necessity of repairing MetSO and recycling methionine residues. MSR mutations render plants more sensitive to oxidative stress, whereas overexpression increases stress resistance, also indicating that oxidation and reduction of MetSO might be an indirect mechanism to extenuate oxidative stress and, as such, prevent further oxidative damage to proteins [30].

Recently, prediction methods have been proposed for investigating the sensitivity differences of individual methionines to ROS [32]. Proof of concept was the confirmation of two methionines near the C-terminal helix of calmodulin that are selectively oxidized, resulting in an activation loss of a plasma membrane Ca-ATPase [33]. Thus, together with proteomic tools, these predictions of sensitive methionines can lead to the discovery of redox stress sensors in response to methionine oxidation.

PROTEOMIC TECHNOLOGIES FOR STUDYING METHIONINE SULFOXIDE

Although methionines are highly susceptible to oxidation, until recently no adequate proteomics methodologies existed to identify the exact sites of oxidation and quantify the degree of oxidation and the available anti-MetSO antibodies suffer from aspecific cross-reactivity [34, 35].

As oxidation of methionine leads to a 16 Da increase, MetSO peptides are often easily detected following LC-MS/MS analysis of proteolytically cleaved proteomes. Although this technique had been tested only on single proteins *in vitro* [36], it was used also on *Arabidopsis* leaf extracts in which protein oxidation could be quantified, combined with stable isotopic calibration [30]. As MetSO-containing peptides were not enriched prior to analysis, these peptides are expected to be underrepresented, given the complex background of the analyte mixture. Another critical point is the lack of distinction between *in vivo* oxidation and the inevitable oxidation arising during sample preparation. The combined fractional diagonal chromatography (COFRADIC) method overcomes this problem by enrichment for MetSO-containing peptides (**Table 1**). Not only does this proteomics technology identify the site of oxidation, it also enables measuring the degree of oxidation and corrects for spontaneous methionine oxidation occurring during sample preparation. In essence, COFRADIC alters MetSO back to methionine through a mixture of recombinant human MsrA and MsrB3, in-between consecutive, identical RP-HPLC peptide separations. Reduction of MetSO results in a hydrophobic shift of the affected peptides, leading to their specific enrichment [37]. An electrophoretic mobility shift assay was another method developed to detect oxidized methionines on polyacrylamide gels (**Table 1**). By alkylation of methionines, a charge change is introduced which shifts the mobility of the protein on an acidic gel relative to the alkylation-resistant sulfoxide form [38].

Recently, also titanium dioxide beads, previously used to enrich phosphopeptides, were exploited to enrich MetO peptides [39] (**Table 1**). By using this approach, oxidation-sensitive proteins were identified in *Arabidopsis* cell cultures treated with a cell-permeant second messenger analogue,

8-bromo-3,5-cyclic guanosine monophosphate (8-Br-cGMP). This cGMP-dependent methionine oxidation was shown to particularly affect stress responsive proteins [39].

Thus far, most methionine oxidation studies in plants focused on the effect of mutant MSRs on stress resistance and have revealed their involvement in signaling pathways and detoxification mechanisms during development and stress conditions [18]. Also, substitution of conserved methionines by leucines is used on *Arabidopsis* proteins to study the biological effect of methionine oxidation [40]. Recently, *Arabidopsis* plastidial MSRB1 substrates have been studied with affinity chromatography to isolate potential substrates [41]. (Table 1). An overview of the enrichment strategies to capture oxidized methionine peptides is given below.

Method	Reference	Enrichment strategy
COFRADIC	[37]	MSR reduction in-between consecutive RP-HPLC separations
mobility shift assay	[38]	electrophoretic shift upon alkylation of methionine
affinity chromatography	[39] [40]	titanium dioxide beads enrich for oxidized peptides MSR binds to its MetO substrates

Table 1. Overview of the enrichment strategies to isolate oxidized methionine peptides.

TYROSINE NITRATION

Nitration of tyrosines is a two-step process, involving the formation of a tyrosyl radical and a nitrogen dioxide radical to generate 3-nitrotyrosine in which the nitro group is added onto one of the two ortho-carbons of the phenolic ring [42] (Figure 3). Peroxynitrite (ONOO^-), *in vivo* responsible for the oxidation and nitration of tyrosine through its radical products $\cdot\text{OH}$ and $\cdot\text{NO}_2$, is formed by an interaction between ROS and RNS. Both the interaction of nitric oxide radicals with superoxide anion ($\cdot\text{NO} + \cdot\text{O}_2^- \rightarrow \text{ONOO}^-$) as well as the heme peroxidase-mediated reaction of nitrite with hydrogen peroxide ($\text{NO}_2^- + \text{H}_2\text{O}_2 \rightarrow \text{ONOO}^-$) are considered to be the two most widely invoked mechanisms leading to nitration [43].

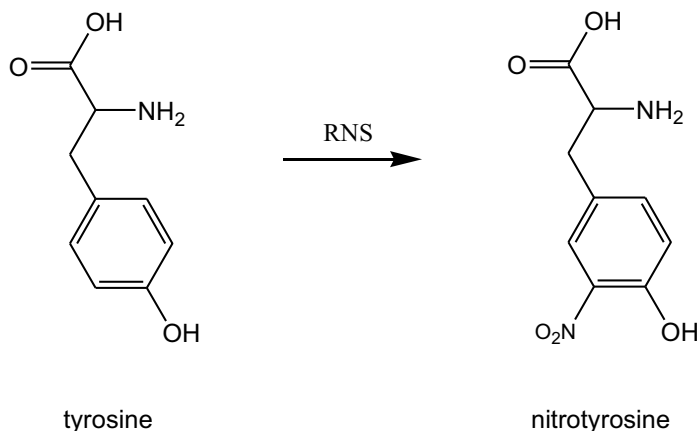


Figure 3: Tyrosine nitration

Tyrosine is susceptible to the interaction with reactive nitrogen species, which results in the formation of 3-nitrotyrosine, where the nitro group is added onto one of the two ortho-carbons of the phenolic ring.

Although a biological denitration enzymatic system is yet to be identified, selective denitration activities have been reported in different mammalian extracts [42]. Tyrosine nitration was found to be selective and dependent on several factors, including the tyrosine location at the protein's surface (positioned in a loop, with exposure of its aromatic ring to the surface-promoting nitration), the proximity of amino acids of opposite charges that promote nitration, the vicinity of cysteine residues, and the proximity of proteins to the site where nitrating agents are generated [44-47]. Addition of a single nitro group can inflict molecular changes, such as a shift in the local pKa-value of the tyrosine hydroxyl group (from 10.1 to 7.2), which, in turn, have functional consequences due to (local) conformational changes [43].

In general, the importance of tyrosine nitration during biotic and abiotic stresses is best studied [48-51], but there is increasing evidence of basal nitration levels, thus suggesting that tyrosine nitration is a constituent of the normal cell physiology [52-54]. By means of anti-nitrotyrosine antibodies, a number of immunoreactive bands were found that intensify or appear under different stresses in different plants. In olive (*Olea europaea*), the intensity and numbers of nitrated proteins in the molecular mass range between 44 and 60 kDa increased during salt stress [55]. Treatment of tobacco (*Nicotiana tabacum*) Bright-Yellow (BY-2) suspension cells with either 3-morpholinopyridone (SIN-1), a peroxynitrite generator, or infestin 1 (INF1), an elicitor protein from *Phytophthora infestans*, resulted in immunostaining of 20 kDa and 50 kDa protein bands [48]. In an antisense nitrite reductase transformant of tobacco, the tyrosine nitration of proteins with molecular masses between 10 and 50 kDa increased as well, as also detected in vitro after addition of peroxynitrite to tobacco leaf extracts [56]. Sunflower (*Helianthus annuus*) cultivars resistant and susceptible to a mildew pathogen (*Plasmopara halstedii*) show different tyrosine nitration profiles after infection: in the uninfected susceptible cultivar, three nitrated proteins of 47, 59, and 68 kDa were detected with intensification of the 68 kDa band after infection, but not in the resistant cultivar [57]. Also in pea (*Pisum sativum*) plants subjected to six different abiotic stresses, the staining of some immunoreactive bands in the range 29–59 kDa was enhanced and only one additional band of 73 kDa appeared after exposure to high or low temperature or high light stress [50]. In the first nitration study in *Arabidopsis*, plants were inoculated with the avirulent strain (avrB) of *Pseudomonas syringae* and changes in the tyrosine nitration status over time were monitored. Western blot analysis again revealed the presence of tyrosine-nitrated proteins in the nontreated sample, but with a strongly intensified signal during the course of infection [51]. Finally, in 2D Western blots, 12 differentially tyrosine-nitrated proteins were identified during the hypersensitivity response and these proteins corresponded to the previously detected nitrated proteins in peroxynitrite-infiltrated *Arabidopsis* leaves that were mainly involved in photosynthesis, glycolysis, and nitrate assimilation [51]. Another study focused on native photosynthetic complexes in the thylakoid membrane of *A. thaliana* leaves adapted to growth light and subsequently exposed to high light. The majority of the 23 tyrosine residues detected in five photosystem I and nine photosystem II proteins with altered nitration levels [58] showed a decrease upon exposure to high light. In *Taxus cuspidata* suspension cells, nitrotyrosine levels increased during shear stress that correlated with the inhibition of glutathione S-transferase by different reactive nitrogen species [49].

Of the few in-depth studies on the functional effect of tyrosine nitration in plant proteins, the first one reported the cytosolic O-acetylserine(thiol)lyase enzyme (OASA1) in *Arabidopsis*, which catalyzes the last step of sulfur assimilation and, hence, is crucial for cysteine homeostasis. Nitration of the Tyr302

residue strongly inhibited its activity due to a drastic reduction of substrate binding (O-acetylserine) and reduced stability of the cofactor (pyridoxal-5'-phosphate) through hydrogen bonds [59]. Nitration of the *Medicago truncatula* nodule enzyme glutamine synthase 1 (MtGS1) on Tyr167 results in a complete loss of enzyme activity [60]. Thereby, a direct relationship between reduced glutamine synthase (GS) activity, increased GS nitration, and reduced nitrogen fixation was found. Another study showed that the nonsymbiotic hemoglobin from *Medicago sativa* (Mhb1) was able to mediate autonitration and nitration of other proteins in the presence of nitrite and H₂O₂. As such, Mhb1 could influence different components of signal transduction cascades during plant pathogen response, which was manifested by selective upregulation of pathogen-inducible genes in *Arabidopsis* Mhb1-overexpressing plants infected with *P. syringae* [61].

Tyrosine nitration is not only considered to occur during exposure to stress, but also has been recognized recently as an integral part of the physiological status of the cell, irrespective of pathological processes. A study on α -tubulin tyrosine nitration in tobacco BY-2 suspension cells [54] was linked with previous reports in rice (*Oryza sativa*) and tobacco cells in which the tubulin nitration had been shown to affect cell division and to decrease mitotic figures as a consequence of reduced microtubule dynamics [62, 63]. Moreover, a possible impact on signaling processes was proposed since nitration of tyrosine residues might directly or indirectly compete, inhibit, block, or even mimic phosphorylation/dephosphorylation of the same residue [64, 65]. Finally, an inventory of potential *in vivo* targets of tyrosine nitration in *Arabidopsis* seedlings has been published [53], leading to the identification of 127 proteins of which 35% corresponded to reported nitrated nonplant homologs, although none of the *in vivo* nitration sites could be identified by MS/MS.

PROTEOMIC TECHNOLOGIES FOR STUDYING TYROSINE NITRATION

In plants, all of the abovementioned nitration studies made use of anti-3-nitrotyrosine antibodies that were used either in Western blots to detect tyrosine-nitrated proteins or as an immunoprecipitant to pull down potential *in vivo* nitrated proteins prior to LC-MS/MS analysis [53] (**Figure 4A**). It is thus not surprising that most of these studies focused on reporting possibly nitrated proteins and only few pinpointed out the exact nitrated sites. Thus far, only a couple of studies have demonstrated the functional impact of tyrosine nitration, among others by mutation studies where tyrosine is replaced by alanine [59]. Until now, the proteomics methods for studying tyrosine nitration have been used in mammalian systems only (**Figure 4B**). They are based on the specific reduction of the nitro group into an amino group. Proteins are digested and the resulting peptide mixture is subjected to a series of steps that enrich for the newly formed aminotyrosine peptides prior to LC-MS/MS analysis. First, primary amines are blocked prior to the reduction of the nitrotyrosine into aminotyrosine. The hence newly introduced, primary amino group is then modified by a reagent containing an affinity anchor, such as biotin [65], N-succinimidyl S-acetylthioacetate (SATA) [66], a fluorogenic derivative, 3R,4S-1-4-aminomethylphenylsulfonyl pyrrolidine-3,4-diol (APPD) [67], or a metal-chelating motif [68], all allowing enrichment of the modified 3-aminotyrosine-containing peptides. The aminotyrosine-containing peptides can also be immobilized on a solid-phase active ester reagent [69]. Table 2 gives an overview of the different methods together with their specific blocking and reducing agents. Another method to study tyrosine nitration is based on the COFRADIC technology [70]. Here, the peptide mixture is separated by RP-HPLC and peptide fractions are treated with sodium dithionite

and, subsequently, separated under identical conditions as the primary RP-HPLC separation step. Due to the reduction of 3-nitrotyrosine into 3-aminotyrosine, the chromatographic behavior of the latter will change (hydrophilic shift), whereas nonaffected peptides elute within the same time interval as during the primary separation. Hence, the peptides with a hydrophilic shift are collected and analyzed by MS.

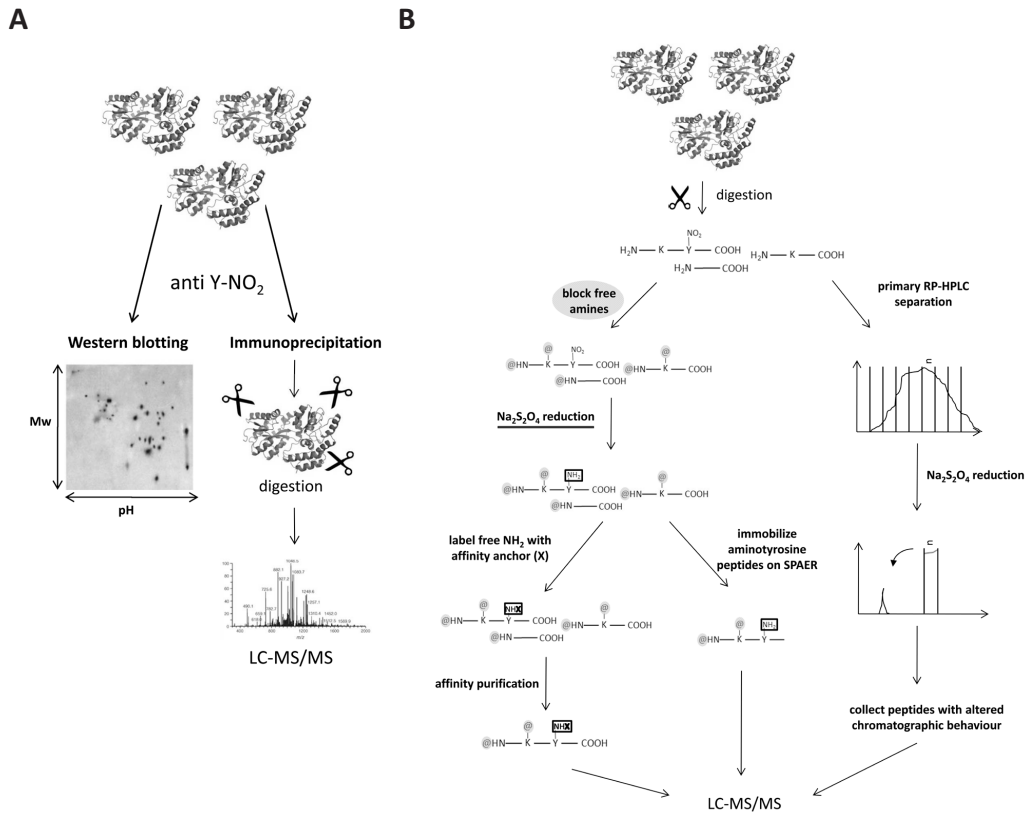


Figure 4. Proteomics technologies to study tyrosine nitration.

Tyrosine nitration can be studied using nitrotyrosine-specific antibodies via Western blotting or by using immunoprecipitation where proteins can be identified via mass spectrometry (LC-MS/MS) (A). Alternative techniques rely on the reduction of nitrotyrosine into aminotyrosine, mostly via addition of sodium dithionite (Na₂S₂O₄). This is followed by affinity labeling or covalent immobilization on a solid-phase active ester reagent (SPAER). (A). The same reduction step is also used in a diagonal chromatography setup (B). The blocking of free amines is omitted in the method with the fluorescent reagent (APPD) [67] since this does not interact with primary amines (*).

Method [Reference]	Blocking of primary amines ^a	Reduction to aminotyrosine	Anchor ^b	Isolation method ^c
[65]	Acetylation with sulfosuccinimidyl acetate	Heme + dithiothreitol	Biotin	Immobilized avidin column
[66]	Acetylation with acetic anhydride	Sodium dithionite	SATA	- Deprotection of S-acetyl on SATA (with NH ₂ OH) - Sulfhydryl peptide enrichment with thiopropyl Sephacrose beads
[67]	/	Sodium dithionite	APPD	Boronate affinity chromatography
[68]	Reductive methylation with formaldehyde and sodium cyanoborohydride	Sodium dithionite	/	Solid phase active ester reagent beads (SPAER)
[69]	Acetylation with sulfosuccinimidyl acetate	Sodium dithionite	Bispyridinylation (metal-chelating motif)	Ni ²⁺ NTA magnetic beads

Table 2. Different methods for isolating nitrotyrosine-containing peptides.

Abbreviations: SATA, N-succinimidyl S-acetylthioacetate; APPD, fluorogenic derivative 3R,4S-1-4-aminomethylphenylsulfonyl pyrrolidine-3,4-diol; Ni-NTA, nickel-nitrilotriacetic acid; SPAER, solid-phase active ester reagent; /, Not applied.

CYSTEINE OXIDATION

Cysteine is, next to methionine, a major site for oxidative modifications within proteins since it also contains an electron rich sulfur atom. Cysteine was shown to be a sensitive target of ROS, appearing in a wide range of oxidation states [71]. Between individual cysteines, the reactivity towards ROS can be hugely different. This is amongst others caused by the dependency on the local electrostatic environment and steric accessibility of cysteine side-chains. Oxidation of cysteines can result in the formation of reversible modifications, such as sulfenic acid (R-SOH) and sulfinic acid (R-SO₂H), and the irreversible sulphonic acid modification (R-SO₃H) (**Figure 5**). The reversibility of the sulfinic acid modification has been debated, but was demonstrated by the presence of an ATP-dependent sulfiredoxin enzyme, capable of reducing sulfinic acids in plant cells [72]. After formation of the highly unstable sulfenic acid intermediate, reaction with free thiols can occur creating a disulfide bond, either intramolecular within one protein or intermolecular between proteins (**Figure 5**). Mixed disulfides are formed when cysteine thiols react with low molecular weight thiols such as glutathione (S-glutathionylation) or cysteine (S-cysteinylation). Also nitrosothiols (R-SNO) can be formed by interaction of cysteine with •NO and its derivatives (**Figure 5**). For an update on mixed disulfides we refer to Lindahl *et al.* (2011) [73].

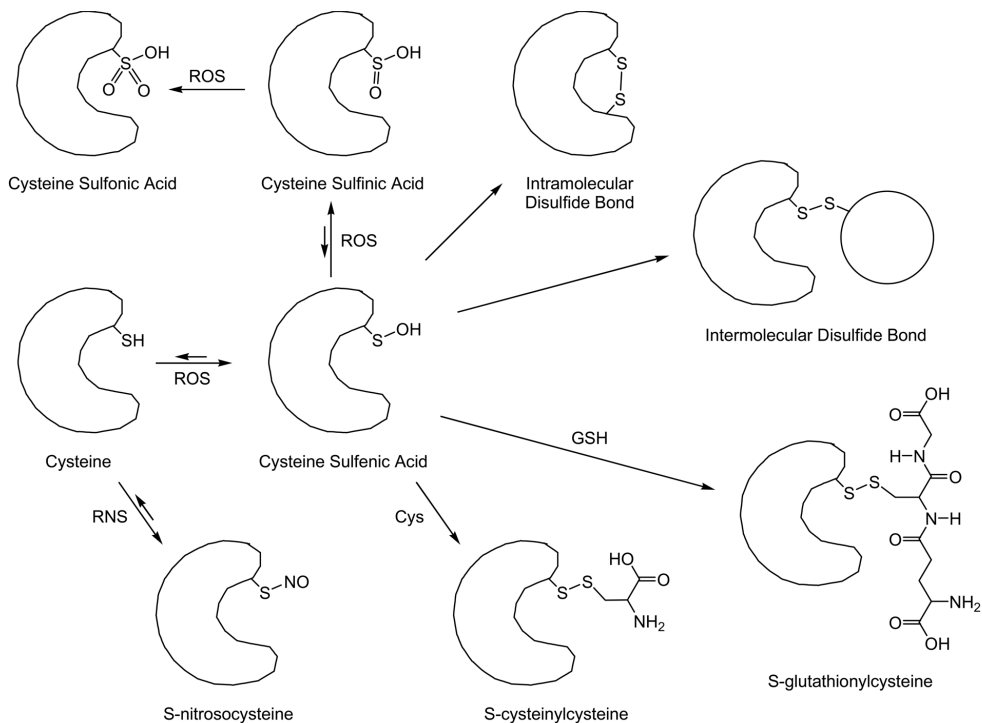


Figure 5: An overview of the different cysteine oxidation products.

Oxidation of cysteines results in the formation of reversible modifications, such as sulfenic acid (R-SOH) and sulfinic acid (R-SO₂H), and the irreversible sulphonic acid modification (R-SO₃H). Also, formation of inter- or intramolecular disulphide bridges occurs next to the formation of S-nitrosocysteine upon interaction with RNS.

The differential reactivity of Cys residues towards ROS and the possibility to be present in different oxidation states permits them to appear on the crossroad of highly dynamic oxidative events. It is a well-recognized concept that profiling of ROS/RNS modified proteins containing cysteine, can unveil key redox sensors involved in signal transduction pathways [74]. An updated and detailed overview of the oxidative post-translational modifications of cysteine residues in plant signal transduction can be found in addendum 1 (Waszczak *et al.*, 2014 –coauthor). To understand the impact and the functional consequences of these cysteine oxidations, redox proteomic techniques have been developed and are discussed in addendum 2 (Akter *et al.*, 2014 –coauthor).

CONCLUDING REMARKS

Excess ROS and RNS will inevitably modify proteins, both at specific sites (e.g. oxidation of methionine and cysteine) and at more random sites (such as carbonylation). In this review, we have touched the tip of the iceberg by describing how methionine oxidation can affect the function and the structure of plant proteins. Although several studies focusing on single plant proteins have been published, the proteomics technologies are just emerging that are required for a more comprehensive catalog of the modified sites within oxidized proteins. In fact, such technologies are highly needed as only these allow the unambiguous identification of oxidation-modified proteins and the characterization of their affected sites. Only following these discovery proteomics studies, further functional studies can be initiated that use, for instance, oxidation-resistant mutant proteins, and only such studies will reveal if the identified modifications are indeed signals or just the result of ROS or RNS scavenging. In addition, the degree of oxidation or nitration should also be considered since, when these modifications are functional, this quantitative information will shed further light on their physiological importance.

ACKNOWLEDGEMENTS

This work was supported by grants from the Fund for Scientific Research-Flanders (grant number G.0038.09N) and the Ghent University Multidisciplinary Research Partnership “Biotechnology for a Sustainable Economy” (project no.01MRB510W). S.J. is indebted to the Agency for Innovation through Science and Technology for a predoctoral fellowship and B.G. is a Postdoctoral Fellow of the Research Foundation-Flanders.

REFERENCES

- [1] Van Breusegem, F., Dat, J. F., Reactive oxygen species in plant cell death. *Plant Physiol.* 2006, 141, 384-390.
- [2] Foyer, C. H., Noctor, G., Redox homeostasis and antioxidant signaling: a metabolic interface between stress perception and physiological responses. *Plant Cell* 2005, 17, 1866-1875.
- [3] Mittler, R., Vanderauwera, S., Suzuki, N., Miller, G., *et al.*, ROS signaling: the new wave? *Trends Plant Sci.* 2011, 16, 300-309.
- [4] Mittler, R., Vanderauwera, S., Gollery, M., Van Breusegem, F., The reactive oxygen gene network of plants. *Trends Plant Sci.* 2004, 9, 490-498.
- [5] Gadjev, I., Vanderauwera, S., Gechev, T. S., Laloi, C., *et al.*, Transcriptomic footprints disclose specificity of reactive oxygen species signaling in *Arabidopsis*. *Plant Physiol.* 2006, 141, 436-445.
- [6] Queval, G., Neukermans, J., Vanderauwera, S., Van Breusegem, F., Noctor, G., Day length is a key regulator of transcriptomic responses to both CO₂ and H₂O₂ in *Arabidopsis*. *Plant Cell Environ.* 2012, 35, 374-387.
- [7] Cheong, Y. H., Chang, H.-S., Gupta, R., Wang, X., *et al.*, Transcriptional profiling reveals novel interactions between wounding, pathogen, abiotic stress, and hormonal responses in *Arabidopsis*. *Plant Physiol.* 2002, 129, 661-677.
- [8] An, D., Yang, J., Zhang, P., Transcriptome profiling of low temperature-treated cassava apical shoots showed dynamic responses of tropical plant to cold stress. *BMC Genomics* 2012, 13, 64.
- [9] Padmalatha, K. V., Dhandapani, G., Kanakachari, M., Kumar, S., *et al.*, Genome-wide transcriptomic analysis of cotton under drought stress reveal significant down-regulation of genes and pathways involved in fibre elongation and up-regulation of defense responsive genes. *Plant Mol. Biol.* 2012, 78, 223-246.
- [10] Spadaro, D., Yun, B.-W., Spoel, S. H., Chu, C., *et al.*, The redox switch: dynamic regulation of protein function by cysteine modifications. *Physiol. Plant.* 2010, 138, 360-371.
- [11] Galetskiy, D., Lohscheider, J. N., Kononikhin, A. S., Popov, I. A., *et al.*, Mass spectrometric characterization of photooxidative protein modifications in *Arabidopsis thaliana* thylakoid membranes. *Rapid Commun. Mass Spectrom.* 2011, 25, 184-190.
- [12] Rajjou, L., Belghazi, M., Catusse, J., Ogé, L., *et al.*, Proteomics and posttranslational proteomics of seed dormancy and germination. *Methods Mol. Biol.* 2011, 773, 215-236.
- [13] Navrot, N., Finnie, C., Svensson, B., Hägglund, P., Plant redox proteomics. *J. Proteomics* 2011, 74, 1450-1462.
- [14] Lindahl, M., Mata-Cabana, A., Kieselbach, T., The disulfide proteome and other reactive cysteine proteomes: analysis and functional significance. *Antioxid. Redox Signal.* 2011, 14, 2581-2642.
- [15] Mikesh, L. M., Ueberheide, B., Chi, A., Coon, J. J., *et al.*, The utility of ETD mass spectrometry in proteomic analysis. *Biochim. Biophys. Acta* 2006, 1764, 1811-1822.

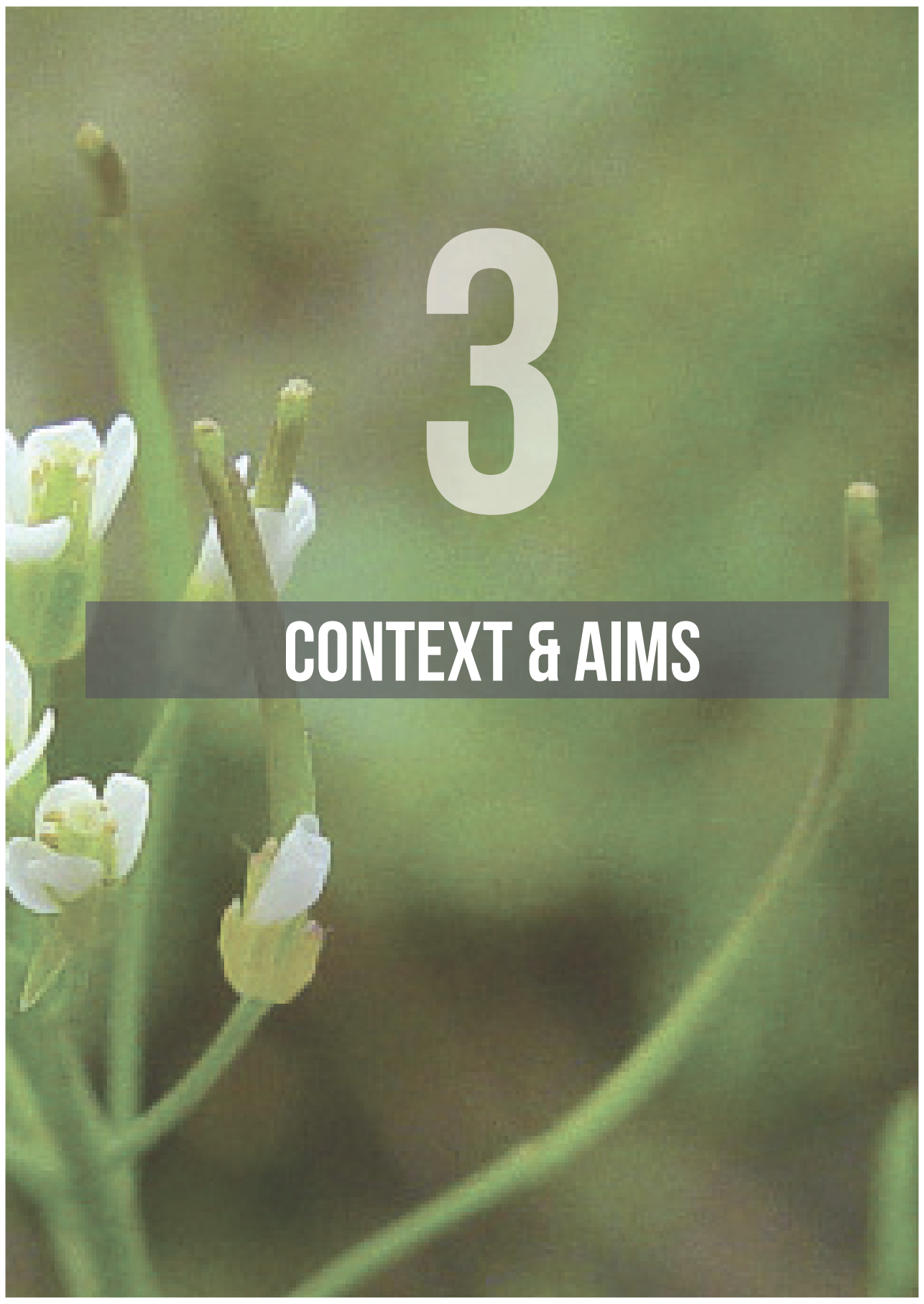
- [16] Savige, W. E., Fontana, A., Interconversion of methionine and methionine sulfoxide. *Methods Enzymol.* 1977, 47, 453-459.
- [17] Boschi-Muller, S., Gand, A., Branlant, G., The methionine sulfoxide reductases: catalysis and substrate specificities. *Arch. Biochem. Biophys.* 2008, 474, 266-273.
- [18] Tarrago, L., Laugier, E., Rey, P., Protein-repairing methionine sulfoxide reductases in photosynthetic organisms: gene organization, reduction mechanisms, and physiological roles. *Mol. Plant* 2009, 2, 202-217.
- [19] Romero, H. M., Berlett, B. S., Jensen, P. J., Pell, E. J., Tien, M., Investigations into the role of the plastidial peptide methionine sulfoxide reductase in response to oxidative stress in *Arabidopsis*. *Plant Physiol.* 2004, 136, 3784-3794.
- [20] Vieira Dos Santos, C., Cuiné, S., Rouhier, N., Rey, P., The *Arabidopsis* plastidic methionine sulfoxide reductase B proteins. Sequence and activity characteristics, comparison of the expression with plastidic methionine sulfoxide reductase A, and induction by photooxidative stress. *Plant Physiol.* 2005, 138, 909-922.
- [21] Kwon, S. J., Kwon, S. I., Bae, M. S., Cho, E. J., Park, O. K., Role of the methionine sulfoxide reductase MsrB3 in cold acclimation in *Arabidopsis*. *Plant Cell Physiol.* 2007, 48, 1713-1723.
- [22] Lowther, W. T., Brot, N., Weissbach, H., Matthews, B. W., Structure and mechanism of peptide methionine sulfoxide reductase, an "anti-oxidation" enzyme. *Biochemistry* 2000, 39, 13307-13312.
- [23] Tarrago, L., Laugier, E., Zaffagnini, M., Marchand, C., et al., Regeneration mechanisms of *Arabidopsis thaliana* methionine sulfoxide reductases B by glutaredoxins and thioredoxins. *J. Biol. Chem.* 2009, 284, 18963-18971.
- [24] Tarrago, L., Laugier, E., Zaffagnini, M., Marchand, C. H., et al., Plant thioredoxin CDSP32 regenerates 1-Cys methionine sulfoxide reductase B activity through the direct reduction of sulfenic acid. *J. Biol. Chem.* 2010, 285, 14964-14972.
- [25] Chen, Q., Vierling, E., Analysis of conserved domains identifies a unique structural feature of a chloroplast heat shock protein. *Mol. Gen. Genet.* 1991, 226, 425-431 [Erratum *Mol. Gen. Genet.* 228, 328].
- [26] Ehrnsperger, M., Gräber, S., Gaestel, M., Buchner, J., Binding of non-native protein to Hsp25 during heat shock creates a reservoir of folding intermediates for reactivation. *EMBO J.* 1997, 16, 221-229.
- [27] Gustavsson, N., Kokke, B. P. A., Härndahl, U., Silow, M., et al., A peptide methionine sulfoxide reductase highly expressed in photosynthetic tissue in *Arabidopsis thaliana* can protect the chaperone-like activity of a chloroplast-localized small heat shock protein. *Plant J.* 2002, 29, 545-553.
- [28] Lim, J. C., Gruschus, J. M., Ghesquière, B., Kim, G., et al., Characterization and solution structure of mouse myristoylated methionine sulfoxide reductase A. *J. Biol. Chem.* 2012, 287, 25589-25595.
- [29] Hardin, S. C., Larue, C. T., Oh, M.-H., Jain, V., Huber, S. C., Coupling oxidative signals to protein phosphorylation via methionine oxidation in *Arabidopsis*. *Biochem. J.* 2009, 422, 305-312.

- [30] Bechtold, U., Rabbani, N., Mullineaux, P. M., Thornalley, P. J., Quantitative measurement of specific biomarkers for protein oxidation, nitration and glycation in *Arabidopsis leaves*. *Plant J.* 2009, 59, 661-671.
- [31] Rouhier, N., Vieira Dos Santos, C., Tarrago, L., Rey, P., Plant methionine sulfoxide reductase A and B multigenic families. *Photosynth. Res.* 2006, 89, 247-262.
- [32] Bigelow, D. J., Squier, T. C., Thioredoxin-dependent redox regulation of cellular signaling and stress response through reversible oxidation of methionines. *Mol. Biosyst.* 2011, 7, 2101-2109.
- [33] Yin, D., Kuczera, K., Squier, T. C., The sensitivity of carboxyl-terminal methionines in calmodulin isoforms to oxidation by H₂O₂ modulates the ability to activate the plasma membrane Ca-ATPase. *Chem. Res. Toxicol.* 2000, 13, 103-110.
- [34] Oien, D. B., Canello, T., Gabizon, R., Gasset, M., et al., Detection of oxidized methionine in selected proteins, cellular extracts and blood serums by novel anti-methionine sulfoxide antibodies. *Arch. Biochem. Biophys.* 2009, 485, 35-40.
- [35] Wehr, N. B., Levine, R. L., Wanted and wanting: antibody against methionine sulfoxide. *Free Radic. Biol. Med.* 2012, 53, 1222-1225.
- [36] Brock, J. W. C., Cotham, W. C., Ames, J. M., Thorpe, S. R., Baynes, J. W., Proteomic method for the quantification of methionine sulfoxide. *Ann. N.Y. Acad. Sci.* 2005, 1043, 284-289.
- [37] Ghesquière, B., Jonckheere, V., Colaert, N., Van Durme, J., et al., Redox proteomics of protein-bound methionine oxidation. *Mol. Cell. Proteomics* 2011, 10, M110.006866.
- [38] Saunders, C. C., Stites, W. E., An electrophoretic mobility shift assay for methionine sulfoxide in proteins. *Anal. Biochem.* 2012, 421, 767-769.
- [39] Maronedze, C., Turek, I., Parrott, B., Thomas, L., Jankovic, B., Lilley, K. S., and Gehring, C. (2013) Structural and functional characteristics of cGMP-dependent methionine oxidation in *Arabidopsis thaliana* proteins. *Cell communication and signaling : CCS* 11, 1
- [40] Gustavsson, N., Kokke, B. P. A., Anzelius, B., Boelens, W. C., Sundby, C., Substitution of conserved methionines by leucines in chloroplast small heat shock protein results in loss of redox-response but retained chaperone-like activity. *Protein Sci.* 2001, 10, 1785-1793.
- [41] Tarrago, L., Kieffer-Jaquinod, S., Lamant, T., Marcellin, M., et al., Affinity chromatography: a valuable strategy to isolate substrates of methionine sulfoxide reductases? *Antioxid. Redox Signal.* 2012, 16, 79-84.
- [42] Abello, N., Kerstjens, H. A. M., Postma, D. S., Bischoff, R., Protein tyrosine nitration: selectivity, physicochemical and biological consequences, denitration, and proteomics methods for the identification of tyrosine-nitrated proteins. *J. Proteome Res.* 2009, 8, 3222-3238.
- [43] Radi, R., Nitric oxide, oxidants, and protein tyrosine nitration. *Proc. Natl. Acad. Sci. USA* 2004, 101, 4003-4008.
- [44] Souza, J. M., Daikhin, E., Yudkoff, M., Raman, C. S., Ischiropoulos, H., Factors determining the selectivity of protein tyrosine nitration. *Arch. Biochem. Biophys.* 1999, 371, 169-178.

- [45] Ischiropoulos, H., Biological selectivity and functional aspects of protein tyrosine nitration. *Biochem. Biophys. Res. Commun.* 2003, 305, 776-783.
- [46] Bartesaghi, S., Ferrer-Sueta, G., Peluffo, G., Valez, V., et al., Protein tyrosine nitration in hydrophilic and hydrophobic environments. *Amino Acids* 2007, 32, 501-515.
- [47] Chaki, M., Valderrama, R., Fernández-Ocaña, A. M., Carreras, A., et al., Protein targets of tyrosine nitration in sunflower (*Helianthus annuus* L.) hypocotyls. *J. Exp. Bot.* 2009, 60, 4221-4234.
- [48] Saito, S., Yamamoto-Katou, A., Yoshioka, H., Doke, N., Kawakita, K., Peroxynitrite generation and tyrosine nitration in defense responses in tobacco BY-2 cells. *Plant Cell Physiol.* 2006, 47, 689-697.
- [49] Gong, Y.-W., Yuan, Y.-J., Nitric oxide mediates inactivation of glutathione S-transferase in suspension culture of *Taxus cuspidata* during shear stress. *J. Biotechnol.* 2006, 123, 185-192.
- [50] Corpas, F. J., Chaki, M., Fernández-Ocaña, A., Valderrama, R., et al., Metabolism of reactive nitrogen species in pea plants under abiotic stress conditions. *Plant Cell Physiol.* 2008, 49, 1711-1722.
- [51] Cecconi, D., Orzetti, S., Vandelle, E., Rinalducci, S., et al., Protein nitration during defense response in *Arabidopsis thaliana*. *Electrophoresis* 2009, 30, 2460-2468.
- [52] Corpas, F. J., Chaki, M., Leterrier, M., Barroso, J. B., Protein tyrosine nitration: a new challenge in plants. *Plant Signal. Behav.* 2009, 4, 920-923.
- [53] Lozano-Juste, J., Colom-Moreno, R., León, J., In vivo protein tyrosine nitration in *Arabidopsis thaliana*. *J. Exp. Bot.* 2011, 62, 3501-3517.
- [54] Yemets, A. I., Krasylenko, Y. A., Lytvyn, D. I., Sheremet, Y. A., Blume, Y. B., Nitric oxide signalling via cytoskeleton in plants. *Plant Sci.* 2011, 181, 545-554.
- [55] Valderrama, R., Corpas, F. J., Carreras, A., Fernández-Ocaña, A., et al., Nitrosative stress in plants. *FEBS Lett.* 2007, 581, 453-461.
- [56] Morot-Gaudry-Talarmain, Y., Rockel, P., Moureaux, T., Quilleré, I., et al., Nitrite accumulation and nitric oxide emission in relation to cellular signaling in nitrite reductase antisense tobacco. *Planta* 2002, 215, 708-715.
- [57] Chaki, M., Fernández-Ocaña, A. M., Valderrama, R., Carreras, A., et al., Involvement of reactive nitrogen and oxygen species (RNS and ROS) in sunflower-mildew interaction. *Plant Cell Physiol.* 2009, 50, 265-279.
- [58] Galetskiy, D., Lohscheider, J. N., Kononikhin, A. S., Popov, I. A., et al., Phosphorylation and nitration levels of photosynthetic proteins are conversely regulated by light stress. *Plant Mol. Biol.* 2011, 77, 461-473.
- [59] Álvarez, C., Lozano-Juste, J., Romero, L. C., Garcia, I., et al., Inhibition of *Arabidopsis* O-acetylserine(thiol) lyase A1 by tyrosine nitration. *J. Biol. Chem.* 2011, 286, 578-586.
- [60] Melo, P. M., Silva, L. S., Ribeiro, I., Seabra, A. R., Carvalho, H. G., Glutamine synthetase is a molecular target of nitric oxide in root nodules of *Medicago truncatula* and is regulated by tyrosine nitration. *Plant Physiol.* 2011, 157, 1505-1517.

- [61] Maassen, A., Hennig, J., Effect of *Medicago sativa* Mhb1 gene expression on defense response of *Arabidopsis thaliana* plants. *Acta Biochim. Pol.* 2011, 58, 427-432.
- [62] Jovanović, A. M., Durst, S., Nick, P., Plant cell division is specifically affected by nitrotyrosine. *J. Exp. Bot.* 2010, 61, 901-909.
- [63] Mallozzi, C., Di Stasi, A. M. M., Minetti, M., Nitrotyrosine mimics phosphotyrosine binding to the SH₂ domain of the src family tyrosine kinase lyn. *FEBS Lett.* 2001, 503, 189-195.
- [64] Monteiro, H. P., Arai, R. J., Travassos, L. R., Protein tyrosine phosphorylation and protein tyrosine nitration in redox signaling. *Antioxid. Redox Signal.* 2008, 10, 843-889.
- [65] Abello, N., Barroso, B., Kerstjens, H. A., Postma, D. S., Bischoff, R., Chemical labeling and enrichment of nitrotyrosine-containing peptides. *Talanta* 2010, 80, 1503-1512.
- [66] Zhang, Q., Qian, W.-J., Knyushko, T. V., Clauss, T. R. W., et al., A method for selective enrichment and analysis of nitrotyrosine-containing peptides in complex proteome samples. *J. Proteome Res.* 2007, 6, 2257-2268.
- [67] Dremina, E. S., Li, X., Galeva, N. A., Sharov, V. S., et al., A methodology for simultaneous fluorogenic derivatization and boronate affinity enrichment of 3-nitrotyrosine-containing peptides. *Anal. Biochem.* 2011, 418, 184-196.
- [68] Prokai-Tatrai, K., Guo, J., Prokai, L., Selective chemoprecipitation and subsequent release of tagged species for the analysis of nitropeptides by liquid chromatography-tandem mass spectrometry. *Mol. Cell. Proteomics* 2011, 10, M110.002923.
- [69] Lee, J. R., Lee, S. J., Kim, T. W., Kim, J. K., et al., Chemical approach for specific enrichment and mass analysis of nitrated peptides. *Anal. Chem.* 2009, 81, 6620-6626.
- [70] Ghesquière, B., Colaert, N., Helsens, K., Dejager, L., et al., In vitro and in vivo protein-bound tyrosine nitration characterized by diagonal chromatography. *Mol. Cell. Proteomics* 2009, 8, 2642-2652.
- [71] Davies, M. J., The oxidative environment and protein damage. *Biochimica et biophysica acta* 2005, 1703, 93-109.
- [72] Rey, P., Becuwe, N., Barrault, M. B., Rumeau, D., et al., The *Arabidopsis thaliana* sulfiredoxin is a plastidic cysteine-sulfinic acid reductase involved in the photooxidative stress response. *Plant J* 2007, 49, 505-514.
- [73] Lindahl, M., Mata-Cabana, A., Kieselbach, T., The disulfide proteome and other reactive cysteine proteomes: analysis and functional significance. *Antioxid Redox Signal* 2011, 14, 2581-2642.
- [74] Couturier, J., Chibani, K., Jacquot, J. P., Rouhier, N., Cysteine-based redox regulation and signaling in plants. *Front Plant Sci* 2013, 4, 105.





3

CONTEXT & AIMS

SCOPE AND OBJECTIVES

Enhanced reactive oxygen species (ROS) production is a common theme in the response of plants to adverse environmental conditions. This leads to an imbalance of the ROS homeostasis and can cause significant cellular damage, but can also initiate defense responses, where the plant uses ROS as signaling molecules [1, 2]. Amongst the different ROS, hydrogen peroxide is particularly suitable to fulfill a signaling function with its relatively long half-life and small size, allowing it to migrate to different cellular compartments [3, 4]. Mutant plants defective in peroxisomal CATALASE 2 are very important tools to study the *in vivo* effects of increased hydrogen peroxide levels [5]. The catalase 2 enzyme is the major leaf catalase isoform out of three encoded in the Arabidopsis genome and acts as the leading scavenger of hydrogen peroxide [5]. The latter became apparent as catalase 2 deficient plants show a reduction in catalase activity to only 10% of that in wild-type plants [6]. Upon photorespiration, wild-type plants produce hydrogen peroxide by glycolate oxidase in the peroxisomes, which is in turn scavenged by CAT2. Hence, exposure of catalase 2 knock-out plants (*cat2-2*) to photorespiratory inducing conditions increases the hydrogen peroxide availability within the plants. This endogenous hydrogen peroxide production renders *cat2-2* plants a physiologically much more relevant model system [7] than rather high hydrogen peroxide levels exogeneously delivered to plant tissues or plant cells [8]. For this reason, we here employ the well-characterized *cat2-2* plants as our model system to study the molecular responses upon oxidative stress. Although multiple genome-wide transcriptome analyses of catalase deficient plants exposed to oxidative stress led to a comprehensive inventory of hydrogen peroxide responsive genes [6, 7, 9-12], very little is known about the outcome of these responses at the protein level. Although proteins are the functional entities of a living cell, there is a large knowledge gap between regulation at the transcriptional level and the consecutive regulatory steps leading to the oxidative stress dependent protein production and stability.

This project aims to fill the gaps by generating the necessary additional omics data, essential to get a multi-angle view of the ROS signaling network, with a focus towards the proteome and beyond.

Our main objective is to inventorize and assess the dynamics of transcript levels, translation and protein abundance during the oxidative stress response in *Arabidopsis thaliana* wild-type and CATALASE 2 knock-out plants (*cat2-2*). Therefore, we will implement and optimize state-of-the art mass spectrometry, i.e. a quantitative gel-free shotgun proteomics approach, and next generation sequencing technologies, namely a ribosome profiling study [13] generating mRNA-seq and ribo-seq data. Ribosome profiling entails the deep sequencing of ribosomal protected messenger RNA, so called ribosomal footprints [14]. Combined with mRNA-sequencing, these data are particularly suited to perform in-depth studies of protein translation. Footprint abundances point out the actual mRNA molecules that are being translated, define the open reading frames and moreover, the efficiency of translation can be inferred [13, 15, 16]. Of note, such ribosome profiling studies were already proven useful to define the landscape of genome-wide regulation of translation in response to hydrogen peroxide in yeast [17].

By combining our mass spectrometry and next-generation sequencing datasets, we aim to provide insights into the complex dynamic interplay of cellular regulation during oxidative stress.

In addition, we will identify and characterize *in vivo* oxidation events of protein-bound methionine during oxidative stress using the proteome-wide COFRADIC technology [13]. Reversible methionine oxidation is a plausible mechanism to perceive oxidative stress and might function in redox signalling. This study will lead to candidate proteins that are able to perceive changes in cellular redox potential.

This global view on how plants, and more specifically *A. thaliana*, react to and cope with accumulated ROS levels, will contribute to a better understanding of plant adaptability to stress. We aspire to reveal important players and possible regulators of the ROS signaling network, resulting in an extended pool of novel targets for engineering abiotic stress tolerance.

REFERENCES

- [1] Suzuki, N., Koussevitzky, S., Mittler, R., Miller, G., ROS and redox signalling in the response of plants to abiotic stress. *Plant Cell Environ* 2012, 35, 259-270.
- [2] Mittler, R., Vanderauwera, S., Suzuki, N., Miller, G., *et al.*, ROS signaling: the new wave? *Trends Plant Sci* 2011, 16, 300-309.
- [3] Bienert, G. P., Schjoerring, J. K., Jahn, T. P., Membrane transport of hydrogen peroxide. *Biochim Biophys Acta* 2006, 1758, 994-1003.
- [4] Petrov, V. D., Van Breusegem, F., Hydrogen peroxide-a central hub for information flow in plant cells. *AoB Plants* 2012, 2012, pls014.
- [5] Mhamdi, A., Queval, G., Chaouch, S., Vanderauwera, S., *et al.*, Catalase function in plants: a focus on *Arabidopsis* mutants as stress-mimic models. *J Exp Bot* 2010, 61, 4197-4220.
- [6] Vandenabeele, S., Van Der Kelen, K., Dat, J., Gadjev, I., *et al.*, A comprehensive analysis of hydrogen peroxide-induced gene expression in tobacco. *Proc Natl Acad Sci U S A* 2003, 100, 16113-16118.
- [7] Vandenabeele, S., Vanderauwera, S., Vuylsteke, M., Rombauts, S., *et al.*, Catalase deficiency drastically affects gene expression induced by high light in *Arabidopsis thaliana*. *Plant Journal* 2004, 39, 45-58.
- [8] Vanderauwera, S., Zimmermann, P., Rombauts, S., Vandenabeele, S., *et al.*, Genome-wide analysis of hydrogen peroxide-regulated gene expression in *Arabidopsis* reveals a high light-induced transcriptional cluster involved in anthocyanin biosynthesis. *Plant Physiol* 2005, 139, 806-821.
- [9] Queval, G., Issakidis-Bourguet, E., Hoeberichts, F. A., Vandenabeele, M., *et al.*, Conditional oxidative stress responses in the *Arabidopsis* photorespiratory mutant *cat2* demonstrate that redox state is a key modulator of daylength-dependent gene expression, and define photoperiod as a crucial factor in the regulation of H₂O₂-induced cell death. *Plant J* 2007, 52, 640-657.
- [10] Queval, G., Neukermans, J., Vanderauwera, S., Van Breusegem, F., Noctor, G., Day length is a key regulator of transcriptomic responses to both CO(2) and H(2)O(2) in *Arabidopsis*. *Plant Cell Environ* 2012, 35, 374-387.
- [11] Vanderauwera, S., Hoeberichts, F. A., Breusegem, F., in: Rio, L. A., Puppo, A. (Eds.), *Reactive Oxygen Species in Plant Signaling*, Springer Berlin Heidelberg 2009, pp. 149-164.
- [12] Ingolia, N. T., Ghaemmaghami, S., Newman, J. R., Weissman, J. S., Genome-wide analysis in vivo of translation with nucleotide resolution using ribosome profiling. *Science* 2009, 324, 218-223.
- [13] Ghesquiere, B., Jonckheere, V., Colaert, N., Van Durme, J., *et al.*, Redox proteomics of protein-bound methionine oxidation. *Mol Cell Proteomics* 2011.



4

SYSTEMS-WIDE ANALYSIS OF THE OXIDATIVE STRESS RESPONSE IN A. THALIANA

**SILKE JACQUES, PIETER-JAN DE BOCK, JONATHAN VANDENBUSSCHE, DARIA GAWRON,
PETRA VAN DAMME, FREDERIK COPPENS,
FRANK VAN BREUSEGEM AND KRIS GEVAERT**

Silke Jacques wrote the chapter with corrections of Petra Van Damme, Frank Van Breusegem and Kris Gevaert

Silke Jacques performed and analyzed all experiments, the ribosome profiling strategy was optimized for plant material together with Daria Gawron and under supervision of Petra Van Damme. Frederik Coppens assisted with sequencing data analysis. Pieter-Jan De Bock and Jonathan Vandenbussche performed the LC-MS/MS measurements.

ABSTRACT

Adverse environmental conditions lead to the accumulation of reactive oxygen and nitrogen species in plants, causing oxidative stress and provoking major crop losses. A comprehensive elucidation on how plants cope with and adjust to oxidative stress is however lacking. Here, an integrated systems-level analysis of the transcriptome, translome and proteome was conducted to disentangle the plant response to oxidative stress. As a model system, we made use of *Arabidopsis thaliana* catalase 2 knock-out plants that can endogenously accumulate higher levels of hydrogen peroxide, and compared their responses to these of wild-type plants. Comparison of mRNA-seq, ribo-seq and protein abundance measurements provided a holistic (comprehensive) view on the oxidative stress response in *A. thaliana* leaves. The gel-free proteome profiling revealed both known (e.g., DHAR2, APX1, UGT1) and new players (e.g., SAHH1, SAHH2, MAT3) in the ROS-responsive network. Combined with the next-generation sequencing data, a prominent role for protein degradation was revealed. Via an active breakdown of ribosomal proteins, translation was severely affected upon high light stress treatment. Co-regulation of transcription and translation is revealed but the translational efficiency of individual mRNAs is highly affected upon increased hydrogen peroxide levels. This study emphasized the necessity of combining state-of-the-art technologies to study different levels of cellular regulation of plants exposed to stress.

INTRODUCTION

Abiotic and biotic stress conditions such as drought, extreme temperature and pest attacks lead to severe crop losses worldwide due to their adverse effect on plant growth and development [1]. A common theme within these adverse conditions is the accumulation of reactive oxygen and nitrogen species (ROS/RNS). In order to avoid ROS-dependent cellular damage, a fine-tuned balance between ROS production and scavenging is essential. In *Arabidopsis* this balance is governed by a complex regulatory network (Mittler et al., 2011). Both non-enzymatic and enzymatic antioxidants, present in each cellular compartment, permit a tight regulation of ROS which in turn allows ROS to be used in a beneficial way: they can act as signalling molecules in different environmental and developmental processes [2, 3]. Hydrogen peroxide was found to be a potent signaling molecule [4], which is involved in a plethora of physiological functions and interacts with multiple hormonal pathways [5]. Catalases are able to dismutate hydrogen peroxide to water and oxygen. From the three catalase encoding genes in *Arabidopsis*, peroxisomal catalase 2 (CAT2) is the main leaf isoform [6]. Hence, CAT2 knock-out (*cat2-2*) plants allow an inducible and endogenous increase in ROS levels through an easy manipulation by external conditions. Perturbation of hydrogen peroxide can be sustained over time without the need for invasive techniques but by inducing photorespiration [7-10]. Previous studies gave insights into the elaborate transcriptional response upon accumulation of hydrogen peroxide in plants defective in CAT2 [7, 8, 10, 11]. However, it is not yet clear how the majority of stress-related redox stimuli are perceived and transduced, rendering it necessary to generate complementary datasets to gain a better understanding of the complex ROS signal transduction network.

Recent advances in next-generation sequencing allow for comprehensive and quantitative measurements of mRNA levels (RNA-seq). However, gene transcript levels are not necessarily accurate proxies of protein levels and even less so for protein activities [12-15]. Posttranscriptional as well as translational and posttranslational (e.g. protein processing/degradation) regulations are important cellular control mechanisms that need to be considered. Recently, a global analysis of mRNA translation at the sub-codon level became possible with the development of ribosome profiling or ribo-seq [16], which monitors ribosome-protected mRNA fragments (footprints) by deep sequencing. Coupled with mRNA-sequencing (mRNA-seq), ribo-seq data exposes the actual mRNA molecules and open reading frames (ORFs) that are translated and their translational efficiencies that are reflected by the ribosomal densities on the mRNA molecules [17-19]. Ribosome profiling has been proven a useful tool to investigate the genome-wide regulation of translation in cells, e.g. mouse fibroblasts and human embryonic kidney cells, in response to stress [20, 21]. Also, the complex translational regulation of organisms, i.e. *Saccharomyces cerevisiae*, to hydrogen peroxide treatment were revealed by a ribosome profiling study [22]. In plants, the first steps towards mapping the translational landscape were made by genome-wide profiling of ribosome footprints in *Arabidopsis* seedlings [23, 24].

However, little is known about the outcome of these responses at the protein level. Proteome-wide studies of the abundance dynamics during oxidative stress are particularly rare, but would be of great value.

In order to generate accurate knowledge of plant responsiveness to environmental stresses, several OMICS approaches, each capturing a segment of the overall plant response, ideally need to be combined [25]. Our main objective; to capture the early dynamics during oxidative stress, steered the choice to analyse early time points of oxidative stress. We here used a bottom-up, quantitative LC-MS/MS approach to capture the proteome dynamics of the plant oxidative stress response over time and integrated this with mRNA-seq and ribo-seq data. We demonstrated that there is a role for active protein degradation to initiate a fast stress response together with a general shutdown of translation. Furthermore, translational efficiency was largely affected by enhanced hydrogen peroxide concentrations. Also, a map of quantified translation events, including information related to expressed upstream open reading frames and N-terminal protein extensions, results in a more accurate knowledge of changes in protein synthesis and responsiveness to environmental stresses.

We examined how plant cells globally cope with oxidative stress by exploring the dynamic interplay between transcription, translation and protein abundance by integrative in-depth and system-level analyses. We anticipate that such global integrated analyses will further aid to reveal yet uncharacterized regulatory mechanisms in the oxidative stress response.

RESULTS

Monitoring multiple systems-level responses during oxidative stress

To assess the cellular responses to hydrogen peroxide accumulation, *Arabidopsis thaliana* plants with a T-DNA insertion in the CAT2 coding sequence (*cat2-2*) were compared to wild-type plants. Perturbation of hydrogen peroxide homeostasis in these knock-out plants can be sustained over time under photorespiratory conditions [11], ultimately leading to cell death while wild-type plants exposed to identical conditions accumulate anthocyanins (resulting in purple colored leaves) [8] (**Figure 1A**, <https://vimeo.com/114873383>). Since photorespiration is the primary source of hydrogen peroxide in photosynthetic tissue [26], wild-type and *cat2-2* plants were grown under high concentrations of CO₂ (3,000 ppm). This was obtained by growing the plants in climate-controlled chambers in a completely randomized experimental block design, with tray-scattering of the genotypes. Growing plants under such elevated CO₂ concentrations is expected to minimize photorespiration and consequently, hydrogen peroxide accumulation. In effect, no obvious phenotypic differences are observed between wild-type and *cat2-2* plants (**Figure 1B**) after 5 weeks growth under 3,000 ppm CO₂. Oxidative stress was induced by transferring plants from high CO₂ concentrations to ambient air conditions (400 ppm CO₂) and high light (HL) irradiation (1,000 μmol m⁻² s⁻¹). The experiment was designed to simultaneously monitor three systems-level processes during oxidative stress, from transcription to protein steady-state levels (**Figure 2**). By focusing on the early stages of ROS-mediated responses, new signal transducers and regulators can be characterized while avoiding secondary effects due to increased cell toxicity, ultimately leading to cell death. Therefore, middle-aged leaves (depicted in red) were sampled at 0, 1, 2 and 3 h following the onset of stress exposure and immediately frozen in liquid nitrogen (**Figure 2**). These time points were chosen based on repetitive sampling at multiple time points from which we assessed transcript levels of various H₂O₂ induced marker genes [8, 9] and CAT2 protein levels. The detailed transcriptional oxidative stress response of wild-type and *cat2-2* leaves is examined by deep sequencing of mRNA (mRNA-seq) before and 3 h after the onset of stress treatment. We pair

this data with ribosome profiling, the deep sequencing of ribosome-protected mRNA fragments during active translation. This combination offers significant insight into proteome synthesis and translational regulation during oxidative stress, not available by monitoring transcript expression alone [18]. To directly measure changes at the protein level and to capture the dynamics of ROS-responsive proteins, wild-type and *cat2-2* leaves sampled at four time points, were subjected to isotopic labelling and tandem mass spectrometry to quantify the dynamic protein abundances during oxidative stress.

A.



B.



Figure 1. Catalase knock-out plants as a model system

Exposure to high light intensities induces cell death in the *cat2-2* line while the control line accumulates anthocyanins, as is evident from the purple coloring of leaves (A). These representative plants were exposed for 3 days to $400 \mu\text{mol m}^{-2} \text{s}^{-1}$ in a controlled growth chamber (see movie). No phenotypic differences can be detected between *cat2-2* and wild-type plants after 5 weeks of growth under elevated CO_2 concentrations (B).

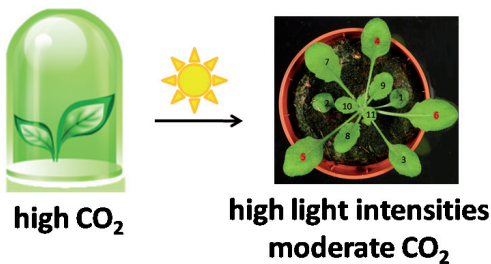


Figure 2. Monitoring multiple systems-level responses in *cat2-2* and wild-type plants during oxidative stress

Wild-type and *cat2-2* plants were grown for five weeks under high CO_2 concentrations before they were exposed to high light intensities and moderate CO_2 levels. Middle-aged leaves (red dots) were sampled at 0, 1, 2 and 3 h following the onset of stress exposure. Transcriptional and translational control is examined by combining deep sequencing of mRNA (mRNA seq) with ribosome profiling (ribo seq) before and 3 h after the onset of stress treatment. To capture the dynamics of ROS-responsive proteins, wild-type and *cat2-2* leaves sampled at all four time points, were subjected to tandem mass spectrometry to quantify the protein abundances during oxidative stress.

As the measurements of the steady-state protein levels is extended to all time points sampled, we will first describe the protein dynamics of wild-type and *cat2-2* plants upon exposure to HL.

A quantitative gel-free proteomics strategy to study protein dynamics

We opted for a quantitative proteomics approach based on stable-isotope labeling of peptides to detect differences in protein abundance between wild-type and *cat2-2* plants exposed to a combination of ambient air conditions and high light (HL).

To allow the inter-comparison of two genotypes and four time points (0, 1, 2, 3 h) with minimal run to run variations, we opted for a reference pool design. This reference pool is made up of equal quantities of all eight samples assayed. Following protein extraction and proteolytic digestion (using endoproteinase Lys-C), post-metabolic labeling of peptides, using light ($^{12}\text{C}_3$) or heavy ($^{13}\text{C}_3$) propionate, was performed [27]. These mass tags allow for a differential and quantitative comparison between genotypes and time points. Every sample, labeled light, is compared to the heavy labeled reference pool leading to a final of eight samples to be analyzed, being the proteomes sampled at the four time points for both wild-type and catalase knock-out plants (Figure 3). Three independent biological repeat experiments were performed, resulting in a total of 24 proteome analyses. After separation of the proteome digests via reversed phase-high performance liquid chromatography (RP-HPLC), fractions were loaded onto the the LTQ Orbitrap XL for subsequent LC-MS/MS analysis.

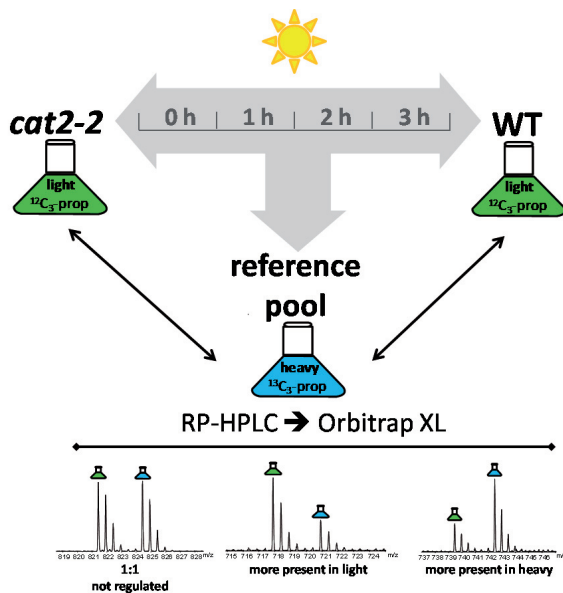


Figure 3. Schematic overview of the shotgun proteomics approach

Five-weeks old *cat2-2* and wild-type plants were exposed to a continuous high light irradiation ($1,000 \mu\text{mol m}^{-2} \text{s}^{-1}$) under ambient air (400 ppm). Leaves were sampled at 0, 1, 2 and 3 h after the onset of high light stress. A reference pool was generated that comprises equivalent amounts of each proteome sample. Peptides were post-metabolically labelled using light ($^{12}\text{C}_3$) or heavy ($^{13}\text{C}_3$) propionate for the sample and reference pool, respectively. These mass tags allow to quantify differences in overall protein abundances over time and between genotypes by looking at isotopic envelopes of 6Da difference.

Proteome data analysis

We made use of the MaxQuant software package [28], which allows to match data between runs while searching with the Andromeda search engine. In this way, identifications across replicate experiments can be increased as peptides eluting in similar time windows and with matching m/z values are now additionally assigned by deduction based on the co-elution profiles of common peptides identified in other LC-MS/MS runs. As such, the missing value problem is partially solved and results in a considerable overlap between biological repeats. Consequently, the MS and MS/MS data of the 24 proteomes were searched using MaxQuant and subsequent data analysis was performed in Perseus.

Normalization and further analysis is performed on data from all three biological repeats (**Supplemental Figure S1**). Missing values are filtered out to continue with valid protein ratios present in both wild-type and *cat2-2* genotypes and over all four time points, resulting in 24 abundance values for 912 proteins out of the 3,327 proteins identified in total. This represents 27% of all identified proteins in all analyzed samples.

Prior to analyzing the dynamics of the commonly identified proteins, we assessed the proteome differences of wild-type and *cat2-2* plants grown under high CO_2 levels. Preceding oxidative stress induction (0 h), an overlap of 1,237 proteins was identified in the wild-type and *cat2-2* proteomes. The only protein whose abundance differed significant ($p < 0.01$) between both genotypes was CAT2 (AT4G35090). The volcano plot (**Supplemental Figure S2**), with the significance threshold set by determining the correct s_0 factor ($s_0 = 0.077$) and a false discovery rate of 1%, shows that the proteins identified in wild-type and *cat2-2* plants were generally unaltered when grown under high CO_2 . Thus, not only do wild-type and *cat2-2* plants show a similar phenotype, also at the proteome level, no significant differences except for CAT2 could be detected. Together, these data show very high levels of uniformity, even at the proteome level, between the two plant lines before the onset of stress treatment.

To identify proteins whose abundance changed during early time points after stress treatment, a SAM (statistical analysis of microarrays) analysis was performed [29]. This method is advantageous over ANOVA since normality, homogeneity and independence are parametric assumptions inherent to it. The variation between our biological repeats as well as the inter-dependence between proteins therefore disfavors ANOVA, whilst determining if the expression of any proteins is significantly related to the response via permutation-based analysis is more favorable. The latter is exactly what SAM does, it carries out multiple protein specific t-tests and computes a statistic d_i for each protein i , measuring the strength of relationship between protein abundance and the response variable [30]. Repeated permutations allow filtering out any gene whose expression is significantly related to the response, e.g. exposure to high light intensities over time. The normalized ratios of the significant proteins ($p < 0.05$) were rescaled to a (-1;1) interval to have a more easy interpretable scale where +1 is most and -1 is least abundant.

Dynamics of ROS-responsive proteins

Proteins with an abundance significantly ($p < 0.05$) changing over time were retained and a Pearson correlation cluster analysis revealed several patterns of changing protein abundances (**Figure 4**). A subdivision of these profiles into seven distinct clusters formed the basis for the further exploration of regulated proteins upon oxidative stress.

Clusters 2, 3 and 5 hold proteins with a general lower abundances in both genotypes prior to the transfer, but of which the levels increase over time, though at different rates. Proteins with the smallest increase make up cluster 2 and here, a slight delay in *cat2-2* plants is observed. The abnormal inflorescence meristem protein (AIM1) categorized in this cluster catalyzes the final steps of jasmonate biosynthesis, being the beta-oxidation of 12-oxo-phytoenoic acid [31]. A link with functional peroxisomes was already demonstrated as, together with AIM1, peroxisomes were found necessary for wound-induced jasmonate biosynthesis.

Cluster 3 comprises proteins with a steep increase in protein abundance, already 1 h after high light exposure in wild-type plants, but whose induction is delayed in *cat2-2* plants. Both S-adenosyl-L-homocysteine hydrolases 1 and 2 (SAHH1; AT4G13940 and SAHH2; AT3G23810), as well as the S-adenosylmethionine synthetase (SAMS) are found in this cluster. This means that high light increases the steady-state levels of three enzymes from the methionine cycle, already at earlier time-points in wild-type plants. Also, two chaperonins (AT1G24510; AT3G03960) were identified whose presence was previously observed in plasmodesma [32]. Two GTPases were also found in this cluster. One is the integral membrane protein TOC159 that functions as a transit-sequence receptor for the co-translational import of proteins and required for chloroplast biogenesis [33]. Up-regulation of chloroplast biogenesis could be a defense strategy to ensure chloroplast reinforcement due to the high light exposure. The other GTPase is the RAS-related nuclear protein (RAN1), which is a soluble GTP-binding protein involved in nuclear translocation of proteins [34]. Also, known proteins implicated in the protection against ROS such as cytokinesis defective 1 (CYT1; AT2G39770) and delta1-pyrroline-5-carboxylate synthase (P5CS1; AT2G39800) were identified. The former provides GDP-mannose used for ascorbate biosynthesis, the core pathway of hydrogen peroxide detoxification by serving a direct anti-oxidant function [35]. P5CS1 catalyzes the rate-limiting step in proline biosynthesis by generating glutamic semialdehyde from glutamate. This gene was shown to be induced by abscisic acid and salt stress in a light-dependent manner and subsequent proline accumulation provides protection from ROS [36].

In cluster 5, hydrogen peroxide exerted an additional inducing effect resulting in an earlier up-regulation of proteins in *cat2-2* plants. This cluster contains proteins from the dehydrin family; LTI29 (AT1G20450), COR47 (AT1G20440) and COR78 (AT5G52310). All these proteins contain highly conserved 7 to 17 residues long lysine, serine, tyrosine and arginine-rich stretches, scattered over their sequences [37]. LTI29 or low temperature induced 29 protein, confers cold tolerance upon overexpression and interacts with the cytoskeleton [38]. The COLD-REGULATED proteins COR47 and COR78 were also found to attribute to cold tolerance, abscisic acid, osmotic stress and dehydration [39]. Also, one of the two arginases encoded in the Arabidopsis genome is present in cluster 5. This arginine amidohydrolase is the final enzyme in the urea cycle and produces ornithine and urea from arginine. An increased pool of ornithine could, like described for P5CS1, lead to glutamic semialdehyde to fuel proline biosynthesis [40].

Clusters 1, 6 and 7 harbour proteins with equal abundances in both wild-type and *cat2-2* plants before stress treatment, while in *cat2-2*, proteins in cluster 7 are down-regulated after 2 h of stress treatment, but were generally not responsive in wild-type plants. The opposite was found for proteins in clusters 1 and 6; their levels dropped in wild-type plants, but hardly changed in *cat2-2* plants. Zooming in on cluster 7 reveals some interesting candidate proteins susceptible to hydrogen peroxide mediated down-regulation in *cat2-2* plants. Two of these code for 3-deoxy-D-arabino-heptulosonate 7-phosphate synthase (DAHPS; AT4G33510 and AT1G22410), which catalyzes the first committed step in the shikimate pathway [41]. Aromatic amino acids in turn derive from shikimate and serve as precursors for a wide range of secondary metabolites, including anthocyanins [42]. Another protein that is subject to hydrogen peroxide dependent down-regulation under high light stress is the cinnamoyl-CoA reductase like (CCL) protein, which catalyzes the first step in the monolignol branch of the phenylpropanoid pathway. Another interesting cluster member is the GUN5 protein, involved in plastid-to-nucleus signal transduction which leads to transcriptional regulation of nuclear genes encoding plastid-localized proteins. This H-subunit of the magnesium chelatase was also shown to bind abscisic acid and mediates stomatal movement [43, 44]. A prominent role for mitochondria in oxidative stress emerges given the identification of several mitochondrial proteins with significant altered protein levels upon high light stress. A representative protein is the 51 kDa subunit of complex I of the mitochondrial respiratory chain (CI51). This NADH dehydrogenase complex releases NAD⁺ and has an established role in maintaining the cellular redox balance since it is the main entrance site for electrons in the respiratory electron transport chain [45]. The mitochondrial malate dehydrogenase 1 is found in cluster 1 and shows unaltered levels in *cat2-2* plants while it is repressed, already 1 h after stress, in wild-type plants. This protein uses electrons of NADH to reduce oxaloacetate to malate that can now freely pass the mitochondrial membrane. Hence, a link to photorespiration emerges, and down-regulation of this protein in wild-type plants is known to lead to a reduction of cytosolic malate, slowing down glycine decarboxylation and limiting photorespiratory carbon flux [46]. The inverse trend found for the CI51 protein described above could be explained by the higher NADH availability in *cat2-2* plants, which in turn can be consumed by higher levels of mMDH1.

Proteins in cluster 6 are significantly down-regulated after 3 h of high light stress in wild-type plants, but their down-regulation appears delayed and reduced in *cat2-2* plants. Importantly, all proteins in cluster 6 are ribosomal proteins, implying that translation is inhibited upon high light exposure. Inhibition of protein synthesis might protect cells against protein misfolding during oxidative stress [47]. The delayed and reduced down-regulation observed in *cat2-2* plants might be explained by a dose-dependent effect of hydrogen peroxide which at high concentrations suppresses the down-regulation of the translational machinery [48]. Also, since *cat2-2* plants suffer from more severe oxidative stress, they might try to adapt for long-term survival in a more selective, translation dependent manner. Accordingly, *cat2-2* plants try to cope with oxidative stress by continuing translation of proteins that alleviate oxidative damage, as is illustrated by the proteins grouped in cluster 4. Here, high light stress in *cat2-2* plants results in a strong up-regulation of well-known antioxidant proteins: ascorbate peroxidase 1, dehydroascorbate reductase 2, UGT1 and isoflavone reductase. All of them were previously shown to respond to oxidative stress [49, 50].

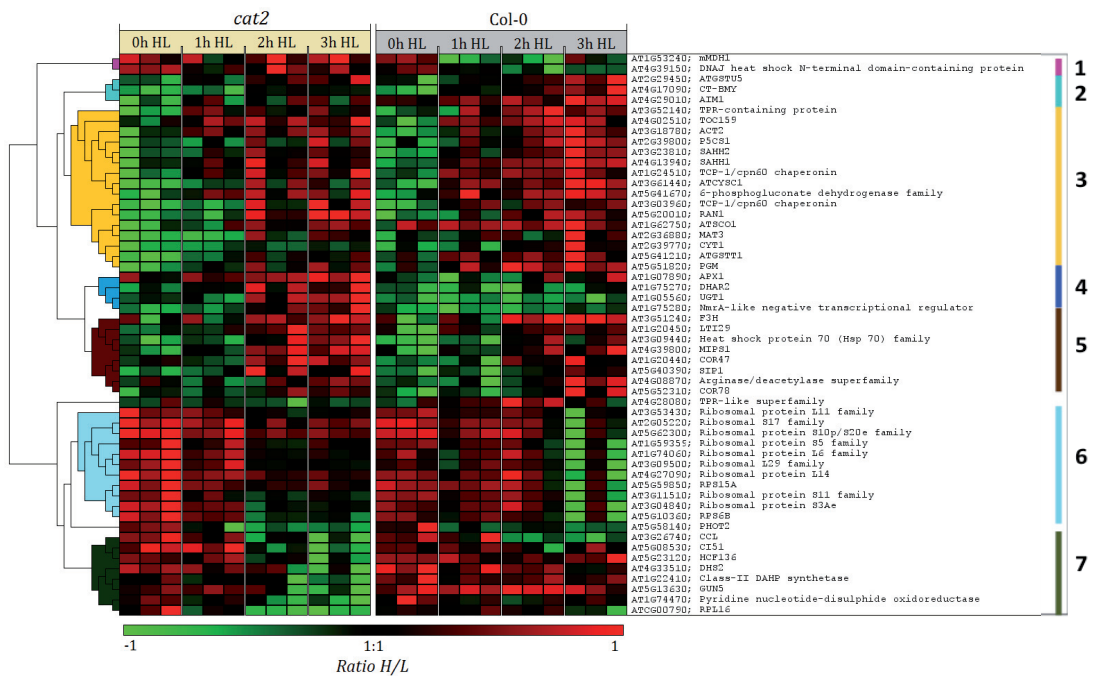


Figure 4. Heat map showing protein dynamics

912 proteins occurring in each biological repeat for all time points were plotted and analyzed via Perseus. Proteins with an abundance significantly changing over time were determined via SAM analysis and cluster analysis revealed similar patterning of protein abundances.

mRNA-seq and ribosome footprinting – a global overview

Here, we measured steady-state protein levels. These are a final outcome of the interplay between transcription, translation and protein degradation. Since proteins are the functional entities of a living cell, our initial focus was on the identification of (the dynamic aspects of) altered protein levels. However, both transcriptional and translational regulations shape the molecular landscape and impact overall protein levels. As measurements of steady-state protein levels might obscure biologically important changes of newly synthesized proteins [51, 52], in-depth studies of transcription and translation events were performed.

Ribosome profiling enables systematic monitoring of mRNA translation by deep sequencing of ribosome-protected mRNA fragments and thereby enables us to quantitatively assess translational regulation in response to oxidative stress [22]. Making use of the translation elongation inhibitor cycloheximide, ribosomes are halted on mRNA molecules they are actively translating [53]. Following nuclease digestion of ribosome unprotected mRNA, only ribosome-protected mRNA fragments are recovered upon density centrifugation. Next, these protected RNA fragments, or ribosome footprints, are converted into a cDNA library [16, 18, 54], which can be analyzed by deep sequencing alongside data from mRNA-sequencing (mRNA-seq). Combined, such datasets provide information on the actively translated mRNA sequences, the identity of the reading frames used and the ribosomal density at each position within these mRNAs. The latter provides a quantitative measurement of the (difference in) efficiency of translation.

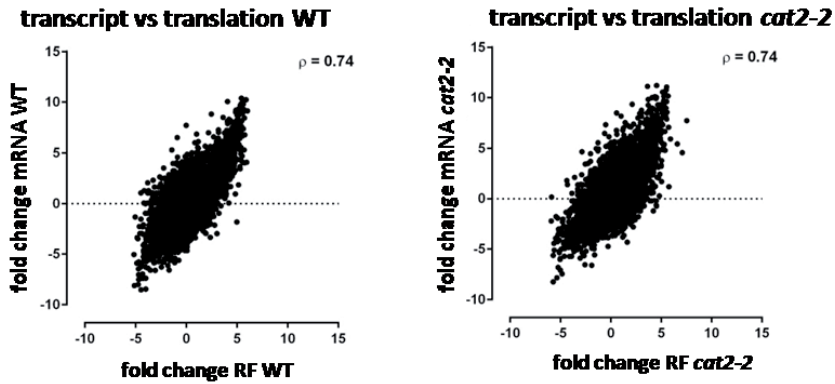
Using this approach, the transcriptomes and translomes of leaf material from wild-type and *cat2-2* plants, both under control conditions (high CO₂, moderate light) and exposed to high light and moderate CO₂ (3 h), were analyzed. The log₂ fold changes of the normalized read counts were calculated to assess transcription (mRNA), translation (ribosome footprint) and translational efficiency (ribosome footprint/mRNA). Of the 27,416 protein-coding genes annotated in TAIR (The *Arabidopsis* Information Resource), changes of 20,596 genes in wild-type and 20,536 genes in *cat2-2* plants could be detected, implying that at least 75% of all protein-coding genes are transcribed in both genotypes at both time points. Fold changes of ribosomal footprints in wild-type and *cat2-2* plants were obtained for 93% and 88% of the transcripts, respectively. A look at global translation shows 1,362 transcripts in wild-type plants and 990 transcripts in *cat2-2* plants with at least a 4-fold reduction in ribosomal occupancy after high light exposure. Similarly, 1,332 transcripts in wild-type plants and 1,653 transcripts in *cat2-2* plants have at least a 4-fold up-regulation of ribosomal footprints upon high light stress. The more pronounced translational down-regulation within wild-type plants correlates with our observed down-regulation of ribosomal proteins in wild-type plants which is delayed in *cat2-2* plants (**cluster 6, Figure 4**).

A quantitative view on regulation: correlation from transcript to protein

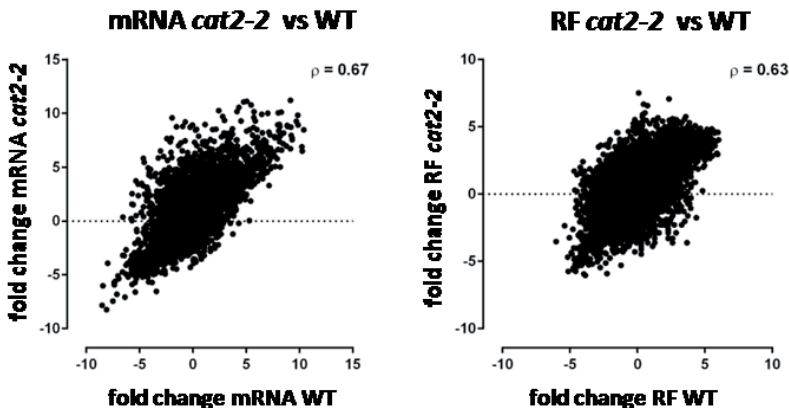
The correlation between the fold changes in transcript levels and ribosomal footprints was relatively high with a Pearson correlation coefficient (ρ) in both genotypes of 0.74 (**Figure 5A**). Further, both at a transcriptional and translational level, fold changes between control wild-type and *cat2-2* plants correlate considerably with a p -value of 0.63 for ribosomal footprints and 0.67 for mRNAs (**Figure 5B**), indicative of non-catalase deficiency dependent, next to catalase deficiency dependent changes in transcriptional and translational control. Translational efficiencies over time correspond well within one genotype, especially in wild-type plants ($\rho = 0.77$) (**Figure 5C**). Interestingly, this correlation is lost when comparing these translational efficiencies between genotypes after stress induction ($\rho = 0.23$, **Figure 5D**). Taken together, these data show that translational efficiency is strongly genotype-dependent and that catalase deficiency, leading to enhanced hydrogen peroxide accumulation, drastically alters transcript-specific efficiency of translation in conditions of oxidative stress. After 3 h of oxidative stress, a strongly decreased translational efficiency (≥ 8 -fold) is observed for 581 transcripts in *cat2-2* plants, while for 229 transcripts (**Figure 5D**), a substantial rise in translational efficiency is evident when compared to wild-type plants. A large group of the former transcripts encode for ethylene responsive transcription factors, calcium binding proteins and kinases, while cell-wall modifying coding genes are enriched in the latter group of transcripts (**Supplemental Table S1**). The inverse correlation between translational efficiency over time and transcriptional regulation of a gene during oxidative stress is intriguing and becomes apparent in both genotypes (**Figure 5E**).

To compare changes in transcription and translation with protein abundances, the quantified proteins in the setups before and after 3 h of stress treatment were considered. In this way, 1,012 proteins identified in all three biological replicates were sampled. In part due to our experimental setup (e.g. making use of a reference pool as intrinsic control), the dynamic range of protein abundance differences here found (using MS) is much lower than that of the transcripts and the ribosomal footprint coverage. For example, the steady state protein abundance levels after 3 h of HL stress vary less than 4-fold at most, while at the transcriptional level, up to a 1350-fold up-regulation could be measured. Further, a list of the top

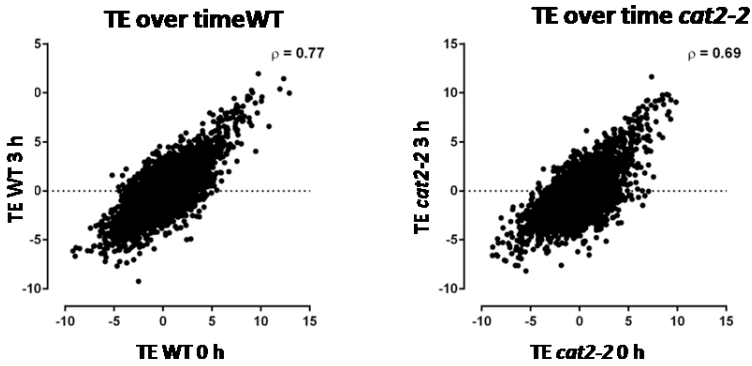
100 most up- and down-regulated genes at the level of transcription, illustrates the limited overlap with protein abundance alterations. Interestingly, the majority of proteins whose abundance lowers during stress treatment are not regulated at the level of transcription or translation (**Supplemental Table S2**). By plotting the fold changes of protein abundance to those of the ribosomal footprint reads in a particular genotype, proteins are revealed with a decreased abundance after 3h of oxidative stress, while their corresponding ribosome occupancy appears unaffected (**Figure 5F**). The same trend can be observed when plotting the protein abundance levels versus transcript levels, albeit at a lower correlation (**Supplemental Figure S3**). Taken together, these data indicate that the reduction in protein levels is regulated at the post-translational level and thus likely caused by protein degradation rather than by changes in transcription and/or translation rates.



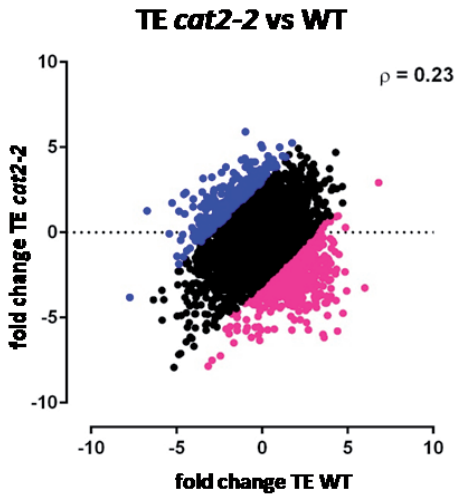
A. Transcript (mRNA FC) versus translation (ribosomal footprint FC) within one genotype



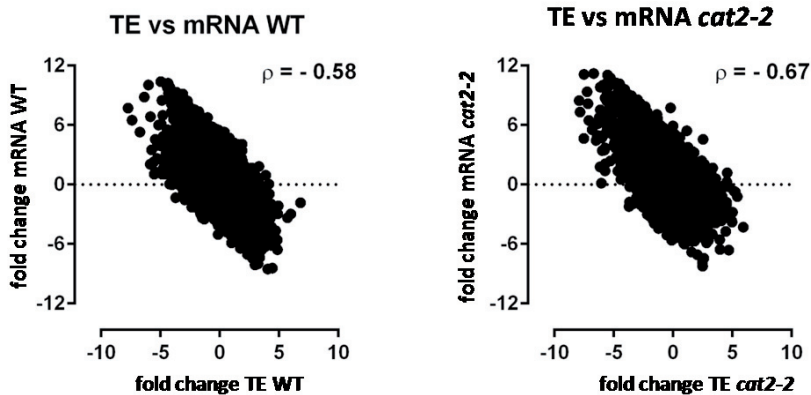
B. transcript (mRNA FC) and translation (ribosomal footprint FC) between genotypes



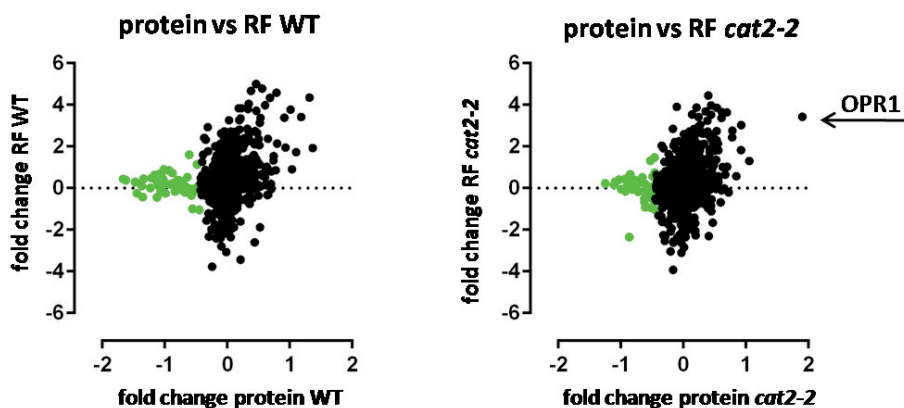
C. Translational efficiency (ribosomal footprint FC/mRNA FC) within one genotype



D. Translational efficiency (ribosomal footprint/mRNA) between genotypes over time (CAT vs WT)



E. Translational efficiency (ribosomal footprint FC/mRNA FC) versus transcriptional regulation (FC mRNA) within one genotype



F. Protein fold changes versus ribosomal footprint fold changes per genotype

Figure 5. Correlations from transcript to protein

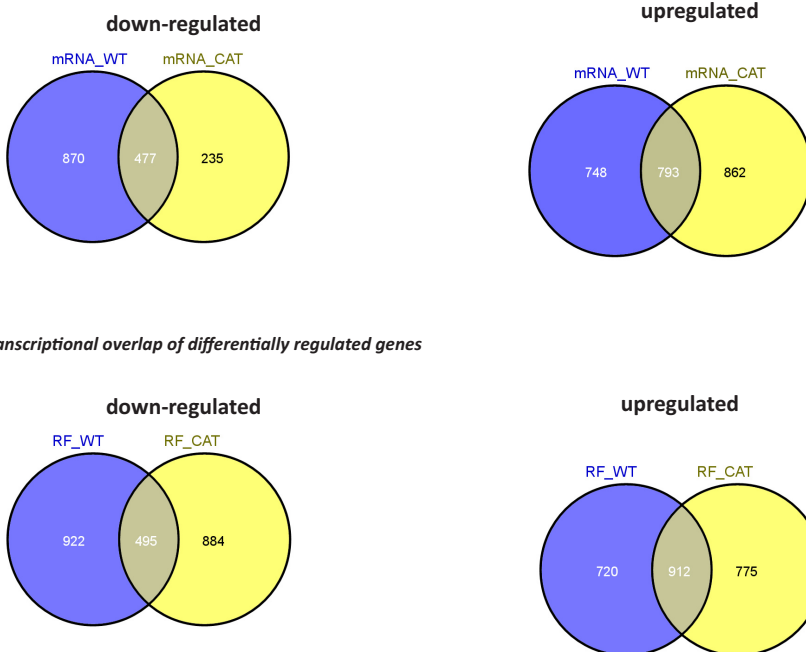
Comparison of normalized log₂ expression ratios after 3 h of high light exposure compared to 0 h (cpm) per protein-coding gene (A-F). Pearson correlation coefficients (ρ) are shown. (A) Normalized mRNA and ribosome footprint read density (cpm) are compared within one genotype. (B) Comparing reads between genotypes results in a reduced correlation of 0.67 for mRNA fold changes and 0.64 for ribosomal footprints. (C) Translational efficiency of individual transcripts in wild-type correlates well ($\rho = 0.77$) before and after oxidative stress, while in *cat2-2* translational efficiency is affected more during stress ($\rho = 0.69$). (D) Translational efficiency fold changes are drastically altered between *cat2-2* and wild-type plants. (E) In both genotypes, a negative correlation is observed when comparing the translational efficiencies and mRNA abundances over time. (F) Protein abundances are compared to the ribosome footprints per genotype. Proteins with a significant lower abundance (green) are hardly regulated at the translational level.

Genotype (in)dependent regulation during oxidative stress

Making use of Huber statistics, differentially regulated genes ($p < 0.05$) were selected and translational regulation was compared to regulation at the transcriptional level. At the level of transcription, 30% of all down-regulated and 33% of all up-regulated genes (each time at $p < 0.05$) overlap between the genotypes (Figure 6A). This overlap of differentially regulated genes represent a core of genes with similar behaviour in response to high light, irrespective of the genotypic background, hence named genotype independent, high light specific genes. There is however also a genotypic effect noticeable since in *cat2-2* plants, only 712 genes with significantly reduced transcript levels after 3 h were identified compared to 1347 in wild-type plants.

At the level of translation, a total of 495 transcripts in both wild-type and *cat2-2* plants showed reduced ribosomal occupancies after 3 h of high light exposure (Figure 6B), which corresponds to 22% of the total number of transcripts displaying a drop in ribosomal occupancy independent of catalase deficiency. In this group, Gene Ontology analysis using DAVID [55] revealed an overrepresentation of cell wall genes, such as expansins and xyloglucan endotransglycosylases, auxin responsive genes, membrane transporters and genes implicated in signalling such as receptor kinases and transcription factors (e.g. WRKY, bHLH, NAC) (Supplemental Table S3). When considering transcripts with increased ribosomal

occupancy, 912 of all transcripts (or 38%) with increased ribosomal occupancy were found in the wild-type and *cat2-2* setups (**Figure 6B**). This set was enriched for genes responsive to jasmonic acid (JA) and abscisic acid (ABA), and genes involved in their biosynthesis. Furthermore, genes responsive to water deprivation, high light intensity and oxidative stress (e.g., MYC2 and MYB75 transcription factors), and genes of the flavonoid and lignin biosynthetic pathways were also found in this subset. Interestingly, when considering translationally up-regulated genes found exclusively in *cat2-2* plants, a strong enrichment ($p < 1.4E-16$) of genes from the ubiquitin/proteasome proteolytic pathway was found, again providing a link to reduced protein levels via increased protein degradation. Also heat-shock protein encoding genes, next to glutathione-S-transferases and UDP-glycosyltransferases were enriched, the former possibly hinting towards a cellular prevention of misfolding and protein aggregation. Also, proteins implicated in transmembrane transport and regulators of transcription regulation represent two enriched gene classes in the *cat2-2* genotype (**Supplemental Table S3**).



A. Transcriptional overlap of differentially regulated genes

B. Translational overlap of differentially regulated genes

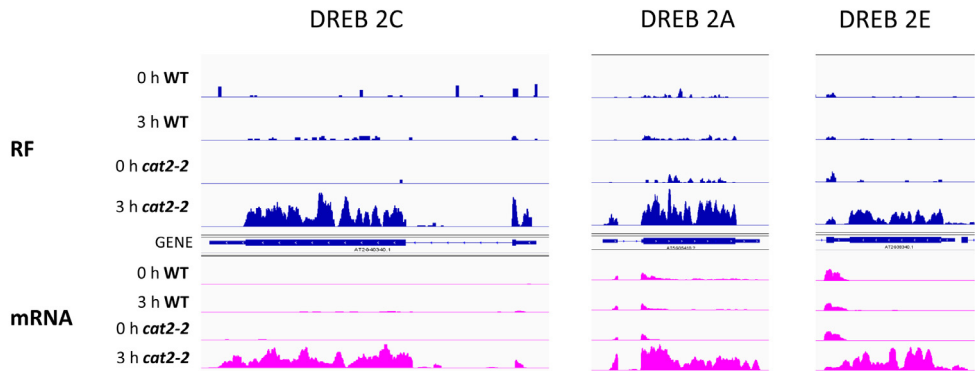
Figure 6. Differentially regulated genes

Significant ($p < 0.05$) transcriptional and translational regulated genes are compared between *cat2-2* and wild-type plants. (A) At the level of transcription, 477 or 30% of the down-regulated genes are shared between the genotypes (left), while this becomes 793 or 33% for all up-regulated genes (right). (B) Between both genotypes, an overlap of 495 transcripts (22%) shows a decline in ribosomal occupancy after 3 h of high light exposure (left). The overlap expands to 921 (or 38%) transcripts with increased ribosomal occupancy.

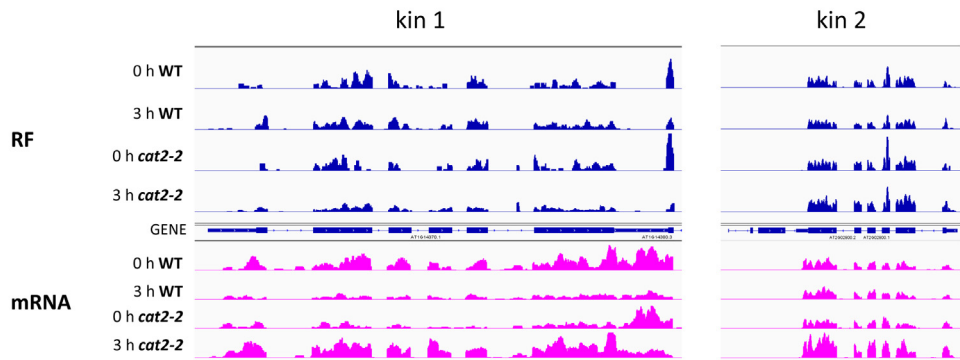
Next, transcriptional regulation was compared to translational regulation within each genotype. For both genotypes, over 56% of the transcripts with increased footprint counts were also up-regulated at the transcriptional level. While for those transcripts with decreased ribosomal occupancy, only 30% and 24% of the translationally controlled transcripts follow transcriptional down-regulation in wild-type and *cat2-2* plants, respectively (**Supplemental Figure S4**).

Regulation of the regulators: a focus on transcription factors

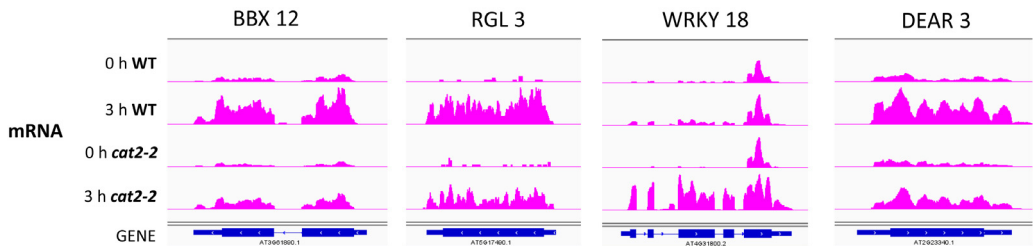
In our transcriptomics and translomics datasets, multiple transcription factors were found highly responsive to high light exposure. In fact, the transcript with the highest fold increase in ribosomal footprints in *cat2-2* plants after stress treatment encodes for a member of the transcription factor ERF/AP2 family. In wild-type plants, the corresponding gene, the dehydration-responsive element binding 2C (DREB2C; AT2G40340) shows only a minor increase at the transcript level and no up-regulation of ribosomal occupancy. DREB2A (AT5G05410) and DREB2E (AT2G38340), two transcription factors belonging to the same subfamily show a similar pattern of transcriptional up-regulation and increased translation in *cat2-2* plants (**Figure 7A**). Interestingly, these DREB2 transcription factors are highly conserved in economically important cereal crops and were previously shown to regulate, mostly in an ABA-independent manner, the expression of many stress-responsive genes upon drought, salinity and high temperature [56]. Moreover and likely due to the presence of a core DRE motif in their promoters, the transcript levels of two downstream signalling kinases, kin 1 and 2 [57], are both up-regulated in *cat2-2* upon high light exposure (**Figure 7B**). In addition, the downstream cold-regulated genes (COR) also contain cis-acting elements, with ICE1 formerly depicted as the master regulator for multiple downstream transcription factors that in turn regulate these COR genes [58]. Although ICE1 is not regulated under these stress conditions, transcription of its downstream transcription factors such as homeobox12 (AT3G61890), RGA-like3 (AT5G17490), WRKY18 (AT4G31800) and DEAR3 (AT2G23340) is clearly increased (**Figure 7C**). Such data reveal a complex interplay of transcription factors that are subject to transcriptional and translational regulation in relation to a genetic (catalase deficiency) and environmental (high light) perturbation. An additional level of complexity is added by the recognition mechanisms of transcription factors, e.g. DREB2 on promoter cis-elements of other transcription factors. Further downstream, three COR proteins were identified of which the protein levels increased significantly during high light stress treatment in both wild-type and *cat2-2* plants (**Figure 4, cluster 5**). This increase in protein abundance was here found to correlate with an up-regulation at both the transcriptional as well as the translational level (**Figure 7D**).



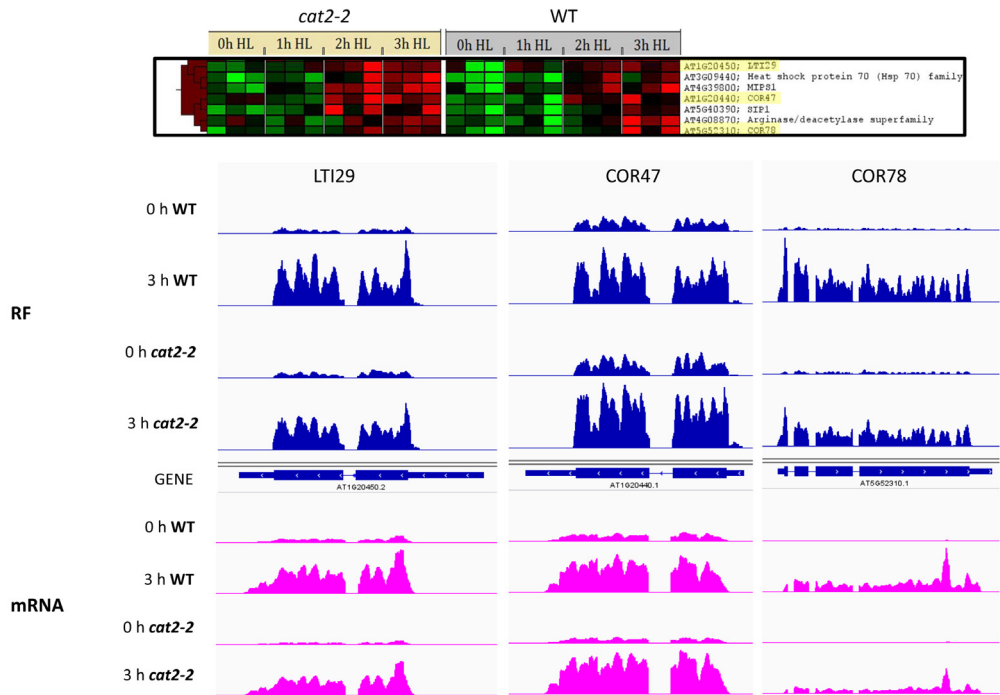
A. DREB TF regulation



B. Kinase regulation



C. Transcriptional regulation of TF



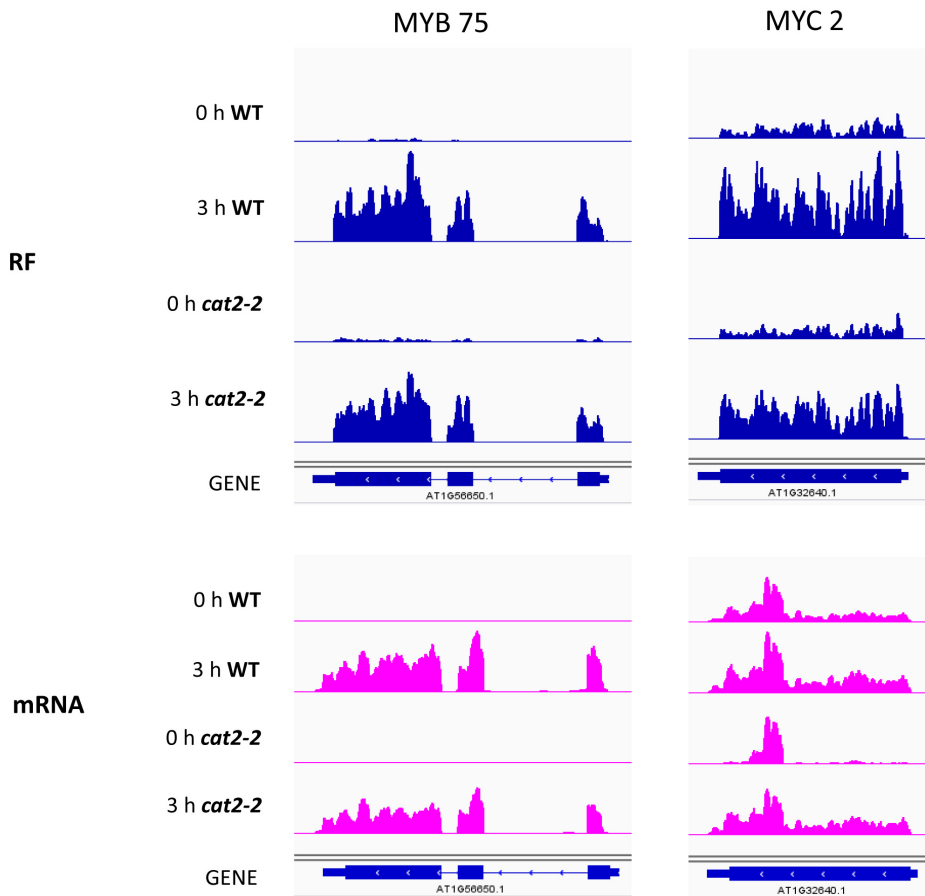
D. COR regulation

Figure 7. DREB transcription factor family

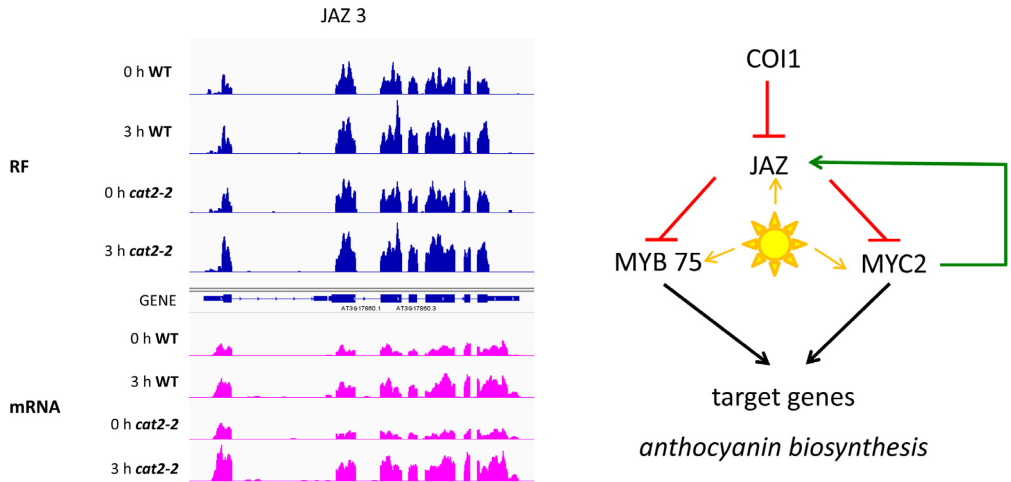
Coverage of ribosomal footprints (blue) and total mRNA reads (pink) on selected genes before and after 3 h of high light exposure. (A) The dehydration-responsive element binding 2 genes (DREB) show a strong transcriptional and translational up-regulation after 3 h in *cat2-2* plants but not in wild-type plants. (B) Two kinases, kin 1 and kin 2 are downstream targets of DREB2C and show an mRNA increase at 3 h in *cat2-2* plants. (C) Transcriptional regulation of transcription factors involved in cold stress acclimation. (D) Three cold regulated proteins were identified of which the abundance increased in both genotypes during high light stress treatment (upper panel). This correlates well with the transcriptional and translational up-regulation that was observed for these three genes (lower panel).

The bHLH TF MYC2 and MYB TF production of anthocyanin 1 (PAP1, also known as MYB75) were here identified in both genotypes and for both there is a clear increase in translational output after stress treatment. This is in agreement with their transcriptional up-regulation, albeit more pronounced for MYB75 (Figure 8). PAP1 was shown to regulate anthocyanin production and MYC2 is considered as the master regulator of JA signalling pathways that also steers anthocyanin biosynthesis [59]. Upon closer inspection, the genes encoding JAZ-family members (JASMONATE-ZIM-DOMAIN) show a clear up-regulation both at the transcription and at the translation level, with the exception of JAZ3 (Figure 8B); more JAZ3 transcripts are present following high light treatment, but translation does not appear to be enhanced. JAZ proteins can interact with MYC2 and MYB75 transcription factors, preventing the activation of their downstream target genes. Perception of JA by its receptor COI1

(coronatine insensitive 1; AT2G39940) triggers proteasome mediated ubiquitination and degradation of JAZ proteins, thereby releasing MYC2 and MYB75 from repression and allowing the activation of JA-responsive genes [60]. MYC2 also binds to the promoters of JAZ genes and regulates their overall expression levels, leading to a negative feedback loop, enabling tight control of JA-responsive gene expression [61] (**Figure 8C**). Further, the jasmonate receptor COI1 is not regulated after stress, which points to the importance of an active degradation of the JAZ proteins upon COI1-mediated JA perception.



A. MYC2 and MYB75 are both induced in translation and transcription after HL stress



B. JAZ3 is only transcriptionally induced

C. Schematic overview of JAZ regulation

Figure 8. MYB75 and MYC2 transcription factors are regulated during oxidative stress

(A) Both MYB75 and MYC2 transcripts have an increase in ribosomal occupancy (blue) after stress treatment, in accordance with their increased mRNA reads (pink), although the latter is more pronounced for the MYB75 encoding gene. (B) Except for JAZ3, for which only a transcriptional up-regulation (pink) can be observed, the JAZ repressors are up-regulated at the transcriptional and translational level. (C) A schematic overview of jasmonate triggered responses upon high light exposure. In the absence of JA, JAZ proteins bind TFs like MYC2 and MYB75, thereby inhibiting their transcriptional activity. MYC2 regulates also JAZ expression levels, leading to a negative feedback loop. High light results in an up-regulation of MYC2 and MYB75, but also of JAZ transcripts, hereby enabling a strict regulation.

A role for increased protein degradation during oxidative stress

Protein abundances are the final outcome of coordinated transcriptional, translational and post-translational control mechanisms. The relative importance of these control relays is examined here. In general, **Figure 5F** points to two factors that we need to take into account: the limited dynamic range when measuring steady-state protein abundance levels and post-translational activities. This limited dynamic range is in fact also partly due to our experimental set-up as we made use of a reference pool design. Indeed, if a protein is present in wild-type but absent in *cat2-2* samples, a maximum two-fold range will be observed, as is exemplified for the CAT2 protein (**Figure 9**).

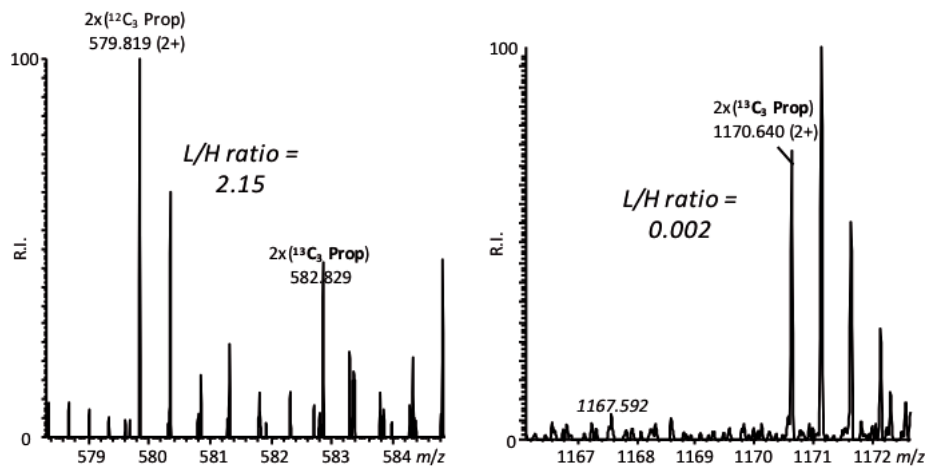


Figure 9. CATALASE2 spectrum illustrates a limited dynamic range of protein abundance measurements

The mass spectra of CAT2 before the onset of high light exposure. The wild-type sample contains 2.15 fold more CAT2 compared to the reference pool (left panel) whereas in the *cat2-2* sample, the CAT2 peptide represents a singleton, only present in the reference pool (right panel).

Ribosomal proteins constitute a large fraction of proteins that are down-regulated after 3 h of stress treatment in both wild-type and *cat2-2* plants, albeit with a delay in the latter (**Figure 4, cluster 6**). For these ribosomal proteins, no regulation occurred at the levels of transcription or translation (**Figure 10**), illustrating that active degradation, rather than transcriptional or translational down-regulation provides a rapid means of influencing the cellular protein balance. By enhanced, yet specific ribosomal catabolism, the whole cell might be quickly redirected towards a defensive system rather than one focused on growth. While indeed several 26S proteasome AAA-ATPase and non-ATPase subunits are up-regulated (**Figure 11A**), especially in *cat2-2* plants, it is also interesting to note the down-regulation of protease inhibitors (**Figure 11B**), all of which may contribute to enhanced proteolytic capacity. Two of the 26S proteasome subunits, RPT1 and RPT2A were also identified in our proteome study as being regulated. Transcription of the RPT1 and RPT2A genes was up-regulated respectively 2.5 and 3 times in wild-type plants, and in *cat2-2* plants, this was about 8-fold. Translational induction followed transcriptional regulation, which, in the end resulted in a 1.7-fold induction of the steady-state levels of the RPT1 protein and 1.9-fold for the RPT2 in both genotypes after 3 h of high light exposure.

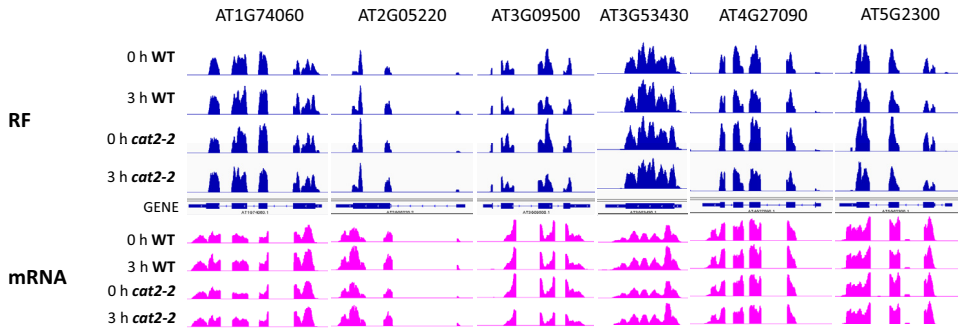
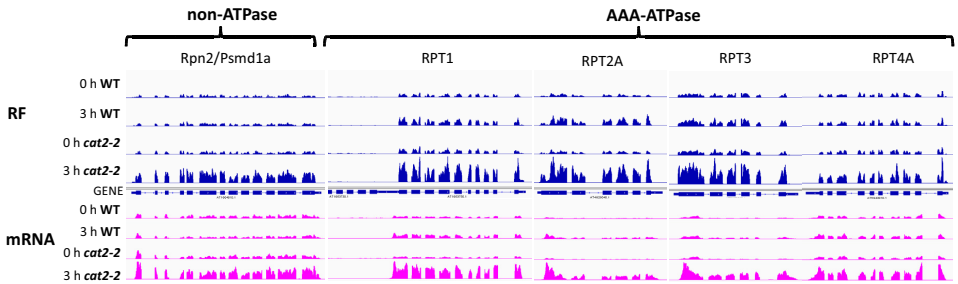
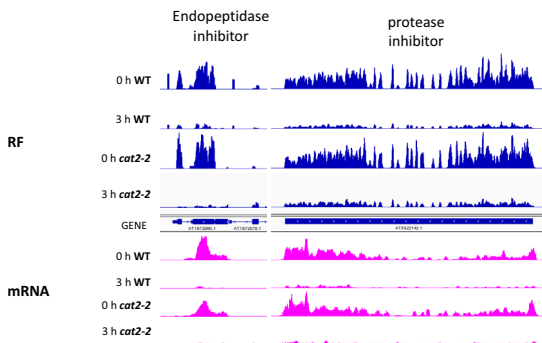


Figure 10. Ribosomal proteins are not subjected to transcriptional or translational control

Many ribosomal genes, including the 6 genes shown here, do not show any change in mRNA (pink) or ribosomal footprint reads (blue), although their protein levels were significantly less abundant during stress treatment.



A. 26S proteasomal subunits



B. Protease inhibitors

Figure 11. Degradation is enhanced in *cat2-2* plants

(A) mRNA (pink) and ribosome footprint reads (blue) of a non-ATPase and four AAA-ATPase subunits of the 26S proteasome complex show an up-regulation in *cat2-2* plants of transcripts and ribosomal occupancies. (B) Two examples of protease inhibitor coding genes (AT1G72060 and AT3G22142) whose transcription (pink) and translation (blue) are down-regulated in both genotypes during high light stress treatment.

Filling the gaps: pathways from transcript to protein

Integration of mRNA, ribosomal footprints and protein abundances allows an in-depth understanding of a system-level response to stress where entire pathways can be examined. By incorporating the regulation on three levels, namely transcription, translation and (dynamic changes) in steady-state protein levels, new insights are gained and as a consequence, strategies to target pathways and redirect a system can be refined.

As *cat2-2* and WT plants react differently upon prolonged exposure to high light intensities, i.e. cell death and purple coloring of leaves, respectively, we first focused on anthocyanin production. Note that transcripts with a significantly increased ribosomal occupancy after 3 h of stress that were commonly identified in both genotypes, are enriched for genes of the flavonoid and lignin biosynthetic pathways. This implies that *cat2-2* plants also produce enzymes implicated in flavonoid biosynthesis after 3 h of oxidative stress. An overview of flavonoid biosynthesis is given with each panel representing a different level; either fold changes of mRNA reads, ribosomal footprint reads or protein abundances after 3 h of high light exposure compared to 0 h (**Figure 12**).

WT

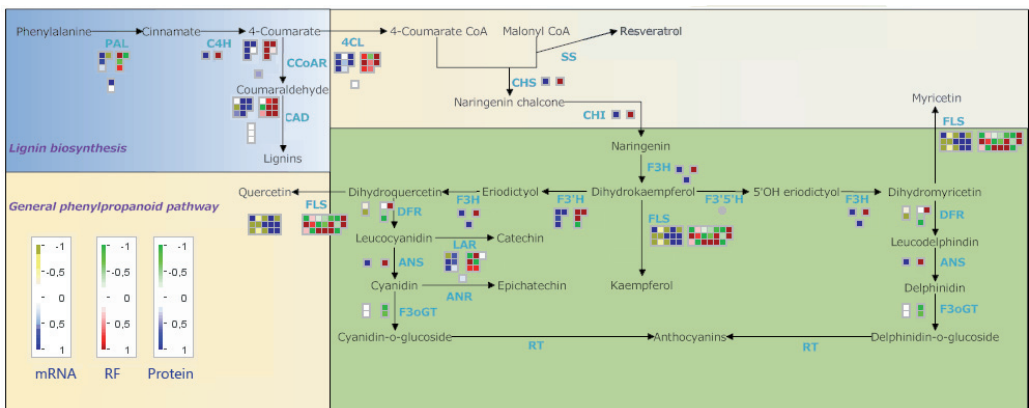
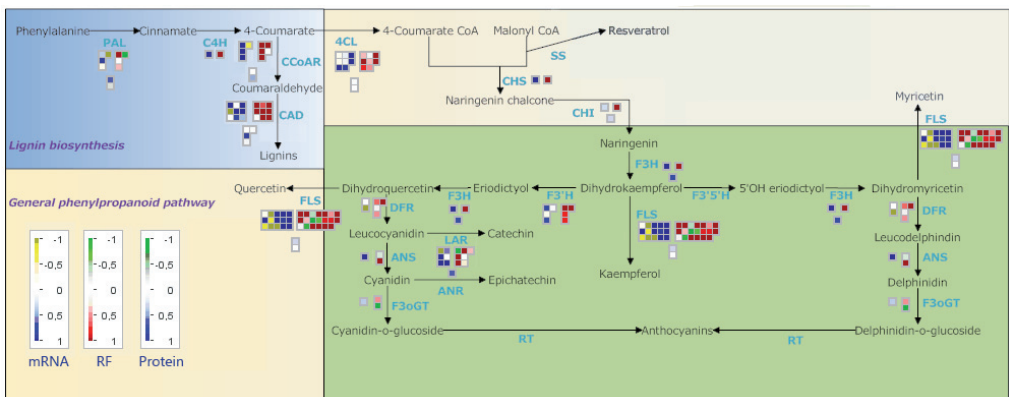
*cat2-2*

Figure 12. Flavonoid biosynthesis pathway: from transcript to protein

Schematic overview of the flavonoid biosynthesis steps showing normalized log₂ fold changes (3 h compared to 0 h) of the identified genes or proteins (squares). Transcript levels with the fold changes of mRNA reads are depicted in a yellow-blue scale, green-red scaling is used to represent translational regulation via the ribosomal footprint reads. Abundances of identified proteins are shown below (green-blue). *F₃H* protein abundances are higher in wild-type plants while this is the case for CAD5 in *cat2-2* plants. In wild-type plants, a stronger increase in transcripts of *F₃H*, *F₃'H* and *CHI* was already observed.

As such, genotypic differences and differential regulation within one genotype can be easily tracked and compared. In wild-type leaves, a stronger transcriptional up-regulation of flavonoid biosynthesis genes, such as chalcone isomerase (CHI), flavanone-3-hydroxylase (F_3H) and flavonoid 3'-monooxygenase ($F_3'H$) is apparent (dark blue), whereas in *cat2-2* the cinnamoyl-CoA reductase (CAD) genes have a higher ribosomal occupancy (dark red). This leads to a higher protein abundance of F_3H in wild-type plants and CAD5 in *cat2-2* plants possibly driving wild-type plants into flavonoid production while *cat2-2* might be steered more to lignin biosynthesis (Figure 12).

The details of the lignin pathway revealed minor, yet important differences between both genotypes. A stronger transcriptional up-regulation of some CAD genes in *cat2-2* plants, i.e. CAD5 and CAD8, also resulted in a higher CAD5 abundance after 3 h of high light stress (Figure 13). Metabolite profiling of both genotypes, exposed to identical stress conditions, showed a significant difference of 5-hydroxyferulic between wild-type and *cat2-2* plants after 2 h of high light exposure (Supplemental Figure S5). The higher levels of this lignin intermediate in *cat2-2* could be a reason why we observe higher CAD expression to detoxify such accumulated intermediates that become toxic for the cell. Hence, minor differences in regulation can have a significant impact on the final outcome.

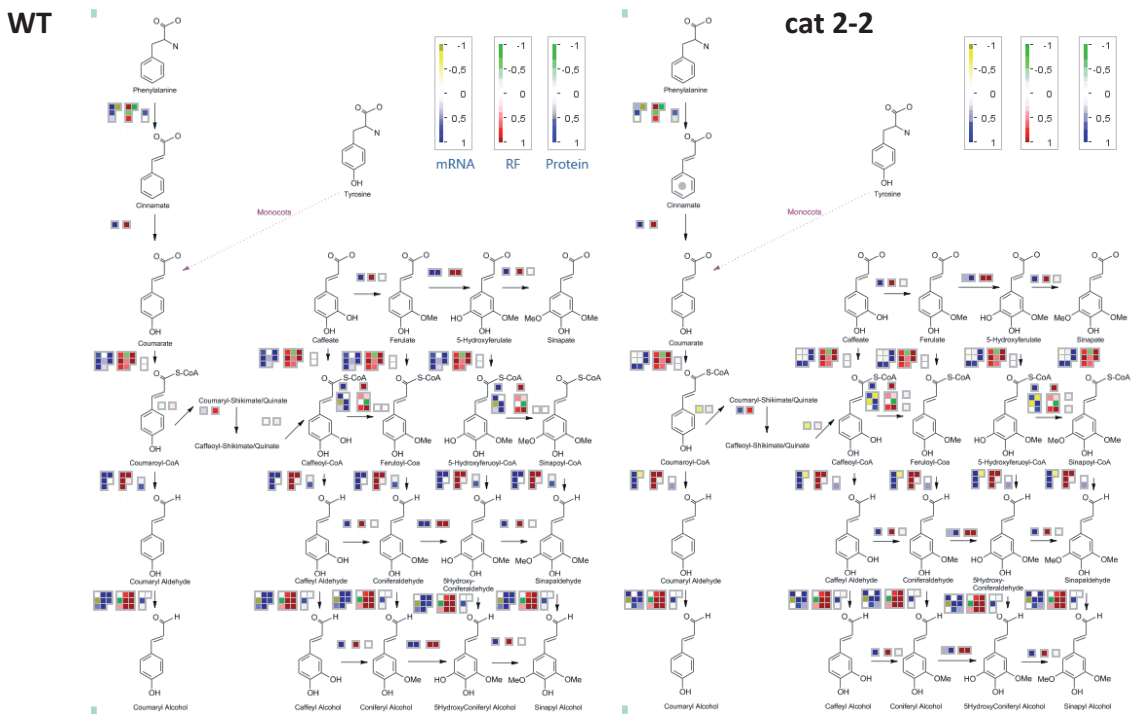


Figure 13. Lignin biosynthesis pathway

Lignin biosynthesis compared at transcription (left boxes; yellow-blue scaling), translation (middle boxes; green-red scaling) and protein level (right boxes; green-red scaling). Every square represents an identified gene or protein and is colored according to its normalized log₂ fold change (3 h compared to 0 h). A stronger transcriptional up-regulation CAD5 and CAD8 in *cat2-2* plants, also resulted in a higher CAD5 abundance after 3 h of high light stress.

JA biosynthesis is an example where translational regulation exerts control over protein abundances (**Figure 14**). The reduction of 12-oxo-phytodienoic acid (OPDA) occurs in the peroxisomes providing a possible link to the photorespiratory burst of hydrogen peroxide. This reaction is catalyzed by OPDA reductases (OPRs) whose transcripts show a steep decrease in ribosomal occupancy in wild-type plants, resulting in largely unchanged steady-state protein levels upon oxidative stress exposure at the time point analysed, a finding in contrast with raised abundance levels in *cat2-2* plants. The OPR1 gene (AT1G76680) can also clearly be distinguished in the correlation plots of protein abundances and ribosomal footprint reads (**Figure 5F**) or mRNA reads (**Supplemental Fig. S3**) as indicated.

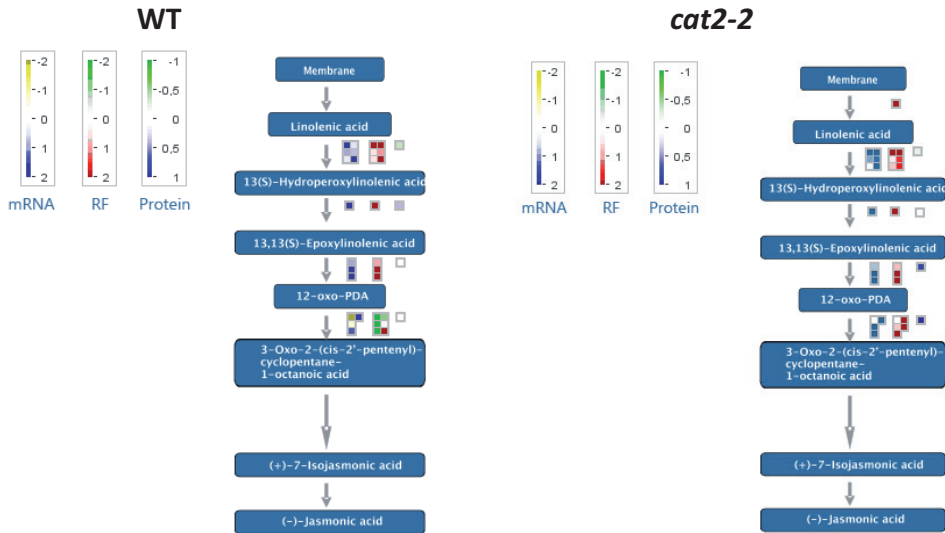


Figure 14. Jasmonate biosynthesis affected by translational control

Overview of the jasmonate biosynthesis pathway where the OPDA reductases (OPR) show a severe decrease in ribosomal occupancy of their transcripts in wild-type plants (green middle boxes). This results in unchanged protein abundances after oxidative stress, while in *cat2-2* plants increased abundance levels are apparent (blue right boxes).

Considering our high light set-up to induce oxidative stress, together with the use of catalase knock-out plants, a global look at both photosynthesis and photorespiration was performed (**Figure 15**). Transcription is firmly down-regulated in *cat2-2* plants, especially for genes involved in the light reactions of the chloroplast. Translation however, seems to be in concordance with the translational regulation in wild-type plants with the exception of rubisco and glycolate oxidase (GO). Not only are these genes in *cat2-2* plants less transcribed, their transcripts are also less translated during oxidative stress. This might be a strategy to circumvent an additional accumulation of hydrogen peroxide, since the oxidation of glycolate to glyoxylate by GO represents the hydrogen peroxide producing step. The translational up-regulation of the concomitant enzymes to metabolize glyoxylate results in increased glyoxylate transaminase protein levels for both genotypes and could steer this carbon source back to the Calvin-cycle (**Figure 15**).

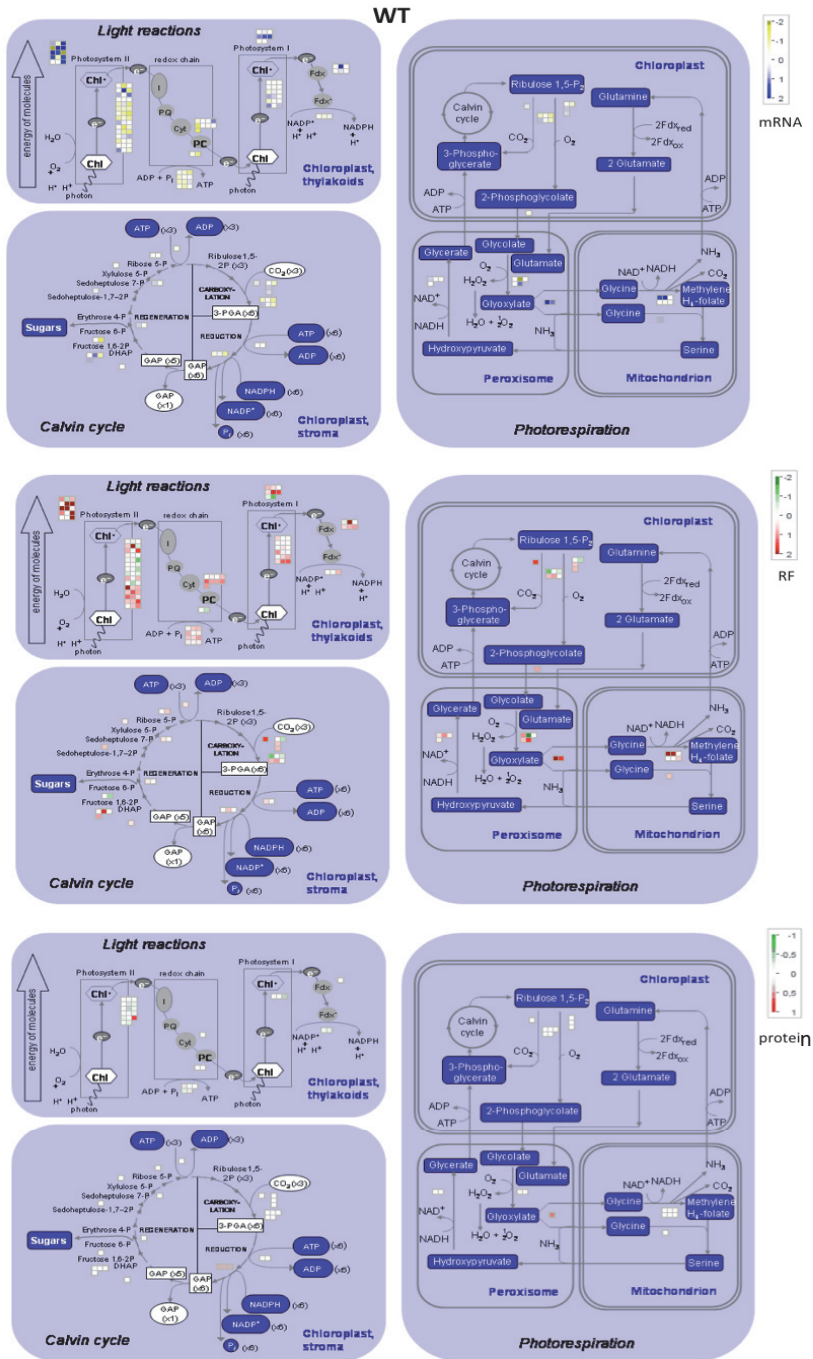
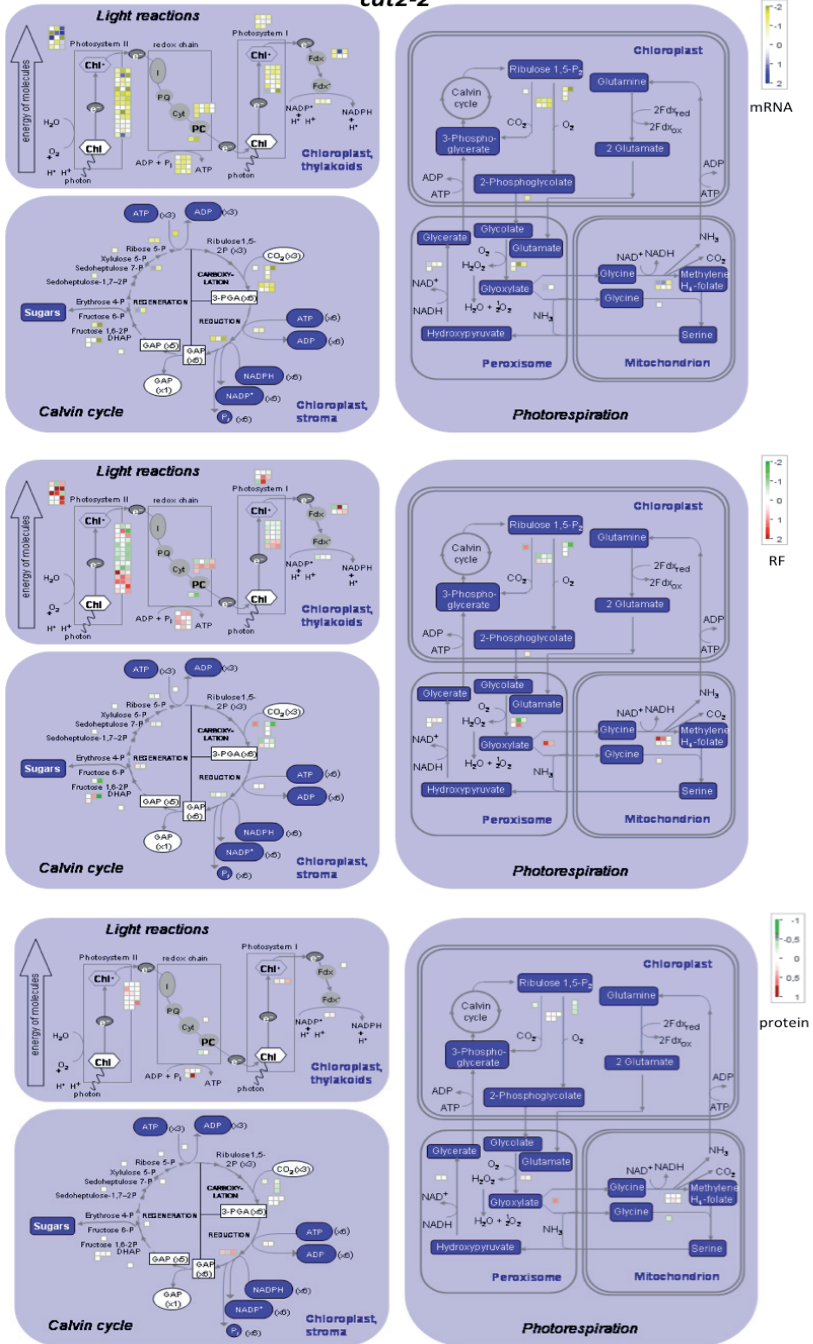


Figure 15. Overview of photosynthesis, photorespiration and Calvin cycle

Normalized \log_2 fold changes (3 h compared to 0 h) of mRNA, ribosome footprint reads and protein abundance levels are shown. Transcription (upper panel) is largely affected, especially in *cat2-2* plants with a strong down-regulation of transcripts involved in the light reactions of the chloroplast (yellow squares). Both genotypes have higher glyoxylate transaminase protein abundances (lower panel). This is in accordance with the translational up-regulation (middle panel) of the concomitant enzymes to metabolize glyoxylate.

cat2-2



These results emphasize the benefits of combining multiple techniques that study different levels of regulation. This way, the most comprehensive overview of ongoing cellular processes can be obtained where both major and minor changes can be detected.

DISCUSSION

We have performed a systems-level study to analyze the consequences of ROS-provoked proteome changes in leaf tissue, measured via a quantitative LC-MS/MS approach. A combination of a genetic perturbation, catalase 2 knock-out plants (*cat2-2*), and an environmental perturbation, high light, enabled us to dissect protein dynamics in response to perturbed hydrogen peroxide homeostasis. Molecular phenotyping of *cat2-2* plants revealed CAT2 as the only significant different protein compared to wild-type plants before the onset of stress treatment. Together with the occurring cell death lesions in *cat2-2* plants upon longer exposure to high light, compared to the accumulated anthocyanin levels in wild-type plants, these findings ascertain *cat2-2* plants as a valuable model system to study the effects of enhanced hydrogen peroxide production.

To analyze our large proteome datasets, we made use of the MaxQuant software package [28], which allows to match data between runs and thereby increases the number of identifications across replicate experiments. Overall, our workflow resulted in a total of 3,327 identified proteins from which 912 proteins had abundance values in all samples. The identification of 54 proteins whose levels changed significantly over time (**Figure 4**), revealed known and new players of the ROS signaling network. Although proteome studies of the oxidative stress response in plants have been reported previously [62-64], the consequences of non-invasive accumulated hydrogen peroxide levels on the proteome is here described for the first time. Moreover, with our gel-free proteome profiling strategy, we also explored the dynamics of these ROS-responsive proteins.

In a next phase, our proteome data were combined with mRNA-seq and ribosome footprinting data, allowing us to assess the importance of transcriptional and post-transcriptional regulation of the plant's response to elevated hydrogen peroxide levels. Only two reports of ribosome profiling in plants preceded this study [23, 24] and announced a new era of in-depth analysis of translational regulation. However, the combination with protein abundance measurements is novel and provided us with a more holistic view of the dynamic interplay between transcription, translation and protein abundance. Comparing steady-state protein levels with ribosomal occupancy of transcripts revealed a prominent role for degradation; proteins with a significant lowered abundance after high light stress show no regulation at the level of transcription nor translation (**Figure 5F**). In addition, levels of 26S proteasome complex components raised during stress treatment, in accordance with the higher translational output of the corresponding transcripts. Although there might be a possible delay to perceive differences at the protein level, also the limited dynamic range when measuring steady-state protein levels needs to be taken into account. We conclude that protein degradation more drastically impacts protein levels, likely resulting into a swift and coordinated manner to respond to stress.

The regulation of the core set of proteins with differential protein levels during stress is summarized in **Figure 16**. Except for the ribosomal protein cluster, the steady-state protein levels are by-and-large in accordance to transcriptional and translational regulation. Although, as deduced from MS intensities,

the fold changes at protein levels are less pronounced. This limit in dynamic range might be reflected because steady-state levels are measured, where small differences in ratios, e.g. a fold change of 1.2, might have a large impact, since there is 20% more of this protein present. The ribosomal proteins that are significantly lowered in abundance in the presence of increased transcripts and footprint reads once again highlights a role for active degradation (**Figure 16, yellow box**). Simultaneously, this points towards another strategy of a cellular system to cope with stress that has long been speculated, namely a general translational shutdown to avoid protein misfolding upon stress [8, 47]. Another cluster shows a strong decrease in ribosomal occupancy in the absence of mRNA decrease, underlining the importance of translational control (**Figure 16, blue box**). Taken together, this emphasizes the strength of combining multiple approaches, each tackling a different regulatory step of protein synthesis.

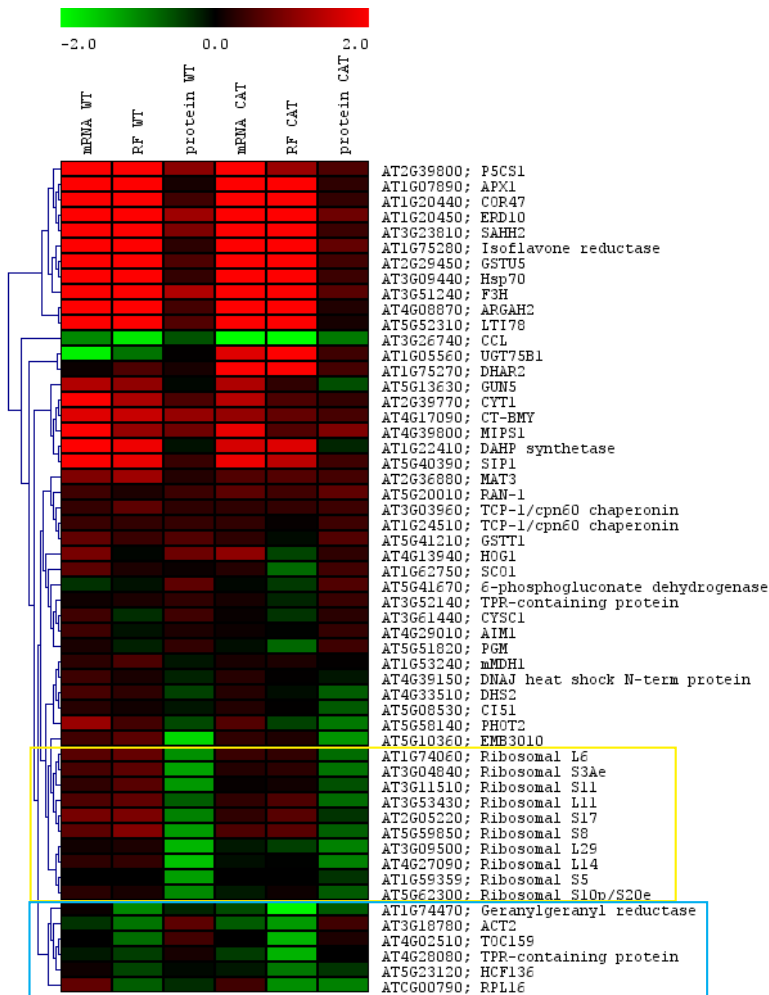


Figure 16. Core of differential proteins compared to transcript levels and ribosomal footprint reads

Comparison of the 54 proteins with changing protein abundance during high light stress treatment. A heatmap of the normalized log₂ fold changes (3 h compared to 0 h) of mRNA, ribosome footprint reads and protein levels is shown. Protein levels have a limited dynamic range but generally follow transcriptional and translational regulation. Ribosomal proteins are degraded (yellow box) while genes in the blue box are down-regulated at the level of translation (decreased ribosomal occupancy) after stress treatment.

The translational efficiencies of various transcripts are strongly genotype dependent (**Figure 7D**), likely reflecting the impact of enhanced hydrogen peroxide concentrations. Hypoxia is another factor previously reported to alter translational efficiency of selective mRNAs [23]. Intriguingly, there is an inverse correlation between translational efficiency and transcript abundance during stress. This might reflect the overall increased inhibition of translation as compared to transcription. As cells will try to cope with this by making more transcripts of specific genes to assure their translation. As a consequence, genes with few transcripts will have a higher translational output, compared to highly up-regulated genes. Since translational regulation only partially follows transcriptional regulation, it is recommended to consider and combine both levels. Further integration of the ribosome footprinting strategy with proteome approaches will become increasingly important to analyze the consequences of ROS-provoked changes. We here examined how plant cells globally cope with oxidative stress by exploring such an integrative in-depth and system-level analyses, thereby creating a multi-angle view on the ROS-network.

EXPERIMENTAL PROCEDURES

Plant material, growth conditions, stress treatments

Catalase knock-out (*cat2-2*) and wild-type (WT) *Arabidopsis thaliana* plants, ecotype Columbia-0 (Col-0), were grown under elevated CO₂ concentrations (3,000 ppm) to impair photorespiration. Individual plants were organized according to a completely randomized block design in a controlled climate chamber (Vötsch Industrietechnik) in a 12:12 day/night regime (relative humidity of 50%, 21°C and an irradiance of 100 μmol m⁻² s⁻¹). For high light treatments, 5 weeks old plants were transferred to a Sanyo Fitotron plant growth chamber in ambient air conditions (400 ppm CO₂, relative humidity of 55%, 21°C) and continuous HL irradiation of 1,200 μmol m⁻² s⁻¹ for one, two or three hours. Middle aged leaves of 15 individual plants per line were sampled, pooled and frozen in liquid nitrogen. This entire set-up was repeated twice to obtain three biological repeats of each time-point analysed per genotype.

Labeling and shotgun proteome set-up

Proteins were extracted from 1 g of grinded tissue by adding 1 ml of 250 mM Tris-HCl buffer (pH 7.4) containing 150 mM NaCl, 2 mM EDTA, 1% 3-[(3-cholamidopropyl)dimethylammonio]-1-propanesulfonate (CHAPS) and the appropriate amount of the Complete Protease Inhibitor cocktail (Roche, Applied Science). After centrifugation at 16,100 x g for 10 min twice, protein concentrations were measured using the Bradford assay. Samples were subsequently desalted on a NAPTM-10 column (Amersham Biosciences) in 1.5 ml of 50 mM triethylammonium bicarbonate (TEAB) buffer (pH 8). After measuring concentrations again using the Bradford assay, the appropriate volumes of TEAB buffer was added to obtain 700 μg per sample in an equal volume of buffer (736 μl). A reference pool was created by combining an additional 700 μg of protein from the eight samples; wild-type and *cat2-2*, each sampled at four time points. Prior to digestion, samples were heated for 10 min at 95°C and cooled on ice. Sequencing-grade endoproteinase Lys-C (Promega) was added in a ratio of 1:370 (enzyme:substrate, w:w) and incubated overnight at 37°C. Next, primary α- and ε-amines were labeled using N-hydroxysuccinimide esters of stable isotopic variants of propionate. Peptides originating from the reference pool were ¹³C₃-propionated, whereas the individual samples were labelled with ¹²C₃-propionate by repeating twice the incubation for 45 min at 30°C to a

final concentration of 10 mM NHS-label. Excess of reagent was removed by quenching the remaining N-hydroxysuccinimide esters with 40 mM of glycine for 15 min at 25°C. A subsequent incubation for 15 min at 25°C with a final concentration of 80 mM hydroxylamine reversed partial O-propionylation of serine, threonine and tyrosine. Samples were acidified to a pH of 3 with acetic acid and after a short spin, the supernatant of each sample was mixed with an equal amount of supernatant from the reference pool. For quantification purposes, a 1:1 ratio is highly desired, and this was checked by an MS-analysis on the mixed sample on the LTQ Orbitrap XL (Fisher Scientific) and if necessary, corrections were made. The mixed samples were separated via reversed phase - high performance liquid chromatography (RP-HPLC) onto a 2.1 mm internal diameter × 150 mm 300SB-C18 column (Zorbax®, Agilent) with an Agilent 1100 Series HPLC system. Via the injector program, oxidation of methionines was performed with 0.3% (w/v) H₂O₂ during 30 min at 30°C. Following a 10 min wash with HPLC solvent A (10 mM ammonium acetate in water/acetonitrile, 98/2 (v/v), water (LC-MS grade, Biosolve), and acetonitrile (HPLC grade, Baker)), a linear gradient to 100% solvent B (10 mM ammonium acetate in water/acetonitrile, 30/70 (v/v)) was applied over 100 min. Using Agilent's electronic flow controller, a constant flow of 80 µl/min was used. Peptides eluting between 20 and 80 min were collected in a 96-well plate in slices of 1 min, resulting in 60 fractions per mixed sample (i.e., sampled tissue/reference pool). Fractions separated by 20 min were pooled and vacuum dried. This resulted in a final of 20 pooled fractions per mixed sample that adds up to a total of 160 pooled fractions per biological repeat (WT and *cat2-2*, each with 4 time points). Each fraction was dissolved in 50 µl 2mM tris(2-carboxyethyl)phosphine (TCEP) in 2% acetonitrile, to reduce disulphide bridges prior to LC-MS/MS analysis.

LC-MS/MS analysis

The obtained peptide mixtures were loaded onto an Ultimate 3000 nano-HPLC system (Dionex) in-line connected to a LTQ Orbitrap XL (Thermo Fisher Scientific) as described (Jacques et al., submitted).

We made use of the Andromeda search engine coupled to MaxQuant. All data were searched against the TAIR10 database (containing 27,416 protein-coding genes). The searches are identical as described before (Jacques et al., submitted; see chapter 5), including the parameter options. The main addition in MaxQuant is the possibility to match data between runs, which we applied.

Data analysis shotgun proteomics

Results from the Andromeda searches were directly imported in Perseus, the downstream bioinformatics platform for MaxQuant data. Here, peptides grouped per protein were normalized over the three biological repeats. Two transformations ($1/x$ and $\log_2(x)$) later, the \log_2 values of the L/H ratios were categorized per genotype and time point. Only proteins with an L/H ratio in all samples (24) were retained and each ratio was subtracted by the sample median. Following width adjustment, the protein ratios changing significant over time were identified via the use of multiple t-testing with a permutation-based FDR of 0.05 and number of randomizations set to 250. Clustering of the significant proteins was performed via Pearson correlation and the protein ratios were rescaled to a [-1;1] interval for visualization. Scatterplots were obtained by subjecting the overlapping proteins per time point to a two-sample t-test and determination of the appropriate s_0 -factor in R.

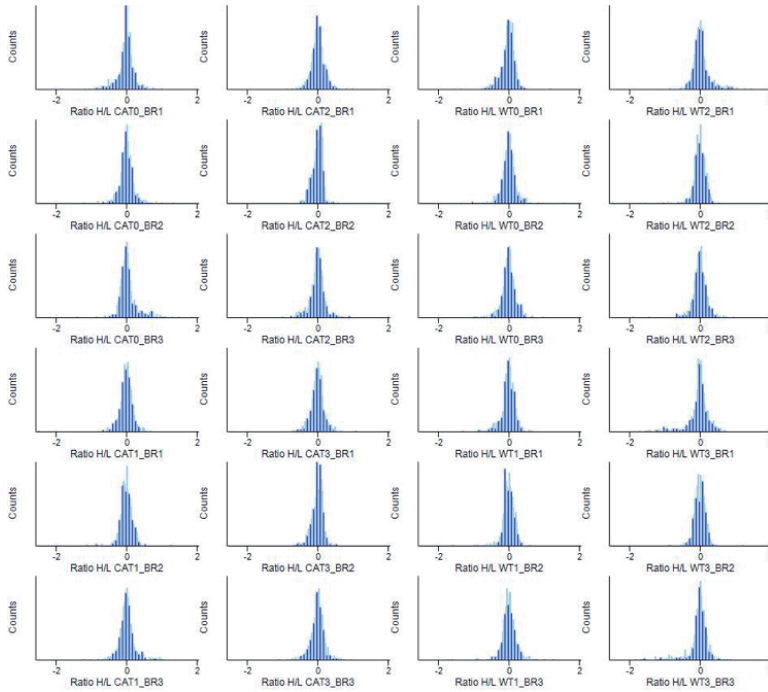
Ribosome footprinting

From the harvested leaf material, also used for shotgun proteomics, 2 ml was crushed in liquid nitrogen to which 2 ml of lysis buffer; 10mM Tris-HCl pH 7.4, 5mM MgCl₂, 100mM KCl, 1% Triton X-100 with freshly added 2mM DDT, 100 µg/ml cycloheximide and protease inhibitor was added. This was put on ice with frequent mixing and filtered over paper spin cups (Pierce) by a 1 min centrifugation (4°C) at 100 x g followed by a 5 min centrifugation at 1000 x g. The supernatant was transferred to new Eppendorf tubes, centrifuged for 15 min (4°C) and incubated on ice for 10 min. Another centrifugation step was performed at 16,000 x g before the supernatant was divided over two Eppendorf tubes; 600 µl for ribosome-protected footprint isolation and 300 µl for total mRNA extraction that was sent for sequencing (GATC Biotech, Constance, Germany). Digestion of the non-protected RNA was initiated by addition of 10 µl RNaseI (100 U/µl stock solution) and incubated for 55 min at room temperature with gentle agitation (thermoblock at 25°C, rotation at 400). The reaction was stopped by adding 30 µl SUPERase• In™ RNase Inhibitor (20 U/µl stock, Life technologies) and the reaction mixture loaded on top of a 1 M sucrose cushion. Ultracentrifugation was performed in a TLA-120.2 rotor at 75,000 rpm for 4 h at 4°C. The supernatant was removed and 570 µl 10 mM Tris HCl pH 7 and 30 µl of 20% SDS were added. Samples were heated to 65°C and footprint fragments were purified using the SDS/phenol method. The ribosome footprints were loaded on gel for subsequent size selection (28-34 nt), after which the extracted gel fragments were dephosphorylated and rRNA was depleted using the Ribo-Zero™ Magnetic Kit (Plant Leaf, Epicentre). This was followed by linker ligation, reverse transcription, circularization and PCR amplification as described before [18]. The obtained cDNA libraries were sequenced on a HiSeq system.

Deep sequencing data analysis

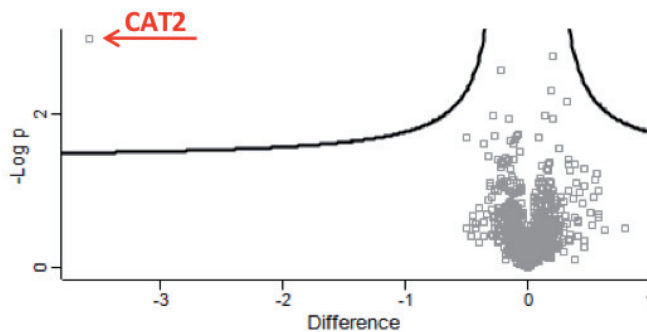
FastQ files were loaded into the Galaxy PSB server for data analysis. The 3' adapter sequences were clipped via the Cutadapt tool by entering a custom adapter sequence and specifying a minimum length of 25 nt. Clipped sequences were retained and mapped using GSNAP to the TAIR10 rRNA sequences to which one additional sequence was added manually (5S rRNA found overrepresented in the datasets but not yet annotated in TAIR10). The unaligned reads were subsequently mapped to the TAIR10 reference genome using GSNAP. Only uniquely mapped reads were retained and summarized using the HTseq tool. Two GFF files were created and uploaded, one with the distinction of exons and coding sequences, and one further specifying 3' and 5' UTRs. These counts were normalized to counts per million (cpm), as well as to transcripts per million (tpm) and reads per kilobase per million (rpKM). Upon comparison, we continued with cpm values as these introduced least biases and gave similar results as tpm and rpKM normalized values. SAM-mapping files were converted into BAM files to create bedgraphs that were loaded into the integrative genome viewer [65] for visualization. Differentially regulated genes were calculated via Huber statistics. Differentially regulated genes were calculated via Huber statistics which correct for the effect of outliers on the standard deviation as described in [66].

SUPPLEMENTAL INFORMATION



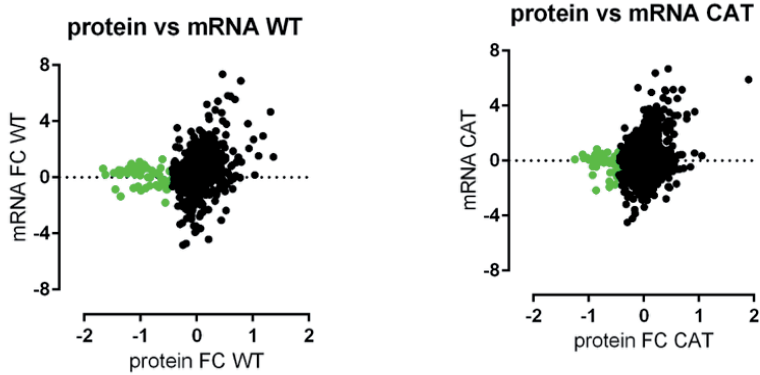
Supplemental Figure S1. Normalization in Perseus.

Normalization is performed in Perseus on the protein ratios of all three biological repeats. First, the values were transformed ($1/x$) and \log_2 scaled, next the normalization consisted of subtracting the median and width adjustment.



Supplemental Figure S2. Protein volcano plot prior to stress induction.

The volcano plot with an $s0$ factor of 0.077 and a false discovery rate of 5%, shows proteins commonly identified in wild-type and *cat2-2* plants (1,237 proteins). No significant differences expect for CATALASE 2 (AT4G35090) could be detected between both genotypes when grown under high CO_2 .

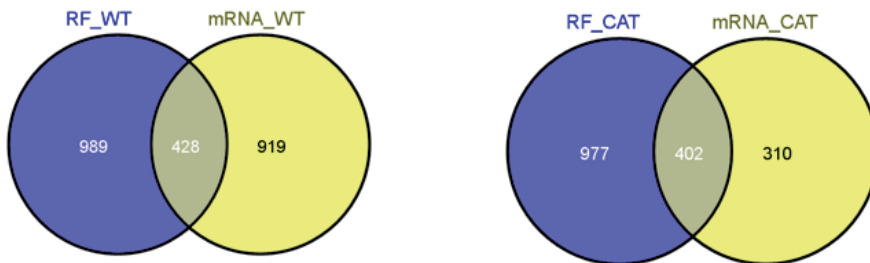


Supplemental Figure S3. Correlation plots between protein and transcript levels.

Comparison of normalized \log_2 mRNA reads to protein abundance levels after 3 h of high light exposure compared to 0 h per protein-coding gene. Proteins with a significant lower abundance (green) are hardly regulated at the level of transcription.



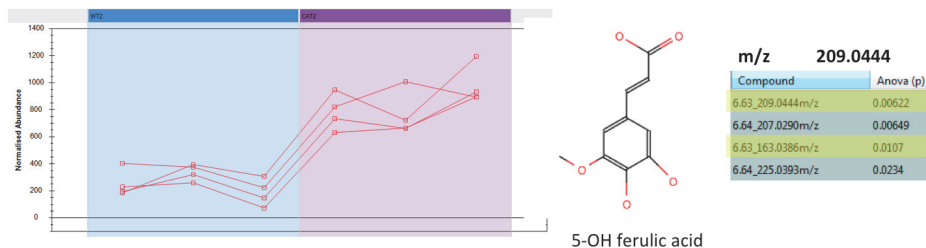
A. Upregulated ($p < 0.05$) genes



B. Downregulated ($p < 0.05$) genes

Supplemental Figure S4. Comparisons of differentially transcriptional and translational regulated genes.

Differentially regulated genes ($p < 0.05$) at transcriptional and translational level are compared with genotypes. (A) In both genotypes, over 56% of the up-regulated genes have both more transcripts and a higher ribosomal occupancy. (B) Similar numbers of genes with a decreased ribosomal occupancy that follow the transcriptional down-regulation: 428 in WT while 402 in *cat2-2* plants. There is a reduction in the number of transcripts with less ribosomal footprint reads (712) compared to genes with less mRNA reads (1,379).



Supplemental Figure S5. 5-hydroxyferulic acid accumulates in cat2-2 plants

Metabolite profiling via LC-MS(/MS) revealed a compound with an m/z value of 209.0444, identified as 5-hydroxyferulic acid, that was significantly more present in cat2-2 samples after 2 h of high light exposure. Also the compound with an m/z value of 163.0386 was shown to be a fragment of the 5-hydroxyferulic acid main peak.

TE cat2-2 versus WT over time	Name	GO ID	enrichment frequency	p-value
decreased	response to ethylene	GO:0009723	10,67	9,48E-51
	calcium ion binding	GO:0005509	4,40	6,65E-03
increased	signal transduction by phosphorylation	GO:0023014	9,57	7,18E-23
	plant-type cell wall modification	GO:0009827	7,29	6,36E-04

Supplemental Table S1. GO enriched categories of genes with an affected translational efficiency

Gene specific translational efficiency is affected upon enhanced hydrogen peroxide levels. Gene ontology analysis of genes with a translational efficiency differing significantly between genotypes is shown here.

Supplemental Table S2. Top 100 of transcriptional up- and down-regulated genes

This table lists the top 100 of up- and down-regulated genes at the transcriptional level (values in \log_2 fold changes) in both wild-type (sheet 1) and cat2-2 plants (sheet 2). Also ribosome footprint (RF) fold changes, protein abundance fold changes and translational efficiencies are shown. The third sheet shows all identified proteins before and after 3 h of stress treatment and lists their behaviour on the level of transcription and translation.

Table with 10 columns: Gene ID, Gene Name, Description, Nucleotide coordinates, and various numerical values. The table lists genes such as AT5G6570.1, AT5G64870.1, AT1G01000.1, etc., along with their functions and associated data points.

A. mRNA_WT

AT264790.1	Pseudo-response regulator PRR. Involved in dock function. PRR7 and PRR9 are involved in the response to oxidative stress. Involved in NADH-dependent histone H4 acetylation. Interacts, binding, with histone H4. Gene name: PRR7. Gene symbol: PRR7. Gene model: PRR7. Gene structure: 21 IRG211	8.83	8.87	2.47	4.52	#N/B	#N/B	2.41	0.31	#N/B	5.03
AT264791.1	Protein encoded by AT264791.1	9.04	8.77	4.54	4.27	#N/B	#N/B	-1.45	2.84	#N/B	-0.09
AT1637990.1	Encodes an aromatic acyl-CoA:MDP+ oxidoreductase whose mRNA levels are induced in response to oxidative stress	9.14	11.22	5.15	4.53	#N/B	#N/B	#N/B	4.13	#N/B	1.37
AT1461340.1	Encodes a gene similar to cellulose synthase protein_coding (ATCSA13)	9.15	6.72	6.02	4.02	#N/B	#N/B	-2.70	#N/B	#N/B	#N/B
AT263830.1	encodes a protein whose sequence is similar to 2-oxoglutarate-dependent dicarboxylate synthetase	9.19	8.73	5.26	4.54	#N/B	#N/B	-0.28	#N/B	#N/B	-0.52
AT1637991.1	encodes a protein whose sequence is similar to 2-oxoglutarate-dependent dicarboxylate synthetase	9.21	7.69	5.12	4.59	#N/B	#N/B	1.10	4.57	#N/B	-3.44
AT1461740.1	alpha/beta-Hydrolase superfamily protein	9.31	7.55	5.65	3.99	#N/B	#N/B	0.10	4.65	#N/B	-0.73
AT15624780.1	encodes an acid phosphatase similar to soybean vegetative storage proteins. It is a member of the acid phosphatase superfamily	9.70	9.27	5.32	3.70	#N/B	#N/B	-1.19	4.65	#N/B	-0.73
AT1562480.1	member of CYP94B protein_coding (CYTOCHROME P450) FAMILY 94, SUBFAMILY 94B, CYTOCHROME P450	9.70	8.53	5.22	4.38	#N/B	#N/B	0.28	4.74	#N/B	-0.42
AT1562479.1	Member of the cytochrome P450 superfamily. Involved in the biosynthesis of flavonoid compounds. It is a member of the cytochrome P450 superfamily	9.86	8.82	5.42	4.19	#N/B	#N/B	-0.28	4.74	#N/B	-0.42
AT1562479.1	Member of the cytochrome P450 superfamily. Involved in the biosynthesis of flavonoid compounds. It is a member of the cytochrome P450 superfamily	9.86	8.82	5.42	4.19	#N/B	#N/B	-0.28	4.74	#N/B	-0.42
AT1651780.1	Encodes a member of the six Arabidopsis BA-amino acid conjugate hydroxylase superfamily	10.07	6.90	4.05	4.51	#N/B	#N/B	1.48	5.70	#N/B	-2.25
AT1632840.1	Encodes an early light-inducible protein. protein_coding (EARLY LIGHT INDUCIBLE PROTEIN)	10.21	6.49	5.71	3.88	#N/B	#N/B	0.91	5.83	#N/B	-3.16
AT1631690.1	encodes a gene similar to cellulose synthase protein_coding (CELLULOSES SYNTHASE)	10.24	6.49	5.89	3.04	#N/B	#N/B	0.08	5.45	#N/B	-0.13
AT163170.1	Encodes a member of the SWEET (saccharine efflux transporter) family proteins.	10.60	6.47	5.41	3.36	#N/B	#N/B	0.08	5.45	#N/B	-0.13

Table with columns: AGI, description, miRNA FC CAT, RF FC CAT, RFC FC WT, protein FC CAT, protein FC WT, FC CAT, protein FC WT, FC CAT, protein FC WT, RFS FC WT, RFS FC CAT, RFS FC WT, RFS FC CAT, FC SVR (CAT vs WT), FC SVR (CAT vs WT), FC SVR (CAT vs WT), FC SVR (CAT vs WT).

B. mRNA_CAT

Gene ID	Description	9,83	3,70	5,62	#N/B	#N/B	-6,13	-4,21	-1,92	#N/B	#N/B	6,59	#N/B	#N/B
AT1G7325.1	Kunitz family trypsin and protease inhibitor protein	9,83	3,70	5,62	#N/B	#N/B	-6,13	-4,21	-1,92	#N/B	#N/B	6,59	#N/B	#N/B
AT5G0220.1	encodes a cupin-domain containing protein that is similar to pif	9,81	4,47	3,15	#N/B	#N/B	-5,44	-3,30	-2,14	#N/B	#N/B	6,59	#N/B	4,36
AT1G0100.1	member of the Nucleoside Diphosphate Kinase (NCKX) family	10,06	4,50	5,38	#N/B	#N/B	-5,46	-2,75	-2,91	#N/B	#N/B	6,59	#N/B	-1,88
AT5G0480.1	member of the ribonuclease T2 family, responds to organic pi	8,28	4,36	5,00	#N/B	#N/B	-5,74	-2,65	-2,47	#N/B	#N/B	4,75	#N/B	0,10
AT1G0740.1	HSP20-like chaperones superfamily protein	5,73	5,25	3,22	#N/B	#N/B	-4,90	-2,51	-2,39	#N/B	#N/B	3,02	#N/B	2,31
AT1G0340.1	isoprenyl diphosphate synthase (N-terminal domain)	4,13	5,67	0,52	#N/B	#N/B	-4,30	-1,89	-1,89	#N/B	#N/B	0,11	#N/B	3,40
AT1G0340.1	isoprenyl diphosphate synthase (C-terminal domain)	4,13	5,67	0,52	#N/B	#N/B	-4,30	-1,89	-1,89	#N/B	#N/B	0,11	#N/B	3,40
AT1G0420.1	member of the Gluc1 small heat shock protein (HSP) family, w	4,30	5,12	1,45	#N/B	#N/B	-5,43	-2,86	-2,58	#N/B	#N/B	0,72	#N/B	4,10
AT1G0320.1	AHSP23.6 mit c-mRNA, nuclear gene encoding mitochondrial	5,45	5,49	1,18	#N/B	#N/B	-5,29	-2,86	-1,02	#N/B	#N/B	1,40	#N/B	4,00
AT5G1200.1	17 kDa class II heat shock protein (HSP17.6II)	4,76	5,53	2,89	#N/B	#N/B	-5,54	-1,87	-3,66	#N/B	#N/B	2,60	#N/B	2,68
AT1G0100.1	member of the Nucleoside Diphosphate Kinase (NCKX) family	8,28	4,50	5,38	#N/B	#N/B	-5,46	-2,75	-2,91	#N/B	#N/B	6,59	#N/B	4,36
AT1G03790.1	Encodes an aromatic alcohol:NADPH oxidoreductase, whose mR	9,14	4,53	5,15	#N/B	#N/B	-4,69	-3,99	-2,70	#N/B	#N/B	4,13	#N/B	1,37

Ribosomal footprints over time	Name	GO ID	enrichment score	p-value	
<i>decreased: overlap cat2-2 & WT</i>	plant-type cell wall	GO:0009505	2,76	2,11E-06	
	response to auxin	GO:0009733	4,15	1,60E-04	
	DNA binding transcription factor activity	GO:0003700	2,75	1,10E-06	
	symporter activity	GO:0015293	1,91	5,50E-03	
	response to jasmonic acid	GO:0009753	17,80	2,90E-23	
	response to abscisic acid stimulus	GO:0009737	17,80	4,40E-15	
	response to water deprivation	GO:0009414	15,78	1,30E-17	
	flavonoid biosynthetic process	GO:0009813	9,31	1,80E-10	
	lignin biosynthetic process	GO:0009809	9,31	7,20E-05	
	response to high light intensity	GO:0009644	6,76	1,20E-09	
<i>increased: overlap cat2-2 & WT</i>	response to oxidative stress	GO:0006979	6,76	2,50E-08	
	proteasome complex	GO:000502	7,81	1,40E-16	
	response to heat	GO:0009408	6,43	1,30E-11	
	glutathione transferase activity	GO:0004364	3,66	9,60E-05	
	UDP-glucosyltransferase activity	GO:0035251	2,93	2,40E-04	
	DNA binding transcription factor activity	GO:0003700	2,50	4,30E-04	
	drug transmembrane transporter activity	GO:0015238	2,03	8,50E-04	
	<i>increased: exclusive in cat2-2</i>				

Supplemental Table S3. GO enriched categories of transcripts with a changed ribosomal occupancy

Gene ontology enriched categories of transcripts with a differential ribosomal occupancy during high light exposure is shown here.

REFERENCES

- [1] Sasson, A. U., The Global Food Crisis: Causes, Prospects, Solutions, *Agri-Bys* 2009.
- [2] Mittler, R., Vanderauwera, S., Suzuki, N., Miller, G., et al., ROS signaling: the new wave? *Trends Plant Sci* 2011, 16, 300-309.
- [3] Choudhury, S., Panda, P., Sahoo, L., Panda, S. K., Reactive oxygen species signaling in plants under abiotic stress. *Plant Signal Behav* 2013, 8, e23681.
- [4] Neill, S. J., Desikan, R., Clarke, A., Hurst, R. D., Hancock, J. T., Hydrogen peroxide and nitric oxide as signalling molecules in plants. *J Exp Bot* 2002, 53, 1237-1247.
- [5] Petrov, V. D., Van Breusegem, F., Hydrogen peroxide-a central hub for information flow in plant cells. *AoB Plants* 2012, 2012, pls014.
- [6] Frugoli, J. A., Zhong, H. H., Nuccio, M. L., McCourt, P., et al., Catalase is encoded by a multigene family in *Arabidopsis thaliana* (L.) Heynh. *Plant Physiol* 1996, 112, 327-336.
- [7] Vandenabeele, S., Vanderauwera, S., Vuylsteke, M., Rombauts, S., et al., Catalase deficiency drastically affects gene expression induced by high light in *Arabidopsis thaliana*. *Plant Journal* 2004, 39, 45-58.
- [8] Vanderauwera, S., Zimmermann, P., Rombauts, S., Vandenabeele, S., et al., Genome-wide analysis of hydrogen peroxide-regulated gene expression in *Arabidopsis* reveals a high light-induced transcriptional cluster involved in anthocyanin biosynthesis. *Plant Physiol* 2005, 139, 806-821.
- [9] Queval, G., Issakidis-Bourguet, E., Hoeberichts, F. A., Vidorpe, M., et al., Conditional oxidative stress responses in the *Arabidopsis* photorespiratory mutant *cat2* demonstrate that redox state is a key modulator of daylength-dependent gene expression, and define photoperiod as a crucial factor in the regulation of H₂O₂-induced cell death. *Plant J* 2007, 52, 640-657.
- [10] Queval, G., Neukermans, J., Vanderauwera, S., Van Breusegem, F., Noctor, G., Day length is a key regulator of transcriptomic responses to both CO₂ and H₂O₂ in *Arabidopsis*. *Plant Cell Environ* 2012, 35, 374-387.
- [11] Mhamdi, A., Queval, G., Chaouch, S., Vanderauwera, S., et al., Catalase function in plants: a focus on *Arabidopsis* mutants as stress-mimic models. *J Exp Bot* 2010, 61, 4197-4220.
- [12] Gygi, S. P., Rochon, Y., Franza, B. R., Aebersold, R., Correlation between protein and mRNA abundance in yeast. *Mol Cell Biol* 1999, 19, 1720-1730.
- [13] Schwanhauser, B., Busse, D., Li, N., Dittmar, G., et al., Global quantification of mammalian gene expression control. *Nature* 2011, 473, 337-342.
- [14] Tian, Q., Stepaniants, S. B., Mao, M., Weng, L., et al., Integrated genomic and proteomic analyses of gene expression in Mammalian cells. *Mol Cell Proteomics* 2004, 3, 960-969.
- [15] Mohammadi, P. P., Moieni, A., Hiraga, S., Komatsu, S., Organ-specific proteomic analysis of drought-stressed soybean seedlings. *Journal of proteomics* 2012, 75, 1906-1923.

- [16] Ingolia, N. T., Ghaemmaghami, S., Newman, J. R., Weissman, J. S., Genome-wide analysis in vivo of translation with nucleotide resolution using ribosome profiling. *Science* 2009, 324, 218-223.
- [17] Brar, G. A., Yassour, M., Friedman, N., Regev, A., et al., High-resolution view of the yeast meiotic program revealed by ribosome profiling. *Science* 2012, 335, 552-557.
- [18] Ingolia, N. T., Brar, G. A., Rouskin, S., McGeachy, A. M., Weissman, J. S., The ribosome profiling strategy for monitoring translation in vivo by deep sequencing of ribosome-protected mRNA fragments. *Nat Protoc* 2012, 7, 1534-1550.
- [19] Ingolia, N. T., Lareau, L. F., Weissman, J. S., Ribosome profiling of mouse embryonic stem cells reveals the complexity and dynamics of mammalian proteomes. *Cell* 2011, 147, 789-802.
- [20] Shalgi, R., Hurt, J. A., Krykbaeva, I., Taipale, M., et al., Widespread regulation of translation by elongation pausing in heat shock. *Mol Cell* 2013, 49, 439-452.
- [21] Liu, B., Han, Y., Qian, S. B., Cotranslational response to proteotoxic stress by elongation pausing of ribosomes. *Mol Cell* 2013, 49, 453-463.
- [22] Gerashchenko, M. V., Lobanov, A. V., Gladyshev, V. N., Genome-wide ribosome profiling reveals complex translational regulation in response to oxidative stress. *Proc Natl Acad Sci U S A* 2012, 109, 17394-17399.
- [23] Juntawong, P., Girke, T., Bazin, J., Bailey-Serres, J., Translational dynamics revealed by genome-wide profiling of ribosome footprints in Arabidopsis. *Proc Natl Acad Sci U S A* 2014, 111, E203-212.
- [24] Liu, M. J., Wu, S. H., Wu, J. F., Lin, W. D., et al., Translational landscape of photomorphogenic Arabidopsis. *Plant Cell* 2013, 25, 3699-3710.
- [25] Sheth, B. P., Thaker, V. S., Plant systems biology: insights, advances and challenges. *Planta* 2014, 240, 33-54.
- [26] Noctor, G., Veljovic-Jovanovic, S., Driscoll, S., Novitskaya, L., Foyer, C. H., Drought and oxidative load in the leaves of C3 plants: a predominant role for photorespiration? *Ann Bot* 2002, 89 Spec No, 841-850.
- [27] Ghesquiere, B., Jonckheere, V., Colaert, N., Van Durme, J., et al., Redox proteomics of protein-bound methionine oxidation. *Mol Cell Proteomics* 2011, 10, M110 006866.
- [28] Cox, J., Mann, M., MaxQuant enables high peptide identification rates, individualized p.p.b.-range mass accuracies and proteome-wide protein quantification. *Nat Biotechnol* 2008, 26, 1367-1372.
- [29] Tusher, V. G., Tibshirani, R., Chu, G., Significance analysis of microarrays applied to the ionizing radiation response. *Proc Natl Acad Sci U S A* 2001, 98, 5116-5121.
- [30] Tusher, V. G., Tibshirani, R., Chu, G., Significance analysis of microarrays applied to the ionizing radiation response. *Proc Natl Acad Sci U S A* 2001, 98, 5116-5121.
- [31] Delker, C., Zolman, B. K., Miersch, O., Wasternack, C., Jasmonate biosynthesis in Arabidopsis thaliana requires peroxisomal beta-oxidation enzymes--additional proof by properties of pex6 and aim1. *Phytochemistry* 2007, 68, 1642-1650.

- [32] Xu, X. M., Wang, J., Xuan, Z., Goldshmidt, A., et al., Chaperonins facilitate KNOTTED1 cell-to-cell trafficking and stem cell function. *Science* 2011, 333, 1141-1144.
- [33] Agne, B., Kessler, F., Modifications at the A-domain of the chloroplast import receptor Toc159. *Plant Signal Behav* 2010, 5, 1513-1516.
- [34] Meier, I., Brkljacic, J., The Arabidopsis nuclear pore and nuclear envelope. *Arabidopsis Book* 2010, 8, e0139.
- [35] Foyer, C. H., Noctor, G., Ascorbate and glutathione: the heart of the redox hub. *Plant Physiol* 2011, 155, 2-18.
- [36] Yoshiba, Y., Nanjo, T., Miura, S., Yamaguchi-Shinozaki, K., Shinozaki, K., Stress-responsive and developmental regulation of Delta(1)-pyrroline-5-carboxylate synthetase 1 (P5CS1) gene expression in Arabidopsis thaliana. *Biochem Biophys Res Commun* 1999, 261, 766-772.
- [37] Graether, S. P., Boddington, K. F., Disorder and function: a review of the dehydrin protein family. *Front Plant Sci* 2014, 5, 576.
- [38] Kim, S. Y., Nam, K. H., Physiological roles of ERD10 in abiotic stresses and seed germination of Arabidopsis. *Plant Cell Rep* 2010, 29, 203-209.
- [39] Nylander, M., Svensson, J., Palva, E. T., Welin, B. V., Stress-induced accumulation and tissue-specific localization of dehydrins in Arabidopsis thaliana. *Plant molecular biology* 2001, 45, 263-279.
- [40] Verslues, P. E., Sharma, S., Proline metabolism and its implications for plant-environment interaction. *Arabidopsis Book* 2010, 8, e0140.
- [41] Herrmann, K. M., Weaver, L. M., The Shikimate Pathway. *Annual review of plant physiology and plant molecular biology* 1999, 50, 473-503.
- [42] Herrmann, K. M., The shikimate pathway as an entry to aromatic secondary metabolism. *Plant Physiol* 1995, 107, 7-12.
- [43] Tsuzuki, T., Takahashi, K., Tomiyama, M., Inoue, S., Kinoshita, T., Overexpression of the Mg-chelatase H subunit in guard cells confers drought tolerance via promotion of stomatal closure in Arabidopsis thaliana. *Front Plant Sci* 2013, 4, 440.
- [44] Shen, Y. Y., Wang, X. F., Wu, F. Q., Du, S. Y., et al., The Mg-chelatase H subunit is an abscisic acid receptor. *Nature* 2006, 443, 823-826.
- [45] Klodmann, J., Sunderhaus, S., Nimtz, M., Jansch, L., Braun, H. P., Internal architecture of mitochondrial complex I from Arabidopsis thaliana. *Plant Cell* 2010, 22, 797-810.
- [46] Tomaz, T., Bagard, M., Pracharoenwattana, I., Linden, P., et al., Mitochondrial malate dehydrogenase lowers leaf respiration and alters photorespiration and plant growth in Arabidopsis. *Plant Physiol* 2010, 154, 1143-1157.
- [47] Holcik, M., Sonenberg, N., Translational control in stress and apoptosis. *Nature reviews. Molecular cell biology* 2005, 6, 318-327.

- [48] Novoa, I., Zhang, Y., Zeng, H., Jungreis, R., et al., Stress-induced gene expression requires programmed recovery from translational repression. *Embo J* 2003, 22, 1180-1187.
- [49] Chen, Z., Gallie, D. R., Dehydroascorbate reductase affects leaf growth, development, and function. *Plant Physiol* 2006, 142, 775-787.
- [50] Maruta, T., Inoue, T., Noshi, M., Tamoi, M., et al., Cytosolic ascorbate peroxidase 1 protects organelles against oxidative stress by wounding- and jasmonate-induced H₂O₂ in Arabidopsis plants. *Biochim Biophys Acta* 2012, 1820, 1901-1907.
- [51] Hinkson, I. V., Elias, J. E., The dynamic state of protein turnover: It's about time. *Trends in cell biology* 2011, 21, 293-303.
- [52] Schwanhausser, B., Gossen, M., Dittmar, G., Selbach, M., Global analysis of cellular protein translation by pulsed SILAC. *Proteomics* 2009, 9, 205-209.
- [53] Schneider-Poetsch, T., Ju, J., Eyler, D. E., Dang, Y., et al., Inhibition of eukaryotic translation elongation by cycloheximide and lactimidomycin. *Nat Chem Biol* 2010, 6, 209-217.
- [54] Michel, A. M., Baranov, P. V., Ribosome profiling: a Hi-Def monitor for protein synthesis at the genome-wide scale. Wiley interdisciplinary reviews. *RNA* 2013, 4, 473-490.
- [55] Huang, D. W., Sherman, B. T., Tan, Q., Collins, J. R., et al., The DAVID Gene Functional Classification Tool: a novel biological module-centric algorithm to functionally analyze large gene lists. *Genome biology* 2007, 8, R183.
- [56] Lata, C., Prasad, M., Role of DREBs in regulation of abiotic stress responses in plants. *J Exp Bot* 2011, 62, 4731-4748.
- [57] Wang, H., Cutler, A. J., Promoters from kin1 and cor6.6, two Arabidopsis thaliana low-temperature- and ABA-inducible genes, direct strong beta-glucuronidase expression in guard cells, pollen and young developing seeds. *Plant molecular biology* 1995, 28, 619-634.
- [58] Chinnusamy, V., Zhu, J. K., Sunkar, R., Gene regulation during cold stress acclimation in plants. *Methods Mol Biol* 2010, 639, 39-55.
- [59] Kazan, K., Manners, J. M., MYC2: the master in action. *Mol Plant* 2013, 6, 686-703.
- [60] De Geyter, N., Gholami, A., Goormachtig, S., Goossens, A., Transcriptional machineries in jasmonate-elicited plant secondary metabolism. *Trends Plant Sci* 2012, 17, 349-359.
- [61] Chini, A., Fonseca, S., Fernandez, G., Adie, B., et al., The JAZ family of repressors is the missing link in jasmonate signalling. *Nature* 2007, 448, 666-671.
- [62] Muthuramalingam, M., Matros, A., Scheibe, R., Mock, H. P., Dietz, K. J., The hydrogen peroxide-sensitive proteome of the chloroplast in vitro and in vivo. *Front Plant Sci* 2013, 4, 54.
- [63] Wang, H., Wang, S., Lu, Y., Alvarez, S., et al., Proteomic analysis of early-responsive redox-sensitive proteins in Arabidopsis. *J Proteome Res* 2012, 11, 412-424.
- [64] Alvarez, S., Zhu, M., Chen, S., Proteomics of Arabidopsis redox proteins in response to methyl jasmonate. *J Proteomics* 2009, 73, 30-40.

[65] Thorvaldsdottir, H., Robinson, J. T., Mesirov, J. P., Integrative Genomics Viewer (IGV): high-performance genomics data visualization and exploration. *Briefings in bioinformatics* 2013, 14, 178-192.

[66] Colaert, N., Helsens, K., Impens, F., Vandekerckhove, J., and Gevaert, K. (2010) Rover: a tool to visualize and validate quantitative proteomics data from different sources. *Proteomics* 10, 1226-1229



5

THE DYNAMICS OF PROTEIN-BOUND METHIONINE OXIDATION EVENTS IN *A.THALIANA* DURING OXIDATIVE STRESS

**SILKE JACQUES, BART GHESQUIÈRE, PIETER-JAN DE BOCK, PATRICK WILLEMS,
FRANK VAN BREUSEGEM AND KRIS GEVAERT**

A modified version of this chapter is re-submitted under the same title to “Molecular and Cellular Proteomics”

Silke Jacques wrote the chapter with corrections of Bart Ghesquiere, Frank Van Breusegem and Kris Gevaert
Silke Jacques designed, performed and analyzed all experiments, Pieter-Jan De Bock performed the LC-MS/MS measurements and Patrick Willems established the online MetOx database

ABSTRACT

Reactive oxygen species such as hydrogen peroxide can modify proteins via direct oxidation of their sulfur-containing amino acids, cysteine and methionine. Methionine oxidation, studied here, is a reversible posttranslational modification, which is increasingly suggested as a mechanism by which proteins perceive oxidative stress and function in redox signalling. Identification of proteins with oxidized methionines is a first prerequisite towards understanding the functional effect of methionine oxidation on proteins and the biological processes in which they are involved. Here, we describe a proteome-wide study of *in vivo* protein-bound methionine oxidation in plants upon oxidative stress, using *Arabidopsis thaliana* CATALASE 2 knock-out plants as a model system. We identified approximately 500 sites of oxidation in about 400 proteins, and quantified the differences in oxidation between wild-type and CATALASE 2 knock-out plants. Further, by sampling over time, we mapped the dynamics of methionine oxidation and gained new insights into this complex and dynamic landscape of the part of the plant proteome that is sculpted by oxidative stress.

INTRODUCTION

Cellular oxidative stress is the result of an imbalance between oxidizing and reducing cellular agents and enzymes, and considered to be a major damaging factor [1]. The identification of those proteins, together with their redox modifications, that are involved in responses to oxidative stress is needed for addressing key questions on understanding how plants perceive and adjust to environmental stress factors. Such adverse environmental conditions indeed impact on plant growth and quality hence, knowing the key protein players might lead to new opportunities to weapon food and feed crops against forecasted climate changes. The latter are expected to trigger sustained exposure of plants to abiotic stress, rendering them vulnerable, thus urging the necessity for sustainable solutions to improve crops. Plant proteomics provides an excellent way to deliver the scientific knowledge that is translatable into useful applications for crop improvement through identification of target proteins affected by the oxidative burden [2-4].

Importantly, the accumulation of reactive oxygen or nitrogen species (ROS/RNS) upon oxidative stress not only leads to damage of proteins, oligonucleotides, sugars and lipids, but ROS and RNS also evoke cellular signaling events [5-6]. Here, hydrogen peroxide is particularly interesting as an oxidative stress signaling molecule [7] due to its relatively long half-life (1 ms) and its size that enables it to oxidize biomolecules in compartments other than the site of hydrogen peroxide generation and even in neighboring cells [8]. However, in plant cells little is known how exactly changes in hydrogen peroxide levels can lead to a final oxidative stress response. Perception of and oxidation by hydrogen peroxide (or derived species) revealed some redox regulating proteins [9] but for the majority of proteins it remains unknown whether oxidation leads to signaling events or to damage. To study the *in vivo* effects of increased hydrogen peroxide levels, *Arabidopsis* CATALASE 2 knock-out plants serve as a good model system since these plants endogenously accumulate (higher) hydrogen peroxide levels, making them a physiologically more relevant model system [10] as compared to the exogenous application of higher hydrogen peroxide levels [11]. The CATALASE 2 enzyme is the major leaf catalase isoform out of three encoded in the *Arabidopsis* genome and as such the leading scavenger of hydrogen peroxide, which is produced by glycolate oxidase in the peroxisomes upon photorespiration [12].

Endogenously produced hydrogen peroxide is capable to directly oxidize the two sulfur-containing amino acids, methionine and cysteine. Oxidation of cysteine in particular has been intensively studied and it is known that its different oxidation states can impact on diverse protein functions [13-14]. Methionine oxidation on the other hand received less attention and, in plants, only a few examples of functional consequences of this modification have been described [15-18]. Due to its low oxidation potential, hydrogen peroxide can readily oxidize methionine to methionine sulfoxide (MetO), which can then be further oxidized to methionine sulfone, although to a much lesser extent [19-20]. Methionine sulfoxidation can be countered by methionine sulfoxide reductases (MSRs) [21]. Upon methionine oxidation, two stereo-isomers may form (R-MetO and S-MetO) and accordingly two families of stereospecific MSRs evolved; MSRA isoforms reduce S-MetO and MSRB R-MetO [22]. *Arabidopsis thaliana* contains 5 MSRA genes encoding three cytosolic (MSRA1, MSRA2 and MSRA3), one chloroplastic (MSRA4) and one isoform targeted to the secretory pathway (MSRA5) [23]. The 9 MSRB proteins present in *Arabidopsis* are also targeted to different organelles; MSRB1 and B2 are localized in the chloroplast,

B3 is designated to the secretory pathway, while the other six MSRB proteins are cytosolic [24-25]. Also other plants such as poplar with 5 MSRAs and 4 MSRBs, and rice, containing 4 MSRAs and 3 MSRBs [26], express a considerably larger number of MSR enzymes as compared to mammals, the latter only containing 4 MSR genes in total [27]. In plants, most of the methionine oxidation studies thus far focused on the different functions of MSRs rather than on the impact and extent of oxidation of protein-bound methionines [28]. Methionine oxidation causes conversion of the hydrophobic methionine into the more hydrophilic methionine sulfoxide. This change in physicochemical properties of methionine triggers the exposure of otherwise inaccessible buried regions as the now hydrophilic methionine sulfoxide is capable to position itself at the surface [29]. In plants, a loss of hydrophobic recognition sites upon methionine oxidation was demonstrated for serine phosphorylation of nitrate reductase [30] and a loss of chaperone-like activity upon oxidation of methionine for the small heat shock protein Hsp21 [31]. The current lack of antibodies that specifically target oxidized methionine residues greatly impaired proteome-wide studies of methionine oxidation events in plants [32]. Here, we implemented the recently developed COFRADIC proteomics technology that relies on diagonal peptide chromatography and the specificity of MSRs to isolate peptides carrying *in vivo* oxidized methionines, which are subsequently analyzed by tandem mass spectrometry [33-34] allowing the identification of the exact sites of methionine oxidation. This enabled us to chart *in vivo* protein-bound methionine oxidation in *Arabidopsis thaliana* following oxidative stress. This pioneering map suggests that under these conditions methionine oxidation is not a random event, but might steer molecular signaling events. Further, we compared differences in methionine oxidation between wild-type and CATALASE 2 mutants and captured the dynamics of oxidation by time-resolved proteome analysis.

RESULTS

Proteome analysis of in vivo protein-bound methionine oxidation

Mapping of oxidation-sensitive methionines in *Arabidopsis thaliana* proteins was done by applying the COFRADIC technology [33] which basically consists of three consecutive steps: (1) peptide fractionation based on hydrophobicity (RP-HPLC), (2) treatment of fractionated peptides with recombinant methionine sulfoxide reductases A and B3, and (3) re-fractionation of the treated fractions by RP-HPLC. *Arabidopsis* CATALASE 2 knock-out line *cat2-2* were used as a model system to study the effects on the proteome upon oxidative stress. Since photorespiration is a primary source of hydrogen peroxide in photosynthetic tissue [38], the catalase knock-out plants as well as wild-type plants were grown under elevated CO₂ levels (3,000 ppm) to block oxygenation of ribulose-1,5-biphosphate and as such hinder photorespiration. Transferring plants after five weeks to a continuous high light irradiation regime under ambient air conditions (400 ppm CO₂), photorespiratory-dependent generation of hydrogen peroxide was endogenously modulated. Indeed, as these growth conditions boost photorespiration, glycolate is produced which is subsequently converted in the peroxisomes to glyoxylate by glycolate oxidase concomitant with the release of hydrogen peroxide [12]. Thus, here we assessed primarily the oxidation of protein-bound methionines caused by increased concentrations of hydrogen peroxide originating from the peroxisomes. Middle aged leaves of five-week old wild-type and catalase knock-out plants were harvested at 1 and 3 h following the onset of photorespiratory stress. These time points were chosen based on our q-PCR results of hydrogen

peroxide responsive genes (**Supplemental Figure S1**) and allowed us to capture the early dynamics of methionine oxidation events during oxidative stress. Following protein extraction and proteolytic cleavage (endoproteinase Lys-C), post-metabolic labeling of peptides, using either light ($^{12}\text{C}_3$) or heavy ($^{13}\text{C}_3$) propionate, was performed to compare WT versus CAT2-2 proteomes. These “mass tags” on the identified MetO peptides will point to the exact origin of the peptides, while the ion signals themselves allow for a quantitative comparison between the genotypes (**Figure 1**). To exclude that the observed differences in the degree of methionine oxidation were caused by differences in protein levels, we performed in parallel a quantitative proteomics screen.

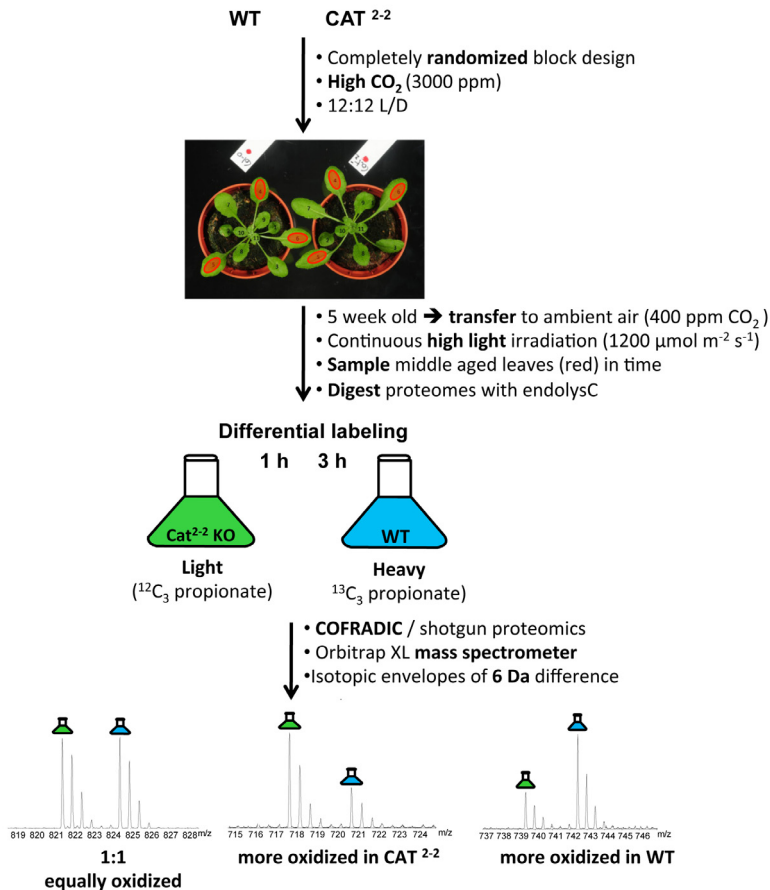


Figure 1: Schematic overview of the experimental workflow.

Catalase knock-out (CAT2-2) and wild-type (WT) plants were grown under high CO₂ concentrations (3,000 ppm) and organized according to a completely randomized block design in a 12:12 L/D regime. Five-week old plants were exposed to continuous high light irradiation (1200 μmol m⁻² s⁻¹) under ambient air (400 ppm). Middle aged leaves (indicated with red dots) of 15 plants per line were sampled 1 h and 3 h after the onset of the high light stress and pooled for further analysis. After digestion with endoproteinase Lys-C and post-metabolic peptide labeling, equal amounts of samples were mixed and applied to COFRADIC-based isolation of MetO peptides. A parallel shotgun proteomics of the same samples allowed correcting for possible differences in overall protein abundance.

We identified 513 oxidation sites in 403 proteins. Following 1 h of high light exposure, 365 MetO peptides in 296 proteins were found, whereas after 3 h, 354 MetO peptides in 294 proteins were identified (**Supplemental Figure S2, Supplemental Table S1**). Interestingly, there is an overlap of 186 proteins with MetO sites identified at both time-points (**Table 1**). An overview of all MetO-containing proteins identified in our study is further made available via <http://www.psb.ugent.be/metox¹>. This website allows to easily track a protein-of-interest using a query interface, shows the identified peptide(s) mapped onto the protein's amino acid sequence and displays quantitative differences in methionine oxidation between catalase knock-out and wild-type plants.

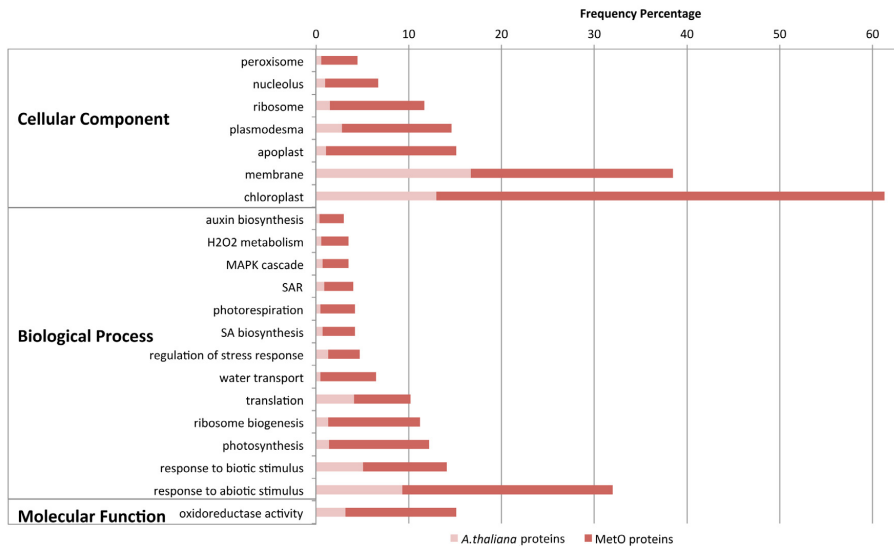
METHIONINE OXIDATION IN NUMBERS	1 h	3 h	total unique IDs
MetO peptides	365	354	507
oxidized proteins	296	294	403
proteins significant more oxidized in CAT vs WT (≥ 2 -fold)	24 (7)	29 (18)	51
proteins significant more oxidized in WT vs CAT (≥ 2 -fold)	40 (14)	18 (8)	57
protein overlap in time (with identical MetO site)	187 (175)		
MetO peptide overlap in time	206		
proteins significant more oxidized over time	17		
proteins significant less oxidized over time	3		
proteins with single oxidation event	236	247	362

Table 1. Overview of the oxidation events identified 1 h and 3 h after the onset of high light stress

A gene ontology enrichment analysis ($p \leq 0.01$) was performed for the 403 oxidized proteins identified with the complete proteome of *Arabidopsis thaliana* used as the background reference set. This GO analysis showed that peroxisomal and chloroplast proteins were significantly more abundant in our dataset (**Figure 2**). Since light irradiation is captured by chloroplasts, excess light could directly affect photosynthetic proteins present in chloroplasts, explaining the prevalence of such proteins when considering the GO terms linked to biological processes. Also, proteins involved in chloroplast relocation [39] were enriched, which might point to the fact that cells try to minimize the captured light by relocating chloroplasts. Higher levels of oxidative stress through the activation of the photorespiratory pathway is illustrated by the enhanced GO classes of proteins involved in photorespiration and hydrogen peroxide metabolism. Nucleolar and ribosomal proteins were also significantly enriched in our dataset, as demonstrated by the enrichment of proteins involved in ribosome biogenesis and translation. Further, proteins known to get localized to plasmodesma and apoplasts were significantly enriched, as well as proteins involved in water transport. This suggests two modes of hydrogen peroxide channeling; plasmodesma provide a gate to neighboring cells, while hydrogen peroxide could also pass into the apoplast, till now known as a free passage for water and solutes. Additionally, aquaporins were found to also transport hydrogen peroxide across membranes [40]. Oxidized membrane proteins also appeared to be an enriched GO class. Other significantly enriched GO terms coupled to biological processes include "response to stress" and, more specifically, response to ROS, and in particular hydrogen peroxide as well as response to light stimulus. In addition, proteins involved in salt and osmotic stress, as well as proteins from the innate immune response, proteins responding to temperature, bacteria or inorganic substances (chemicals, acids, metals) are enriched. Taken together, the enriched GO classes of response towards abiotic and biotic stimulus point to a general stress response cluster upon oxidation. Of note is that not only executors but also regulators of the cellular response to stress are enriched among the oxidized

¹Note that a username "metox" and a password "methi0nine" are needed to access the site.

proteins. Additionally, links to hormone signaling appear as salicylic acid (SA) biosynthesis and systemic acquired resistance (SAR) mediated by SA signaling are found enriched, as well as proteins involved in auxin biosynthesis. Proteins linked to the GO term “oxidoreductase activity” include thioredoxin, two MSRs (MSRA2/A3), and the mitochondrial LPD1 and 2 proteins that are part of the glycine decarboxylase complex that releases CO₂ during photorespiration. Finally, proteins involved in signal transduction by phosphorylation, more specifically members of MAPK cascades, were also enriched.



	gene ontology term	dataset (out of 403)	total Arabidopsis proteome(30495)	fold enrichment	p-value
cellular component	peroxisome	19	235	5,9	1,0E-06
	nucleolus	27	385	5,2	5,8E-09
	ribosome	48	520	7,0	7,4E-23
	plasmodesma	60	862	5,3	1,0E-22
	apoplast	61	467	10,1	1,2E-38
	membrane	160	6885	1,8	1,5E-11
	chloroplast	247	4112	4,5	6,3E-109
	biological process	auxin biosynthesis	12	147	6,0
H2O2 metabolism		14	187	5,8	5,3E-04
MAPK cascade		14	232	4,4	7,0E-03
SAR		24	468	4,0	4,9E-05
photorespiration		17	178	7,0	6,5E-07
SA biosynthesis		17	211	6,0	8,8E-06
regulation of stress response		19	394	3,6	3,7E-03
water transport		26	141	13,0	5,9E-19
translation		51	1444	2,7	4,6E-07
ribosome biogenesis		45	511	6,6	2,0E-20
photosynthesis		52	455	8,6	1,5E-29
molecular function	response to biotic stimulus	58	1895	2,3	5,2E-06
	response to abiotic stimulus	129	2885	3,4	1,6E-33
	oxidoreductase activity	70	1703	3,1	5,2E-14

Figure 2: Gene ontology enrichment analysis of oxidized proteins.

The 403 proteins identified to contain sites of methionine oxidation upon high light stress were submitted to a gene ontology (GO) enrichment analysis using AmiGO. The complete proteome of *A. thaliana* was chosen as a reference set. Significant enriched GO categories ($p < 0.01$) discussed in the main text are listed and the enriched frequencies of methionine oxidized proteins (dark red) are shown. The frequency of all *A. thaliana* proteins in these enriched categories is also shown (light red) as part of the total enriched MetO protein frequency bars. The table lists the significant p-values and number of proteins identified in our dataset compared to the complete proteome for the enriched gene ontology categories.

Quantification of methionine oxidation between genotypes

Post-metabolic peptide labeling enabled us to assess the influence of the plant genotypic background (*cat2-2* vs. wild-type) on methionine oxidation. 51 proteins were significantly more oxidized in catalase knock-out plants when considering both time-points ($p \leq 0.05$; 24 proteins after 1 h, and 29 proteins after 3 h of high light stress, respectively (**Table 1**)). For most of these proteins (18 out of 24 after 1 h, and all after 3 h of high light stress) only one MetO peptide was identified, although multiple methionines, e.g. up to 69 for the NADH-dependent glutamate synthase 1 (AT5G53460), are present in their sequences (**Supplemental Table S1**). Of note is one protein, At4G23670, that was identified at both time points and found oxidized on two sites; methionines 134 and 140. This protein of 151 amino acids is a member of the polyketide cyclase/dehydrase and lipid transport superfamily. It is involved in defense and stress responses as well as in cysteine biosynthesis. Moreover, the levels of this protein dropped to about 65% in the catalase mutant compared to wild-type plants, which might hint to increased degradation of this protein upon oxidation.

Several proteins were more oxidized in HL stressed wild-type plants. For instance, upon 3 h of high light stress, these 18 proteins are all but one oxidized on a single methionine and all are equally or less abundant in wild-type plants which could again suggest increased protein degradation caused by methionine oxidation. 14 and 8 proteins with at least two-fold higher oxidation in wild-type plants were identified after 1 h and 3h of high light stress, respectively. In catalase knock-out plants oxidation events rise from 7 to 18 proteins over time (**Table 1**). This increase of more strongly oxidized proteins in the catalase knock-out plant might be explained by elevated hydrogen peroxide production over time which cannot be eliminated in these plants and as such enhances the overall oxidative stress condition. In wild-type plants on the other hand, the vast majority of proteins with a two-fold higher oxidation degree are localized to plastids.

To conclude, quantification of methionine oxidation revealed 55 MetO peptides in 51 proteins that are significantly more oxidized in the catalase knock-out. Noteworthy, enhanced oxidation was not restricted to the catalase loss-of-function genotype but was also seen in wild-type plants, suggesting a boost in methionine oxidation of proteins that are sensitive towards high light stress.

Dynamics of methionine oxidation

Applying time-resolved analysis by sampling at 1 h and 3 h during oxidative stress allowed to capture the dynamics of protein-bound methionine oxidation. The overlap of 186 proteins identified in both time-points served as a base for exploring this dynamics of oxidation. More specifically, dynamics of oxidation of 175 proteins on identical methionine sites could be compared (**Figure 3**). 17 proteins displayed significant higher oxidation ($p \leq 0.05$) after 3 h compared to 1 h, whereas only 3 proteins showed a decrease in methionine oxidation over time. The proteins with a time-dependent increase in oxidation are metabolic enzymes, a chaperone, a transporter, a protease and a transcription factor, amongst others, and their increased oxidation can be explained by increased concentrations of hydrogen peroxide as the high light stress continues in time in combination with a possible decreased reduction of these MetO-sites by methionine sulfoxide reductases. Several of these proteins have been previously linked to stress response such as the RNA-binding protein Tudor-SN (AT5G61780) that stabilizes stress-responsive mRNA molecules encoding for secreted proteins and proved essential for salt stress

resistance [41]. The basic transcription factor 3 (AT1G17880) homolog in higher plants impairs tolerance of wheat against drought and freezing stresses when silenced, and was also found to be differentially regulated by diverse abiotic stresses and hormone treatments [42]. Also, the photorespiratory enzyme NADH-dependent glutamate synthase 1 was identified to be more oxidized after 3 h which might be a consequence of the proximity to the site of hydrogen peroxide production. On the other hand, proteins of which the levels of methionine oxidation drop over time might have been repaired by the methionine sulfoxide reductases, numerous present in plant cells [28]. Remarkably, the three proteins whose oxidation is lowered over time show increased protein levels after 3 h of stress treatment.

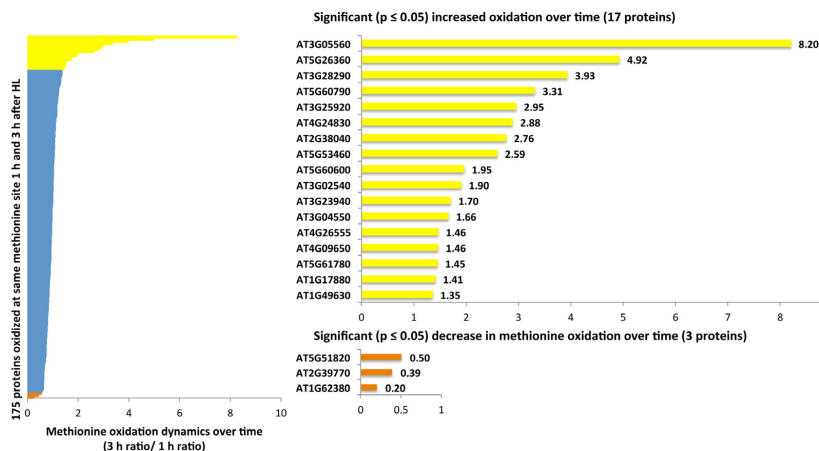


Figure 3: The dynamics of methionine oxidation.

The 186 proteins identified at both time points of high light stress share 175 MetO peptides. Comparing their signals shows the dynamics of methionine oxidation over time; 17 proteins (yellow bars) were significantly ($p \leq 0.05$) more oxidized after 3 h of high light stress, while only 3 proteins (orange bars) showed a significant decrease in methionine oxidation.

Specificity of methionine oxidation

To assess potential specificity of methionine oxidation linked to molecular signaling, different parameters were analyzed such as methionine frequency, the correlation of protein abundance and number of methionines with the oxidation degree, and the amino acid sequence surroundings of the MetO sites. By plotting the overall amino acid frequencies of all annotated *A. thaliana* proteins (35,386 sequences in TAIR10), the occurrence of protein-bound methionine was 2.46% (**Figure 4A**). When correcting for the fact that the initiator methionine is frequently removed in nascent polypeptides [43], the overall methionine content of *Arabidopsis* proteins drops further to 2.21%. Tarrago *et al.* (2011) postulated a positive correlation of methionine oxidation with protein abundance and methionine content as one of the *A. thaliana* methionine sulfoxide reductases, MSRB1, was found to preferentially interact with proteins with high methionine content [44]. Interestingly, about half of the oxidized proteins here identified have a lower than average methionine frequency (**Figure 4B**), meaning that the presence of more methionines in a protein is not a prerequisite for its oxidation. Additionally, out of the 403 proteins bearing an oxidized methionine, 362 proteins were identified with a single MetO peptide, which accounts

for 90% of the identified proteins. When spectral counts from the shotgun analysis are taken into account as a proxy for protein abundance [45], an average of 4.8 and 4.9 spectra were linked to identified proteins in the 1 h and 3 h high light stressed samples, respectively. A comparison of these averages to the spectral counts of proteins with significantly altered oxidation levels showed that only 21 out of the 76 proteins after 1 h, and 18 out of the 62 proteins after 3 h high light intensities are above average abundance. Taken together, these data show that a high methionine content or high protein levels are not prerequisites for oxidation to occur on methionine. As such, these data argue against random methionine oxidation as an alternative ROS scavenging mechanism, leading to indiscriminate protein damage [17].

Further indications for a possible specific regulatory role of methionine oxidation events appear when comparing the protein sequence surrounding the MetO sites identified in oxidized proteins belonging to the same family (**Supplemental Table S2**). One such example are of the rubredoxin protein family (AT3G15640 and AT1G80230), which consists of three proteins with cytochrome c activity and in which the sequence patch surrounding the oxidized methionine is conserved amongst 43 homologous proteins across the plant kingdom (19 species) (**Supplemental Figure S2**). The third *Arabidopsis* gene (AT1G52710) lost this patch and was not picked up in our analysis. Interestingly, both oxidized rubredoxin-like proteins were found to be four times more oxidized in the catalase mutant compared to the wild-type, and this already 1 h after high light irradiance.

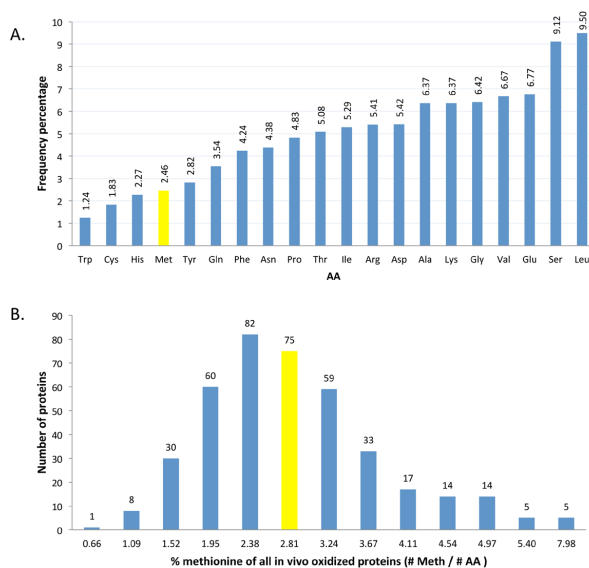


Figure 4: Methionine frequency plots across all *A. thaliana* proteins (A) and within oxidized proteins (B).

A. Amino acid abundance plot of all annotated *A. thaliana* proteins. Across all annotated TAIR10 proteins, methionine makes up 2.46% of all amino acids (yellow bar), and this drops to 2.21% when excluding the initiator methionine.

B. Methionine frequency plot of the identified in vivo oxidized proteins. By plotting the percentage of methionines in all the identified oxidized proteins, a large majority of these proteins was found to contain less than the expected methionine content of 2.46% (yellow bin).

To further investigate a possible role for the primary structure in the oxidation sensitivity of methionines, an iceLogo sequence alignment [46] of neighboring amino acids was generated for the proteins identified at both time-points. As a positive input, the 17 overlapping proteins with a significant increased oxidation

over time at identical methionines were selected. The remaining 158 proteins with MetO peptides identified at both time-points were selected as the reference set. Methionine was fixed at position 6 (P6) and the five surrounding amino acids, both N- and C-terminal to this site were retrieved (P1 to P11). MetO peptides with significant higher oxidation levels ($p \leq 0.05$) after 3 h compared to 1 h revealed a motif of hydrophobic amino acids such as valine, leucine, isoleucine and methionine in proximity of the oxidation site (**Figure 5**). In addition, the polar amino acid threonine was also found. This enriched motif can be explained by either an increased susceptibility of oxidation due to the hydrophobic environment, or by a decreased reduction by MSRs due to the less preferred substrate recognition of these MetO sites. Concerning the latter, a closer look at the expression profiles of the different *Arabidopsis* MSRs shows a clear up-regulation of MSRB7 and B9 under elevated ROS levels [47-48]. Furthermore, both MSRs cluster together upon transcriptional response towards various perturbations (**Supplemental Figure S3A**). Multiple alignment of the *Arabidopsis* MSR protein sequences was used to generate a phylogenetic tree and revealed a close proximity of MSRB7 and MSRB9. The vast majority of MSRs present in *Arabidopsis*, together with a sequence preference surrounding the oxidation site, thus hint towards specificity of either chemical oxidation or enzymatic reduction. However, which of these two is actually causative, remains to be explored.

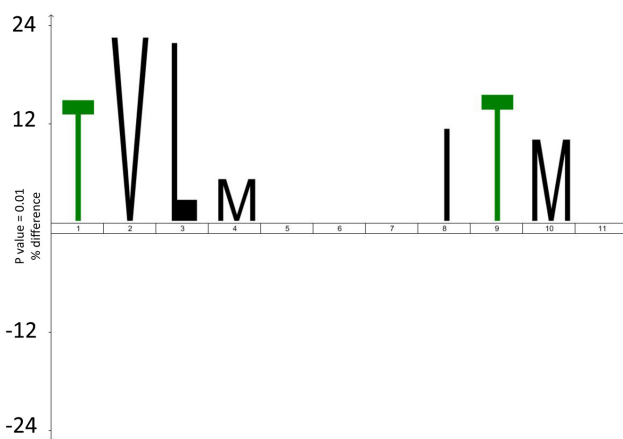


Figure 5: An iceLogo of the amino acid context of the oxidized methionine.

The sequence context of proteins with a significant ($p \leq 0.05$) increased oxidation over time ($n = 17$) reveals a preference ($p \leq 0.01$) for hydrophobic amino acids surrounding the site of methionine oxidation. As a negative reference set, the remaining 158 proteins with identical MetO peptides identified in both time points were chosen. Methionine was fixed at position 6 (P6) and the five surrounding amino acids, both N-terminal (P1-P5) and C-terminal (P7-P11) are shown.

DISCUSSION

Methionine and cysteine are the two sulfur-containing amino acids, and both are rather rare amino acids. Both amino acids can be reversibly oxidised, indicating that such modifications might serve functional roles. Considering the sequence motif (**Figure 5**) in which the most oxidation-sensitive methionines reside, and the identification of identical oxidation sites in proteins belonging to the same family (**Supplemental Table 2**) further hint towards a possible specificity of methionine oxidation, rather than being a random event. Oxidation of methionine increases the polarity of this hydrophobic amino acid and was previously linked to the exposure of otherwise hydrophobic buried regions [27]. The sites of methionine oxidation that increase during the timeframe of exposure to high light intensities show a preference of surrounding

hydrophobic amino acids which might have a protective nature and prevent the exposure of the hydrophilic methionine sulfoxide which would render it susceptible to reduction by methionine sulfoxide reductases. This oxidation-prone motif might as well point to those oxidized methionines that are the least efficiently reduced by the MSR enzymes, as the detected methionine oxidation events are the end result of the interplay between chemical oxidation and enzymatic reduction. The importance of the latter comes from the presence of 14 MSR enzymes found in different cellular compartments of plant cells.

Our compendium of *Arabidopsis thaliana* proteins of which methionines get oxidized upon oxidative stress, available at <http://www.psb.ugent.be/metox> constitutes currently the largest dataset of its kind in plants and forms a base for future studies on functional impact of methionine oxidation. We further discuss some of these proteins that are particularly interesting, given previous findings reported in literature.

One such protein is the small zinc-finger protein methylene blue sensitive 1 (MBS1) (AT3G02790) that acts as a mediator of singlet oxygen responses in the unicellular green alga *Chlamydomonas reinhardtii* [49]. Upon exposure to high light, this protein translocates to distinct granules in the cytosol but the mechanism remains unclear. However, in view of the example of the recently reported hypochlorite-responsive transcription factor in *E. coli* which is activated by methionine oxidation upon oxidative stress [50], oxidation of methionine 62 in MBS1 might well be a plausible mechanism to induce this positional shift. Of further note is the nearly 4 times higher oxidation degree of this protein in light stressed CATALASE 2 knock-out plants.

An interesting class of proteins that were oxidized both after 1 h and 3 h of high light treatment are three members of the rotamase family: cyclophilin 38 (AT3G01480), CYP3 (AT2G16600) and CYP4 (AT3G62030). CYP4 was identified to interact with 12-oxo-phytodienoic acid (OPDA) and links OPDA signaling to amino acid biosynthesis and cellular redox homeostasis in response to stress [51]. Upon interaction, the formation of a complex with O-acetylserine (thiol) lyase B and cysteine synthase is triggered, which leads to an increase of thiol metabolites and the buildup of the cellular reduction potential [52]. Interestingly, all members of this complex were here identified to get oxidized upon high light stress, thus possibly methionine oxidation regulates a cluster of interacting proteins via a redox modification. Also, several photorespiratory enzymes were found to be oxidized, which could be a direct way of sensing elevated hydrogen peroxide levels, in turn directly regulating the pathway involved by methionine oxidation.

Studies related to methionine oxidation in plants thus far focused on the different functions of MSRs. Tarrago *et al.* explored the possibilities to fish for MSRB1 substrates via affinity chromatography and identified 24 possible candidate interactors [44]. Of note is that 23 of these were also identified in our dataset, amongst which CATALASE 2 and 3, confirming oxidation of methionine and demonstrating affinity chromatography as a valuable strategy to look for specific MSR substrates. Recently, glutathione S-transferases F2 and F3 were identified as substrates for MSRB7, where reduction of methionine sulfoxides confers tolerance of *A. thaliana* to oxidative stress [18]. We identified three members of the GST family, GST F9, T21 and T23, of which the tau family members (GST T21 and T23) carried identical sites of methionine oxidation at both time-points sampled. Our results thus indicate the extension of methionine oxidation within the GST family, possibly expanding the general line of defense against oxidative damage. Along this line, two methionine sulfoxide reductases, MSRA2 and MSRA3, were subjected to methionine oxidation themselves. This could suggest a self-regulatory mechanism of methionine reductase activity.

To summarize, we provide the largest dataset of methionine oxidation in plants during oxidative stress treatment, where we compare differences in oxidation between *Arabidopsis* wild-type and CATALASE 2 knock-out, captured the dynamics of oxidation by time-resolved proteome analysis and pinpoint the exact sites of oxidation.

EXPERIMENTAL PROCEDURES

Plant material, growth conditions, stress treatments

Catalase knock-out (*cat2-2*) [35] and wild-type (WT) *Arabidopsis thaliana* plants, ecotype Columbia-0 (Col-0), were grown under elevated CO₂ concentrations (3000 ppm) to impair photorespiration. Individual plants were organized according to a completely randomized block design in a controlled climate chamber (Vötsch Industrietechnik) in a 12:12 day/night regime (relative humidity of 50%, a temperature of 21°C and an irradiance of 100 μmol m⁻² s⁻¹). For high light (HL) treatments, 5 week old plants were transferred to a Sanyo Fitotron plant growth chamber in ambient air conditions (400 ppm CO₂, relative humidity of 55%, 21°C) and continuous HL irradiation of 1,200 μmol m⁻² s⁻¹ for one and three hours. Middle aged leaves (as depicted in Fig. 1) of 15 individual plants per line were sampled, pooled and frozen in liquid nitrogen.

Methionine-sulfoxide COFRADIC

Proteins were extracted from 0.5 g of grinded tissue by adding 0.5 ml of 250 mM Tris-HCl buffer (pH 8.7) containing 150 mM NaCl, 2 mM EDTA, 1 M guanidinium hydrochloride, 1% 3-[(3-cholamidopropyl)dimethylammonio]-1-propane-sulfonic acid (Sigma-Aldrich) and the appropriate amount of the Complete Protease Inhibitor cocktail (Roche, Applied Science). After centrifugation at 16,100 x g for 10 min twice, protein concentrations were measured using the Bradford assay. By adding the appropriate volumes of extraction buffer, the protein concentration of all samples was adjusted to 1.2 mg/ml. Then, cysteines were reduced and alkylated in 10 mM triscarboxyethylphosphine (Pierce) and 20 mM iodoacetamide (Sigma-Aldrich) upon incubation in the dark for 30 min at 30°C. Samples were subsequently desalted on a NAPTM-5 column (Amersham Biosciences) in 1 ml of 50 mM triethylammonium bicarbonate buffer (pH 8), heated for 10 min at 95°C and cooled on ice before adding sequencing-grade endoproteinase Lys-C (Promega) in a ratio of 1:200 (enzyme:substrate, w:w) to digest the samples overnight at 37°C. Next, primary α- and ε-amines were labeled with N-hydroxysuccinimide esters of stable isotopic variants of propionate. Peptides originating from *cat2-2* proteomes were ¹²C₃-propionated, whereas those from Col-0 proteomes were ¹³C₃-propionated by incubation for 1 h at 30°C to a final concentration of 10 mM NHS-label. After quenching remaining N-hydroxysuccinimide esters in 50 mM of glycine for 15 min at 25°C, partial O-propionylation of serine, threonine and tyrosine was reversed by adding hydroxylamine to a final concentration of 50 mM and an incubation for 15 min at 37°C. The samples were acidified to a pH of 3 with acetic acid and equal amounts of peptides were mixed. The COFRADIC technology, relying on diagonal peptide chromatography and the specificity of MSRA and MSRB3 (Jena Bioscience) to specifically isolate peptides carrying *in vivo* oxidized methionines was applied to the equivalent of 500 μg of protein material as described [33] after which peptides were analyzed by LC-MS/MS.

Shotgun proteome analysis

In parallel, shotgun proteomics was applied on peptides fractionated during the first HPLC runs used for the COFRADIC setup. These fractions were pooled per 4, and of each fraction, 10% was kept for LC-MS/MS analysis. These peptide mixtures were vacuum-dried and resolved in 20 μ l of 2% acetonitrile, of which 2.5 μ l was injected for LC-MS/MS analysis as described below.

LC-MS/MS analysis

The obtained peptide mixtures were introduced into an LC-MS/MS system; the Ultimate 3000 RSLC nano (Dionex, Amsterdam, The Netherlands) in-line connected to an LTQ Orbitrap XL (Thermo Fisher Scientific, Bremen, Germany) for analysis. The peptide mixture was first loaded on a trapping column at a flow rate of 10 μ l/min (made in-house, 100 μ m internal diameter (I.D.) x 20 mm, 5 μ m beads C18 Repronil-HD, Dr. Maisch). After flushing from the trapping column, the sample was loaded on a reverse-phase column (made in-house, 75 μ m I.D. x 150 mm, 5 μ m beads C18 Repronil-HD, Dr. Maisch). Peptides were loaded with solvent A (0.1% trifluoroacetic acid, 2% acetonitrile), and were separated with a linear gradient from 2% solvent A' (0.05% formic acid) to 55% solvent B' (0.05% formic acid and 80% acetonitrile) at a flow rate of 300 nl/min followed by a wash reaching solvent B'.

The mass spectrometer was operated in data-dependent mode, automatically switching between MS and MS/MS acquisition for the six most abundant peaks in a given MS spectrum. In the LTQ-Orbitrap XL, full scan MS spectra were acquired in the Orbitrap at a target value of 1E6 with a resolution of 60,000. The six most intense ions were then isolated for fragmentation in the linear ion trap, with a dynamic exclusion of 60 s. Peptides were fragmented after filling the ion trap at a target value of 1E4 ion counts. From the MS/MS data in each LC run, Mascot Generic Files were created using the Mascot Distiller software (version 2.3.2.0, Matrix Science). While generating these peak lists, grouping of spectra was allowed with a maximum intermediate retention time of 30 s and maximum intermediate scan count of 5 was used where possible. Grouping was done with 0.005 Da precursor tolerance. A peak list was only generated when the MS/MS spectrum contained more than 10 peaks. There was no de-isotoping and the relative signal to noise limit was set at 2. These peak lists were then searched with the Mascot search engine (Matrix Science) using the Mascot Daemon interface (version 2.3, Matrix Science). Spectra were searched against the TAIR database (version 10 containing 27,416 protein-coding genes). Two searches were performed as described [36]. In a first search, the quantitation configuration in Mascot was employed where propionate labels were set exclusive to lysines and peptide N-termini. The second search left out the propionate label on peptide N-termini, but considered protein N-terminal acetylation and pyroglutamate formation of glutamine as variable modifications. In both searches methionine oxidation was set as a fixed modification. If a MS/MS spectrum was matched to two different peptides following both searches, the match with the highest score was retained. Mass tolerance on precursor ions was set to \pm 10 ppm (with Mascot's C13 option set to 1) and on fragment ions to \pm 0.5 Da. The peptide charge was set to 1+,2+,3+ and the instrument setting was on ESI-TRAP. The enzyme was set to endoproteinase-LysC, allowing for 1 missed cleavage, and cleavage was also allowed when lysine was followed by proline. Only peptides that were ranked one and scored above the threshold score, set at 99% confidence, were withheld. We calculated a false discovery rate of 2% by creating a reverse database of the *Arabidopsis thaliana* TAIR database. Searches were performed both against the forward and reverse database and the

false discovery rate was calculated based on the method of Elias and Gygi (2007) [37] using the following formula: $FDR = (\#false\ positives)/(\#true\ identifications) * 100$. Identified peptides were quantified using the Mascot Distiller Toolbox (MatrixScience) in the precursor mode. This software tries to fit an ideal isotopic distribution on the experimental data based on the peptide average amino acid composition. This is followed by extraction of the XIC signal of both peptide components (light and heavy) from the raw data. Ratios are calculated from the area below the light and heavy isotopic envelope of the corresponding peptide (integration method 'trapezium', integration source 'survey'). To calculate this ratio value, a least squares fit to the component intensities from the different scans in the XIC peak was created. MS scans used for this ratio calculation are situated in the elution peak of the precursor determined by the Distiller software (XIC threshold 0.3, XIC smooth 1, Max XIC width 250). To validate the calculated ratio, the standard error on the least square fit has to be below 0.16 and correlation coefficient of the isotopic envelope should be above 0.97.

The data have been uploaded in PRIDE with the following details:

Project Name: The dynamics of protein-bound methionine oxidation events in Arabidopsis thaliana during oxidative stress

Project accession: PXD001286 Project DOI: 10.6019/PXD001286

Reviewer account details: Username: reviewer67801@ebi.ac.uk Password: WzQy9ri5

Quantitative data analysis

Using Huber robust statistics, the median, standard deviation and 95% confidence intervals were calculated in R for both the methionine sulfoxide datasets as well as for the shotgun datasets. In each set-up the median ratio value was subtracted from the calculated log₂ ratio values to rescale the distribution of ratio values around $\mu = 0$. All significant spectra (95% CI, $p \leq 0.05$) as well as the peptides denominated "FALSE" by Mascot were manually validated using XCalibur (Thermo Scientific). After recalculation of the Huber limits (95% confidence interval (CI) settings) and rescaling, the ratio values of methionine-containing peptides were corrected for protein abundance differences (when available) by subtracting the rescaled log₂ values, thus correcting for possible altered protein synthesis/degradation. A final calculation was then done of the 95% CI enables to identify significantly differently oxidized proteins after 1 h and 3 h of exposure to HL stress.

ACKNOWLEDGEMENTS

S.J. is supported by a Ph.D grant of the Institute for the Promotion of Innovation through Science and Technology in Flanders (IWT-Vlaanderen). B.G. is a Postdoctoral Fellow of the Research Foundation - Flanders (FWO-Vlaanderen). F.V.B. and K.G. acknowledge support of a research grant from the Fund for Scientific Research – Flanders (Belgium) (grant number G.0038.09N). F.V.B. further acknowledges the Ghent University Multidisciplinary Research Partnership ["Ghent BioEconomy" (Project 01MRB 510W)] and Bijzondere Onderzoeksfonds (BOF 01J11311).

SUPPLEMENTAL INFORMATION

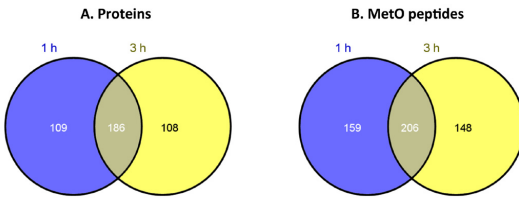


Figure S1: Venn diagrams of the identified oxidized proteins (A) and MetO peptides (B).

Following 1 h of high light exposure 365 MetO peptides were identified in 296 proteins, whereas after 3 h there were 354 MetO peptides in 294 proteins. There is a considerable overlap of 186 proteins that contain 206 identical MetO sites at the two time points sampled.

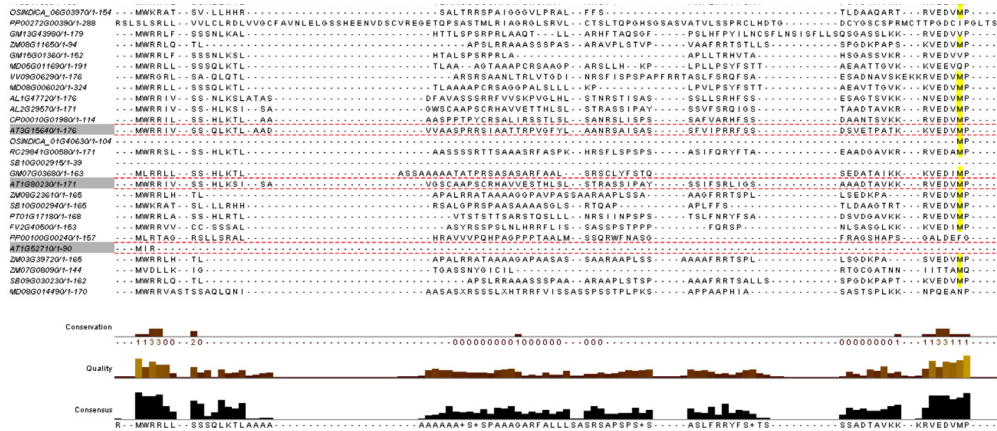
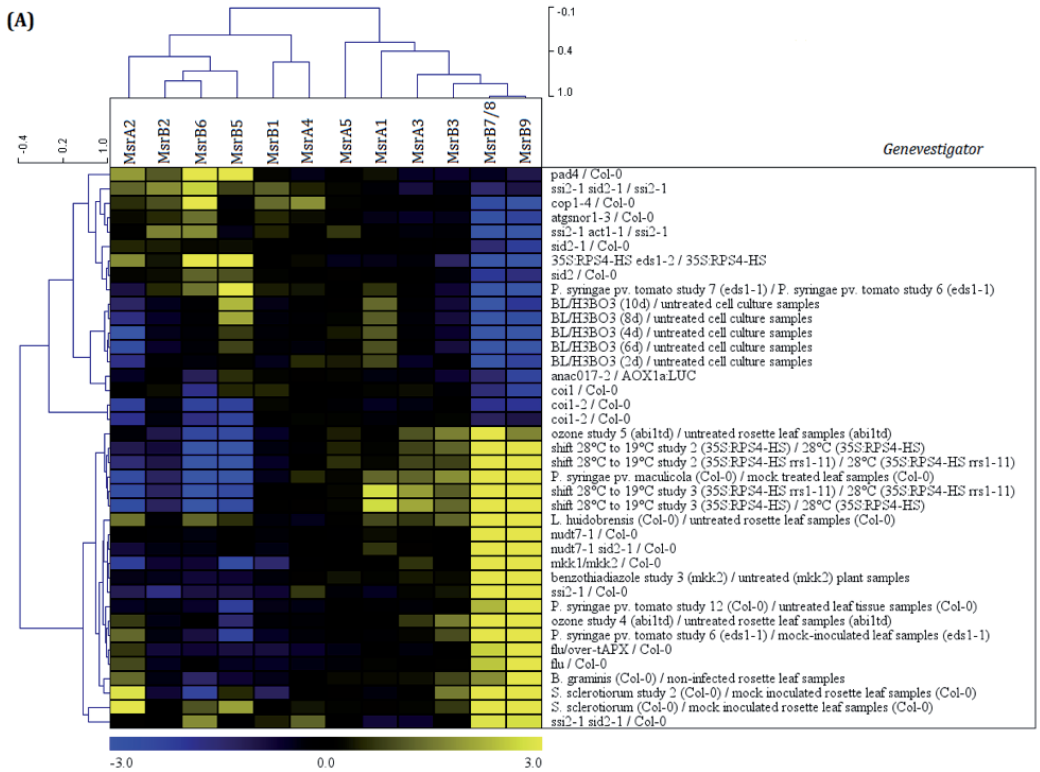


Figure S2: Multiple sequence alignment of the rubredoxin-like superfamily protein genes.

Sequence alignment of all homologous rubredoxin genes (43) across the plant kingdom (19 species) shows that the site of methionine oxidation (highlighted in yellow) lies within a conserved sequence patch. The 3 Arabidopsis genes are boxed with red dotted lines.



(B)

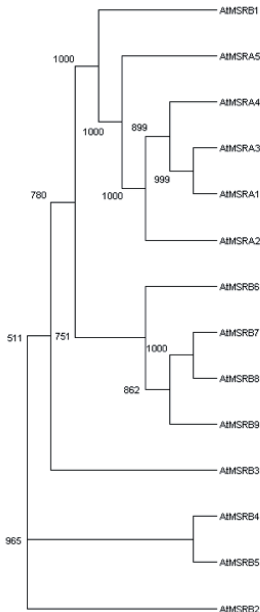


Figure S3: Hierarchical clustering of the expression profiles of the Arabidopsis thaliana MSR genes.

The expression profiles of the Arabidopsis MsrA and MsrB genes were clustered using GENEVESTIGATOR. Upon different perturbations, both biotic and abiotic stresses (A), in the different anatomical parts (B) or during development (C), the expression profiles cluster differently, while MSRB7 and B9 always cluster together. These genes also show an initial low expression profile going through different stages during development suggesting a stress responsive role.

A11G4Z50.1	419	SDGTIGERSVERMK	54	28	2,162	0,797
A11G4B85.0.1	245	MIAADAVRTK	53	31	1,549	0,467
A11G77180.1	442	VALGMASGTGK	59	30	2,391	0,842
A12G77680.1	353	SVLSLMMVPTLEK	46	31	2,238	0,847
A12G4390.1	138	ELMVAQPTK	33	31	1,745	0,653
A13G4697.0.1	172	ELMVAQPTK	32	31	1,745	0,653
A13G4697.0.1	605	TVPTVMVIGK	57	31	1,212	0,664
A11G31180.1	359	MIEDAVDAHK	49	31	0,728	-0,801
A12G4084.0.1	90	SVLRSEFGMK	48	30	1,289	-0,816
A13G2030.1	377	DLVGWVK	35	32	0,674	-0,884
A13G2030.1	456	EVDVILVGGMTRVPK	40	31	1,019	-0,996
A13G2030.1	456	DVYTRMK	38	28	2,800	-0,996
A11G3990.1	34	ELMVAQPTK	4	28	2,800	-0,996
A11G3990.1	2	AKASTMVAQPTK	36	33	0,952	-1,792
A12G4090.1	50	IAGFSTHLMK	62	32	1,773	-1,519
A12G4090.1	138	MHSYDQVGGQK	48	29	1,232	-1,757
A14G17040.1	204	GNRSALPSSTIMIK	53	32	0,980	-2,321
407	419	SDGTIGERSVERMK	54	28	2,162	0,797
245	255	MIAADAVRTK	53	31	1,549	0,467
442	462	VALGMASGTGK	59	30	2,391	0,842
353	366	SVLSLMMVPTLEK	46	31	2,238	0,847
138	145	ELMVAQPTK	33	31	1,745	0,653
172	182	ELMVAQPTK	32	31	1,745	0,653
605	615	TVPTVMVIGK	57	31	1,212	0,664
359	370	MIEDAVDAHK	49	31	0,728	-0,801
90	99	SVLRSEFGMK	48	30	1,289	-0,816
377	342	DLVGWVK	35	32	0,674	-0,884
456	462	DVYTRMK	38	28	2,800	-0,996
456	392	EVDVILVGGMTRVPK	40	31	1,019	-0,996
34	34	ELMVAQPTK	4	28	2,800	-0,996
2	16	AKASTMVAQPTK	36	33	0,952	-1,792
50	59	IAGFSTHLMK	62	32	1,773	-1,519
138	150	MHSYDQVGGQK	48	29	1,232	-1,757
204	217	GNRSALPSSTIMIK	53	32	0,980	-2,321
plastid movement impaired1						
chorismate synthase, putative / 5-enolpyr						
chromatin protein family						
Pyridoxal phosphate (PLP)-dependent tran						
Ribosomal protein L3 family protein						
Ribosomal protein L3 family prote						
alpha-glucan phosphorylase 2						
isopropylmalate dehydrogenase 3						
disproportionating enzyme 2						
PRIMIDINE B						
mitochondrial heat shock protein 70-1						
heat shock protein 90.1						
heat shock protein 90.1						
chlorophyll a/b binding protein 3 (LEA3) [ar						
chlorophyll a/b binding protein 3						
Ribosomal S17 family protein						
starch branching enzyme 2.1						
CLP protease R-subunit 4						

Supplemental Table S1: Identified MetO sites.

All identified MetO sites are here described. The column "ion coverage" depicts the identified y-ions in red while b-ions are underlined>. All ratios are shown as log2 values and the column "corr Ratios" are the normalized manually validated ratios that have been corrected for protein abundance.

A.

AGI	number of Met	MetO peptide	description
AT3G09820	10	HLPMYDEMSQK	adenosine kinase 1
AT5G03300	10	HLPMYDEMSSK	adenosine kinase 2
AT2G19830	10	ATTETVDALRTGASAMK	SNF7 family protein
AT4G29160	11	ATTETVDALRSGASAMK	SNF7 family protein
AT4G14880	10	DRIGFSMISDAEK	O-acetylserine (thiol) lyase (OAS-TL) isoform A1
AT2G43750	9	DRIGYSMITDAEEK	O-acetylserine (thiol) lyase B
AT3G59760	16	DRIGYSMVTDAEQK	O-acetylserine (thiol) lyase isoform C
AT1G23190	12	ELVARMGLGK	Phosphoglucosyltransferase/phosphomannosyltransferase family protein
AT1G70730	12	ELVARMGLSK	Phosphoglucosyltransferase/phosphomannosyltransferase family protein
AT1G62380	11	EPFPAAMK	ACC oxidase 2
AT1G05010	9	EPFPAAMK	ethylene-forming enzyme
AT3G09980	11	EVAMVRK	Family of unknown function (DUF662)
AT5G03660	8	EVTMVRK	Family of unknown function (DUF662)
AT1G12270	17	LISAGIVQMK	stress-inducible protein, putative
AT1G62740	20	LISSGIVQMK	stress-inducible protein, putative
AT1G03680	5	MIDPIVNELAQK	thioredoxin M-type 1
AT4G03520	4	MIDPLVNDLQAHTYTKG	Thioredoxin superfamily protein
AT1G66200	8	SMREGGYEIK	glutamine synthase clone F11
AT5G35630	5	SMREGGFEVIK	glutamine synthetase 2
AT1G78360	6	SPLLLEMPHIK	glutathione S-transferase TAU 21
AT1G78320	5	SPLLQMPHIK	glutathione S-transferase TAU 23
AT2G35370	4	VKPSSPAELESIMGPK	glycine decarboxylase complex H
AT1G32470	4	VKPSSPAELEALMGPK	glycine decarboxylating activity
AT4G34110	25	VMRDPNGTSK	poly(A) binding protein 2
AT2G23350	27	VMRDPSTGSK	poly(A) binding protein 4
AT3G04940	8	ERIAYGMIK	cysteine synthase D1
AT5G28020	9	DRIAYSMIK	cysteine synthase D2
AT2G42680	3	AIMQARTDK	multi-protein bridging factor 1A
AT3G58680	2	AIMQARGEK	multi-protein bridging factor 1B
AT2G19730	2	EFPRMSK	Ribosomal L28e protein family
AT4G29410	2	EFSRMSK	Ribosomal L28e protein family
AT1G80230	3	RVEDVMIPIATGHEK	Rubredoxin-like superfamily protein
AT3G15640	2	KVEDVMIPIATGHEK	Rubredoxin-like superfamily protein

AGI	number of Met	MetO peptide	description
AT3G09820	10	HLPMYDEMSQK	adenosine kinase 1
AT5G03300	10	HLPMYDEMSSK	adenosine kinase 2
AT5G13280	12	FGSSVASAERMK	aspartate kinase 1
AT5G14060	12	FGSSVESAEERMK	Aspartate kinase family protein
AT1G58080	6	GRMAADAIDLK	ATP phosphoribosyl transferase 1
AT1G09795	7	GRMAADSLDLK	ATP phosphoribosyl transferase 2
AT1G66200	8	SMREEGGYEIK	glutamine synthase clone F11
AT5G35630	5	SMREEGGFEVIK	glutamine synthetase 2
AT1G78360	6	SPLLEMNPIHK	glutathione S-transferase TAU 21
AT1G78320	5	SPLLQMNPIHK	glutathione S-transferase TAU 23
AT4G16830	3	EMTLDEYEK	Hyaluronan / mRNA binding family
AT4G17520	4	EMTLEEYEK	Hyaluronan / mRNA binding family
AT3G03780	17	QMSAAGIK	methionine synthase 2
AT5G17920	18	QMSAAGTK	Cobalamin-independent synthase family protein
AT2G42680	3	AIMQARTDK	multi-protein bridging factor 1A
AT3G58680	2	AIMQARGEK	multi-protein bridging factor 1B
AT4G14880	10	DRIGFSMISDAEK	O-acetylserine (thiol) lyase (OAS-TL) isoform A1
AT3G61440	17	DRPAIAMIADAEK	cysteine synthase C1
AT4G23400	5	MEGKEEDVMVGANK	plasma membrane intrinsic protein 1*5
AT1G01620	5	MEGKEEDVRVGANK	plasma membrane intrinsic protein 1C
AT4G34110	25	VMRDPNGTSK	poly(A) binding protein 2
AT2G23350	27	VMRDPGTSK	poly(A) binding protein 4
AT1G32470	4	VKPSPAELEALMGPK	Single hybrid motif superfamily protein
AT2G35370	4	VKPSPAELESIMGPK	glycine decarboxylase complex H
AT1G12270	17	LISAGIVQMK	stress-inducible protein, putative
AT1G62740	20	LISSGIVQMK	stress-inducible protein, putative

Supplemental Table S2: MetO sites in protein families are identical.

Identified proteins at 1 h (A) as well as 3 h (B) show a similar sequential context of oxidized methionines within a protein family. This AA specificity surrounding the MetO site is also conserved over time for adenosine kinase, OAS-TL, stress-inducible protein, glutamine synthetase, poly-A binding protein, glutathione S-transferase and multi-protein bridging factor protein families.

REFERENCES

- [1] Van Breusegem, F., Bailey-Serres, J., Mittler, R., Unraveling the tapestry of networks involving reactive oxygen species in plants. *Plant Physiol* 2008, 147, 978-984.
- [2] Ischiropoulos, H., Biological selectivity and functional aspects of protein tyrosine nitration. *Biochem Biophys Res Commun* 2003, 305, 776-783.
- [3] Souza, J. M., Daikhin, E., Yudkoff, M., Raman, C. S., Ischiropoulos, H., Factors determining the selectivity of protein tyrosine nitration. *Arch Biochem Biophys* 1999, 371, 169-178.
- [4] Fries, D. M., Paxinou, E., Themistocleous, M., Swanberg, E., et al., Expression of inducible nitric-oxide synthase and intracellular protein tyrosine nitration in vascular smooth muscle cells: role of reactive oxygen species. *J Biol Chem* 2003, 278, 22901-22907.
- [5] Mittler, R., Vanderauwera, S., Suzuki, N., Miller, G., et al., ROS signaling: the new wave? *Trends Plant Sci* 2011, 16, 300-309.
- [6] Choudhury, S., Panda, P., Sahoo, L., Panda, S. K., Reactive oxygen species signaling in plants under abiotic stress. *Plant Signal Behav* 2013, 8, e23681.
- [7] Neill, S., Desikan, R., Hancock, J., Hydrogen peroxide signalling. *Curr Opin Plant Biol* 2002, 5, 388-395.
- [8] Bienert, G. P., Schjoerring, J. K., Jahn, T. P., Membrane transport of hydrogen peroxide. *Biochim Biophys Acta* 2006, 1758, 994-1003.
- [9] Balsera, M., Uberegui, E., Schurmann, P., Buchanan, B. B., Evolutionary Development of Redox Regulation in Chloroplasts. *Antioxid Redox Signal* 2014.
- [10] Vandenabeele, S., Vanderauwera, S., Vuylsteke, M., Rombauts, S., et al., Catalase deficiency drastically affects gene expression induced by high light in *Arabidopsis thaliana*. *Plant Journal* 2004, 39, 45-58.
- [11] Claeys, H., Van Landeghem, S., Dubois, M., Maleux, K., Inze, D., What Is Stress? Dose-Response Effects in Commonly Used in Vitro Stress Assays. *Plant Physiol* 2014, 165, 519-527.
- [12] Mhamdi, A., Queval, G., Chaouch, S., Vanderauwera, S., et al., Catalase function in plants: a focus on *Arabidopsis* mutants as stress-mimic models. *J Exp Bot* 2010, 61, 4197-4220.
- [13] Couturier, J., Chibani, K., Jacquot, J. P., Rouhier, N., Cysteine-based redox regulation and signaling in plants. *Front Plant Sci* 2013, 4, 105.
- [14] Waszczak, C., Akter, S., Eeckhout, D., Persiau, G., et al., Sulfenome mining in *Arabidopsis thaliana*. *Proc Natl Acad Sci U S A* 2014, 111, 11545-11550.
- [15] Drazic, A., Winter, J., The physiological role of reversible methionine oxidation. *Biochim Biophys Acta* 2014.
- [16] Jacques, S., Ghesquiere, B., Van Breusegem, F., Gevaert, K., Plant proteins under oxidative attack. *Proteomics* 2013, 13, 932-940.
- [17] Kim, G., Weiss, S. J., Levine, R. L., Methionine oxidation and reduction in proteins. *Biochim Biophys*

Acta 2014, 1840, 901-905.

[18] Lee, S. H., Li, C. W., Koh, K. W., Chuang, H. Y., et al., MSR7 reverses oxidation of GSTF2/3 to confer tolerance of *Arabidopsis thaliana* to oxidative stress. *J Exp Bot* 2014.

[19] Savige, W. E., Fontana, A., Interconversion of methionine and methionine sulfoxide. *Methods in enzymology* 1977, 47, 453-459.

[20] Davies, M. J., The oxidative environment and protein damage. *Biochim Biophys Acta* 2005, 1703, 93-109.

[21] Zhang, X. H., Weissbach, H., Origin and evolution of the protein-repairing enzymes methionine sulfoxide reductases. *Biol Rev Camb Philos Soc* 2008, 83, 249-257.

[22] Boschi-Muller, S., Gand, A., Branlant, G., The methionine sulfoxide reductases: Catalysis and substrate specificities. *Arch Biochem Biophys* 2008, 474, 266-273.

[23] Corpas, F. J., Chaki, M., Fernandez-Ocana, A., Valderrama, R., et al., Metabolism of reactive nitrogen species in pea plants under abiotic stress conditions. *Plant Cell Physiol* 2008, 49, 1711-1722.

[24] Vieira Dos Santos, C., Cuine, S., Rouhier, N., Rey, P., The *Arabidopsis* plastidic methionine sulfoxide reductase B proteins. Sequence and activity characteristics, comparison of the expression with plastidic methionine sulfoxide reductase A, and induction by photooxidative stress. *Plant Physiol* 2005, 138, 909-922.

[25] Le, D. T., Tarrago, L., Watanabe, Y., Kaya, A., et al., Diversity of plant methionine sulfoxide reductases B and evolution of a form specific for free methionine sulfoxide. *PLoS one* 2013, 8, e65637.

[26] Rouhier, N., Vieira Dos Santos, C., Tarrago, L., Rey, P., Plant methionine sulfoxide reductase A and B multigenic families. *Photosynthesis research* 2006, 89, 247-262.

[27] Corpas, F. J., Del Rio, L. A., Barroso, J. B., Post-translational modifications mediated by reactive nitrogen species: Nitrosative stress responses or components of signal transduction pathways? *Plant Signal Behav* 2008, 3, 301-303.

[28] Tarrago, L., Laugier, E., Rey, P., Protein-repairing methionine sulfoxide reductases in photosynthetic organisms: gene organization, reduction mechanisms, and physiological roles. *Mol Plant* 2009, 2, 202-217.

[29] Zhao, Y. L., Li, H. L., Gao, Z. H., Gong, Y. F., Xu, H. B., Effects of flavonoids extracted from *Scutellaria baicalensis* Georgi on hemin-nitrite-H₂O₂ induced liver injury. *European journal of pharmacology* 2006, 536, 192-199.

[30] Hardin, S. C., Larue, C. T., Oh, M. H., Jain, V., Huber, S. C., Coupling oxidative signals to protein phosphorylation via methionine oxidation in *Arabidopsis*. *Biochem J* 2009, 422, 305-312.

[31] Gustavsson, N., Kokke, B. P., Anzelius, B., Boelens, W. C., Sundby, C., Substitution of conserved methionines by leucines in chloroplast small heat shock protein results in loss of redox-response but retained chaperone-like activity. *Protein science : a publication of the Protein Society* 2001, 10, 1785-1793.

[32] Wehr, N. B., Levine, R. L., Wanted and wanting: Antibody against methionine sulfoxide. *Free Radic Biol Med* 2012, 53, 1222-1225.

- [33] Ghesquiere, B., Jonckheere, V., Colaert, N., Van Durme, J., et al., Redox proteomics of protein-bound methionine oxidation. *Mol Cell Proteomics* 2011, 10, M110 006866.
- [34] Ghesquiere, B., Gevaert, K., Proteomics methods to study methionine oxidation. *Mass Spectrom Rev* 2014, 33, 147-156.
- [35] Queval, G., Issakidis-Bourguet, E., Hoeberichts, F. A., Vandorpe, M., et al., Conditional oxidative stress responses in the *Arabidopsis* photorespiratory mutant *cat2* demonstrate that redox state is a key modulator of daylength-dependent gene expression, and define photoperiod as a crucial factor in the regulation of H₂O₂-induced cell death. *Plant J* 2007, 52, 640-657.
- [36] Moruz, L., Staes, A., Foster, J. M., Hatzou, M., et al., Chromatographic retention time prediction for posttranslationally modified peptides. *Proteomics* 2012, 12, 1151-1159.
- [37] Elias, J. E., Gygi, S. P., Target-decoy search strategy for increased confidence in large-scale protein identifications by mass spectrometry. *Nat Methods* 2007, 4, 207-214.
- [38] Noctor, G., Veljovic-Jovanovic, S., Driscoll, S., Novitskaya, L., Foyer, C. H., Drought and oxidative load in the leaves of C3 plants: a predominant role for photorespiration? *Ann Bot* 2002, 89 Spec No, 841-850.
- [39] Kagawa, T., Wada, M., Blue light-induced chloroplast relocation. *Plant Cell Physiol* 2002, 43, 367-371.
- [40] Bienert, G. P., Chaumont, F., Aquaporin-facilitated transmembrane diffusion of hydrogen peroxide. *Biochim Biophys Acta* 2014, 1840, 1596-1604.
- [41] Frei dit Frey, N., Muller, P., Jammes, F., Kizis, D., et al., The RNA binding protein Tudor-SN is essential for stress tolerance and stabilizes levels of stress-responsive mRNAs encoding secreted proteins in *Arabidopsis*. *Plant Cell* 2010, 22, 1575-1591.
- [42] Kang, G., Ma, H., Liu, G., Han, Q., et al., Silencing of TaBTF3 gene impairs tolerance to freezing and drought stresses in wheat. *Mol Genet Genomics* 2013, 288, 591-599.
- [43] Frottin, F., Martinez, A., Peynot, P., Mitra, S., et al., The proteomics of N-terminal methionine cleavage. *Mol Cell Proteomics* 2006, 5, 2336-2349.
- [44] Tarrago, L., Kieffer-Jaquinod, S., Lamant, T., Marcellin, M. N., et al., Affinity chromatography: a valuable strategy to isolate substrates of methionine sulfoxide reductases? *Antioxid Redox Signal* 2012, 16, 79-84.
- [45] Kannaste, O., Suomi, T., Salmi, J., Uusipaikka, E., et al., Cross-correlation of spectral count ranking to validate quantitative proteome measurements. *J Proteome Res* 2014.
- [46] Colaert, N., Helsens, K., Martens, L., Vandekerckhove, J., Gevaert, K., Improved visualization of protein consensus sequences by iceLogo. *Nat Methods* 2009, 6, 786-787.
- [47] Kim, C. H., Meskauskiene, R., Apel, K., Laloi, C., No single way to understand singlet oxygen signalling in plants. *Embo Rep* 2008, 9, 435-439.
- [48] Laloi, C., Stachowiak, M., Pers-Kamczyc, E., Warzych, E., et al., Cross-talk between singlet oxygen- and hydrogen peroxide-dependent signaling of stress responses in *Arabidopsis thaliana*. *Proc Natl Acad Sci U S A* 2007, 104, 672-677.

[49] Shao, N., Duan, G. Y., Bock, R., A mediator of singlet oxygen responses in *Chlamydomonas reinhardtii* and *Arabidopsis* identified by a luciferase-based genetic screen in algal cells. *Plant Cell* 2013, 25, 4209-4226.

[50] Drazic, A., Miura, H., Peschek, J., Le, Y., et al., Methionine oxidation activates a transcription factor in response to oxidative stress. *Proc Natl Acad Sci U S A* 2013, 110, 9493-9498.

[51] Kopriva, S., 12-Oxo-phytodienoic acid interaction with cyclophilin CYP20-3 is a benchmark for understanding retrograde signaling in plants. *Proc Natl Acad Sci U S A* 2013, 110, 9197-9198.

[52] Park, S. W., Li, W., Viehhauser, A., He, B., et al., Cyclophilin 20-3 relays a 12-oxo-phytodienoic acid signal during stress responsive regulation of cellular redox homeostasis. *Proc Natl Acad Sci U S A* 2013, 110, 9559-9564.



6

FUNCTIONAL IMPLICATIONS OF METHIONINE OXIDATION: GST AS A CASE STUDY

**SILKE JACQUES , KHADIJA WAHNI, HANS DEMOL,
FRANK VAN BREUSEGEM, JORIS MESSENS AND KRIS GEVAERT**

Silke Jacques wrote the chapter with corrections by Frank Van Breusegem, Joris Messens and Kris Gevaert. Silke Jacques performed the experiments with the help of Khadija Wahni for the enzymatic assays, at the lab of Joris Messens (VUB), Hans Demol optimized the oxidation conditions via LC-MS measurements.

ABSTRACT

The *Arabidopsis thaliana* genome encodes 55 glutathione S-transferases (GSTs), which are most commonly known for their detoxifying capacities via conjugation of glutathione to electrophilic substrates. Interestingly, crops such as rice, maize and soybean, encode larger numbers of GSTs than competing weeds, making GSTs an interesting target for selected engineering since GSTs are accumulating in biotic and abiotic stress conditions. Recently, members of the plant-specific phi and tau GST classes were identified as targets of *in vivo* methionine oxidation upon oxidative stress. Here, we evaluated the impact of oxidation on GSTF9 and GSTT23 enzyme activity. After determination of the methionine oxidation site, hydrogen peroxide mediated oxidation was used to mimic *in vivo* oxidation.. Not only do we provide kinetic parameters of the GSTF9 and GSTT23 enzymes, we also show that oxidation negatively affects their activity. Furthermore, GSTF9 and GSTT23 are prone to stereospecific methionine oxidation as MSRA can only restore GST9 activity, while MSRB is only able to re-establish GSTT23 activity.

INTRODUCTION

Plant cellular physiology is dependent on a fine-tuned redox balance between reactive oxygen species (ROS) production and ROS-scavenging [1]. The ROS homeostasis is governed by a set of antioxidant systems, diversified in their scavenging capacity in terms of specificity and affinity toward the multiple ROS species [2]. Perturbation of ROS homeostasis leads to transient or permanent changes in the redox status and is exploited by plants in different stress signalling mechanisms [3, 4]. Our knowledge on how ROS are perceived and how plants translate this into downstream cellular responses is still fragmented. ROS can provoke reversible and irreversible modifications to proteins. These so-called oxidative posttranslational modifications (Ox-PTMs) not only cause oxidative damage but may also trigger structural changes, affect protein stability, enzyme activity, intracellular localization and alter protein-protein interactions [5]. Since ROS can directly oxidise amino acids, the Ox-PTMs are a plausible mechanism for cells to sense ROS. The sulphur containing amino acids, cysteine and methionine are prone to these oxidations as most ROS are electron-deficient and react preferably with electron-rich amino acid side chains. Cysteine oxidation has a diverse palette of oxidation states such as sulfenylation (R-SOH), formation of disulfide bridges (R-S-S), S-glutathionylation (R-S-SG), sulfinylation (R-SO₂H) and sulfonylation (R-SO₃H). The functional impact of these oxidation states has been studied extensively [6-8]. However, methionine oxidation has only recently emerged as a trigger for reversible regulation of protein function [9, 10].

Previous chapter 4 described the identification of in vivo oxidized methionines in plants exposed to oxidative stress. We mapped the modifications back to single amino acids which is key for the understanding of the possible consequences of this PTM on a protein function. Characterization of the effect of methionine oxidation on individual proteins is essential to a better understanding of how cells interpret oxidative signals that arise from developmental cues and stress conditions. Here, we assess the consequences of methionine oxidation on two members of the glutathione S-transferase (GST) family. In *Arabidopsis thaliana*, 55 genes have been identified to encode this heterogeneous group of cell detoxifying enzymes [11]. GSTs catalyze the conjugation of reduced glutathione (GSH) with electrophilic, often phytotoxic, compounds and are responsive to a range of abiotic and biotic stresses [12-14]. Based on sequence homology, plant GSTs are subdivided into eight classes; phi, tau, theta, zeta, lambda, DHAR, TCQHD and microsomal [15]. Phi and tau constitute the largest classes of GSTs with 13 and 28 members in *Arabidopsis*, respectively. Although plant GSTs share as little as 10% amino acid identity, crystallography studies revealed a high degree of structural conservation resulting in highly similar overall protein folds [16-19]. Soluble GSTs are dimeric hydrophobic protein of 50 kDa with an N-terminal glutathione binding domain (G-site) and a C-terminal alpha-helical domain, which is the binding site for the hydrophobic co-substrate (H-site) [20]. Because of their role in herbicide metabolism, GSTs are interesting candidates to direct selective chemical weed control [21]. Since major crops such as rice, wheat, maize and soybean contain much higher levels of herbicide detoxifying GSTs than competing weeds which creates possibilities for weed control based on relative rates of detoxification [22].

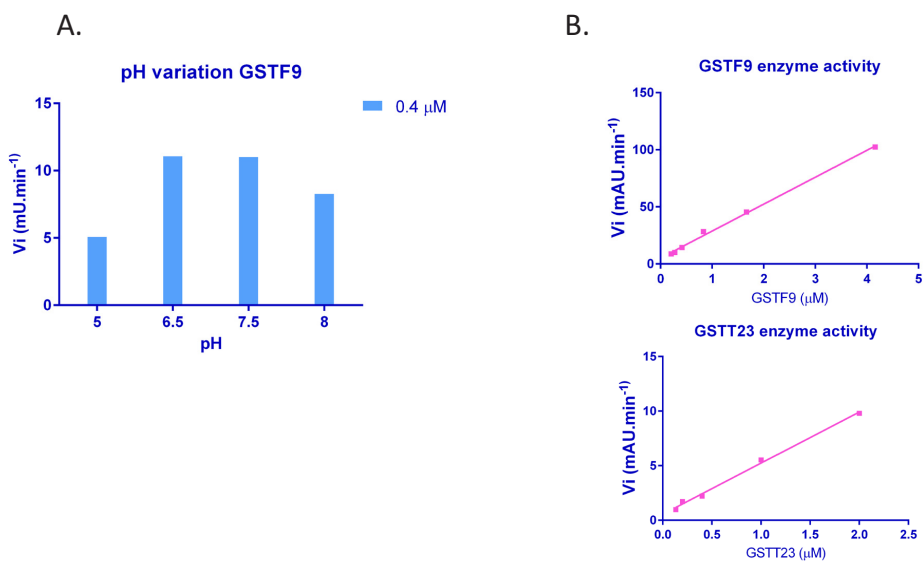
In this chapter the impact of oxidation on the enzyme activity of GST phi9 and GST tau23 that were previously identified as in vivo targets of methionine oxidation was assessed. Conditions of hydrogen peroxide addition were first optimized to mimic the in planta identified oxidations. Next, the kinetic parameters of

both enzymes were characterized. Methionine oxidation was shown to reduce enzyme activity and proven stereospecific with GSTF9 carrying an oxidized methionine S-epimer, while GSTT23 contains an R-epimer.

RESULTS

Kinetic parameters of plant-specific GST phi 9 (F9) and tau 23 (T23)

GST enzyme activity of recombinant GSTF9 and GSTT23 was determined by measuring the conjugation of reduced glutathione with 1-chloro-2,4-dinitrobenzene (CDNB), which is read out by an increase in absorbance at 340 nm. Dialysis of recombinant GSTF9 (AT2G30860) and GSTT23 (AT1G78320) is essential to remove the glutathione that was used during protein purification (see methods section). Whereas the CDNB-assay is typically performed at pH 6.5, we tested a range of pH conditions given that GSTs reside in different subcellular localizations with different pH ($n = 3$). Optimal activity of GSTF9 was noted at pH 6.5 and 7.5. Subsequent experiments were conducted at a pH of 6.5 which is a standard buffer pH for CDNB assays (**Figure 1A**). Initial velocities of the enzymes were calculated via the slope of the absorbance plotted in function of time. GSTF9 and GSTT23 were both active and, as expected, their initial velocities show a linear correlation with the concentration of GST added (**Figure 1B**). To further determine kinetic parameters for GSTF9 and GSTT23, CDNB assays were conducted with varying concentrations of CDNB ($n \geq 3$). In this way, V_{max} , K_M and k_{cat} were determined using the Michaelis-Menten model (**Table 1**). By plotting the initial velocities divided by the enzyme concentration in function of CDNB concentration, the turnover number k_{cat}^{CDNB} was found to be $34.20 \pm 3.60 \text{ min}^{-1}$ and $23.26 \pm 2.55 \text{ min}^{-1}$ for GSTF9 and GSTT23 respectively (**Figure 1C**). By multiplying k_{cat} with the enzyme concentration, the maximum reaction rate (V_{max}) was determined at $13.68 \mu\text{M}/\text{min}$ for GSTF9 while for GSTT23 this becomes $9.30 \mu\text{M}/\text{min}$. The substrate concentration at which the rate of the reaction is at half-maximum (K_M^{CDNB}) was $1.67 \pm 0.36 \text{ mM}$ for GSTF9 and $1.79 \pm 0.37 \text{ mM}$ for GSTT23. This points to an equal preference of GSTF9 and GSTT23 towards CDNB, as the K_M value is inversely related to the affinity of GST for CDNB. However, the turnover number is higher for GSTF9. When comparing the catalytic efficiency using the k_{cat}/K_M value, which is $341.32 \pm 1.83 \text{ M}^{-1}\text{s}^{-1}$ for GSTF9 and $216.45 \pm 1.14 \text{ M}^{-1}\text{s}^{-1}$ for GSTT23, we can conclude that recombinant GSTF9 is more efficient in transferring reduced glutathione to CDNB than GSTT23.



C.

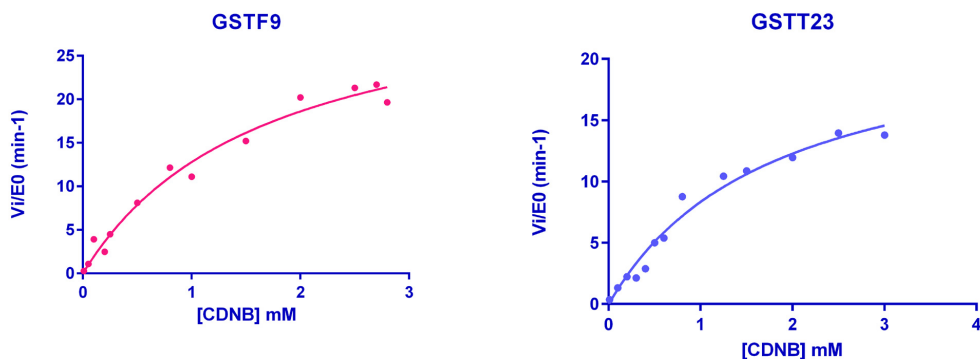


Figure 1: Kinetics of GSTF9 and GSTT23.

Enzyme activities of GSTF9 and GSTT23 were determined via the CDNB assay in different conditions, and a pH of 6.5 was judged optimal for further analysis (A). Both recombinant GSTs transfer GSH to CDNB with initial velocities (V_i) linear to the concentration of added GST with a constant 1 mM f.c. of substrate (B). Kinetic parameters were calculated from the Michaelis-Menten model by plotting $V_i/[GST]$ in function of varying concentrations of CDNB (C).

	k_{cat}^{CDNB} (min^{-1})	K_M^{CDNB} (mM)	k_{cat}/K_M ($\text{M}^{-1} \text{s}^{-1}$)	V_{max} ($\mu\text{M} \text{min}^{-1}$)
GSTF9	34.20 ± 3.60	1.67 ± 0.36	341.32	13.68
GSTT23	23.26 ± 2.55	1.79 ± 0.37	216.45	9.30

Table 1: Overview of the kinetic parameters from GSTF9 and GSTT23.

The kinetic parameters (V_{max} , K_M , k_{cat}) were calculated in GraphPad Prism 6 (GraphPad Software) using the Michaelis-Menten model.

In vitro oxidation of GST proteins

Previously we showed that GSTF9 is oxidized at Met-35, while GSTT21 and GSTT23 were oxidized at Met-48 and Met-47, respectively (Jacques *et al.*, submitted). To assess a possible influence of protein methionine oxidation on GST enzymatic activity, recombinant GSTF9 and GSTT23 were now oxidized with hydrogen peroxide (H_2O_2) prior to the CDNB assay. First, conditions of in vitro H_2O_2 dependent oxidation were optimized to mimic as closely as possible the methionine oxidation found in our previous study. LC-MS measurements were performed on GSTF9 oxidized with varying concentrations H_2O_2 (0.1% – 0.03%) and different incubation times (10 min – 10 h), and at different temperatures (10°C – 22°C). After 135 min of incubation at 10°C with 0.03% H_2O_2 , a single oxidized species of the GSTF9 was most prominently present (Figure 2), whereas at higher doses and longer incubation times LC-MS spectra displayed multiple peaks indicative for multiple oxidation events on the recombinant GST. After purification of this single oxidized GSTF9 protein, endoproteinase Lys-C digestion and peptide analysis by LC-MS/MS, we detected the $\text{G}_{24}\text{VAFETIPVDLMK}_{36}$ peptide that contains a methionine sulfoxide. This peptide is identical to the one previously identified in planta from GSTF9, also oxidized on Met 35. In fact, two forms of this peptide were found, one with and one without the oxidized Met-35 and both were identified by their MS/MS spectrum (Figure 3). A closer look at these MS/MS spectra shows that the mass values of the detected

y-ions of the oxidized and non-oxidized peptides differ by 16 Da from the y_2 -ion onwards, indicative for oxidation of Met-35. Also, as expected, the oxidized peptide elutes earlier from the RP-HPLC column. Taken together, our data show that the in vitro oxidized GSTF9 protein resembles the in vivo oxidized GSTF9 protein, and can thus now be used to determine possible effects of oxidation on enzyme activity.

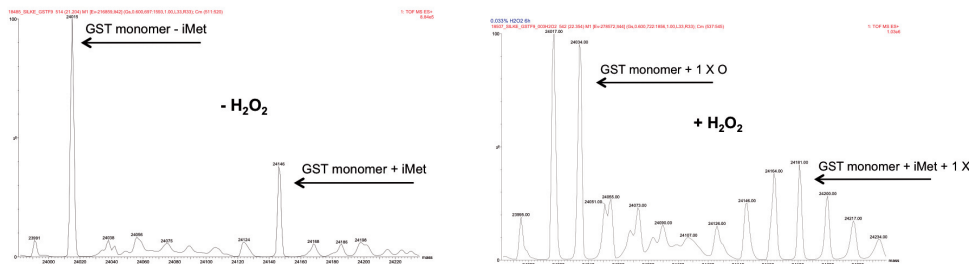


Figure 2: Optimization of in vitro GSTF9 oxidation.

LC-MS (Q-TOF) measurements of GSTF9 before and after addition of 0.03% H_2O_2 and incubation for 135 min at 10°C. GSTF9 is present as a monomer due to the denaturing effect of acetonitrile and the low pH. Also a population of GSTF9 without the initiator methionine was detected. Upon oxidation, a prominent peak of single oxidized GSTF9 appears.

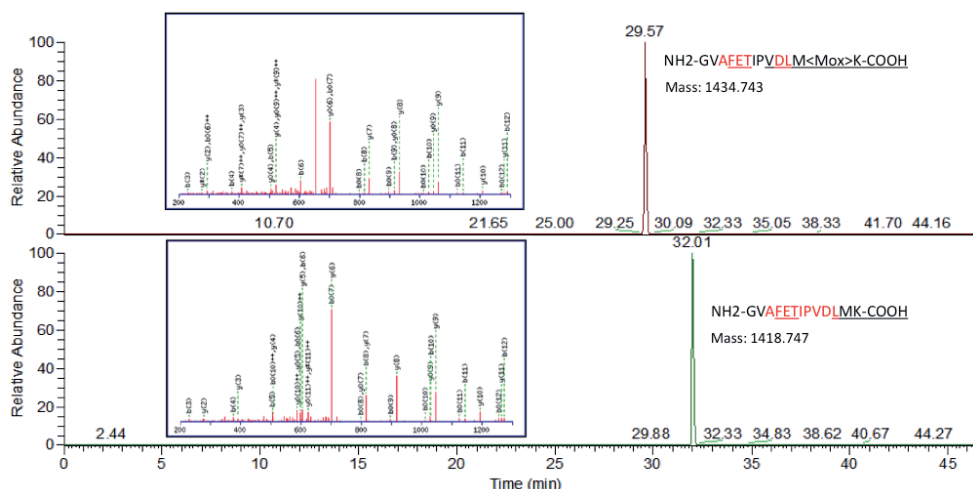


Figure 3: Oxidation of Met-35 in GSTF9.

LC-MS/MS analysis identified the $G_{24}VAFETIPVDLMK_{36}$ peptide after in vitro oxidation of GSTF9. This peptide, previously identified to contain a target for in vivo methionine oxidation (Met-35), is present in two forms; with or without Met-35 oxidized. The extracted-ion chromatogram shows that, as expected, the oxidized peptide with a mass of 1434.743 Da elutes earlier than the non-oxidized peptides (mass of 1418.747 Da). The MS/MS spectra are also shown with b- and y-ions indicated and displayed as underlined residues or residues in red on the peptide sequence, respectively.

Stereospecific methionine oxidation of GST *phi9* and *tau23* reduces enzyme activity

We tested whether the oxidation of GSTF9 and GSTT23 proteins influences their activity. In the CDNB assay both the GSTF9 and GSTT23 activity was significantly ($p \leq 0.01$) reduced upon oxidation and this observation was even more pronounced for higher enzyme concentrations (**Figure 4**) ($n \geq 3$). We observe a loss of 45% of the total GSTF9 enzyme activity, which is in agreement with the mixed population of oxidized and non-oxidized enzyme upon our mild conditions of oxidation.

To assess if this decrease in activity is due to methionine oxidation, the oxidized samples were incubated with methionine sulfoxide reductases, MSRA and MSRB, prior to the CDNB assay ($n \geq 3$). To avoid a possible recovery of GST activity due to the presence of the reducing agent DTT – DTT was used to reduce the MSR enzymes –, DTT was first removed by filtration. In addition, we also tested for possible effects of DTT on GST activity by adding it directly to the oxidized GST proteins. DTT itself induces partial recovery of enzyme activity (**Figure 5**). Our data show thus that an addition of MSRs together with DTT to assess for a direct effect of methionine oxidation on GST activity must be avoided. As such, we continued the CDNB assays with reduced MSRs but in the absence of DTT. Here, the enzymatic activities of GST were restored for up to 88% for GSTT23 and fully restored for GSTF9, indicating that reversible methionine oxidation was responsible for decreased GST activity (Figure 5). Moreover, oxidation of GSTF9 and GSTT23 is stereospecific as GSTF9 activity could only be restored by MSRA, implying that the methionine-sulfoxide is an S-epimer, while the opposite holds true for GSTT23 which appears to hold a methionine-sulfoxide R-epimer that can only be reduced by MSRB (**Figure 5**).

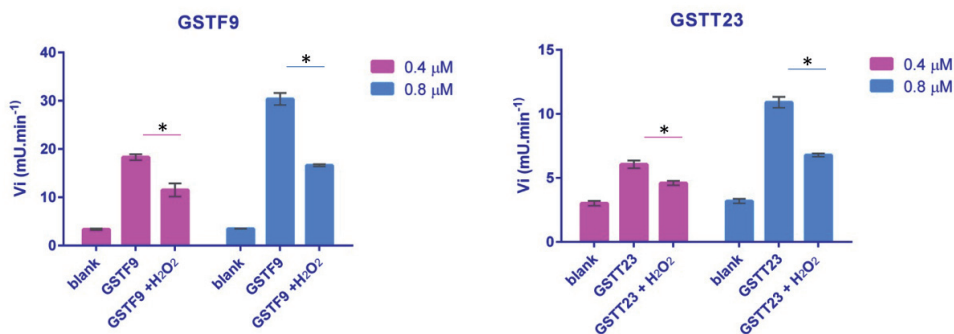


Figure 4: Oxidation negatively affects GSTF9 and GSTT23 activity.

Enzyme activity measurements via the CDNB assay show a significant ($p \leq 0.01$, depicted as *) negative impact for both GSTs upon oxidation. Oxidized GSTF9 has a loss of up to 45% of the total enzyme activity, while the activity of oxidized GSTT23 drops with about 38%.

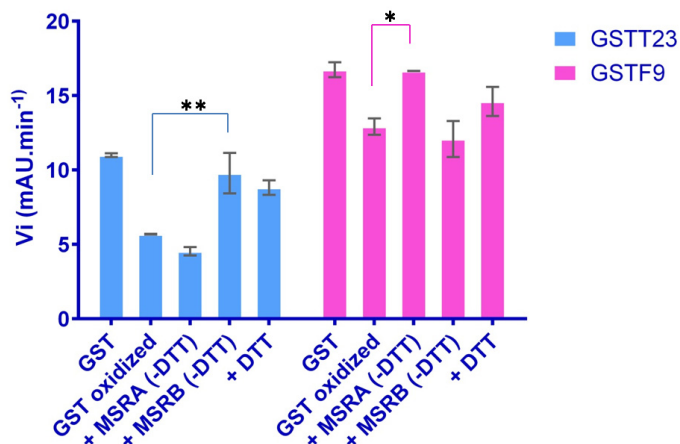


Figure 5: MSR enzymes repair stereospecific oxidation of GSTF9 and GSTT23.

Enzyme activities of oxidized GST can be restored by MSRs. Oxidized GSTF9 is restored to its maximum enzyme activity by MSRA ($p \leq 0.01$, depicted as *), while oxidized GSTT23 is restored to 88% of its activity by MSRB ($p \leq 0.05$, depicted as **). DTT itself also has a positive effect on GST enzyme activity and as such was not added in the buffer solution of the reaction mixture.

Additional proof of concept that it is methionine oxidation in GSTF9 and GSTT23 that is causing the reduced activity is provided by showing that MSRs are active when the oxidized GST proteins are the given substrates. In a coupled enzyme assay, the MSR activity was evaluated by in vitro reconstituting the complete redox cycle necessary to recycle MSR enzymes when active on the provided substrates L-MetO, oxidized GSTF9 or oxidized GSTT23 (**Figure 6A**). Here, thioredoxin and thioredoxin reductase were incubated with the MSR enzymes and NADPH, after which substrate was added and NADPH consumption was followed over time. To exclude possible oxidative effects of remnants of hydrogen peroxide leading to NADPH depletion, addition of hydrogen peroxide (0.03%) instead of substrate was also tested (**Figure 6A**). Once again, stereospecificity was shown as NADPH was consumed when oxidized GSTF9 was added to the redox cycle containing MSRA, but not MSRB. Also, residual hydrogen peroxide from the oxidized samples, which might cause additional oxidation in the redox chain, can be neglected, as no influence on NADPH consumption was observed. By plotting the initial velocities of the progress curves (**Fig. 6A**), it becomes clear that GSTF9 carries a methionine (S)-S-oxide, while GSTT23 contains a methionine (R)-S-oxide (**Figure 6B**). Together, these data show that two members of plant-specific GST proteins ($\phi 9$ and $\tau 23$) are prone to stereospecific methionine oxidation, which negatively affects their enzyme activity.

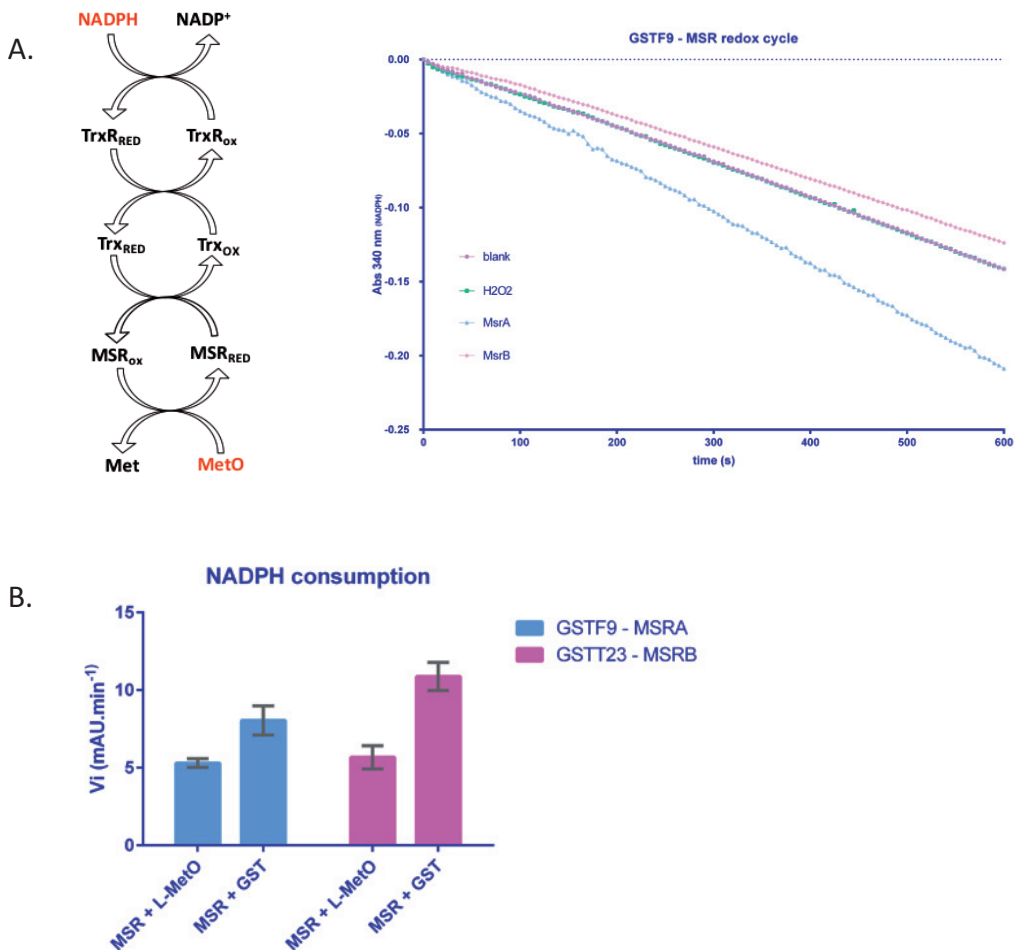


Figure 6: NADPH consumption in the MSR redox cycle.

By addition of NADPH, thioredoxin reductase, thioredoxin, and MSRs in a coupled enzyme assay to the substrates oxidized GSTF9, oxidized GSTT23 or L-MetO, a redox cycle is created in which NADPH consumption is directly linked to MSR activity (**A left panel**).

Progress curves show that MSRA but not MSRB or remnants of H_2O_2 causes NADPH oxidation when GSTF9 was added as a substrate. (**A right panel**). Plotting the initial velocities by which NADPH is consumed depicts MSRA activity upon addition of oxidized GSTF9, while MSRB is only active on oxidized GSTT23. Oxidized L-methionine was included as a positive control for MSR activity (**B**).

DISCUSSION

Glutathione S-transferases are ubiquitously present in plants and are divided into seven classes of which the two largest, the phi and tau classes, have no counterparts in animals [26]. Here, we studied the oxidative post-translational modification of a member of the phi (GSTF9) and tau (GSTT23) classes. Although several functional studies on plant GSTs have been described, enzyme kinetics studies are rarely reported and even non-existing for *Arabidopsis* GST proteins. More specifically for GSTT23 and GSTF9, nothing is known about a specific function or localization other than that GSTF9 is a highly abundant and constitutively expressed protein [27]. The K_M values of GSTF9 (1.9 mM) and GSTT23 (1.8 mM) agree with previously reported values of a GST I in maize (1.6 mM) [28] and a GSTA1/A1 in sorghum (1.9 mM) [29]. Also, the maximum reaction rates, 13.68 $\mu\text{M}/\text{min}$ for GSTF9 and 9.30 $\mu\text{M}/\text{min}$ for GSTT23, correspond to those reported GSTs in sorghum (29.27 $\mu\text{M}/\text{min}$ for GSTA1/A1 and 7.32 $\mu\text{M}/\text{min}$ for GSTB1/B2) [29]. These results indicate that the CDNB assay is indeed a valuable strategy for determining kinetic parameters of isolated plant GSTs. In this particular case, the recombinant GSTF9 and GSTT23 proteins have a tolerable affinity for the substrate, although the turnover numbers and the catalytic efficiencies are relatively low.

GSTF9 and GSTT23 were previously identified in a proteomics survey to discover *in vivo* targets of methionine oxidation upon oxidative stress in *A. thaliana* leaves. To elucidate the possible impact of oxidation on the enzymatic properties, *in vitro* activity assays were performed which simultaneously served as a validation for the previously reported methionine oxidation. Since the exact sites of oxidation are also specified, the conditions of hydrogen peroxide exposure were optimized as to create specific methionine oxidation (**Figures 2-3**). Both enzymes were sensitive towards oxidation, which had a negative impact on their glutathione transferase activities (**Figure 4**). Interestingly, the enzyme activities of both oxidized GSTs can be restored by MSRs, but MSRA repairs GSTF9, while MSRB repairs GSTT23. This clearly points towards stereospecific methionine oxidation of GSTs, where GSTF9 carries an S-epimer and GSTT23 an R-epimer. Rebuilding the complete redox cycle to reduce oxidized methionine sulfoxide reductases after a single catalytic event was used as an alternative method to evidence MSR activity by measuring NADPH consumption in function of time. Apart from this, it also emphasizes the conservation of the reduction-oxidation systems across species as the building blocks to assemble the redox cycle were descending from *Corynebacterium* up to *Arabidopsis*.

The oxidized methionine residues in GSTF9 and GSTT23 are residing in the N-terminal domain, which has evolved from the thioredoxin fold and is structurally similar to it [20]. Since this domain forms the glutathione binding pocket, a reduction of enzyme activity might be due to a hindrance of the hydrophilic oxygen atom attached to the otherwise hydrophobic methionine. Since GSTs are so numerous present in *Arabidopsis*, it is difficult to predict the outcome of decreased GST activity on cellular viability. If oxidation is specifically directed towards only a few members of the large GST family, they might target very precise processes. Thus far, no specific functions have been assigned to GSTF9 and GSTT23, nor is their localization specified. Allocation of exact functions for these enzymes is a first step to get insights into the *in vivo* consequences of reduced activity upon oxidation. In analogy to a petunia GST involved in anthocyanin sequestration through the binding of flavonoids [30], GSTF9 and GSTT23 might be involved in particular metabolic pathways. It could also be hypothesized that upon oxidative stress, methionine oxidation prevents binding of glutathione to GST, hereby increasing the pool of available glutathione. This

could lead to a higher rate of hydrogen peroxide detoxification via the glutathione-ascorbate cycle [31]. Multiple sequence alignment of the homologous GSTF9 and GSTT23 protein families further hints towards the importance of this oxidation. Despite the overall little sequence homology between GST proteins, methionine of the identified oxidation sites is conserved in a remarkable set of plant species. Met-35 of GSTF9 is, amongst others, conserved in the homologous genes of soybean, grape vine, sorghum and papaya while Met-47 of GSTT23 is conserved in proteins of poplar, apple, rice, cassava and strawberry. Recently, two other members of the GST phi class (GSTF2/F3) were shown to be substrates of MSRB7 upon hypochlorous acid treatment [32]. MSRB7 was capable of restoring the activities of oxidized GSTF2 and GSTF3 in vitro, although these results must be interpreted with the necessary caution, as 10 mM DTT was present in the incubation buffer of MSR and GST. Indeed, we here demonstrated that such conditions are far from optimal as DTT itself has a positive effect on the readout of GST enzyme activity (**Figure 5**).

EXPERIMENTAL PROCEDURES

Recombinant protein expression and purification

Gateway™ custom pENTR223 vectors (TAIR) containing coding sequences of full-length GSTF9 (AT2G30860) and GSTT23 (AT1G78320) proteins were recombined into pDEST14 Gateway™ destination vectors. BL21 Star™ One Shot chemically competent *E. coli* cells (Invitrogen) were transformed and GSTF9 and GSTT23 protein production was induced with 0.2 mM isopropyl β -d-1-thiogalactopyranoside (IPTG) in growing cultures of *E. coli* cells reaching an OD_{600} of 0.8. After incubation overnight at 16°C, cells were centrifuged for 10 min at 2700 x g, re-suspended in 20 ml cold phosphate buffer saline with 1 mM DTT, 1% Triton X-100 and cComplete Protease Inhibitor Cocktail (Roche). Sonication for 5 min with 10 s pulses was followed by centrifugation for 10 min at 10000 x g to remove cellular debris, after which the recombinant GST proteins were purified from the supernatant by affinity chromatography using immobilized glutathione (GSTrap HP Columns, GE Healthcare). Elution of the affinity-trapped GST proteins was done using a 50 mM Tris-HCl (pH 8) buffer containing 10 mM of reduced glutathione.

LC-MS(/MS) measurements of the oxidized recombinant GSTF9 protein

The reduced glutathione that was present in the elution buffer was removed by desalting over a 0.7 ml Polyacrylamide Spin Desalting Column (Thermo Scientific Pierce) following the instructions of the manufacturer. During this step, the GSTF9 protein buffer was exchanged with 10 mM ammonium acetate, pH 7. Then, multiple conditions of hydrogen peroxide induced protein oxidation were tested (varying concentration of H_2O_2 , incubation time and temperature) in order to obtain the highest amount of a single oxidized form of GSTF9.

The oxidized GSTF9 protein was first analyzed by LC-MS on a nanoACQUITY UPLC in-line connected to a Q-TOF Premier (Waters). The samples (6 μ l) were first loaded on a trapping column (made in-house, 100 μ m internal diameter (I.D.) x 20 mm, 5 μ m beads Reprosil-pure 300 C4, Dr. Maisch) at a flow rate of 10 μ l/min in 0.1% TFA and 2% ACN. After 4 min, the trapping column was placed in-line with the analytical

reverse-phase column (made in-house, 75 mm I.D. x 150 mm, 3 μm beads Reprosil-pure 300 C4, Dr. Maisch). The proteins were eluted using a standard linear water-acetonitrile gradient with 0.1% formic acid as ion pairing agent. Optimal conditions of selective oxidation of the GSTF9 proteins were found when 0.03% H_2O_2 was used for 135 min at 10°C . For such oxidized proteins, the Q-TOF Premier mass spectrometer was uncoupled and replaced by a UV detector (214 nm) to trace and collect the single oxidized species of GSTF9. This protein fraction was then digested overnight at 37°C by sequencing-grade endoproteinase Lys-C (Wako, 1:50, enzyme:substrate, w:w). Finally, LC-MS/MS analysis (Orbitrap Velos, Thermo Fisher Scientific) was used for peptide identification as described in [23] using the Mascot search engine (Matrix Science) with the Mascot Daemon interface (version 2.3, Matrix Science). Spectra were searched against the TAIR10 database (containing 27,416 protein-coding genes) and methionine oxidation was set as a variable modification. The enzyme was set to endoproteinase-LysC, allowing for 1 missed cleavage, and cleavage was also allowed when lysine was followed by proline. Only peptides that were ranked one and scored above the threshold score, set at 99% confidence, were withheld.

GST enzyme activity assays

Reduced glutathione was removed from the recombinant GSTF9 and GSTT23 proteins by dialysis in 100 mM potassium phosphate buffer (pH 6.5) with 0.1% Triton X100. Glutathione S-transferase activity was measured by conjugation of reduced glutathione with 1-chloro-2,4-dinitrobenzene (CDNB), which is accompanied by an increase in absorbance at 340 nm [24]. The reaction took place in 200 μl with 2 mM reduced glutathione and 1 mM CDNB as final concentrations. Every 20 s during 8 min the absorbance was measured from which the initial velocities in milli-absorbance units per min were deduced (V_i). For determination of the kinetic parameters (V_{max} , K_m , k_{cat}), calculated in GraphPad Prism 6 (GraphPad Software), the concentration of CDNB was varied and plotted against the initial velocities divided by the enzyme concentrations according to the formula: $\frac{V_i}{E_0} = \frac{V_i}{\epsilon (\text{CDNB}) \times \text{pathlength per well} \times E_0} = k_{\text{cat}} \times \frac{[S]}{K_M + [S]}$ where E_0 corresponds to the GST enzyme concentration, ϵ to the extinction coefficient of CDNB and V_i to the initial velocity. Activity measurements were also performed with oxidized GST proteins that were obtained after incubation in 0.03% H_2O_2 for 135 min at 10°C . Recombinant human MSRA and MSRB3 (Jena Bioscience) were pre-incubated with 10 mM DTT for 30 min at room temperature and filtered over a Bio-Spin column (Bio-Rad). Subsequently, the oxidized GST proteins were co-incubated with either 10 mM DTT or with the reduced MSRA or MSRB3 in a 1:1 MSR:GST concentration ratio in 100 mM Tris-HCl buffer pH 7.4 for 30 min at room temperature before activity measurements. All measurements were performed at least in triplicate.

Redox cycle

The redox cycle of the MSR enzyme is rebuilt by addition of 500 μM NADPH (Sigma), 12 μM Cg thioredoxin and 6 μM Cg thioredoxin reductase (both enzymes were recombinantly produced from *Corynebacterium glutamicum* as described in [25]), to 1 μM MSR (human MSRB3 – Jena Bioscience, or *Corynebacterium diphtheriae* recombinant MSRA [25]). After incubation for 10 min at 37°C , 1.6 μM oxidized methionine (L-MetO) or oxidized GST sample was added. MSR activity was measured during 10 min as a decrease of absorbance at 340 nm due to NADPH consumption. Measurements were performed in triplicate.

REFERENCES

- [1] Wrzaczek, M., Brosche, M., Kangasjarvi, J., ROS signaling loops - production, perception, regulation. *Curr Opin Plant Biol* 2013, 16, 575-582.
- [2] Mittler, R., Vanderauwera, S., Gollery, M., Van Breusegem, F., Reactive oxygen gene network of plants. *Trends Plant Sci* 2004, 9, 490-498.
- [3] Mittler, R., Vanderauwera, S., Suzuki, N., Miller, G., et al., ROS signaling: the new wave? *Trends Plant Sci* 2011, 16, 300-309.
- [4] Suzuki, N., Koussevitzky, S., Mittler, R., Miller, G., ROS and redox signalling in the response of plants to abiotic stress. *Plant Cell Environ* 2012, 35, 259-270.
- [5] Karve, T. M., Cheema, A. K., Small changes huge impact: the role of protein posttranslational modifications in cellular homeostasis and disease. *Journal of amino acids* 2011, 2011, 207691.
- [6] Spadaro, D., Yun, B. W., Spoel, S. H., Chu, C., et al., The redox switch: dynamic regulation of protein function by cysteine modifications. *Physiologia plantarum* 2010, 138, 360-371.
- [7] Waszczak, C., Akter, S., Eeckhout, D., Persiau, G., et al., Sulfenome mining in *Arabidopsis thaliana*. *Proc Natl Acad Sci U S A* 2014, 111, 11545-11550.
- [8] Couturier, J., Chibani, K., Jacquot, J. P., Rouhier, N., Cysteine-based redox regulation and signaling in plants. *Front Plant Sci* 2013, 4, 105.
- [9] Drazic, A., Winter, J., The physiological role of reversible methionine oxidation. *Biochim Biophys Acta* 2014.
- [10] Jacques, S., Ghesquiere, B., Van Breusegem, F., Gevaert, K., Plant proteins under oxidative attack. *Proteomics* 2013, 13, 932-940.
- [11] Dixon, D. P., Hawkins, T., Hussey, P. J., Edwards, R., Enzyme activities and subcellular localization of members of the *Arabidopsis* glutathione transferase superfamily. *J Exp Bot* 2009, 60, 1207-1218.
- [12] Frova, C., Glutathione transferases in the genomics era: new insights and perspectives. *Biomol Eng* 2006, 23, 149-169.
- [13] Sappl, P. G., Carroll, A. J., Clifton, R., Lister, R., et al., The *Arabidopsis* glutathione transferase gene family displays complex stress regulation and co-silencing multiple genes results in altered metabolic sensitivity to oxidative stress. *Plant J* 2009, 58, 53-68.
- [14] Dixon, D. P., Skipsey, M., Edwards, R., Roles for glutathione transferases in plant secondary metabolism. *Phytochemistry* 2010, 71, 338-350.
- [15] Dixon, D. P., Edwards, R., Glutathione transferases. *Arabidopsis Book* 2010, 8, e0131.
- [16] Thom, R., Cummins, I., Dixon, D. P., Edwards, R., et al., Structure of a tau class glutathione S-transferase from wheat active in herbicide detoxification. *Biochemistry* 2002, 41, 7008-7020.
- [17] McGonigle, B., Keeler, S. J., Lau, S. M., Koeppe, M. K., O'Keefe, D. P., A genomics approach to the comprehensive analysis of the glutathione S-transferase gene family in soybean and maize. *Plant Physiol* 2000, 124, 1105-1120.

- [18] Thom, R., Dixon, D. P., Edwards, R., Cole, D. J., Laphorn, A. J., The structure of a zeta class glutathione S-transferase from *Arabidopsis thaliana*: characterisation of a GST with novel active-site architecture and a putative role in tyrosine catabolism. *Journal of molecular biology* 2001, 308, 949-962.
- [19] Prade, L., Huber, R., Bieseler, B., Structures of herbicides in complex with their detoxifying enzyme glutathione S-transferase - explanations for the selectivity of the enzyme in plants. *Structure* 1998, 6, 1445-1452.
- [20] Atkinson, H. J., Babbitt, P. C., Glutathione transferases are structural and functional outliers in the thioredoxin fold. *Biochemistry* 2009, 48, 11108-11116.
- [21] Skipsey, M., Cummins, I., Andrews, C. J., Jepson, I., Edwards, R., Manipulation of plant tolerance to herbicides through co-ordinated metabolic engineering of a detoxifying glutathione transferase and thiol cosubstrate. *Plant Biotechnol J* 2005, 3, 409-420.
- [22] Edwards, R., Dixon, D. P., Walbot, V., Plant glutathione S-transferases: enzymes with multiple functions in sickness and in health. *Trends Plant Sci* 2000, 5, 193-198.
- [23] De Antonellis, P., Carotenuto, M., Vandenbussche, J., De Vita, G., et al., Early Targets of miR-34a in Neuroblastoma. *Mol Cell Proteomics* 2014, 13, 2114-2131.
- [24] Habig, W. H., Pabst, M. J., Jakoby, W. B., Glutathione S-transferases. The first enzymatic step in mercapturic acid formation. *J Biol Chem* 1974, 249, 7130-7139.
- [25] Ordonez, E., Van Belle, K., Roos, G., De Galan, S., et al., Arsenate reductase, mycothiol, and mycoredoxin concert thiol/disulfide exchange. *J Biol Chem* 2009, 284, 15107-15116.
- [26] Edwards, R., Dixon, D. P., Plant glutathione transferases. *Methods in enzymology* 2005, 401, 169-186.
- [27] Wagner, U., Edwards, R., Dixon, D. P., Mauch, F., Probing the diversity of the *Arabidopsis* glutathione S-transferase gene family. *Plant molecular biology* 2002, 49, 515-532.
- [28] Labrou, N. E., Mello, L. V., Clonis, Y. D., Functional and structural roles of the glutathione-binding residues in maize (*Zea mays*) glutathione S-transferase I. *Biochem J* 2001, 358, 101-110.
- [29] Gronwald, J. W., Plaisance, K. L., Isolation and characterization of glutathione S-transferase isozymes from sorghum. *Plant Physiol* 1998, 117, 877-892.
- [30] Mueller, L. A., Goodman, C. D., Silady, R. A., Walbot, V., AN9, a petunia glutathione S-transferase required for anthocyanin sequestration, is a flavonoid-binding protein. *Plant Physiol* 2000, 123, 1561-1570.
- [31] Noctor, G., Foyer, C. H., ASCORBATE AND GLUTATHIONE: Keeping Active Oxygen Under Control. *Annual review of plant physiology and plant molecular biology* 1998, 49, 249-279.
- [32] Lee, S. H., Li, C. W., Koh, K. W., Chuang, H. Y., et al., MSRB7 reverses oxidation of GSTF2/3 to confer tolerance of *Arabidopsis thaliana* to oxidative stress. *J Exp Bot* 2014, 65, 5049-5062.





7

CONCLUSIONS AND PERSPECTIVES

GENERAL CONCLUSIONS AND PERSPECTIVES

Reactive oxygen species (ROS) are by-products of aerobic metabolism and as such form an inevitable part of life. Plants need to cope with increased ROS levels, since their sessile lifestyle leads to permanent exposure of changing environmental conditions that impact on ROS homeostasis.

This study focused on the dynamics of the early responses in plants mediated by ROS and led to a global view of the oxidative stress response in *A. thaliana*. We combined next-generation mRNA sequencing, ribosomal profiling and mass spectrometry based proteomics, and made use of a non-invasive model system for hydrogen peroxide modulation (*A. thaliana* catalase 2 knock-out plants). It enabled us to create a multi-angle view of the plant's response to oxidative stress for which transcriptional, translational and post-translational regulation were explored.

Research chapter 3 consists of a comparative omics study in wild-type and CATALASE 2 knock-out plants (*cat2-2*). Because CAT2 is a major peroxisomal H₂O₂ scavenger, *cat2-2* plants will generate accumulated H₂O₂ concentrations when exposed to photorespiratory inducing conditions such as high light and moderate CO₂ concentrations. To perturb ROS-homeostasis, both wild-type and *cat2-2* plants were exposed to these inducing conditions and sampled at multiple time points. Since proteins are the functional entities of a living cell, our initial focus was on the identification of dynamic ROS-responsive proteins. Via a bottom-up, quantitative LC-MS/MS approach, differences in wild-type and *cat2-2* protein abundances were captured in Arabidopsis leaves during the oxidative stress response. Knowledge of the effects of enhanced hydrogen peroxide concentrations on the plant proteome is fragmented and is based on external addition of H₂O₂ [1-4]. Our study of the proteome dynamics upon accumulated hydrogen peroxide levels, without its exogenous addition is therefore unique. This gel-free proteome profiling in *A. thaliana* revealed both known (e.g., DHAR2, APX1, UGT1) and new players (e.g., SAHH1, SAHH2, MAT3) in the ROS-responsive network.

By measuring steady-state protein abundances, the final outcome of the interplay between transcription, translation and (protein-modification linked) degradation is measured. Ribosome profiling [5], an emerging technique to study translational regulation to the highest resolution possible, was used to complement the retrieved proteome data. By exploring the dynamic interplay of transcriptional and translational regulations with steady state protein levels, some general trends could be observed. A prominent role for protein degradation was revealed, which could be an effective strategy of a cell to initiate a fast stress response. Translation was severely affected upon high light stress treatment via an active breakdown of ribosomal proteins. Transcription factors were tightly regulated at the level of transcription, while, as expected due to their general low levels, only few of these were identified in the proteome study. Enhanced hydrogen peroxide accumulation was shown to affect translational efficiency of individual mRNAs, as was previously described for hypoxia [6]. Gene-specific alteration of translational efficiencies upon oxidative stress, illustrate the need of additional data to complement the available transcriptome studies since changes in transcript levels are only the beginning of the story.

The power of an integrative systems-wide approach is the possibility to study complete pathways at different levels of regulation. This contributes greatly to the general understanding of plant adaptability to stress and allows deciphering the key regulators. These insights can be exploited and will allow for a better understanding of processes and pathways that are involved in stress tolerance in plants. We optimized the ribosome profiling technique for *Arabidopsis* cell cultures and grinded leaf tissue, hereby preparing the ground for its application in other plant species such as maize and rice. Moreover, platforms for data analysis (i.e. KNIME and Perseus workflows for proteome analysis and Galaxy workflow for ribo-seq and mRNA seq data) were created and can be consulted and adapted easily. Next to the possibility of implementing these omics technologies for crops, these data contain unparalleled capacities for generating new hypotheses. These data can be employed to verify how genes previously identified in other stress responses behave in response to high light exposure. Doing so, the general stress response can be distinguished from oxidative and high light specific responses. In addition to creating new hypotheses, our data can be used to interpret previous observations, thereby clarifying proposed hypotheses. Also, by looking into the transcriptional and translational regulation of genes, different functional classes could be distinguished. As such, comparing expression patterns could be a way of distinguishing functional groups of (equally annotated) genes, based on the guilt-by-association principle.

Plants can perceive a change in hydrogen peroxide concentrations, which can lead to either a defense response or to cell death [7], implying that plants are capable of using hydrogen peroxide as a signaling molecule. How plants perceive these hydrogen peroxide fluctuations still remains speculative [8]. A direct modification of redox-sensitive transcription factors was suggested [9]. Oxidation of methionine could also be a direct way of sensing hydrogen peroxide and was even found to link to protein phosphorylation [10]. Hence, the identification of proteins with oxidized methionines is a first prerequisite towards understanding the functional effect of methionine oxidation on proteins and the biological processes in which they are involved.

In research chapter 4, we mapped in vivo protein bound methionine oxidation using the COFRADIC proteomics technology [11]. This technology relies on diagonal peptide chromatography and the specificity of MSRs to isolate peptides carrying in vivo oxidized methionines that are subsequently analyzed by tandem mass spectrometry. We compared the differences in methionine oxidation between wild-type and *cat2-2* plants during oxidative stress. We were able to identify the exact sites of methionine oxidation, namely 513 oxidation sites in 403 proteins, as well as to capture the dynamics of oxidation by time-resolved proteome analysis. Our results suggest that methionine oxidation is not a random event, but might steer molecular signaling. Our compendium of *A. thaliana* proteins of which methionines get oxidized upon oxidative stress, available at <http://www.psb.ugent.be/metox¹>, currently constitutes the largest dataset of its kind in plants and forms a base for future studies on functional impact of methionine oxidation. These oxidation sensitive proteins can result in a new era of biotechnology applications in the field, where single amino acid mutations lead to a population of proteins not prone to oxidation. In turn, these proteins might result in an enhanced resistance of plants against a range of adverse environmental conditions

¹Note that a username "metox" and a password "methi0nine" are needed to access the site.

As a case study, the influence of methionine oxidation on the enzyme activity of two members of plant-specific glutathione S-transferases (*phi9* and *tau23*) was examined in chapter 5. We optimized the conditions of *in vitro* hydrogen peroxide mediated oxidation via LC-MS(/MS) measurements to mimic *in vivo* oxidation as closely as possible. Oxidation negatively affects the enzyme activity of both GST *phi 9* and *tau 23*. Intriguingly, MSRA can only restore GST9 activity, while MSRB is only able to re-establish GSTT23 activity, which shows a stereospecific oxidation of methionine residues where GSTF9 carries an S-epimer and GSTT23 an R-epimer. A conformational change could be a possible outcome of the methionine oxidation, resulting in the ob

served loss of activity. Ongoing research aims to monitor conformational changes of GSTF9 and GSTT23 upon oxidation where both limited proteolysis and native MS are deployed strategies, together with the crystallization of non-oxidized and oxidized GST.

This single example shows the explorative power of the methionine oxidation dataset since this reversible posttranslational modification might influence activity (as described for GSTF9 and GSTT23), localization or interaction between proteins. Moreover, this list provides new possible hydrogen peroxide perceptrors, with a particular interest for proteins of the MAPK clade. Methionine oxidation was found to couple oxidative signals to phosphorylation [10], rendering methionine oxidation as a possible missing link between stress and signaling responses in plants. In addition, phenotypic screens of knock-out lines from genes encoding for methionine oxidation-sensitive proteins can reveal interesting candidate stress sensors (ongoing). If a deviating phenotype is observed, a plausible regulation mechanism, namely a reversible oxidation of methionine, is revealed. Also, photosynthetic performance can be determined via chlorophyll fluorescence measurements (ongoing). Knock-out lines complemented either with a wild-type gene or a single amino-acid methionine mutant version, can give further insights how methionine oxidation is related to the observed phenotype. Also, the dynamic trafficking of proteins during stress is a possible regulatory mechanism to render ROS signaling highly flexible to initiate a fast defense response. Consequently, also localization studies of a methionine oxidation-sensitive protein (AT3G02790) are ongoing, where this protein is fused to a GFP fluorescent tag and is under the control of its endogenous promoter. So far, this revealed a re-localization of the protein upon high light exposure, from the plasma membrane towards the nucleolus and the endoplasmic reticulum. Methionine oxidation might be the mechanism behind this stress-induced re-localization and should be further investigated.

The validation and functional characterization of those identified proteins for their biochemical, functional and structural aspects will be the main challenge for the near future. This validation of proteomic results requires a dedicated effort that in most cases focuses on one single protein at a time.

This thesis provides new insights in the dynamics of the oxidative stress response at multiple levels. A multi-angle view on the ROS-mediated responses allows to elucidate complete pathway responsiveness as well as single gene regulation, up to the level of posttranslational methionine oxidation. Future validation studies of this hypothesis-creating data will further contribute to the general understanding of plant adaptability to environmental stresses.

REFERENCES

- [1] Muthuramalingam, M., Matros, A., Scheibe, R., Mock, H. P., Dietz, K. J., The hydrogen peroxide-sensitive proteome of the chloroplast in vitro and in vivo. *Front Plant Sci* 2013, 4, 54.
- [2] Tanou, G., Job, C., Belghazi, M., Molassiotis, A., et al., Proteomic signatures uncover hydrogen peroxide and nitric oxide cross-talk signaling network in citrus plants. *J Proteome Res* 2010, 9, 5994-6006.
- [3] Tanou, G., Job, C., Rajjou, L., Arc, E., et al., Proteomics reveals the overlapping roles of hydrogen peroxide and nitric oxide in the acclimation of citrus plants to salinity. *Plant J* 2009, 60, 795-804.
- [4] Zhou, L., Bokhari, S. A., Dong, C. J., Liu, J. Y., Comparative proteomics analysis of the root apoplasts of rice seedlings in response to hydrogen peroxide. *PloS one* 2011, 6, e16723.
- [5] Ingolia, N. T., Brar, G. A., Rouskin, S., McGeachy, A. M., Weissman, J. S., The ribosome profiling strategy for monitoring translation in vivo by deep sequencing of ribosome-protected mRNA fragments. *Nat Protoc* 2012, 7, 1534-1550.
- [6] Juntawong, P., Girke, T., Bazin, J., Bailey-Serres, J., Translational dynamics revealed by genome-wide profiling of ribosome footprints in Arabidopsis. *Proc Natl Acad Sci U S A* 2014, 111, E203-212.
- [7] Van Breusegem, F., Bailey-Serres, J., Mittler, R., Unraveling the tapestry of networks involving reactive oxygen species in plants. *Plant Physiol* 2008, 147, 978-984.
- [8] Petrov, V. D., Van Breusegem, F., Hydrogen peroxide-a central hub for information flow in plant cells. *AoB Plants* 2012, 2012, pls014.
- [9] Miller, G., Shulaev, V., Mittler, R., Reactive oxygen signaling and abiotic stress. *Physiologia plantarum* 2008, 133, 481-489.
- [10] Hardin, S. C., Larue, C. T., Oh, M. H., Jain, V., Huber, S. C., Coupling oxidative signals to protein phosphorylation via methionine oxidation in Arabidopsis. *Biochem J* 2009, 422, 305-312.
- [11] Ghesquiere, B., Jonckheere, V., Colaert, N., Van Durme, J., et al., Redox proteomics of protein-bound methionine oxidation. *Mol Cell Proteomics* 2011, 10, M110 006866.



8

SAMENVATTING

SAMENVATTING

Om te overleven moeten planten zich snel kunnen aanpassen aan veranderende omgevingsfactoren. Hiervoor moet een plant de omgeving kunnen waarnemen om een gepaste respons te genereren en zich te verweren. Zowel biotische als abiotische stress zorgen voor de productie van vrije zuurstofradicalen (VZR) in de cel wat leidt tot een verstoring van het evenwicht in de redox-status. Zo kunnen planten veranderende VZR concentraties waarnemen en vervolgens gebruiken als een signalisatiemechanisme. Het ontrafelen van de VZR responsieve moleculaire signalisaties waarmee de plant in staat is om deze VZR concentraties te bepalen en om te zetten naar de correcte cellulaire stress respons blijft een grote uitdaging.

Met deze studie willen we een globaal inzicht verwerven in de eerste stappen betrokken bij de responsiviteit van *A. thaliana* gedurende oxidatieve stress, waarbij de verstoring van de VZR balans een signaliserende rol vervult. Hiertoe werden meerdere analysetechnieken toegepast zoals sequenceringsmethoden van mRNA, ribosoom profilering alsook massaspectrometrische toepassingen voor proteoomwijde analyses. Voor dit project werd gebruikt gemaakt van catalase-deficiënte planten (*cat2-2*) die werden blootgesteld aan een hoge lichtintensiteit. Aangezien catalase het voornaamste antioxidantenzym van waterstofperoxide is, kunnen *cat2-2* planten als een niet invasief modelsysteem gebruikt worden om verhoogde waterstofperoxide concentraties te bestuderen. De planten dienen hiertoe enkel blootgesteld te worden aan externe condities die fotorespiratie induceren, zoals hoge lichtintensiteit. In **hoofdstukken 2 en 3** wordt respectievelijk het VZR-gevoelige proteoom geschetst als inleiding en de hoofddoelstellingen van deze thesis gegeven.

Hoofdstuk 4 beschrijft de dynamische wisselwerking van transcriptionele en translationele regulatie, hetgeen invloed heeft op de finale eiwithoeveelheden in planten onder stress. Hiervoor werd een staalname in functie van de tijd uitgevoerd in wild-type en *cat2-2* planten, blootgesteld aan stress inducerende condities. Een kwantitatieve vergelijking van de dynamische VZR-responsieve eiwitten werd mogelijk door peptiden met stabiele isotopen post-metabolisch te merken. Ook werd er een ribosoom profileringsstudie uitgevoerd waarbij de verkregen mRNA-seq en ribo-seq data gecomplementeerd werden met de eiwitdata. Onze data tonen een belangrijke rol van eiwitdegradatie aan, vooral van ribosomale eiwitten. Dit zorgt voor een algemene vermindering van translatie gedurende oxidatieve stress. Bovendien zien we een sterk effect op de translatie-efficiëntie van individuele transcripten tussen beide genotypes. Deze bevindingen steunen onze integratieve aanpak om inzicht te verwerven, van transcript tot eiwit, van de signalisatiemechanismen gedurende stressadaptatie bij planten.

In **hoofdstukken 5 en 6** ligt de focus op methionine oxidatie als een reversibele posttranslationele modificatie (PTM) gedurende oxidatieve stress. De directe oxidatie van aminozuren in eiwitten is namelijk een mogelijks mechanisme van de plant om veranderende VZR concentraties op te merken. Via de COFRADIC technologie waren we in staat om de oxidatiesites te mappen in wild-type en *cat2-2* planten gedurende blootstelling aan hoge lichtintensiteit. Ook de dynamiek van deze oxidatie werd bestudeerd door stalen te nemen bij twee tijdstippen. Het labelen van peptiden met stabiele isotopen stelde ons ook nu in staat om oxidatie te kwantificeren tussen wild-type en *cat2-2* planten. In totaal werden 513 oxidatiesites geïdentificeerd in 403 eiwitten. Onze resultaten ondersteunen de hypothese dat methionine

oxidatie niet enkel een schadelijk gevolg is van oxidatieve stress maar ook bijdraagt tot de moleculaire signalisatie.

De validatie van deze kandidaateiwitten en de invloed van methionine oxidatie op de structuur en functie van deze eiwitten, zullen een belangrijke rol spelen in het begrijpen van de VZR signalisatie op moleculair niveau. In deze thesis werd reeds de impact van oxidatie getest voor twee glutathione S-transferases, phi 9 en tau 23 (**hoofdstuk 7**). Methionine oxidatie van deze enzymen bleek stereospecifiek en had een negatieve impact op hun enzymactiviteit.

Deze thesis heeft getracht om een globaal beeld te schetsen van de oxidatieve stress respons van *A. thaliana*, waarbij transcriptionele, translationele en posttranslationele regulatie onderzocht werden. De verworven kennis draagt bij tot nieuwe inzichten in de regulerende mechanismen van de stressrespons in planten en kan leiden tot nieuwe toepassingen in het verkrijgen van verbeterde stresstolerante gewassen.





9

ADDENDA

ADDENDUM 1. OXIDATIVE POST-TRANSLATIONAL MODIFICATIONS OF CYSTEINE RESIDUES IN PLANT SIGNAL TRANSDUCTION

Cezary Waszczak^{1,2,3,4,5#}, **Salma Akter**^{1,2,3,4,5,8}, **Silke Jacques**^{1,2,6,7}, **Jingjing Huang**^{3,4,5}, **Joris Messens**^{3,4,5*} and **Frank Van Breusegem**^{1,2*}

1 Department of Plant Systems Biology, VIB, 9052 Ghent, Belgium

2 Department of Plant Biotechnology and Bioinformatics, Ghent University, 9052 Ghent, Belgium

3 Structural Biology Research Center, VIB, 1050 Brussels, Belgium

4 Brussels Center for Redox Biology, 1050 Brussels, Belgium

5 Structural Biology Brussels, Vrije Universiteit Brussel, 1050 Brussels, Belgium

6 Department of Medical Protein Research, VIB, 9000 Gent, Belgium

7 Department of Biochemistry, Ghent University, 9000 Gent, Belgium

8 Faculty of Biological Sciences, University of Dhaka, 1000 Dhaka, Bangladesh

present address: Division of Plant Biology, Department of Biosciences, University of Helsinki, 00014 Helsinki, Finland

* To whom correspondence may be addressed: E-mail: joris.messens@vib-vub.be; frank.vanbreusegem@psb.vib-ugent.be

E-mail addresses: Cezary Waszczak: cezary.waszczak@helsinki.fi; Salma Akter: Salma.Akter@vub.ac.be; Silke Jacques: sijac@psb.vib-ugent.be; Jingjing Huang: jingjing.huang@vub.ac.be

Corresponding authors:

Frank Van Breusegem

Department Plant Systems Biology, VIB - Ghent University

Technologiepark 927, B-9052 Ghent, Belgium

Tel.: +32 9 331 39 20; Fax : +32 9 331 38 09

E-mail: frank.vanbreusegem@psb.vib-ugent.be

Joris Messens

Structural Biology Research Center, VIB - Vrije Universiteit Brussel

Pleinlaan 2, B-1050 Brussel, Belgium

Tel.: +32 2 6291992; Fax: +32 2 6291963

E-mail: joris.messens@vib-vub.be

Date of submission: December 16, 2014

Abbreviations: ABA, abscisic acid; ABI1, ABA insensitive 1; APX, ascorbate peroxidase; Asc, ascorbate; CAT, catalase; Cys, cysteine; DsPPT, double specificity protein tyrosine phosphatase; Fdx, ferredoxin; FNR, Fdx:NADP+ reductase; FTR, ferredoxin-thioredoxin reductase; Gpx, glutathione peroxidase; GR, glutathione reductase; Grx, glutaredoxin; GSH, glutathione; JA, jasmonate; MAPK, mitogen-activated protein kinase; NTR, NADPH-dependent thioredoxin reductases; OPDA, 12 oxo phytodienoic acid; Ox-PTMs, oxidative post-translational modifications; PR, pathogenesis-related; Prx, peroxiredoxin; PTP, protein tyrosine phosphatase; RNG, reactive nitrogen species; ROS, reactive oxygen species; SA, salicylic acid; SAR, systemic acquired resistance; SOD, superoxide dismutase; Srx, sulfiredoxin; Trx, thioredoxin.

ABSTRACT

In plants, fluctuation of the redox balance by altered levels of reactive oxygen species (ROS) can affect many aspects of cellular physiology. ROS homeostasis is governed by a diversified set of antioxidant systems that allow maintaining redox homeostasis. Perturbation of this homeostasis leads to transient or permanent changes in the redox status and is exploited by plants in different stress signaling mechanisms. Understanding how plants sense ROS and transduce these stimuli into downstream biological responses is still a major challenge. ROS can provoke reversible and irreversible modifications to proteins that are acting in diverse signaling pathways. These oxidative post-translational modifications (Ox-PTMs) either lead to oxidative damage and/or trigger structural alterations in these target proteins. Characterization of the effect of individual Ox-PTMs on individual proteins is the key to a better understanding of how cells interpret oxidative signals that arise from developmental cues and stress conditions. This review focuses on ROS-mediated Ox-PTMs on cysteine residues. The cysteine side chain, with its high nucleophilic capacity, appears to be the principle target of ROS. Ox-PTMs on cysteine residues participate in various signaling cascades initiated by other plant stress hormones. We review the mechanistic aspects and functional consequences of cysteine Ox-PTMs on specific target proteins in view of stress signaling events.

Key words: redox regulation, cysteine oxidative post-translational modification, phytohormone signaling, reactive oxygen species

INTRODUCTION

Plants continuously need to adapt their development towards fluctuating environmental conditions in order to survive and aim for optimal fitness (Wituszyńska et al., 2013a; Wituszyńska et al., 2013b). These adaptations require mechanisms that are constantly monitoring, sensing and transducing a diverse array of environmental stimuli. Besides changes in phytohormone levels, signaling via perturbed reactive oxygen species (ROS) homeostasis can participate in the necessary steps leading to an efficient cellular and organismal response (Gilroy et al., 2014; Wrzaczek et al., 2013).

The accumulation of ROS has not only been demonstrated for multiple stress conditions like wounding (Orozco-Cardenas and Ryan, 1999), chilling (Wise and Naylor, 1987), excess light (Fryer et al., 2003), pathogen infections (Apostol et al., 1989; Levine et al., 1994), but also during developmental processes like root growth (Foreman et al., 2003), gravitropism (Joo et al., 2001), extracellular ATP signaling (Song et al., 2006), pollen tube growth (Kaya et al., 2014; Potocký et al., 2007) and its rupture (Duan et al., 2014). Cellular production units involved in ROS production include core cellular processes like mitochondrial respiration (Navrot et al., 2007), photosynthesis (Asada, 2006), photorespiration (Bauwe et al., 2012; Foyer et al., 2009), peroxisomal β -fatty acid oxidation (Jiang et al., 2011) and purine degradation (Sandalio et al., 1988; Zarepour et al., 2010). Over more than three decades, the general concepts of redox regulation in plants have been shaped (Montrichard et al., 2009; Schürmann and Buchanan, 2008). However, it is yet not clear how the majority of stress-related redox stimuli are perceived and transduced. One mechanism to sense ROS/reactive nitrogen species (RNS) is by the modification of proteins on specific cysteine and methionine residues (Jacques et al., 2013; Roos and Messens, 2011). The availability of different oxidation states of both sulfur containing amino acids permits the formation of a diverse palette of oxidative post-translational modifications (Ox-PTMs), including nitric oxide (NO)-mediated S-nitrosylation (SNO; Yu et al., 2014), hydrogen sulfide (H₂S)-mediated sulfhydration (SSH; Álvarez et al., 2012; Mustafa et al., 2009; Paul and Snyder, 2012), and ROS-mediated changes (sulfenylation, R-SOH; formation of intra-/intermolecular disulfide bridges, R-S-S-R/R-S-S-R'; S-glutathionylation, R-S-SG; sulfinylation, R-SO₂H; and sulfonylation, R-SO₃H).

The best-studied cases for ROS-mediated PTMs are those on enzymes involved in the Calvin cycle (Schürmann and Buchanan, 2008), sulfur metabolism (Kopriva et al., 2012) and starch metabolism (Glaring et al., 2012). Next to these redox-sensitive metabolic components, Ox-PTMs also emerge as regulatory switches on various signal transduction proteins, including transcription factors (excellently reviewed by Dietz, 2014), kinases, phosphatases, proteases and RNA-binding proteins. In this review, we focus on hydrogen peroxide-mediated thiol-based redox signaling, including kinase modules, proteases and RNA-binding proteins. Special attention is given to cysteine (Cys) Ox-PTMs that mediate the cross-talk between ROS and signaling pathways initiated by stress-related hormones.

Cys Ox-PTMs in plant ROS control systems

Plants have evolved various strategies to keep ROS levels under a tight control governed by enzymatic and non-enzymatic ROS producing and scavenging systems (Apel and Hirt, 2004; Mittler et al., 2011; Fig. 1A). Glutathione (GSH) and ascorbate (Asc) are the major non-enzymatic cellular redox systems, with

tocopherol and diverse alkaloid, carotenoid and flavonoid metabolites often listed, but sometimes debated as physiologically relevant antioxidants (Apel and Hirt, 2004; Hernández et al., 2009). Maintenance of a reduced glutathione pool (high GSH/GSSG ratio) is crucial for cellular redox homeostasis, since GSH is utilized to regenerate oxidized ascorbate in the glutathione-ascorbate cycle (Fig. 1A; Foyer and Halliwell, 1976). GSH and Asc are working hand in hand with glutathione peroxidases (Gpxs; Mills, 1957) and ascorbate peroxidases (APXs; Groden and Beck, 1979; Nakano and Asada, 1981) respectively, which together with catalases (CATs), superoxide dismutases (SODs) and peroxiredoxins (Prxs) constitute the major enzymatic classes involved in ROS scavenging (Mittler et al., 2004). Due to its relatively high pKa (8.9; Van Laer et al., 2013), glutathione is fully protonated at physiological pH, thereby its reactivity toward disulfides and ROS is rather limited.

Oxidative post-translational modifications of cysteine residues

Chemical properties of the sulfur atom (i.e. wide range of oxidation states) make cysteine and methionine residues the major sites of oxidation within proteins (Davies, 2005). In Cys Ox-PTMs, the thiol group (-SH) represents the -2 oxidation state of the sulfur atom, which is the fully reduced form. Not all cysteines within the protein context are prone to ROS-mediated modifications and the reactivity of different thiol-proteins toward ROS varies according to their physiological function and local redox environment. Between individual cysteines, the reactivity is strongly correlated with their pKa – i.e. the ability to form the anionic form of the sulfur, called thiolate (R-S⁻), that is much more reactive than the thiol (R-SH). If the pKa of the sulfur atom is higher than the pH of the solution, the protonated thiol will be the dominant species. However, if the pKa is lower than the pH, the majority of the thiols will be present as a thiolate (cysteine prone to oxidation). The pKa of Cys residues is largely determined by the local electrostatic environment, i.e. the presence of proximal charged residues or dipoles and the hydrogen bonding between thiols/thiolates and neighboring residues (Harris and Turner, 2002). Hydrogen bonding has a strong influence on the pKa of reactive cysteines. In general, the more hydrogen bonds a cysteine-sulfur receives, the lower the pKa is and the more the thiolate form is stabilized (Roos et al., 2013). Nucleophilicity of the Cys is also an important factor for its reactivity; in some cases, a lower stabilization of the thiolate in Cys residues increases its nucleophilicity, while a highly stabilized thiolate needs a larger amount of energy to reach the transition state (Ferrer-Sueta et al., 2011). Another important factor that controls the reactivity of Cys residues is their steric accessibility within the 3D structure of the protein (Marino and Gladyshev, 2010).

The first step in ROS-dependent signaling involves the reversible oxidation of reactive Cys residues to sulfenic acid (R-SOH; Fig 1 B). Unless stabilized within its protein environment, this modification is highly unstable and leads to further modifications (Claiborne et al., 1993). An excess concentration of oxidant can lead to further oxidation to sulfinic acid (R-SO₂H), and subsequently to irreversible sulfonic acid (R-SO₃H; Roos and Messens, 2011). The reversion of the R-SO₂H modification is catalyzed by an ATP-dependent sulfiredoxin enzyme (Srx) that is capable of reducing R-SO₂H to R SOH in Arabidopsis (Rey et al., 2007). However, thus far, R-SO₂H reduction is rather exceptional with the only two known substrates of AtSrx: the chloroplast 2-Cys Prx (Iglesias-Baena et al., 2010; Rey et al., 2007) and mitochondrial PrxIIIF (Iglesias-Baena et al., 2011). Alternatively, R SOH can react with free protein thiols to form intra- or intermolecular disulfide bonds (RS-SR') or is modified by low-molecular-weight thiols (like

GSH in plants), leading to cysteine S-glutathionylation (Fig 1 B). S-glutathionylation events were initially considered to serve as a protective mechanism on active-site Cys residues, preventing overoxidation and subsequent permanent protein damage. Only recently, S-glutathionylation gained recognition for its role in redox signaling (Zaffagnini et al., 2012). The reduction of disulfide bonds and deglutathionylation are controlled by glutaredoxins (Grxs) and thioredoxins (Trxs), respectively (Fig. 1B). Compared to prokaryotes and animals, plants are equipped with a much more complex Trx/Grx network. The Arabidopsis genome encodes 44 Trx/Trx-like and 50 Grx/Grx-like proteins (Meyer et al., 2012). Depending on the subcellular localization, Trxs utilize multiple sources of reducing equivalents to perform the reduction of intra-/intermolecular disulfide bonds. In chloroplasts, light reactions reduce ferredoxin (Fdx) that in turn reduces ferredoxin-thioredoxin reductase (FTR), which ultimately regenerates the Trx sulfhydryl groups (Fig. 1C; Schürmann and Buchanan, 2008). Another general source of reducing equivalents, common for the Trx and Grx systems is NADPH, that after oxidation to NADP⁺ is reduced by Fdx:NADP⁺ reductase (FNR) within the chloroplast stroma, as well as during the oxidative pentose phosphate pathway. While Trxs are directly reduced by NADPH-dependent thioredoxin reductases (NTRs), Grxs engage a two-step reaction involving GSH and NADPH-dependent glutathione reductases (GRs; Fig. 1B, C).

Cross-talk between ROS and phytohormone signaling mediated by Cys Ox-PTMs

Abscisic acid signaling

Thus far, the best described cross-talk between ROS and abscisic acid (ABA) occurs during guard cell movement (Fig. 2; Kwak et al., 2003; Pei et al., 2000). In response to stress conditions (e.g. pathogen attack, drought), the rising concentration of ABA within guard cells triggers a signaling cascade which ultimately results in stomatal closure and reduced transpiration. Perception (binding) of ABA by PYRABACTIN RESISTANCE/PYR1 LIKE/REGULATORY COMPONENT OF ABA RECEPTOR (PYR/PYL/RCAR) receptor proteins (Ma et al., 2009; Park et al., 2009) results in conformational changes within their protein structure, leading to binding and inhibition of PROTEIN PHOSPHATASE 2C (PP2C) family members that act as constitutive repressors of SnRK2/OST1 kinase (Cutler et al., 2010). Upon de-repression, SnRK2/OST1 achieves full activation by autophosphorylation and further activates (phosphorylates) its target proteins such as NADPH oxidases RbohD/F, leading to apoplast-localized ROS production (Kwak et al., 2003; Sirichandra et al., 2009). This oxidative burst activates Ca²⁺ influx channels (Pei et al., 2000). In parallel, SnRK2/OST1 activates the anion channel SLOW ANION CHANNEL-ASSOCIATED 1 (SLAC1; Lee et al., 2009; Vahisalu et al., 2008), which has a central role in guard cells. Another ion channel targeted by SnRK2/OST1 is the KAT1 potassium channel that loses its activity upon phosphorylation (Sato et al., 2009). The rise in cytoplasmic Ca²⁺ concentration activates multiple calcium-dependent protein kinases CPK3, CPK6 (Mori et al., 2006); CPK4, CPK11 (Zhu et al., 2007); CPK5 (Dubiella et al., 2013); CPK21 and CPK23 (Geiger et al., 2010). Among them, CPK21 activates SLAC1 (Geiger et al., 2010) and SLAC1 homolog 3 (SLAH3; Demir et al., 2013; Geiger et al., 2010). Together, these signaling steps lead to the coordinated action of membrane channels that control the levels of osmotically active ions within guard cells (Song et al., 2014). Two members of the PP2C family (ABA insensitive 1 (ABI1) and ABI2), which act as negative regulators of ABA signaling (Merlot et al., 2001), were shown to undergo H₂O₂-dependent inhibition (Fig. 2). Oxidizing conditions lead to the inactivation of phosphatase activities in vitro, presumably via formation of an intramolecular disulfide bond

(Meinhard and Grill, 2001; Meinhard et al., 2002). This oxidative inactivation amplifies ABA signaling and effects in guard cells. In planta, ABI2 oxidation is mediated by GLUTATHIONE PEROXIDASE 3 (GPX3). GPX3 acts as a sensor protein that, upon perception of increased ROS levels, relays the oxidizing equivalents to ABI2 via thiol-disulfide exchange to inhibit its phosphatase activity (Miao et al., 2006). Similar scenarios have been described as well in yeast and mammalian cells exposed to oxidative stress (Delaunay et al., 2002; Gutscher et al., 2009). In yeast, oxidation of the H₂O₂ sensor Oxidant Receptor Peroxidase 1 (ORP1/Gpx3) triggers a thiol disulfide relay mechanism that ultimately leads to nuclear accumulation of the Yeast AP-1 (YAP1) transcription factor (Delaunay et al., 2002) and subsequent induction of H₂O₂ responsive genes (Lee et al., 1999). Together with their strong sequence similarities within kingdoms (Margis et al., 2008), these notions plead for thiol peroxidases to act as widespread redox sensors.

Next to the GPX3-mediated inhibition of ABI1/2, also the activity of CPK21 kinase is redox dependent (Fig. 2). CPK21 undergoes H₂O₂-dependent inhibition that is linked to the formation of an intramolecular disulfide bond (Cys97-Cys108) and is effectively restored by Trx h1 (Ueoka-Nakanishi et al., 2013).

Recent evidence suggests that ANNEXIN1 (AtANN1) mediates the ROS-dependent Ca²⁺ fluxes in Arabidopsis roots (Laohavisit et al., 2012). ANNEXIN1 binds to lipid membranes in a Ca²⁺-dependent manner and stimulates Ca²⁺ influx in a hydroxyl radical- (HO[•]; Laohavisit et al., 2012) and peroxide-dependent manner (Richards et al., 2014). AtANN1 deficient mutants are impaired in the ROS-mediated increase in the cytoplasmic Ca²⁺ concentration (Laohavisit et al., 2012). This process is of particular importance for root growth, since it largely relies on cell expansion that is dependent on the activation of Ca²⁺ channels downstream of NADPH oxidase RbohC (Foreman et al., 2003). Besides impaired root development, ann1 mutants are hypersensitive to drought (Konopka-Postupolska et al., 2009). ANNEXIN1 is S-glutathionylated on both of its cysteine residues (Cys111 and Cys239), resulting in a 50% decrease in Ca²⁺ affinity (Konopka-Postupolska et al., 2009). This mechanism probably serves to restrict the AtANN1 membrane association and inhibit ROS-mediated Ca²⁺ fluxes in a negative feedback loop.

Salicylic acid signaling

Salicylic acid (SA) regulates both local and systemic acquired resistance (SAR) to limit the progress of pathogen infections. SA governs a drastic transcriptional response that is largely mediated by a coordinated action of the NONEXPRESSER OF PR GENES 1 (NPR1) transcriptional co-activator and interacting TGA transcription factors (Fig. 3). Both NPR1 and TGAs are regulated by changes in the cellular redox status that occur upon pathogen infection (Mou et al., 2003; Tada et al., 2008). Normally, NPR1 localizes to the cytoplasm in the form of oligomers formed through intramolecular RS-SR' bonds involving cysteine residues Cys82 and Cys216 (Mou et al., 2003). SA triggers perturbation of the cellular redox status that leads to a Trxh3/h5-dependent reduction of disulfides and subsequent monomerization of NPR1 and nuclear import. This activation process directly competes with oligomerization promoted by S-nitrosylation of Cys156. The interplay between these two modifications provides a tight control for NPR1-dependent signaling (Tada et al., 2008). A recent characterization of NPR1 denitrosylation by a Trx h5/NTRA system revealed a double role for Trx h5 in the control of NPR1 cytoplasmic retention (Kneeshaw et al., 2014). Upon import into the nucleus, NPR1 interacts with TGA basic leucine-zipper transcription factors to promote transcription of pathogenesis-related (PR) genes. Clade 2 TGA transcription factors

(TGA2/5/6) act as constitutive repressors of PR transcription. Binding of NPR1 to TGA2 results in the co-activation of transcription and depends on NPR1 Cys521 and Cys529, which are required for activation of the NPR1 trans-activation domain (Rochon et al., 2006). It has been demonstrated that NPR1 is a SA receptor and that these two Cys residues are involved in the stabilization of copper atoms that are necessary for SA binding (Wu et al., 2012). Furthermore, TGA2/6 interact with glutaredoxin GRX480 (ROXY 19), suggesting that GRX480 might control their redox status. This complex might also involve NPR1, which implies the role of GRX480 in the regulation of the interaction between TGA and NPR1 (Ndamukong et al., 2007), however, the precise function of GRX480 remains to be elucidated.

The interaction of NPR1 with clade 1 TGA transcription factors (TGA1/4) relies on their redox status. When oxidized, TGA1 and/or TGA4 form an intramolecular disulfide bridge (Cys260-Cys266) that hinders interaction with NPR1. Reduction of this disulfide stimulates the formation of a complex with NPR1, and subsequent binding to the as-1 element for activation of PR genes (Després et al., 2003). Recent data indicate that the two remaining TGA1 Cys residues Cys172 and Cys287 are also involved and act as a regulatory disulfide (Lindermayr et al., 2010). Furthermore, all four residues were found to undergo S-nitrosylation/S-glutathionylation upon treatment with S-nitrosoglutathione (GSNO). These modifications serve to protect the Cys residues from oxidation and consequently lead to an increase in the DNA binding activity of TGA1 (Lindermayr et al., 2010).

Jasmonate signaling

The biologically active form of jasmonate (JA), the JA-Ile conjugate, triggers the 26S proteasome-mediated proteolysis of the JASMONATE ZIM-domain (JAZ) transcriptional repressors by mediating their interaction with the F box protein CORONATINE INSENSITIVE1 (COI1), which is a part of the Skp1/Cullin/F-boxCOI1 ubiquitin E3 ligase complex. Proteolysis of JAZ proteins de-represses multiple transcription factors (i.e. MYC2) and leads to panoramic changes in gene expression (Pauwels and Goossens, 2011). Besides JA derivatives, also JA precursors, such as 12-oxo-phytodienoic acid (OPDA), are able to exert transcriptional responses (Taki et al., 2005). A recent study has extended our knowledge about OPDA signaling by the identification of its chloroplastic receptor CYCLOPHYLIN 20-3 (CYP20-3; Park et al., 2013). Cyclophilins are characterized by a highly conserved peptidyl-prolyl isomerase (PPIase) domain that, if functional, assists proper folding of their target proteins (Trivedi et al., 2012). CYP20-3 is reduced by m-type Trx (Motohashi et al., 2001) and was demonstrated to undergo oxidative inhibition mediated by the formation of two intramolecular RS-SR (Cys53-Cys170; Cys128-Cys175; Motohashi et al., 2003). Thus far, in *Arabidopsis*, the only identified target of CYP20-3 is the chloroplast SERINE ACETYL-TRANSFERASE1 (SAT1), which catalyzes the rate-limiting step in cysteine synthesis. The physical interaction of CYP20-3 with SAT1 is crucial for optimal synthesis of cysteine. Consequently, *cyp20-3* mutant plants exhibit a low thiol content and are impaired in light-dependent stress responses (Dominguez-Solis et al., 2008). Direct binding of OPDA to CYP20-3 was shown to stimulate this interaction and ultimately promote the production of cellular antioxidants (Park et al., 2013). Therefore, CYP20-3 is a redox sensitive cross-talk point linking OPDA signaling with maintenance of the cellular redox balance.

Cys Ox-PTMs: control switches in plant signal transduction

Protein tyrosine phosphatases and mitogen-activated protein kinases

Mitogen-activated protein kinases (MAPKs) are involved in the regulation of almost every aspect of plant growth, development and stress responses (Beckers et al., 2009; Betsuyaku et al., 2011; Kosetsu et al., 2010; Pitzschke et al., 2009; Takahashi et al., 2007). The three component MAPK signaling cascades are initiated by stimulus-triggered activation of MAPK kinase kinases (MAPKKKs) that in turn phosphorylate MAPK kinases (MAPKKs), which phosphorylate specific MAPKs. The Arabidopsis genome encodes more than 60 MAPKKKs, 10 MAPKKs and 20 MAPKs (Ichimura et al., 2002), which, depending on the environmental and developmental stimuli, regulate respective cellular processes. The potential complexity of signaling combinations that could arise from numerous members of MAPKKK/MAPKK/MAPK families suggests that these proteins might function as convergence points linking multiple rather than single hormonal pathways. Moreover, recent data indicate that apart from the classical MAPK signaling cascades, MAPKs might be subjected to direct regulation by calcium-dependent protein kinases (Xie et al., 2014) or ROS, providing a multi-level control of their activity.

In yeast and mammalian cells, several MAPKs undergo Ox-PTMs (Cross and Templeton, 2004; Day and Veal, 2010; Templeton et al., 2010). So far, no reports that describe direct Ox-PTMs on plant MAPKs are available. However, there are several indications that plant MAPKs are activated in response to oxidative stress. The ABA-dependent stomatal closure is positively regulated by MAPK9 and MAPK12, that both function downstream of ROS in the signaling cascade (Fig. 2). The kinase activity of MPK12 is stimulated by both ABA and H₂O₂ (Jammes et al., 2009), although the exact mechanism of this regulation needs further investigation. Similarly, H₂O₂ was demonstrated to induce MAPKKK1 (ANP-1), which in turn activates MAPK3 and MAPK6 (Kovtun et al., 2000), however the redox sensing capabilities of MAPKKK1 are yet to be demonstrated. The redox regulation of MAPK signaling cascades is likely to be evolutionary conserved, since tomato (*Solanum lycopersicum*) MAPK2, which is an ortholog of Arabidopsis MAPK6, also undergoes oxidative activation (Zhou et al., 2014). Direct Ox-PTMs of plant MAPKs need further investigation; however, growing evidence suggests that such modifications can take place, since three members of the MAPK family, MAPK 2, 3 and 7, have been found to undergo H₂O₂-dependent sulfenylation (Waszczak et al., 2014).

Thus far, in plants, the only well-established link between the cellular redox status and MAPK activity is the oxidative stress-related negative regulation of MAPK repressors. The activity of MAPKs positively depends on the phosphorylation status of threonine and tyrosine residues within the conserved TXY motif in the activation loop (Canagarajah et al., 1997; Zhang et al., 1994). As such, the protein tyrosine phosphatases (PTPs) have been implemented in the control of various processes that involve MAPK signaling components such as guard cell signaling (MacRobbie, 2002), oxidative stress tolerance (Lee and Ellis, 2007), SA homeostasis (Bartels et al., 2009), disease responses (Lumbreras et al., 2010) and development (Strader et al., 2008; Walia et al., 2009). ROS mediate the inactivation of PTPs and double specificity PTPs (DsPTPs) that act on both phosphotyrosine and phosphothreonine residues and repress MAPKs (Gupta et al., 1998; Xu et al., 1998). The activity of PTPs and DsPTPs, that apart from their active site motif do not share any sequence similarity, requires a highly conserved Cys residue, Cys265 in AtPTP1 (Xu et al., 1998) and Cys135 in AtDsPTP1 (Gupta et al., 1998). The activity of AtPTP1 is negatively influenced by H₂O₂ treatment both in vitro and in vivo. Furthermore, this inactivation is positively correlated with MAPK6 activation by H₂O₂, indicating

that AtPTP1 acts as a redox sensor linking oxidative stress with MAPKs activity (Gupta and Luan, 2003). The soybean (*Glycine max*) GmPTP has a low sensitivity to inhibition through H_2O_2 and displays hypersensitivity toward GSSG-induced S-glutathionylation. GmPTP activity is governed by two redox active cysteine residues (Cys78 and Cys176) that control the catalytic Cys266, which itself is not a primary target for oxidation. S-glutathionylation of Cys176 leads to a rapid inactivation of the enzyme, followed by S-glutathionylation of Cys78, and further leading to the formation of Cys78-Cys266 intra/intermolecular disulfides, probably protecting the Cys266 from oxidation (Dixon et al., 2005). The general paradigm of oxidative inactivation of PTPs has recently been challenged by the discovery of a reductant inhibited PTP from maize (*Zea mays*; ZmRIP1). ZmRIP1 phosphatase activity is insensitive to H_2O_2 and irreversibly decreases upon reduction with of Cys181 with dithiothreitol (DTT) (Li et al., 2012). It has been suggested that Cys181 might be involved in RS-SR formation, however the exact mechanism of this redox regulation needs to be elucidated. Interestingly, upon H_2O_2 treatment, ZmRIP1 undergoes chloroplast-to-nucleus translocation, which is indicative for a role in signal transduction, however the target proteins of ZmRIP1 are currently not known.

Cys Ox-PTMs control protein translation and stability

Next to the regulation of transcription, the control of mRNA translation by trans-acting factors is crucial for fine-tuned protein expression. Thus far, the best-studied case of redox-regulated control of mRNA translation occurs during expression of *Chlamydomonas reinhardtii* photosystem II reaction center protein D1 that is encoded by the chloroplast *psbA* gene (Alergand et al., 2006; Kim and Mayfield, 1997; Yohn et al., 1998). This two-component system involves the polyadenylation-binding protein RB47 and the protein disulfide isomerase RB60. Binding of RB47 to the 5' UTR of the *psbA* mRNA is required for translation and depends on RB60 that regulates this process in a light-dependent manner. During the photosynthetic light reactions, a reducing environment is generated by PSI. The reducing equivalents are relayed through the Fdx/FTR/Trx system to the chloroplast RB60. RB60 contains two Trx-like CGHC-sites that serve to interact with Cys143 or Cys259 of RB47. This interaction results in the reduction of the RB47 regulatory disulfides (Cys259-Cys143 or Cys259-Cys55) and activates the binding of RB47 to the *psbA* mRNA (Alergand et al., 2006). Upon translation, the D1 protein is incorporated into PSII complexes. Importantly, under oxidizing conditions, RB60 facilitates the conversion of reduced RB47 to its inactive oxidized form (Kim and Mayfield, 1997). An analogous system could control the *psbA* mRNA translation in *Arabidopsis*, since two yet unidentified RNA-binding proteins have been found to interact with *psbA* mRNA in a redox-dependent manner (Shen et al., 2001). In addition, mRNA stability might be subjected to redox control. SALT OVERLY SENSITIVE 1 (SOS1) transcripts are stabilized after H_2O_2 treatment. SOS1 codes for a plasma membrane Na⁺/H⁺ antiporter crucial for the maintenance of ion homeostasis in saline stress conditions. Under normal conditions, SOS1 mRNA is highly unstable, but via yet unknown mechanisms stress-induced production of H_2O_2 positively influences its stability and promotes salt stress tolerance (Chung et al., 2008). Although the molecular mechanism behind this process is unknown, a plausible scenario could involve redox-regulated RNA-binding protein(s) (Lorković, 2009).

A recent study demonstrates that the proteolytic control of protein maturity can also be subjected to redox regulation. The activity of major Arabidopsis thylakoidal processing peptidase PLASTIDIC TYPE I SIGNAL PEPTIDASE 1 (PLSP1), which functions in the removal of the thylakoid-transfer signal upon import of proteins from the chloroplast stroma into the thylakoid lumen, depends on the regulatory disulfide bond between Cys166 and Cys286. Formation of the regulatory disulfide leads to the activation of proteolytic activity *in vitro* probably via facilitating the entry of substrate proteins into the protease binding pocket (Midorikawa et al., 2014). Proteolytic regulation of protein stability gains recognition in the field of plant cell death research (Coll et al., 2010; Wrzaczek et al., 2014), however it is not yet clear whether any of the signaling components involved in these processes is directly targeted by ROS.

Perspectives

The portfolio of proteins that potentially undergo Ox-PTMs is continuously growing. Many studies have been performed to understand reversible Cys Ox-PTMs and the repertoire of techniques that enable identification of these PTMs is continuously expanding (Montrichard et al., 2009). We have recently identified a set of sulfenylated proteins, which are potential ROS sensors, in Arabidopsis thaliana (Waszczak et al., 2014; Akter et al., submitted). Besides the Cys Ox-PTMs, formation of methionine sulfoxide and tyrosine nitration are emerging redox PTMs affecting protein structure and function (Jacques et al., 2013). In this relatively new field, we expect that in the near future, many more proteins undergoing Ox-PTMs at cysteine, methionine and tyrosine residues will be identified. Now we face the challenge to validate and functionally characterize those proteins for their biochemical, functional and structural aspects in order to get extra insights into the ROS signal transduction mechanism at the molecular level. The validation of proteomic results requires a dedicated effort that in most cases focuses on one single protein at a time. A closer look at the results of current investigations reveals an apparent huge gap between the number of identified proteins and the number of proteins for which the occurrence of Ox-PTMs has been validated. This is caused by the difficulty to recombinantly express plant proteins, the lack of suitable activity assays, the absence of mutant phenotypes hampering the complementation studies, and finally, the scarce information about the role and function of the identified proteins. We anticipate that future efforts in the field of plant redox biology will explore the sets of already identified, but not yet validated proteomic findings. Furthermore, it is important to realize that proteins identified by redox proteomics approaches might be secondary, rather than primary targets for Ox-PTMs due to their relatively low reactivity with ROS when compared to e.g. thiol peroxidases. As discussed earlier, the thiol-disulfide relays initiated by thiol peroxidases have been demonstrated for multiple ROS sensory modules (Delaunay et al., 2002; Miao et al., 2006) which, complemented with most recent discoveries (Sobotta et al., 2014), argues for an universal nature of such systems. Finally, in the view of future potential of redox sensory systems for manipulation of plant stress tolerance, we believe that, whenever possible, the relevance of all results obtained from *in vitro* experiments should be assessed *in vivo*.

ACKNOWLEDGEMENTS

We thank Jaakko Kangasjärvi for useful comments on the manuscript. This work was supported by grants from EU-R 435 OS (BMBS COST Action BM1203), Research Foundation Flanders (FWO project GOD7914N “Sulfenomics: oxidatieve schakelaars in planten. Hoe zwavelhoudende planteneiwitten via ‘agressieve’ zuurstof praten”), the Interuniversity Attraction Poles Programme (IUAP P7/29 “MARS”) initiated by the Belgian Science Policy Office, Ghent University [Multidisciplinary Research Partnership “Biotechnology for a Sustainable Economy” (Grant 01MRB510W) and “Bijzonder Onderzoeksfonds – Post-translational modifications” (BOF 01J11311)] the Agency for Innovation by Science and Technology (IWT; predoctoral fellowship to S.J.), and the VIB International PhD Program (predoctoral fellowship to C.W.). We would like to thank Annick Bleys for help in preparing the manuscript.

REFERENCES

- Alegand T, Peled-Zehavi H, Katz Y, Danon A. 2006. The chloroplast protein disulfide isomerase RB60 reacts with a regulatory disulfide of the RNA-binding protein RB47. *Plant and Cell Physiology* 47, 540-548.
- Álvarez C, García I, Moreno I, Pérez-Pérez ME, Crespo JL, Romero LC, Gotor C. 2012. Cysteine-generated sulfide in the cytosol negatively regulates autophagy and modulates the transcriptional profile in *Arabidopsis*. *Plant Cell* 24, 4621-4634.
- Apel K, Hirt H. 2004. REACTIVE OXYGEN SPECIES: metabolism, oxidative stress, and signal transduction. *Annual Review of Plant Biology* 55, 373-399.
- Apostol I, Heinsteint PF, Low PS. 1989. Rapid stimulation of an oxidative burst during elicitation of cultured plant cells. Role in defense and signal transduction. *Plant Physiology* 90, 109-116.
- Asada K. 2006. Production and scavenging of reactive oxygen species in chloroplasts and their functions. *Plant Physiology* 141, 391-396.
- Bartels S, Anderson JC, Besteiro MAG, Carreri A, Hirt H, Buchala A, Métraux J-P, Peck SC, Ulm R. 2009. MAP KINASE PHOSPHATASE1 and PROTEIN TYROSINE PHOSPHATASE1 are repressors of salicylic acid synthesis and SNC1-mediated responses in *Arabidopsis*. *Plant Cell* 21, 2884-2897.
- Bauwe H, Hagemann M, Kern R, Timm S. 2012. Photorespiration has a dual origin and manifold links to central metabolism. *Current Opinion in Plant Biology* 15, 269-275.
- Beckers GJM, Jaskiewicz M, Liu Y, Underwood WR, He SY, Zhang S, Conrath U. 2009. Mitogen-activated protein kinases 3 and 6 are required for full priming of stress responses in *Arabidopsis thaliana*. *Plant Cell* 21, 944-953.
- Betsuyaku S, Takahashi F, Kinoshita A, Miwa H, Shinozaki K, Fukuda H, Sawa S. 2011. Mitogen-activated protein kinase regulated by the CLAVATA receptors contributes to shoot apical meristem homeostasis. *Plant and Cell Physiology* 52, 14-29.
- Canagarajah BJ, Khokhlatchev A, Cobb MH, Goldsmith EJ. 1997. Activation mechanism of the MAP kinase ERK2 by dual phosphorylation. *Cell* 90, 859-869.
- Chung J-S, Zhu J-K, Bressan RA, Hasegawa PM, Shi H. 2008. Reactive oxygen species mediate Na⁺-induced

SOS1 mRNA stability in Arabidopsis. *Plant Journal* 53, 554-565.

Claiborne A, Miller H, Parsonage D, Ross RP. 1993. Protein-sulfenic acid stabilization and function in enzyme catalysis and gene regulation. *FASEB Journal* 7, 1483-1490.

Coll NS, Vercammen D, Smidler A, Clover C, Van Breusegem F, Dangl JL, Epple P. 2010. Arabidopsis type I metacaspases control cell death. *Science* 330, 1393-1397.

Cross JV, Templeton DJ. 2004. Oxidative stress inhibits MEK1 by site-specific glutathionylation in the ATP-binding domain. *Biochemical Journal* 381, 675-683.

Cutler SR, Rodriguez PL, Finkelstein RR, Abrams SR. 2010. Abscisic acid: emergence of a core signaling network. *Annual Review of Plant Biology* 61, 651-679.

Davies MJ. 2005. The oxidative environment and protein damage. *Biochimica et Biophysica Acta - Proteins and Proteomics* 1703, 93-109.

Day AM, Veal EA. 2010. Hydrogen peroxide-sensitive cysteines in the Sty1 MAPK regulate the transcriptional response to oxidative stress. *Journal of Biological Chemistry* 285, 7505-7516.

Delaunay A, Pflieger D, Barrault M-B, Vinh J, Toledano MB. 2002. A thiol peroxidase is an H₂O₂ receptor and redox-transducer in gene activation. *Cell* 111, 471-481.

Demir F, Horntrich C, Blachutzyk JO, et al. 2013. Arabidopsis nanodomain-delimited ABA signaling pathway regulates the anion channel SLAH3. *Proceedings of the National Academy of Sciences of the United States of America* 110, 8296-8301.

Després C, Chubak C, Rochon A, Clark R, Bethune T, Desveaux D, Fobert PR. 2003. The Arabidopsis NPR1 disease resistance protein is a novel cofactor that confers redox regulation of DNA binding activity to the basic domain/leucine zipper transcription factor TGA1. *Plant Cell* 15, 2181-2191.

Dietz K-J. 2011. Peroxiredoxins in plants and cyanobacteria. *Antioxidants & Redox Signaling* 15, 1129-1159.

Dietz K-J. 2014. Redox regulation of transcription factors in plant stress acclimation and development. *Antioxidants & Redox Signaling* 21, 1356-1372.

Dixon DP, Fordham-Skelton AP, Edwards R. 2005. Redox regulation of a soybean tyrosine-specific protein phosphatase. *Biochemistry* 44, 7696-7703.

Dominguez-Solis JR, He Z, Lima A, Ting J, Buchanan BB, Luan S. 2008. A cyclophilin links redox and light signals to cysteine biosynthesis and stress responses in chloroplasts. *Proceedings of the National Academy of Sciences of the United States of America* 105, 16386-16391.

Duan Q, Kita D, Johnson EA, Aggarwal M, Gates L, Wu H-M, Cheung AY. 2014. Reactive oxygen species mediate pollen tube rupture to release sperm for fertilization in Arabidopsis. *Nature Communications* 5, 3129.

Dubiella U, Seybold H, Durian G, Komander E, Lassig R, Witte C-P, Schulze WX, Romeis T. 2013. Calcium-dependent protein kinase/NADPH oxidase activation circuit is required for rapid defense signal propagation. *Proceedings of the National Academy of Sciences of the United States of America* 110, 8744-8749.

- Ferrer-Sueta G, Manta B, Botti H, Radi R, Trujillo M, Denicola A. 2011. Factors affecting protein thiol reactivity and specificity in peroxide reduction. *Chemical Research in Toxicology* 24, 434-450.
- Foreman J, Demidchik V, Bothwell JHF, et al. 2003. Reactive oxygen species produced by NADPH oxidase regulate plant cell growth. *Nature* 422, 442-446.
- Foyer CH, Bloom AJ, Queval G, Noctor G. 2009. Photorespiratory metabolism: genes, mutants, energetics, and redox signaling. *Annual Review of Plant Biology* 60, 455-484.
- Foyer CH, Halliwell B. 1976. The presence of glutathione and glutathione reductase in chloroplasts: A proposed role in ascorbic acid metabolism. *Planta* 133, 21-25.
- Fryer MJ, Ball L, Oxborough K, Karpinski S, Mullineaux PM, Baker NR. 2003. Control of Ascorbate Peroxidase 2 expression by hydrogen peroxide and leaf water status during excess light stress reveals a functional organisation of Arabidopsis leaves. *Plant Journal* 33, 691-705.
- Geiger D, Scherzer S, Mumm P, et al. 2010. Guard cell anion channel SLAC1 is regulated by CDPK protein kinases with distinct Ca²⁺ affinities. *Proceedings of the National Academy of Sciences of the United States of America* 107, 8023-8028.
- Gilroy S, Suzuki N, Miller G, Choi W-G, Toyota M, Devireddy AR, Mittler R. 2014. A tidal wave of signals: calcium and ROS at the forefront of rapid systemic signaling. *Trends in Plant Science* 19, 623-630.
- Glaring MA, Skryhan K, Kötting O, Zeeman SC, Blennow A. 2012. Comprehensive survey of redox sensitive starch metabolising enzymes in Arabidopsis thaliana. *Plant Physiology and Biochemistry* 58, 89-97.
- Groden D, Beck E. 1979. H₂O₂ destruction by ascorbate-dependent systems from chloroplasts. *Biochimica et Biophysica Acta - Bioenergetics* 546, 426-435.
- Gupta R, Huang Y, Kieber J, Luan S. 1998. Identification of a dual-specificity protein phosphatase that inactivates a MAP kinase from Arabidopsis. *Plant Journal* 16, 581-589.
- Gupta R, Luan S. 2003. Redox control of protein tyrosine phosphatases and mitogen-activated protein kinases in plants. *Plant Physiology* 132, 1149-1152.
- Gutscher M, Sobotta MC, Wabnitz GH, Ballikaya S, Meyer AJ, Samstag Y, Dick TP. 2009. Proximity-based protein thiol oxidation by H₂O₂-scavenging peroxidases. *Journal of Biological Chemistry* 284, 31532-31540.
- Harris TK, Turner GJ. 2002. Structural basis of perturbed pK_a values of catalytic groups in enzyme active sites. *International Union of Biochemistry and Molecular Biology Life* 53, 85-98.
- Hernández I, Alegre L, Van Breusegem F, Munné-Bosch S. 2009. How relevant are flavonoids as antioxidants in plants? *Trends in Plant Science* 14, 125-132.
- Ichimura K, Shinozaki K, Tena G, et al. 2002. Mitogen-activated protein kinase cascades in plants: a new nomenclature. *Trends in Plant Science* 7, 301-308.
- Iglesias-Baena I, Barranco-Medina S, Lázaro-Payo A, López-Jaramillo FJ, Sevilla F, Lázaro J-J. 2010. Characterization of plant sulfiredoxin and role of sulphinic form of 2-Cys peroxiredoxin. *Journal of Experimental Botany* 61, 1509-1521.

- Iglesias-Baena I, Barranco-Medina S, Sevilla F, Lázaro J-J. 2011. The dual-targeted plant sulfiredoxin retroreduces the sulfinic form of atypical mitochondrial peroxiredoxin. *Plant Physiology* 155, 944-955.
- Jacques S, Ghesquière B, Van Breusegem F, Gevaert K. 2013. Plant proteins under oxidative attack. *Proteomics* 13, 932-940.
- Jammes F, Song C, Shin D, et al. 2009. MAP kinases MPK9 and MPK12 are preferentially expressed in guard cells and positively regulate ROS-mediated ABA signaling. *Proceedings of the National Academy of Sciences of the United States of America* 106, 20520-20525.
- Jiang T, Zhang X-F, Wang X-F, Zhang D-P. 2011. Arabidopsis 3-ketoacyl-CoA thiolase-2 (KAT2), an enzyme of fatty acid β -oxidation, is involved in ABA signal transduction. *Plant and Cell Physiology* 52, 528-538.
- Joo JH, Bae YS, Lee JS. 2001. Role of auxin-induced reactive oxygen species in root gravitropism. *Plant Physiology* 126, 1055-1060.
- Kaya H, Nakajima R, Iwano M, et al. 2014. Ca²⁺-activated reactive oxygen species production by Arabidopsis RbohH and RbohJ is essential for proper pollen tube tip growth. *Plant Cell* 26, 1069-1080.
- Kim J, Mayfield SP. 1997. Protein disulfide isomerase as a regulator of chloroplast translational activation. *Science* 278, 1954-1957.
- Kneeshaw S, Gelineau S, Tada Y, Loake GJ, Spoel SH. 2014. Selective protein denitrosylation activity of thioredoxin-h5 modulates plant immunity. *Molecular Cell* 56, 153-162.
- Konopka-Postupolska D, Clark G, Goch G, Debski J, Floras K, Cantero A, Fijolek B, Roux S, Hennig J. 2009. The role of annexin 1 in drought stress in Arabidopsis. *Plant Physiology* 150, 1394-1410.
- Kopriva S, Mugford SG, Baraniecka P, Lee B-R, Matthewman CA, Koprivova A. 2012. Control of sulfur partitioning between primary and secondary metabolism in Arabidopsis. *Frontiers in Plant Science* 3, 163.
- Kosetsu K, Matsunaga S, Nakagami H, Colcombet J, Sasabe M, Soyano T, Takahashi Y, Hirt H, Machida Y. 2010. The MAP kinase MPK4 is required for cytokinesis in Arabidopsis thaliana. *Plant Cell* 22, 3778-3790.
- Kovtun Y, Chiu W-L, Tena G, Sheen J. 2000. Functional analysis of oxidative stress-activated mitogen-activated protein kinase cascade in plants. *Proceedings of the National Academy of Sciences of the United States of America* 97, 2940-2945.
- Kwak JM, Mori IC, Pei Z-M, et al. 2003. NADPH oxidase AtrbohD and AtrbohF genes function in ROS-dependent ABA signaling in Arabidopsis. *EMBO Journal* 22, 2623-2633.
- Laohavisit A, Shang Z, Rubio L, et al. 2012. Arabidopsis annexin1 mediates the radical-activated plasma membrane Ca²⁺- and K⁺-permeable conductance in root cells. *Plant Cell* 24, 1522-1533.
- Lee J, Godon C, Lagniel G, Spector D, Garin J, Labarre J, Toledano MB. 1999. Yap1 and Skn7 control two specialized oxidative stress response regulons in yeast. *Journal of Biological Chemistry* 274, 16040-16046.
- Lee JS, Ellis BE. 2007. Arabidopsis MAPK phosphatase 2 (MKP2) positively regulates oxidative stress tolerance and inactivates the MPK3 and MPK6 MAPKs. *Journal of Biological Chemistry* 282, 25020-25029.
- Lee SC, Lan W, Buchanan BB, Luan S. 2009. A protein kinase-phosphatase pair interacts with an ion channel to regulate ABA signaling in plant guard cells. *Proceedings of the National Academy of Sciences of*

the United States of America 106, 21419-21424.

Levine A, Tenhaken R, Dixon R, Lamb C. 1994. H₂O₂ from the oxidative burst orchestrates the plant hypersensitive disease resistance response. *Cell* 79, 583-593.

Li B, Zhao Y, Liang L, et al. 2012. Purification and characterization of ZmRIP1, a novel reductant-inhibited protein tyrosine phosphatase from maize. *Plant Physiology* 159, 671-681.

Lindermayr C, Sell S, Müller B, Leister D, Durner J. 2010. Redox regulation of the NPR1-TGA1 system of *Arabidopsis thaliana* by nitric oxide. *Plant Cell* 22, 2894-2907.

Lorković ZJ. 2009. Role of plant RNA-binding proteins in development, stress response and genome organization. *Trends in Plant Science* 14, 229-236.

Lumbreras V, Vilela B, Irar S, Solé M, Capellades M, Valls M, Coca M, Pagès M. 2010. MAPK phosphatase MKP2 mediates disease responses in *Arabidopsis* and functionally interacts with MPK3 and MPK6. *Plant Journal* 63, 1017-1030.

Ma Y, Szostkiewicz I, Korte A, Moes D, Yang Y, Christmann A, Grill E. 2009. Regulators of PP2C phosphatase activity function as abscisic acid sensors. *Science* 324, 1064-1068.

MacRobbie EAC. 2002. Evidence for a role for protein tyrosine phosphatase in the control of ion release from the guard cell vacuole in stomatal closure. *Proceedings of the National Academy of Sciences of the United States of America* 99, 11963-11968.

Margis R, Dunand C, Teixeira FK, Margis-Pinheiro M. 2008. Glutathione peroxidase family – an evolutionary overview. *FEBS Journal* 275, 3959-3970.

Marino SM, Gladyshev VN. 2010. Cysteine function governs its conservation and degeneration and restricts its utilization on protein surfaces. *Journal of Molecular Biology* 404, 902-916.

Meinhard M, Grill E. 2001. Hydrogen peroxide is a regulator of ABI1, a protein phosphatase 2C from *Arabidopsis*. *FEBS Letters* 508, 443-446.

Meinhard M, Rodriguez PL, Grill E. 2002. The sensitivity of ABI2 to hydrogen peroxide links the abscisic acid-response regulator to redox signalling. *Planta* 214, 775-782.

Merlot S, Gosti F, Guerrier D, Vavasseur A, Giraudat J. 2001. The ABI1 and ABI2 protein phosphatases 2C act in a negative feedback regulatory loop of the abscisic acid signalling pathway. *Plant Journal* 25, 295-303.

Meyer Y, Belin C, Delorme-Hinoux V, Reichheld J-P, Riondet C. 2012. Thioredoxin and glutaredoxin systems in plants: molecular mechanisms, crosstalks, and functional significance. *Antioxidants & Redox Signaling* 17, 1124-1160.

Miao Y, Lv D, Wang P, Wang X-C, Chen J, Miao C, Song C-P. 2006. An *Arabidopsis* glutathione peroxidase functions as both a redox transducer and a scavenger in abscisic acid and drought stress responses. *Plant Cell* 18, 2749-2766.

Midorikawa T, Endow JK, Dufour J, Zhu J, Inoue K. 2014. Plastidic type I signal peptidase 1 is a redox-dependent thylakoidal processing peptidase. *Plant Journal* 80, 592-603.

- Mills GC. 1957. Hemoglobin catabolism: I. Glutathione peroxidase, an erythrocyte enzyme which protects hemoglobin from oxidative breakdown. *Journal of Biological Chemistry* 229, 189-197.
- Mittler R, Vanderauwera S, Gollery M, Van Breusegem F. 2004. Reactive oxygen gene network of plants. *Trends in Plant Science* 9, 490-498.
- Mittler R, Vanderauwera S, Suzuki N, Miller G, Tognetti VB, Vandepoele K, Gollery M, Shulaev V, Van Breusegem F. 2011. ROS signaling: the new wave? *Trends in Plant Science* 16, 300-309.
- Montrichard F, Alkhalfioui F, Yano H, Vensel WH, Hurkman WJ, Buchanan BB. 2009. Thioredoxin targets in plants: The first 30 years. *Journal of Proteomics* 72, 452-474.
- Mori IC, Murata Y, Yang Y, et al. 2006. CDPKs CPK6 and CPK3 function in ABA regulation of guard cell S-type anion- and Ca²⁺-permeable channels and stomatal closure. *PLoS Biology* 4, e327.
- Motohashi K, Kondoh A, Stumpp MT, Hisabori T. 2001. Comprehensive survey of proteins targeted by chloroplast thioredoxin. *Proceedings of the National Academy of Sciences of the United States of America* 98, 11224-11229.
- Motohashi K, Koyama F, Nakanishi Y, Ueoka-Nakanishi H, Hisabori T. 2003. Chloroplast cyclophilin is a target protein of thioredoxin - Thiol modulation of the peptidyl-prolyl cis-trans isomerase activity. *Journal of Biological Chemistry* 278, 31848-31852.
- Mou Z, Fan W, Dong X. 2003. Inducers of plant systemic acquired resistance regulate NPR1 function through redox changes. *Cell* 113, 935-944.
- Mustafa AK, Gadalla MM, Sen N, et al. 2009. H₂S signals through protein S-sulfhydration. *Science Signaling* 2, ra72.
- Nakano Y, Asada K. 1981. Hydrogen peroxide is scavenged by ascorbate-specific peroxidase in spinach chloroplasts. *Plant and Cell Physiology* 22, 867-880.
- Navrot N, Rouhier N, Gelhaye E, Jacquot J-P. 2007. Reactive oxygen species generation and antioxidant systems in plant mitochondria. *Physiologia Plantarum* 129, 185-195.
- Ndamukong I, Al Abdallat A, Thurow C, Fode B, Zander M, Weigel R, Gatz C. 2007. SA-inducible Arabidopsis glutaredoxin interacts with TGA factors and suppresses JA-responsive PDF1.2 transcription. *Plant Journal* 50, 128-139.
- Orozco-Cardenas M, Ryan CA. 1999. Hydrogen peroxide is generated systemically in plant leaves by wounding and systemin via the octadecanoid pathway. *Proceedings of the National Academy of Sciences of the United States of America* 96, 6553-6557.
- Park S-W, Li W, Viehhauser A, et al. 2013. Cyclophilin 20-3 relays a 12-oxo-phytodienoic acid signal during stress responsive regulation of cellular redox homeostasis. *Proceedings of the National Academy of Sciences of the United States of America* 110, 9559-9564.
- Park S-Y, Fung P, Nishimura N, et al. 2009. Abscisic acid inhibits PP2Cs via the PYR/PYL family of ABA-binding START proteins. *Science* 324, 1068-1071.
- Paul BD, Snyder SH. 2012. H₂S signalling through protein sulfhydration and beyond. *Nature Reviews*

Molecular Cell Biology 13, 499-507.

Pauwels L, Goossens A. 2011. The JAZ proteins: a crucial interface in the jasmonate signaling cascade. *Plant Cell* 23, 3089-3100.

Pei Z-M, Murata Y, Benning G, Thomine S, Klüsener B, Allen GJ, Grill E, Schroeder JI. 2000. Calcium channels activated by hydrogen peroxide mediate abscisic acid signalling in guard cells. *Nature* 406, 731-734.

Pitzschke A, Djamei A, Bitton F, Hirt H. 2009. A major role of the MEKK1-MKK1/2-MPK4 pathway in ROS signalling. *Molecular Plant* 2, 120-137.

Potocký M, Jones MA, Bezdova R, Smirnov N, Žárský V. 2007. Reactive oxygen species produced by NADPH oxidase are involved in pollen tube growth. *New Phytologist* 174, 742-751.

Rey P, Bécuwe N, Barrault M-B, Rumeau D, Havaux M, Biteau B, Toledano MB. 2007. The Arabidopsis thaliana sulfiredoxin is a plastidic cysteine-sulfinic acid reductase involved in the photooxidative stress response. *Plant Journal* 49, 505-514.

Richards SL, Laohavisit A, Mortimer JC, Shabala L, Swarbreck SM, Shabala S, Davies JM. 2014. Annexin 1 regulates the H₂O₂-induced calcium signature in Arabidopsis thaliana roots. *Plant Journal* 77, 136-145.

Rochon A, Boyle P, Wignes T, Fobert PR, Després C. 2006. The coactivator function of Arabidopsis NPR1 requires the core of its BTB/POZ domain and the oxidation of C-terminal cysteines. *Plant Cell* 18, 3670-3685.

Roos G, Foloppe N, Messens J. 2013. Understanding the pK_a of redox cysteines: the key role of hydrogen bonding. *Antioxidants & Redox Signaling* 18, 94-127.

Roos G, Messens J. 2011. Protein sulfenic acid formation: From cellular damage to redox regulation. *Free Radical Biology and Medicine* 51, 314-326.

Sandalio LM, Fernández VM, Rupérez FL, Del Río LA. 1988. Superoxide free radicals are produced in glyoxysomes. *Plant Physiology* 87, 1-4.

Sato A, Sato Y, Fukao Y, et al. 2009. Threonine at position 306 of the KAT1 potassium channel is essential for channel activity and is a target site for ABA-activated SnRK2/OST1/SnRK2.6 protein kinase. *Biochemical Journal* 424, 439-448.

Schürmann P, Buchanan BB. 2008. The ferredoxin/thioredoxin system of oxygenic photosynthesis. *Antioxidants & Redox Signaling* 10, 1235-1273.

Shen Y, Danon A, Christopher DA. 2001. RNA binding-proteins interact specifically with the Arabidopsis chloroplast psbA mRNA 5' untranslated region in a redox-dependent manner. *Plant and Cell Physiology* 42, 1071-1078.

Sirichandra C, Gu D, Hu H-C, et al. 2009. Phosphorylation of the Arabidopsis AtrbohF NADPH oxidase by OST1 protein kinase. *FEBS Letters* 583, 2982-2986.

Sobotta MC, Liou W, Stöcker S, Talwar D, Oehler M, Ruppert T, Scharf AND, Dick TP. 2014. Peroxiredoxin-2 and STAT3 form a redox relay for H₂O₂ signaling. *Nature Chemical Biology* 10.1038/nchembio.1695.

Song CJ, Steinebrunner I, Wang X, Stout SC, Roux SJ. 2006. Extracellular ATP induces the accumulation of

superoxide via NADPH oxidases in Arabidopsis. *Plant Physiology* 140, 1222-1232.

Song Y, Miao Y, Song C-P. 2014. Behind the scenes: the roles of reactive oxygen species in guard cells. *New Phytologist* 201, 1121-1140.

Strader LC, Monroe-Augustus M, Bartel B. 2008. The IBR5 phosphatase promotes Arabidopsis auxin responses through a novel mechanism distinct from TIR1-mediated repressor degradation. *BMC Plant Biology* 8, 41.

Tada Y, Spoel SH, Pajerowska-Mukhtar K, Mou Z, Song J, Wang C, Zuo J, Dong X. 2008. Plant immunity requires conformational changes of NPR1 via S-nitrosylation and thioredoxins. *Science* 321, 952-956.

Takahashi F, Yoshida R, Ichimura K, Mizoguchi T, Seo S, Yonezawa M, Maruyama K, Yamaguchi-Shinozaki K, Shinozaki K. 2007. The mitogen-activated protein kinase cascade MKK3-MPK6 is an important part of the jasmonate signal transduction pathway in Arabidopsis. *Plant Cell* 19, 805-818.

Taki N, Sasaki-Sekimoto Y, Obayashi T, et al. 2005. 12-oxo-phytodienoic acid triggers expression of a distinct set of genes and plays a role in wound-induced gene expression in Arabidopsis. *Plant Physiology* 139, 1268-1283.

Templeton DJ, Aye M-S, Rady J, Xu F, Cross JV. 2010. Purification of reversibly oxidized proteins (PROP) reveals a redox switch controlling p38 MAP kinase activity. *PLoS ONE* 5, e15012.

Trivedi DK, Yadav S, Vaid N, Tuteja N. 2012. Genome wide analysis of Cyclophilin gene family from rice and Arabidopsis and its comparison with yeast. *Plant Signaling & Behavior* 7, 1653-1666.

Ueoka-Nakanishi H, Sazuka T, Nakanishi Y, Maeshima M, Mori H, Hisabori T. 2013. Thioredoxin h regulates calcium dependent protein kinases in plasma membranes. *FEBS Journal* 280, 3220-3231.

Vahisalu T, Kollist H, Wang Y-F, et al. 2008. SLAC1 is required for plant guard cell S-type anion channel function in stomatal signalling. *Nature* 452, 487-491.

Van Laer K, Hamilton CJ, Messens J. 2013. Low-molecular-weight thiols in thiol-disulfide exchange. *Antioxidants & Redox Signaling* 18, 1642-1653.

Walia A, Lee JS, Wasteney G, Ellis B. 2009. Arabidopsis mitogen-activated protein kinase MPK18 mediates cortical microtubule functions in plant cells. *Plant Journal* 59, 565-575.

Waszczak C, Akter S, Eeckhout D, et al. 2014. Sulfenome mining in Arabidopsis thaliana. *Proceedings of the National Academy of Sciences of the United States of America* 111, 11545-11550.

Wise RR, Naylor AW. 1987. Chilling-enhanced photooxidation: evidence for the role of singlet oxygen and superoxide in the breakdown of pigments and endogenous antioxidants. *Plant Physiology* 83, 278-282.

Wituszyńska W, Gałązka K, Rusaczonek A, Vanderauwera S, Van Breusegem F, Karpiński S. 2013a. Multivariable environmental conditions promote photosynthetic adaptation potential in Arabidopsis thaliana. *Journal of Plant Physiology* 170, 548-559.

Wituszyńska W, Ślesak I, Vanderauwera S, et al. 2013b. LESION SIMULATING DISEASE1, ENHANCED DISEASE SUSCEPTIBILITY1, and PHYTOALEXIN DEFICIENT4 conditionally regulate cellular signaling homeostasis, photosynthesis, water use efficiency, and seed yield in Arabidopsis. *Plant Physiology* 161, 1795-1805.

- Wrzaczek M, Brosché M, Kangasjärvi J. 2013. ROS signaling loops – production, perception, regulation. *Current Opinion in Plant Biology* 16, 575-582.
- Wrzaczek M, Vainonen JP, Stael S, et al. 2014. GRIM REAPER peptide binds to receptor kinase PRK5 to trigger cell death in Arabidopsis. *EMBO Journal* 10.15252/embj.201488582.
- Wu Y, Zhang D, Chu JY, Boyle P, Wang Y, Brindle ID, De Luca V, Després C. 2012. The Arabidopsis NPR1 protein is a receptor for the plant defense hormone salicylic acid. *Cell Reports* 1, 639-647.
- Xie K, Chen J, Wang Q, Yang Y. 2014. Direct phosphorylation and activation of a mitogen-activated protein kinase by a calcium-dependent protein kinase in rice. *Plant Cell* 26, 3077-3089.
- Xu Q, Fu H-H, Gupta R, Luan S. 1998. Molecular characterization of a tyrosine-specific protein phosphatase encoded by a stress-responsive gene in Arabidopsis. *Plant Cell* 10, 849-857.
- Yohn CB, Cohen A, Rosch C, Kuchka MR, Mayfield SP. 1998. Translation of the chloroplast psbA mRNA requires the nuclear-encoded poly(A)-binding protein, RB47. *Journal of Cell Biology* 142, 435-442.
- Yu M, Lamattina L, Spoel SH, Loake GJ. 2014. Nitric oxide function in plant biology: a redox cue in deconvolution. *New Phytologist* 202, 1142-1156.
- Zaffagnini M, Bedhomme M, Marchand CH, Morisse S, Trost P, Lemaire SD. 2012. Redox regulation in photosynthetic organisms: focus on glutathionylation. *Antioxidants & Redox Signaling* 16, 567-586.
- Zarepour M, Kaspari K, Stagge S, Rethmeier R, Mendel RR, Bittner F. 2010. Xanthine dehydrogenase AtXDH1 from Arabidopsis thaliana is a potent producer of superoxide anions via its NADH oxidase activity. *Plant Molecular Biology* 72, 301-310.
- Zhang F, Strand A, Robbins D, Cobb MH, Goldsmith EJ. 1994. Atomic structure of the MAP kinase ERK2 at 2.3 Å resolution. *Nature* 367, 70-711.
- Zhou J, Xia X-J, Zhou Y-H, Shi K, Chen Z, Yu J-Q. 2014. RBOH1-dependent H₂O₂ production and subsequent activation of MPK1/2 play an important role in acclimation-induced cross-tolerance in tomato. *Journal of Experimental Botany* 65, 595-607.
- Zhu S-Y, Yu X-C, Wang X-J, et al. 2007. Two calcium-dependent protein kinases, CPK4 and CPK11, regulate abscisic acid signal transduction in Arabidopsis. *Plant Cell* 19, 3019-3036.

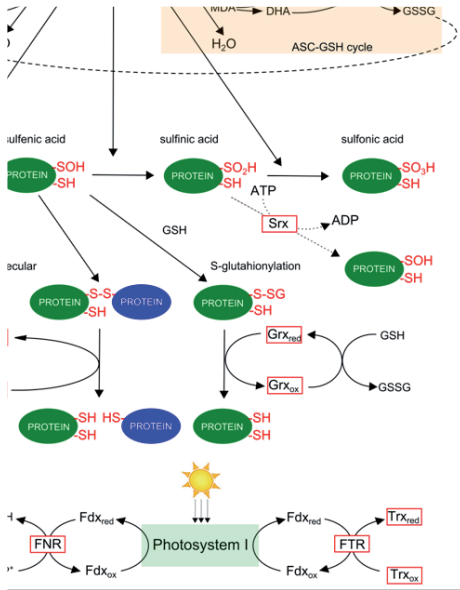


Fig. 1. The impact of H₂O₂ on plant cells. (A) Production and enzymatic scavenging of H₂O₂. SOD, superoxide dismutase; Prx, peroxiredoxin; CAT, catalase; GR, glutathione reductase; GPX, glutathione peroxidase; APX, ascorbate peroxidase; MDAR, monodehydroascorbate reductase; DHAR, dehydroascorbate reductase, Srx, sulfiredoxin. Adapted from Dietz (2011) and Mittler et al. (2004). (B) Oxidative post-translational modifications of cysteine residues, adapted from Roos and Messens (2011). (C) Light-dependent reduction of thioredoxins within the chloroplast. Fdx, ferredoxin; FTR, ferredoxin-thioredoxin reductase; NTR, NADPH-dependent thioredoxin reductase, FNR, ferredoxin-NADP+ reductase.

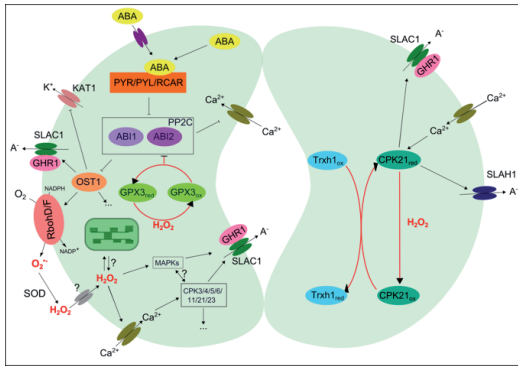


Fig. 2. Schematic representation of cysteine post-translational modifications in guard cell signaling. Red arrows indicate reactions involving thiol/disulfide exchange. For description of abbreviations and specific regulatory events, we refer to the main text.

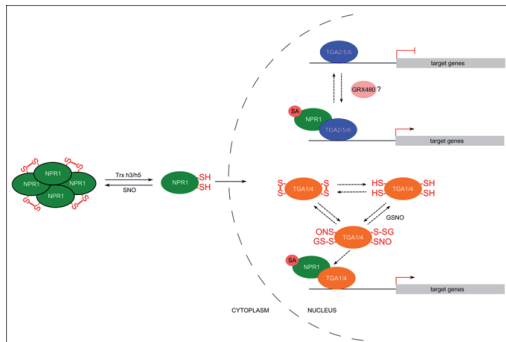


Fig. 3. Schematic representation of NPR1-based plant immune signaling. Upon pathogen infection and initial oxidative burst, the cytoplasm gets reduced by cell antioxidant systems. This leads to the monomerization of transcriptional co-activator NPR1 and its subsequent translocation to the nucleus. Upon import, NPR1 interacts with transcriptional repressors TGA2/5/6 and de-represses the expression of pathogenesis-related (PR) genes. Binding with TGA1/4 is promoted by S glutathionylation/S-nitrosylation of their Cys residues and results in the activation of PR gene expression.

ADDENDUM 2. CYSTEINES UNDER ROS ATTACK IN PLANTS: A PROTEOMICS VIEW

Salma Akter^{1,2,3,4,5,8,§}, Cezary Waszczak^{1,2,3,4,5,§,#}, Jingjing Huang^{3,4,5}, Silke Jacques^{1,2,6,7}, Kris Gevaert^{6,7}, Frank Van Breusegem^{1,2,*}, and Joris Messens^{3,4,5,*}

1Department of Plant Systems Biology, VIB, 9052 Ghent, Belgium; 2Department of Plant Biotechnology and Bioinformatics, Ghent University, 9052 Ghent, Belgium; 3Structural Biology Research Center, VIB, 1050 Brussels, Belgium; 4Brussels Center for Redox Biology, 1050 Brussels, Belgium; 5Structural Biology Brussels, Vrije Universiteit Brussel, 1050 Brussels, Belgium; 6Department of Medical Protein Research, VIB, 9000 Gent, Belgium; 7Department of Biochemistry, Ghent University, 9000 Gent, Belgium; 8Faculty of Biological Sciences, University of Dhaka, 1000 Dhaka, Bangladesh

§These authors contributed equally to this work.

#present address: Division of Plant Biology, Department of Biosciences, University of Helsinki, 00014 Helsinki, Finland

*To whom correspondence should be addressed: E-mail: joris.messens@vib-vub.be;

frank.vanbreusegem@psb.vib-ugent.be.

E-mail addresses: Salma Akter:; saakt@psb.vib-ugent.be; Cezary Waszczak: cezary.waszczak@helsinki.fi; Jingjing Huang: jihua@psb.vib-ugent.be; Silke Jacques: sijac@psb.vib-ugent.be; Kris Gevaert: Kris.Gevaert@UGent.be

Corresponding authors:

Frank Van Breusegem

Department Plant Systems Biology, VIB Ghent University

Technologiepark 927, B-9052 Ghent, Belgium

Tel.: +32 9 331 39 20; Fax : +32 9 331 38 09 ; E-mail: frank.vanbreusegem@psb.vib-ugent.be

Joris Messens

Structural Biology Research Center, VIB - Vrije Universiteit Brussel

Pleinlaan 2, B-1050 Brussel, Belgium

Tel.: +32 2 6291992; Fax: +32 2 6291963; E-mail: joris.messens@vib-vub.be.

ABSTRACT

Plants generate reactive oxygen species (ROS) as part of their metabolism and as response to various external stress factors, potentially causing significant damage to cell structures, known as oxidative stress. During the course of evolution, plants have adapted to this ROS toxicity, and today, plants use ROS as a signaling messenger that activates defense responses. Cysteine (Cys) residues in proteins are one of the sensitive targets for ROS-mediated post-translational modifications (PTMs), and they have become a crucial key residue for ROS signaling studies. The reactivity of Cys residues toward ROS and the possibility to be present in different oxidation states permit them to appear on the crossroad of highly dynamic oxidative events. As such, a redox active cysteine can be present as S-glutathionylated (-SSG), disulfide bonded (S-S), sulfenylated (-SOH), sulfinylated (-SO₂H), and also sulfonylated (-SO₃H). The sulfenic acid (-SOH) form has been considered as part of ROS sensing pathways, as it leads to further modifications which affect protein structure and function. To understand why and how cysteines undergo oxidative PTMs and to explore the ROS sensor proteins of plants, redox proteomic studies are required. Here, we update the current knowledge of the cysteine reactivity with ROS. Further, we give an overview of the proteomic techniques applied to identify different redox modified cysteines in plants. Special focus goes to the identification of sulfenylated proteins, which have the potential to be involved in plant signal transduction.

Key words: Cysteine, oxidative post-translational modification, redox proteomics, redox regulation, reactive oxygen species, sulfenic acid

Abbreviations: BCN, bicyclo[6.1.0]nonyne; c-CRD, carboxy-terminal, cysteine-rich domain; Cys, cysteine; cystMT, cysteine tandem mass tag; 2-DE, two-dimensional electrophoresis; DTT, dithiothreitol; Fdx, ferredoxin; FNR, Fdx:NADP reductase; FTR, ferredoxin-thioredoxin reductase; GEE-biotin, biotinylated reduced glutathione ethyl ester; GSH, glutathione; H₂O₂, hydrogen peroxide; IAF, iodoacetamidofluorescein; IAM, iodoacetamide; ICAT, isotope coded affinity tag; iTRAQ, isobaric tag labeling; NEM, N-ethylmaleimide; NO, nitric oxide; Ox-PTMs, oxidative post-translational modifications; PTMs, post-translational modifications; RNS, reactive nitrogen species; ROS, reactive oxygen species; R-SO₂H, sulfinic acid; RSSH, persulfide species; -SSG, ROS-triggered S-glutathionylation; RS-SR', ROS-triggered disulfide bond formation; -S-, thiolate anion; -SH, thiol; -SNO, S- S-nitrosylation; -SOH, sulfenic acid; -SO₂H, sulfinic acid; -SO₃H, sulfonic acid; Srx, sulfiredoxin; S-S, disulfide bond formation; SSG, S glutathionylation; TCEP, tris 2-carboxyethyl phosphine; Trx, thioredoxin reductase; YAP1, yeast AP-1.

INTRODUCTION

During stress conditions, plants accumulate reactive oxygen species (ROS), such as hydrogen peroxide (H₂O₂), and reactive nitrogen species (RNS), such as nitric oxide (NO). ROS/RNS have a dual face, since they can either lead to oxidative damage or trigger signal transduction via redox sensors (Huang et al., 2012; Miller et al., 2010). However, the molecular mechanism of how the ROS/RNS signal is sensed and traveling within or across different cells is still unsolved. Exploring which and how proteins sense ROS/RNS and transduce these stimuli into downstream biological effects is one of the major challenges in plant redox biology.

ROS/RNS interact with multiple signaling pathways and transmit signals through the post-translational modifications (PTMs) of signaling proteins. Cysteine (Cys) is one of the sensitive targets of ROS/RNS, as it contains the electron rich sulfur atom appearing in a wide range of oxidation states that make Cys residues the major sites of oxidative modifications within proteins (Davies, 2005). It is a well-recognized concept that profiling of ROS/RNS modified proteins containing cysteine, can unveil key

redox sensors involved in signal transduction pathways (Couturier et al., 2013). The availability of different oxidation states permits the formation of a diverse range of cysteine oxidative PTMs (Ox-PTMs), including ROS-triggered S-glutathionylation (RSSG), disulfide bond formation (RS-SR'), sulfenylation (-SOH), sulfinylation (-SO₂H), sulfonylation (-SO₃H), and RNS-mediated S-nitrosylation (-SNO). Protein S-nitrosylation, the covalent attachment of NO to Cys residues to form S-nitrosothiol (-SNO), has been considered as the most important route to transfer the bioactivity of NO in plants to date (Yu et al., 2014). S-nitrosylation of crucial signaling proteins affects their enzyme activity (Lindermayr et al., 2005; Romero-Puertas et al., 2007; Wang et al., 2009; Yun et al., 2011), localization (Tada et al., 2008), structure (Tavares et al., 2014), and interaction with other proteins (Bellin et al., 2013; Hara et al., 2006; Yu et al., 2014). Different technologies have been developed and applied for the identification of S-nitrosylation, either experimentally or computationally (Bellin et al., 2013; Lee et al., 2011). Numerous plant proteins have been identified by proteomics studies to undergo S-nitrosylation, of which many are implicated in signaling pathways as crucial physiological regulators, especially in plant disease resistance (Puyaubert et al., 2014). In this review, NO-mediated S-nitrosylation will not be discussed, but it is the topic of Romero-Puertas et al. (2013).

So far, the main focus of ROS-triggered Cys Ox-PTM studies in plants was on reversible modification, such as disulfides and S-glutathionylated proteomes. These Cys Ox-PTMs play important roles in the cellular redox balance and prevent oxidative damage through the cellular redox regulation systems, like glutaredoxin (Grx) or thioredoxin (Trx) (Balmer et al., 2004; Balmer et al., 2006; Buchanan and Balmer, 2005; Fernandes and Holmgren, 2004; Marchand et al., 2006; Marchand et al., 2010; Yoshida et al., 2013). The formation of a sulfenic acid, the initial oxidation product of the Cys residue, has been shown to function as a redox sensor involved in many physiological pathways, by affecting the enzymatic and metal binding activities of crucial signaling proteins, and the activity of transcription factors modulating gene expression (Oger et al., 2012; Poole et al., 2004; Poole and Nelson, 2008; Reddie and Carroll, 2008; Roos and Messens, 2011). Similarly to NO-mediated S-nitrosylation, H₂O₂-mediated sulfenylation appears to be a global signaling pathway, which can be considered to be analogous to the well-known PTM, phosphorylation (Paulsen et al., 2012; Yu et al., 2014). However, because of the lack of well-established technologies for the identification of sulfenylation, the knowledge of the plant sulfenome remains quite limited.

CYS PTMS UNDER ROS ATTACK

ROS-mediated modifications do not happen to all Cys residues in an individual protein, and different thiol-proteins react with ROS at different rates (Marinho et al., 2014). The subtle structural environment within a protein will determine the final fate of the cysteine, and as such also the function of the respective protein. Crucial is the thermodynamic and kinetic stability of the first oxidation state of the Cys residue, the sulfenic acid (Fig. 1), which makes that the Cys-SOH can be regarded as the central PTM on the crossroad toward different destinations.

As already mentioned, the reactivity of Cys residues toward ROS can be largely different, and this reactivity is strongly correlated with its pKa (Roos et al., 2013). The structural environment of a protein will determine the pKa of a specific cysteine, and as such the balance between the thiol (SH) and the

thiolate anion (S⁻) state of the cysteine (Roos and Messens, 2011). By the presence of polar, positively charged amino acids, or local dipoles, like at the N-terminus of an α -helix, the thiolate is stabilized through electrostatic interactions, which decrease the pKa of the cysteine (Roos et al., 2013). If the pKa is lower than the pH, the majority of the thiols will be present as a thiolate. While free cysteine has a pKa of 8.3-8.5 (Luo et al., 2005; Tajc et al., 2004), the most oxidation sensitive Cys residues described thus far have a pKa \leq 3.5 (Gan et al., 1990; Nelson and Creighton, 1994). Also, hydrogen bonding has a strong influence on the pKa of cysteines. Thioredoxin (Trx) with two hydrogen bonds directed to the thiolate of the active-site nucleophilic cysteine has a pKa \sim 7.0, while the respective cysteine in the Trx-fold of glutaredoxin (Grx) receives three hydrogen bonds, which results in a pKa of \sim 4.0 (Roos et al., 2013). In general, the more hydrogen bonds a cysteine-sulfur receives, the lower its pKa, the more the thiolate form is stabilized. Other factors that play a role in the reactivity of a cysteine-sulfur are the accessibility and its presence in specific binding sites (Marino and Gladyshev, 2010), like for example in peroxiredoxins. (Roos and Messens, 2011).

The kinetic stability of the sulfenic acid strongly depends on the presence of nearby cysteines and on the accessibility to low molecular weight thiols, like the tri-peptide glutathione (GSH). The electrophilic sulfenic acid will then react and form an intermolecular disulfide or a mixed disulfide (i.e. S-glutathionylation) (Fig. 1). These disulfides are reversible as they can be reduced by the GSH/Grx system or the Trx/thioredoxin reductase (TxR) systems (Collet and Messens, 2010; Messens and Collet, 2013). S-glutathionylation is long believed to serve as a kind of safeguard of sulfenic acids against overoxidation and permanent protein damage. More recently, S-glutathionylation starts to gain recognition for its role in redox signaling (Zaffagnini et al., 2012b; Zaffagnini et al., 2012c).

Plants are equipped with a complex network of Trx/Grx systems, the Arabidopsis genome encodes 44 Trx and 50 Grx proteins (Meyer et al., 2012). These Trx and Grx proteins also need to be reduced, and therefore plants have multiple sources of reducing equivalents in different subcellular localizations. The major reducing equivalents are coming from NADPH, which is known to be the general electron donor for both Trx and Grx reducing systems. In chloroplasts, Trx is being reduced by light (Meyer et al., 2009). Electrons released in the oxidation of H₂O are transferred along the photosynthetic electron transfer chain via Photosystems I and II to ferredoxin (Fdx) which reduces either Trx via ferredoxin-thioredoxin reductase (FTR) or NADP via Fdx:NADP reductase (FNR).

In the case that the structural determinants in the protein environment are not stabilizing the sulfenic acid, it can undergo an additional reaction with H₂O₂ and form sulfinic acid (SO₂H) and sulfonic acid (SO₃H), although the rate of these reactions is slower than that of the reaction of H₂O₂ with a thiolate (Hugo et al., 2009; Hugo et al., 2014). In most cases, overoxidation is irreversible and it will lead to protein degradation. However, the reversibility of a sulfinic acid (R-SO₂H) modification has been debated. For example, it has been shown that an ATP-dependent sulfiredoxin (Srx) enzyme was capable of reducing R-SO₂H in plant cells (Rey et al., 2007). Since thus far the only known substrates of AtSrx are chloroplast 2-Cys peroxiredoxins and mitochondrial PrxIIIF (Iglesias-Baena et al., 2011; Rey et al., 2007), the reduction of R-SO₂H cannot be regarded as a general rule.

Finally, an alternative way to protect sulfenic acids from overoxidation is the reaction of a sulfenic acid with the backbone nitrogen of the adjacent residue, forming a sulfenylamide (Fig. 1), which is well known for the human protein tyrosine phosphatase (PTP1B) (Haque et al., 2011; Salmeen et al., 2003).

Whether plant proteins use sulfenylamide formation as a cysteine protection strategy remains unclear.

PROTEOMICS FOR STUDYING CYS OX-PTMS

Since the advent of proteomics, numerous studies have aimed at the identification of proteins with an oxidative modified cysteine. Basically, all proteomic technologies consist of three basic steps: I) tagging of the oxidative modifications, II) isolation or enrichment of the modified proteins, and III) identification of the modified proteins. Here we focus on the redox proteomics applied in plants to understand the Cys Ox-PTMs (Table 1 and 2).

DIFFERENTIAL ALKYLATION-BASED INDIRECT PROTEOMICS

Currently, differential alkylation methods are the most widely used to indirectly detect and study the cysteine status in proteins, which undergo all kind of reversible Cys Ox-PTMs. This method comprises three consecutive steps: blocking of the free thiols, specific reduction of the modified Cys Ox-PTM, and finally isolation or labeling of the newly obtained thiols (Table 1).

The free thiols are blocked using alkylating reagents such as iodoacetamide (IAM), or N-ethylmaleimide (NEM), which form an irreversible S-carbamidomethylated thiol or a thioether, respectively (Hansen et al., 2009). The reversible cysteine modifications are then reduced by a general reductant like tris 2-carboxyethyl phosphine (TCEP) or dithiothreitol (DTT). Subsequently, the newly obtained thiols are isolated by thiol affinity chromatography (Lee et al., 2004) or labeled with a tagged alkylating agent such as biotin-conjugated IAM/NEM/maleimide/HDPD, iodoacetamidofluorescein (IAF), mBBr, cysteine tandem mass tag (cysTMT), isobaric tag labeling (iTRAQ), isotope coded affinity tag (ICAT) etc. This differential labeling allows downstream analysis by Western blot or fluorescence-based visualization of the redox active protein spots on a two-dimensional electrophoresis (2-DE) gel, or avidin affinity enrichment, and finally mass spectrophotometical identification (Alvarez et al., 2009; Bykova et al., 2011b; Liu et al., 2014; Parker et al., 2012; Wang et al., 2012). Quantification of the cysteine redox state of individual proteins is possible by using ICAT, iTRAQ, cysTMT tags, as they enable selective labeling and relative quantitation of cysteine-containing peptides representing their redox status in the samples.

In alkylation-based proteomics, specific reversible cysteine modifications can be identified using a specific reducing agent. Arsenite is applied as a specific reductant to study sulfenylation (Saurin et al., 2004; Tyther et al., 2010). The peroxide inactivation of papain through sulfenic acid modification has been reported by using this reducing agent (Lin et al., 1975), however, this approach has not been used in plant redox proteomics research. Trxs have been used for the reduction of disulfide bonds and Grxs to reduce S-gluthionylated proteins (Yano et al., 2001; Lind et al., 2002). Application of this strategy at the cellular level provides a global scenario of the reversible cysteine oxidation status, including S-S, -SSG, and SOH, and has been explored in plants both at cellular and subcellular levels (Table 1). However, application of this technique for sulfenome proteomics is limited due to the highly reactive, transient nature of sulfenic acids. Although in vitro blocking, reduction and labeling steps are performed under acidic or anaerobic conditions, it does not completely preclude the chance of de novo sulfenylation due to

an altered cysteine redox state in the cell lysates, or that the sulfenic acid modifications are insufficiently trapped due to protection or overoxidation (Couturier et al., 2013; Leonard and Carroll, 2011).

DIRECT PROTEOMICS FOR CYS OX-PTMS

Apart from the alkylation-based indirect technologies, direct detections have been developed for the identification of Cys Ox-PTMs. Most of these direct proteomics are based on specific probes for direct trapping or labeling of the modified proteins, or for affinity enrichment of the targets (Table 2).

Sulfenylation (-SOH)

Direct detection of -SOH is based on the electrophilic character of the sulfur within the sulfenic acid (Gupta and Carroll, 2014), which can react with a highly selective 5,5-dimethyl-1,3-cyclohexanedione (dimedone). Subsequently, dimedone-tagged proteins can be identified by mass spectrometry (Carballal et al., 2003; Waszczak et al., 2014). However, dimedone has limited applications for the identification of the cellular sulfenome due to the lack of a functional group to enrich for dimedone-tagged sulfenylated proteins. Therefore, dimedone-biotin/fluorophores conjugates, such as the DCP-bio series, the DCP-FL series, and the DCP-Rho series, have been developed, which allow sensitive detection and enrichment of SOH modified proteins (Charles et al., 2007; Poole et al., 2005). One potential drawback of these chemical probes is that the bulky chemical tags compromise cell-permeability (Poole et al., 2007; Seo and Carroll, 2009). A subsequent alternative approach was the development of azido- and alkyne-functionalized dimedone analogs termed DAz-1 (Reddie et al., 2008; Seo and Carroll, 2009), DAz-2 (Leonard et al., 2009), DYn-1 and DYn-2 (Paulsen and Carroll, 2013), which enable the direct trapping and tagging of protein-SOH modifications in living cells. DYn-2 has been reported as a non-toxic probe with no influence on the intracellular redox balance (Paulsen et al., 2012; Yang et al., 2014). This alkyne functionalized probe has recently been applied for the first time in plants, leading to the identification of 226 sulfenylated proteins in H₂O₂ treated Arabidopsis cells (Akter et al. submitted). Two recent reports expand the list of chemical probes: 1,3-cyclopentadione (Qian et al., 2011) and the linear β -ketoester (Qian et al., 2012). However, the linear β -ketoester probe has been debated with an issue of unspecific recognition (Gupta and Carroll, 2014). More recently, a new chemical probe for SOH detection, termed bicyclo[6.1.0]nonyne (BCN) derivatives, has been published (Poole et al., 2014). It is characterized with a reaction rate that is more than two orders of magnitude faster as compared to dimedone-based probes.

In situ trapping approaches with these chemical probes have their own limitations, as the addition of a small membrane permeable molecule to cells might interfere with the signaling pathways. This issue can be addressed, at least in part, by adding the probe to cells after signal pathway activation and/or by monitoring the effect of probe addition on relevant downstream biological markers (Paulsen and Carroll, 2009). Another important consideration with chemical probes is the rate at which the probes react with the modified Cys residue. If the reaction is slow, transient cysteine oxidation events might be missed. The modest second order rate constant for the reaction of many dimedone analogs with sulfenic acid is only $2.7 \times 10^{-2} \text{ M}^{-1}\text{s}^{-1}$ (Paulsen and Carroll, 2013), which might not be sufficient to trap especially transient modifications. Therefore, it will be important to develop chemical probes with a high reaction rate to trap

these transiently formed sulfenic acids. The DYn-2 probe, however, is doing much better, since its reaction rate with dipeptide-SOH is estimated to be $11 \text{ M}^{-1}\text{s}^{-1}$ (Gupta and Carroll, 2014). In recent work of Poole et al. (2014), it has been shown that strained cycloalkynes react with sulfenic acids to yield a stable alkenyl sulfoxide with a reaction rate that is 100 times faster than that of most dimedone-based 1,3 dicarbonyl reagents. However, increasing the probe concentration can also compensate for relatively modest reaction rates, but appropriate controls must be performed to ensure that the underlying biology is not disturbed.

Alternatively, a yeast AP-1 (YAP1)-based genetic probe offers a way to trap -SOH in vivo for the identification of redox sensitive proteins undergoing sulfenylation under oxidative stress conditions (Takanishi et al., 2007b). To develop a YAP1 genetic probe, the C-terminal cysteine rich domain of the YAP1 transcription factor was mutated, leaving a single Cys598 for trapping sulfenylated proteins through the formation of disulfide bonds. This genetic probe equipped with an affinity tag was expressed in *Escherichia coli* and used to co-purify proteins undergoing H₂O₂-dependent sulfenylation. In a follow-up study, this technique was applied to yeast (Takanishi and Wood, 2011) to profile sulfenylated proteins under H₂O₂ stress. Using a combination of the DCP-Bio1 and YAP1 probe in the *Medicago truncatula* and *Sinorhizobium meliloti* symbiosis, 44 proteins were found sulfenylated in inoculated roots and 65 proteins in the functioning symbiotic organ (Oger et al., 2012). We developed and applied successfully the YAP1-based sulfenome mining strategy in *Arabidopsis thaliana* with the identification of 97 sulfenylated proteins in *Arabidopsis* cell suspensions under H₂O₂ stress (Waszczak et al., 2014).

In contrast to chemical probes, the YAP1-based sulfenome probe is non-invasive and more physiological. The use of the YAP1 protein probe enables exploration of organellar sulfenomes, as it can be easily modified with target peptide sequences (Takanishi et al., 2007a; Takanishi and Wood, 2011). In addition, if we compare the rate constant of YAP1 disulfide formation with target sulfenic acids with that of the reaction of sulfenic acids with thiols to form a disulfide bond ($21.6 \text{ M}^{-1}\text{s}^{-1}$) (Gupta and Carroll, 2014; Paulsen and Carroll, 2013), the YAP1 genetic probe should be more efficient in trapping sulfenic acids than the chemical probe. The drawbacks of the YAP1-based strategy are the relative low efficiency and the somewhat high risk of false identifications (Furdui and Poole, 2014). The number of detected sulfenic acid-forming proteins could be underestimated due to the reduction of disulfide bonds (between YAP1 and target sulfenylated proteins) by glutathione or redox enzymes or other cysteine containing proteins, or by the resolving cysteine of the trapped protein itself. Another limitation could be the steric effects, since the Yap1-carboxy-terminal, cysteine-rich domain (c-CRD) variant must be expressed in host cells and, since it is protein-based, it may exhibit substrate bias when compared to chemical-based probes (Gupta and Carroll, 2014). Moreover, there is a chance of co-elution of non-sulfenic acid proteins due to complex protein-protein interactions.

At this stage, the combination of the genetic probe and a chemical probe would be an appropriate strategy to explore the complete sulfenome in plants, because both probes have their specific advantages. Moreover, future research should be focused on mapping and quantifying the sulfenylation sites in the signal transduction proteins to assess their role in oxidative stress signal transduction events. A recent work of Yang et al. (2014) reports a proteomic workflow for the quantitative identification of sulfenylation sites combining DYn-2 with a functionalized biotin reagent containing a cleavable linker. In human cells, this probe allows to identify about 1,000 sulfenylation sites in more than 700 proteins.

DISULFIDE BONDS (S-S)

A direct *in vitro* disulfide proteomics method called redox two-dimensional electrophoresis (redox 2-DE) or diagonal two-dimensional electrophoresis (diagonal 2-DE) is used to identify intra- or intermolecular disulfides under non-reducing and reducing conditions based on the differential migration in the gel (Cumming, 2008). Non-disulfide proteins will migrate on a diagonal since they have the same electrophoretic mobility in both dimensions. However, proteins containing intramolecular disulfide bonds have a lower electrophoretic mobility in their reduced state and therefore migrate above the diagonal, whereas cross-linked proteins with intermolecular disulfides will appear below the diagonal since they migrate slower in the first dimension than in the second one.

Disulfide bonds are targeted and reduced by Trxs. Based on the finding that the intermolecular disulfide bonds during the thiol disulfide exchange reaction between target proteins and Trxs are stabilized when the second cysteine of Trxs is mutated, a monocysteinic Trx trapping method with only the N-terminal nucleophilic cysteine was developed (Brandes et al., 1996; Goyer et al., 1999). Proteomic approaches based on Trx affinity chromatography using immobilized monocysteinic CXXA Trx as a ligand, have been extensively employed for the identification of the disulfide proteome of Trx targets in many plant species (Balmer et al., 2004; Balmer et al., 2006; Marchand et al., 2006; Marchand et al., 2010; Wong et al., 2004; Yoshida et al., 2013). However, this proteomics approach may result in a lack of specificity, since Trxs or Trx-like enzymes can reduce Cys Ox-PTMs such as S-glutathionylation and sulfhydration (Bedhomme et al., 2012; Krishnan et al., 2011).

S-GLUTATHIONYLATION (-SSG)

A number of direct methods have been developed to identify and analyze plant S-glutathionylated proteins. The most widely used techniques for S-glutathionylated proteomic analyses in plants are based on the use of ³⁵S-radiolabeled cysteine, biotinylated glutathione (GSH-biotin/GSSG-biotin), or biotinylated reduced glutathione ethyl ester (GEE-biotin) (Dixon et al., 2005; Ito et al., 2003; Michelet et al., 2005; Michelet et al., 2008; Zaffagnini et al., 2012a).

With the ³⁵S-radiolabeled cysteine technique, the glutathione pool of growing cells will be labeled. The first step of this method is the inhibition of protein synthesis in both the cytosol and organelles by cycloheximide, followed by incubation with radiolabeled cysteine for four hours, so that it enters the cell and gets incorporated into glutathione molecules (Dixon et al., 2005). After an oxidative stress treatment, radiolabeled -SSG proteins are visualized by fluorography of a 2D-gel. The spots in the gel that disappear after the reduction with DTT correspond to those of S-glutathionylated proteins. Subsequently, the proteins of these spots are identified by mass spectrometry.

With a biotinylated glutathione labeling technique, the biotin tag allows downstream analysis of the glutathionylated proteins by Western blot or avidin affinity chromatography (Michelet et al., 2008).

Based on the same principle as for monocysteinic Trx trapping, monocysteinic Grx trapping also has been developed for the identification of S-glutathionylated proteins (Nordstrand et al., 1999). Using a monocysteinic mutant of Grx (poplar GrxC4 mutated on the second active-site cysteine) has led to the identification of the

Grx-interacting proteins from poplar, Arabidopsis, potato and pea (Rouhier et al., 2005) (Table 2). Other strategies, like biotin labeled GST (Cheng et al., 2005), and immobilized GSH/GSSG affinity matrices to trap the glutathionylated proteins (Niture et al., 2005), have not been applied for plant proteomic studies so far.

SULFINYLATION (-SO₂H) AND SULFONYLATION (-SO₃H)

Sulfinylated (-SO₂H) proteins can be detected by mass spectrometry with a 32 Da increase in the mass (Witze et al., 2007). However, confusion might occur, as hydrogen sulfide leads to persulfide species (RSSH) with the same nominal mass shift. Therefore, it is necessary to develop specific methods for monitoring the formation of -SO₂H within proteins. Antibodies directed against proteins containing -SO₂H have been developed (Woo et al., 2003), but they are not suited for global profiling studies. Apart from that aryl-nitroso compounds can act as chemo-selective probes for -SO₂H (Lo Conte and Carroll, 2012), which might open a new avenue for studying -SO₂H at the proteomic level. Like -SO₂H, the role of -SO₃H in redox regulation has for a long time been hindered by a lack of means to selectively detect this irreversible Cys Ox-PTMs. Recently, a method has been developed that permits selective enrichment of proteins containing -SO₃H using poly-arginine (PA)-coated nano-diamonds as high affinity probes (Chang et al., 2010), but due to the competition with phosphorylated peptides, the number of detected -SO₃H containing proteins is limited.

PERSPECTIVE

The application of proteomic methods has increased the number of proteins that potentially undergo ROS-triggered Ox-PTMs in plants. In plant redox biology, there was a missing list of the proteins forming sulfenic acids, the first oxidation stage of the redox regulatory chain, until the recent research reported by Waszczak et al. (2014) and Akter et al., submitted. The next challenge is to validate the sulfenylated proteins in all their biochemical, functional and structural aspects in order to get an in-depth insight into the mode of action of ROS signal transduction at the molecular level. Apart from that, site-specific mapping and quantification of protein sulfenylation might give us a broader view on the plant sulfenome. Therefore, the development of new tools, like the UV cleavable dimedone probe (Yang et al., 2014), will be important to boost the redox field. We anticipate that future efforts toward deciphering the ROS signal transduction events will focus on the functional characterization of already identified proteins, thereby exploring the sets of non-validated proteomic findings. Finally, we expect that the growing knowledge of ROS signal transduction events will stimulate efforts toward the manipulation of plant stress tolerance and future translation of this knowledge into crops.

ACKNOWLEDGEMENTS

This work was supported by grants from EU-ROS (BMBS COST Action BM1203), Research Foundation Flanders (FWO project GOD7914N "Sulfenomics: oxidatieve schakelaars in planten. Hoe zwavelhoudende planteneiwitten via 'agressieve' zuurstof praten"), IWT (projects Phoenix and Stressnet), the Interuniversity Attraction Poles Programme (IUAP P7/29

“MARS”) initiated by the Belgian Science Policy Office and Ghent University (Multidisciplinary Research Partnership “Biotechnology for a Sustainable Economy” (Grant 01MRB510W)).

REFERENCES

- Alkhalifioui F, Renard M, Vensel WH, Wong J, Tanaka CK, Hurkman WJ, Buchanan BB, Montrichard F. 2007. Thioredoxin-linked proteins are reduced during germination of *Medicago truncatula* seeds. *Plant Physiol* 144, 1559-1579.
- Alvarez S, Zhu M, Chen S. 2009. Proteomics of *Arabidopsis* redox proteins in response to methyl jasmonate. *J Proteomics* 73, 30-40.
- Anderson LE, Manabe K. 1979. Disulfide-linked peptides in the chloroplast thylakoid membrane. *Biochimica et biophysica acta* 579, 1-9.
- Balmer Y, Koller A, Val GD, Schurmann P, Buchanan BB. 2004. Proteomics uncovers proteins interacting electrostatically with thioredoxin in chloroplasts. *Photosynth Res* 79, 275-280.
- Balmer Y, Vensel WH, Hurkman WJ, Buchanan BB. 2006. Thioredoxin target proteins in chloroplast thylakoid membranes. *Antioxid Redox Signal* 8, 1829-1834.
- Bedhomme M, Adamo M, Marchand CH, Couturier J, Rouhier N, Lemaire SD, Zaffagnini M, Trost P. 2012. Glutathionylation of cytosolic glyceraldehyde-3-phosphate dehydrogenase from the model plant *Arabidopsis thaliana* is reversed by both glutaredoxins and thioredoxins in vitro. *Biochem J* 445, 337-347.
- Bellin D, Asai S, Delledonne M, Yoshioka H. 2013. Nitric oxide as a mediator for defense responses. *Mol Plant Microbe Interact* 26, 271-277.
- Brandes HK, Larimer FW, Hartman FC. 1996. The molecular pathway for the regulation of phosphoribulokinase by thioredoxin f. *J Biol Chem* 271, 3333-3335.
- Buchanan BB, Balmer Y. 2005. Redox regulation: a broadening horizon. *Annu Rev Plant Biol* 56, 187-220.
- Bykova NV, Hoehn B, Rampitsch C, Banks T, Stebbing J-A, Fan T, Knox R. 2011a. Redox-sensitive proteome and antioxidant strategies in wheat seed dormancy control. *Proteomics* 11, 865-882.
- Bykova NV, Hoehn B, Rampitsch C, Banks T, Stebbing JA, Fan T, Knox R. 2011b. Redox-sensitive proteome and antioxidant strategies in wheat seed dormancy control. *Proteomics* 11, 865-882.
- Carballal S, Radi R, Kirk MC, Barnes S, Freeman BA, Alvarez B. 2003. Sulfenic acid formation in human serum albumin by hydrogen peroxide and peroxyxynitrite. *Biochemistry* 42, 9906-9914.
- Chang YC, Huang CN, Lin CH, Chang HC, Wu CC. 2010. Mapping protein cysteine sulfonic acid modifications with specific enrichment and mass spectrometry: an integrated approach to explore the cysteine oxidation. *Proteomics* 10, 2961-2971.
- Charles RL, Schroder E, May G, Free P, Gaffney PR, Wait R, Begum S, Heads RJ, Eaton P. 2007. Protein sulfenation as a redox sensor: proteomics studies using a novel biotinylated dimedone analogue. *Mol Cell Proteomics* 6, 1473-1484.

- Cheng G, Ikeda Y, Iuchi Y, Fujii J. 2005. Detection of S-glutathionylated proteins by glutathione S-transferase overlay. *Arch Biochem Biophys* 435, 42-49.
- Collet JF, Messens J. 2010. Structure, function, and mechanism of thioredoxin proteins. *Antioxid Redox Signal* 13, 1205-1216.
- Couturier J, Chibani K, Jacquot JP, Rouhier N. 2013. Cysteine-based redox regulation and signaling in plants. *Front Plant Sci* 4, 105.
- Cumming RC. 2008. Analysis of global and specific changes in the disulfide proteome using redox two-dimensional polyacrylamide gel electrophoresis. *Methods in molecular biology (Clifton, N.J.)* 476, 165-179.
- Davies MJ. 2005. The oxidative environment and protein damage. *Biochimica et biophysica acta* 1703, 93-109.
- Dixon DP, Skipsey M, Grundy NM, Edwards R. 2005. Stress-induced protein S-glutathionylation in *Arabidopsis*. *Plant Physiol* 138, 2233-2244.
- Fernandes AP, Holmgren A. 2004. Glutaredoxins: glutathione-dependent redox enzymes with functions far beyond a simple thioredoxin backup system. *Antioxid Redox Signal* 6, 63-74.
- Furdui CM, Poole LB. 2014. Chemical approaches to detect and analyze protein sulfenic acids. *Mass Spectrom Rev* 33, 126-146.
- Galant A, Koester RP, Ainsworth Ea, Hicks LM, Jez JM. 2012. From climate change to molecular response: redox proteomics of ozone-induced responses in soybean. *New Phytol* 194, 220-229.
- Gan ZR, Sardana MK, Jacobs JW, Polokoff MA. 1990. Yeast thioltransferase--the active site cysteines display differential reactivity. *Arch Biochem Biophys* 282, 110-115.
- Goyer A, Decottignies P, Lemaire S, Ruelland E, Issakidis-Bourguet E, Jacquot JP, Miginiac-Maslow M. 1999. The internal Cys-207 of sorghum leaf NADP-malate dehydrogenase can form mixed disulphides with thioredoxin. *FEBS Lett* 444, 165-169.
- Gupta V, Carroll KS. 2014. Sulfenic acid chemistry, detection and cellular lifetime. *Biochim Biophys Acta* 1840, 847-875.
- Hagglund P, Bunkenborg J, Maeda K, Svensson B. 2008. Identification of thioredoxin disulfide targets using a quantitative proteomics approach based on isotope-coded affinity tags. *J Proteome Res* 7, 5270-5276.
- Hansen RE, Roth D, Winther JR. 2009. Quantifying the global cellular thiol-disulfide status. *Proc Natl Acad Sci U S A* 106, 422-427.
- Haque A, Andersen JN, Salmeen A, Barford D, Tonks NK. 2011. Conformation-sensing antibodies stabilize the oxidized form of PTP1B and inhibit its phosphatase activity. *Cell* 147, 185-198.
- Hara MR, Thomas B, Cascio MB, Bae BI, Hester LD, Dawson VL, Dawson TM, Sawa A, Snyder SH. 2006. Neuroprotection by pharmacologic blockade of the GAPDH death cascade. *Proc Natl Acad Sci U S A* 103, 3887-3889.
- Huang GT, Ma SL, Bai LP, Zhang L, Ma H, Jia P, Liu J, Zhong M, Guo ZF. 2012. Signal transduction during cold,

salt, and drought stresses in plants. *Mol Biol Rep* 39, 969-987.

Hugo M, Turell L, Manta B, Botti H, Monteiro G, Netto LE, Alvarez B, Radi R, Trujillo M. 2009. Thiol and sulfenic acid oxidation of AhpE, the one-cysteine peroxiredoxin from *Mycobacterium tuberculosis*: kinetics, acidity constants, and conformational dynamics. *Biochemistry* 48, 9416-9426.

Hugo M, Van Laer K, Reyes AM, Vertommen D, Messens J, Radi R, Trujillo M. 2014. Mycothiol/mycoredoxin 1-dependent reduction of the peroxiredoxin AhpE from *Mycobacterium tuberculosis*. *J Biol Chem* 289, 5228-5239.

Iglesias-Baena I, Barranco-Medina S, Sevilla F, Lázaro J-J. 2011. The dual-targeted plant sulfiredoxin retroreduces the sulfinic form of atypical mitochondrial peroxiredoxin. *Plant Physiol* 155, 944-955.

Ito H, Iwabuchi M, Ogawa K. 2003. The sugar-metabolic enzymes aldolase and triose-phosphate isomerase are targets of glutathionylation in *Arabidopsis thaliana*: detection using biotinylated glutathione. *Plant Cell Physiol* 44, 655-660.

Juarez-Diaz JA, McClure B, Vazquez-Santana S, Guevara-Garcia A, Leon-Mejia P, Marquez-Guzman J, Cruz-Garcia F. 2006. A novel thioredoxin h is secreted in *Nicotiana glauca* and reduces S-RNase in vitro. *J Biol Chem* 281, 3418-3424.

Krishnan N, Fu C, Pappin DJ, Tonks NK. 2011. H₂S-Induced sulfhydration of the phosphatase PTP1B and its role in the endoplasmic reticulum stress response. *Sci Signal* 4, ra86.

Lee K, Lee J, Kim Y, Bae D, Kang KY, Yoon SC, Lim D. 2004. Defining the plant disulfide proteome. *Electrophoresis* 25, 532-541.

Lee TY, Chen YJ, Lu TC, Huang HD, Chen YJ. 2011. SNOsite: exploiting maximal dependence decomposition to identify cysteine S-nitrosylation with substrate site specificity. *PLoS One* 6, e21849.

Leonard SE, Carroll KS. 2011. Chemical 'omics' approaches for understanding protein cysteine oxidation in biology. *Curr Opin Chem Biol* 15, 88-102.

Leonard SE, Reddie KG, Carroll KS. 2009. Mining the Thiol Proteome for Sulfenic Acid Modifications Reveals New Targets for Oxidation in Cells. *ACS chemical biology* 4, 783-799.

Lin WS, Armstrong DA, Gaucher GM. 1975. Formation and repair of papain sulfenic acid. *Can J Biochem* 53, 298-307.

Lindermayr C, Saalbach G, Durner J. 2005. Proteomic identification of S-nitrosylated proteins in *Arabidopsis*. *Plant Physiol* 137, 921-930.

Liu P, Zhang H, Wang H, Xia Y. 2014. Identification of redox-sensitive cysteines in the *Arabidopsis* proteome using OxiTRAQ, a quantitative redox proteomics method. *Proteomics* 14, 750-762.

Lo Conte M, Carroll KS. 2012. Chemoselective ligation of sulfinic acids with aryl-nitroso compounds. *Angewandte Chemie (International ed. in English)* 51, 6502-6505.

Luo D, Smith SW, Anderson BD. 2005. Kinetics and mechanism of the reaction of cysteine and hydrogen peroxide in aqueous solution. *J Pharm Sci* 94, 304-316.

Marchand C, Le Maréchal P, Meyer Y, Decottignies P. 2006. Comparative proteomic approaches for the

isolation of proteins interacting with thioredoxin. *Proteomics* 6, 6528-6537.

Marchand CH, Vanacker H, Collin V, Issakidis-Bourguet E, Marechal PL, Decottignies P. 2010. Thioredoxin targets in Arabidopsis roots. *Proteomics* 10, 2418-2428.

Marinho HS, Real C, Cyrne L, Soares H, Antunes F. 2014. Hydrogen peroxide sensing, signaling and regulation of transcription factors. *Redox Biol* 2, 535-562.

Marino SM, Gladyshev VN. 2010. Cysteine function governs its conservation and degeneration and restricts its utilization on protein surfaces. *J Mol Biol* 404, 902-916.

Messens J, Collet JF. 2013. Thiol-disulfide exchange in signaling: disulfide bonds as a switch. *Antioxid Redox Signal* 18, 1594-1596.

Meyer Y, Belin C, Delorme-Hinoux V, Reichheld J-P, Riondet C. 2012. Thioredoxin and glutaredoxin systems in plants: molecular mechanisms, crosstalks, and functional significance. *Antioxidants & redox signaling* 17, 1124-1160.

Meyer Y, Buchanan B, Vignols F, Reichheld J. 2009. Thioredoxins and Glutaredoxins: Unifying Elements in Redox Biology. *Annu Rev Genet*.

Michelet L, Zaffagnini M, Marchand C, Collin V, Decottignies P, Tsan P, Lancelin JM, Trost P, Miginiac-Maslow M, Noctor G, Lemaire SD. 2005. Glutathionylation of chloroplast thioredoxin f is a redox signaling mechanism in plants. *Proc Natl Acad Sci U S A* 102, 16478-16483.

Michelet L, Zaffagnini M, Vanacker H, Le Marechal P, Marchand C, Schroda M, Lemaire SD, Decottignies P. 2008. In vivo targets of S-thiolation in *Chlamydomonas reinhardtii*. *J Biol Chem* 283, 21571-21578.

Miller G, Suzuki N, Ciftci-Yilmaz S, Mittler R. 2010. Reactive oxygen species homeostasis and signalling during drought and salinity stresses. *Plant Cell Environ* 33, 453-467.

Montrichard F, Alkhalifiou F, Yano H, Vensel WH, Hurkman WJ, Buchanan BB. 2009. Thioredoxin targets in plants: the first 30 years. *J Proteomics* 72, 452-474.

Muthuramalingam M, Matros A, Scheibe R, Mock HP, Dietz KJ. 2013. The hydrogen peroxide-sensitive proteome of the chloroplast in vitro and in vivo. *Front Plant Sci* 4, 54.

Nelson JW, Creighton TE. 1994. Reactivity and ionization of the active site cysteine residues of DsbA, a protein required for disulfide bond formation in vivo. *Biochemistry* 33, 5974-5983.

Niture SK, Velu CS, Bailey NI, Srivenugopal KS. 2005. S-thiolation mimicry: quantitative and kinetic analysis of redox status of protein cysteines by glutathione-affinity chromatography. *Arch Biochem Biophys* 444, 174-184.

Nordstrand K, Slund F, Holmgren A, Otting G, Berndt KD. 1999. NMR structure of Escherichia coli glutaredoxin 3-glutathione mixed disulfide complex: implications for the enzymatic mechanism. *J Mol Biol* 286, 541-552.

Oger E, Marino D, Guigonis JM, Pauly N, Puppo A. 2012. Sulfenylated proteins in the Medicago truncatula-Sinorhizobium meliloti symbiosis. *J Proteomics* 75, 4102-4113.

Parker J, Zhu N, Zhu M, Chen S. 2012. Profiling thiol redox proteome using isotope tagging mass

spectrometry. *J Vis Exp*.

Paulsen CE, Carroll KS. 2009. Chemical dissection of an essential redox switch in yeast. *Chemistry & biology* 16, 217-225.

Paulsen CE, Carroll KS. 2013. Cysteine-mediated redox signaling: chemistry, biology, and tools for discovery. *Chem Rev* 113, 4633-4679.

Paulsen CE, Truong TH, Garcia FJ, Homann A, Gupta V, Leonard SE, Carroll KS. 2012. Peroxide-dependent sulfenylation of the EGFR catalytic site enhances kinase activity. *Nat Chem Biol* 8, 57-64.

Poole LB, Karplus PA, Claiborne A. 2004. Protein sulfenic acids in redox signaling. *Annu Rev Pharmacol Toxicol* 44, 325-347.

Poole LB, Klomsiri C, Knaggs SA, Furdui CM, Nelson KJ, Thomas MJ, Fetrow JS, Daniel LW, King SB. 2007. Fluorescent and affinity-based tools to detect cysteine sulfenic acid formation in proteins. *Bioconjug Chem* 18, 2004-2017.

Poole LB, Nelson KJ. 2008. Discovering mechanisms of signaling-mediated cysteine oxidation. *Curr Opin Chem Biol* 12, 18-24.

Poole LB, Zeng BB, Knaggs SA, Yakubu M, King SB. 2005. Synthesis of chemical probes to map sulfenic acid modifications on proteins. *Bioconjug Chem* 16, 1624-1628.

Poole TH, Reisz Ja, Zhao W, Poole LB, Furdui CM, King SB. 2014. Strained cycloalkynes as new protein sulfenic acid traps. *J Am Chem Soc* 136, 6167-6170.

Puyaubert J, Fares A, Reze N, Peltier JB, Baudouin E. 2014. Identification of endogenously S-nitrosylated proteins in Arabidopsis plantlets: effect of cold stress on cysteine nitrosylation level. *Plant Sci* 215-216, 150-156.

Qian J, Klomsiri C, Wright MW, King SB, Tsang AW, Poole LB, Furdui CM. 2011. Simple synthesis of 1,3-cyclopentanedione derived probes for labeling sulfenic acid proteins. *Chemical communications (Cambridge, England)* 47, 9203-9205.

Qian J, Wani R, Klomsiri C, Poole LB, Tsang AW, Furdui CM. 2012. A simple and effective strategy for labeling cysteine sulfenic acid in proteins by utilization of β -ketoesters as cleavable probes. *Chemical communications (Cambridge, England)* 48, 4091-4093.

Reddie KG, Carroll KS. 2008. Expanding the functional diversity of proteins through cysteine oxidation. *Curr Opin Chem Biol* 12, 746-754.

Reddie KG, Seo YH, Muse Iii WB, Leonard SE, Carroll KS. 2008. A chemical approach for detecting sulfenic acid-modified proteins in living cells. *Mol Biosyst* 4, 521-531.

Rey P, Bécuwe N, Barrault M-B, Rumeau D, Havaux M, Biteau B, Toledano MB. 2007. The Arabidopsis thaliana sulfiredoxin is a plastidic cysteine-sulfenic acid reductase involved in the photooxidative stress response. *The Plant journal : for cell and molecular biology* 49, 505-514.

Romero-Puertas MC, Laxa M, Matte A, Zaninotto F, Finkemeier I, Jones AM, Perazzolli M, Vandelle E, Dietz KJ, Delledonne M. 2007. S-nitrosylation of peroxiredoxin II E promotes peroxynitrite-mediated tyrosine

nitration. *Plant Cell* 19, 4120-4130.

Romero-Puertas, M. C., Rodriguez-Serrano, M., Sandalio, L. M. 2013. Protein S-nitrosylation in plants under abiotic stress: an overview. *Front Plant Sci* 2013, 4, 373.

Roos G, Foloppe N, Messens J. 2013. Understanding the pK(a) of redox cysteines: the key role of hydrogen bonding. *Antioxid Redox Signal* 18, 94-127.

Roos G, Messens J. 2011. Protein sulfenic acid formation: from cellular damage to redox regulation. *Free Radic Biol Med* 51, 314-326.

Rouhier N, Villarejo A, Srivastava M, Gelhaye E, Keech O, Droux M, Finkemeier I, Samuelsson G, Dietz KJ, Jacquot JP, Wingsle G. 2005. Identification of plant glutaredoxin targets. *Antioxid Redox Signal* 7, 919-929.

Salmeen A, Andersen JN, Myers MP, Meng TC, Hinks JA, Tonks NK, Barford D. 2003. Redox regulation of protein tyrosine phosphatase 1B involves a sulphenyl-amide intermediate. *Nature* 423, 769-773.

Saurin AT, Neubert H, Brennan JP, Eaton P. 2004. Widespread sulfenic acid formation in tissues in response to hydrogen peroxide. *Proc Natl Acad Sci U S A* 101, 17982-17987.

Seo YH, Carroll KS. 2009. Profiling protein thiol oxidation in tumor cells using sulfenic acid-specific antibodies. *Proc Natl Acad Sci U S A* 106, 16163-16168.

Tada Y, Spoel SH, Pajeroska-Mukhtar K, Mou Z, Song J, Wang C, Zuo J, Dong X. 2008. Plant immunity requires conformational changes [corrected] of NPR1 via S-nitrosylation and thioredoxins. *Science* 321, 952-956.

Tajc SG, Tolbert BS, Basavappa R, Miller BL. 2004. Direct determination of thiol pKa by isothermal titration microcalorimetry. *J Am Chem Soc* 126, 10508-10509.

Takanishi CL, Ma L-H, Wood MJ. 2007a. A genetically encoded probe for cysteine sulfenic acid protein modification in vivo. *Biochemistry* 46, 14725-14732.

Takanishi CL, Ma L-H, Wood MJ. 2007b. A genetically encoded probe for cysteine sulfenic acid protein modification in vivo. *Biochemistry* 46, 14725-14732.

Takanishi CL, Wood MJ. 2011. A genetically encoded probe for the identification of proteins that form sulfenic acid in response to H₂O₂ in *Saccharomyces cerevisiae*. *J Proteome Res* 10, 2715-2724.

Tavares CP, Vernal J, Delena RA, Lamattina L, Cassia R, Terenzi H. 2014. S-nitrosylation influences the structure and DNA binding activity of AtMYB30 transcription factor from *Arabidopsis thaliana*. *Biochim Biophys Acta* 1844, 810-817.

Tyther R, Ahmeda A, Johns E, McDonagh B, Sheehan D. 2010. Proteomic profiling of perturbed protein sulfenation in renal medulla of the spontaneously hypertensive rat. *J Proteome Res* 9, 2678-2687.

Wang H, Wang S, Lu Y, Alvarez S, Hicks LM, Ge X, Xia Y. 2012. Proteomic analysis of early-responsive redox-sensitive proteins in *Arabidopsis*. *J Proteome Res* 11, 412-424.

Wang YQ, Feechan A, Yun BW, Shafiei R, Hofmann A, Taylor P, Xue P, Yang FQ, Xie ZS, Pallas JA, Chu CC, Loake GJ. 2009. S-nitrosylation of AtSABP3 antagonizes the expression of plant immunity. *J Biol Chem* 284, 2131-2137.

- Waszczak C, Akter S, Eeckhout D, Persiau G, Wahni K, Bodra N, Van Molle I, De Smet B, Vertommen D, Gevaert K, De Jaeger G, Van Montagu M, Messens J, Van Breusegem F. 2014. Sulfenome mining in *Arabidopsis thaliana*. *Proc Natl Acad Sci U S A* 111, 11545-11550.
- Winger AM, Taylor NL, Heazlewood JL, Day DA, Millar AH. 2007. Identification of intra- and intermolecular disulphide bonding in the plant mitochondrial proteome by diagonal gel electrophoresis. *Proteomics* 7, 4158-4170.
- Witze ES, Old WM, Resing KA, Ahn NG. 2007. Mapping protein post-translational modifications with mass spectrometry. *Nature methods* 4, 798-806.
- Wong JH, Balmer Y, Cai N, Tanaka CK, Vensel WH, Hurkman WJ, Buchanan BB. 2003. Unraveling thioredoxin-linked metabolic processes of cereal starchy endosperm using proteomics. *FEBS Lett* 547, 151-156.
- Wong JH, Cai N, Balmer Y, Tanaka CK, Vensel WH, Hurkman WJ, Buchanan BB. 2004. Thioredoxin targets of developing wheat seeds identified by complementary proteomic approaches. *Phytochemistry* 65, 1629-1640.
- Woo HA, Kang SW, Kim HK, Yang KS, Chae HZ, Rhee SG. 2003. Reversible oxidation of the active site cysteine of peroxiredoxins to cysteine sulfinic acid. Immunoblot detection with antibodies specific for the hyperoxidized cysteine-containing sequence. *J Biol Chem* 278, 47361-47364.
- Yang J, Gupta V, Carroll KS, Liebler DC. 2014. Site-specific mapping and quantification of protein S-sulphenylation in cells. *Nat Commun* 5, 4776.
- Yoshida K, Noguchi K, Motohashi K, Hisabori T. 2013. Systematic exploration of thioredoxin target proteins in plant mitochondria. *Plant Cell Physiol* 54, 875-892.
- Yu M, Lamattina L, Spoel SH, Loake GJ. 2014. Nitric oxide function in plant biology: a redox cue in deconvolution. *New Phytol* 202, 1142-1156.
- Yun BW, Feechan A, Yin M, Saidi NB, Le Bihan T, Yu M, Moore JW, Kang JG, Kwon E, Spoel SH, Pallas JA, Loake GJ. 2011. S-nitrosylation of NADPH oxidase regulates cell death in plant immunity. *Nature* 478, 264-268.
- Zaffagnini M, Bedhomme M, Groni H, Marchand CH, Puppo C, Gontero B, Cassier-Chauvat C, Decottignies P, Lemaire SD. 2012a. Glutathionylation in the photosynthetic model organism *Chlamydomonas reinhardtii*: a proteomic survey. *Mol Cell Proteomics* 11, M111 014142.
- Zaffagnini M, Bedhomme M, Lemaire SD, Trost P. 2012b. The emerging roles of protein glutathionylation in chloroplasts. *Plant Sci* 185-186, 86-96.
- Zaffagnini M, Bedhomme M, Marchand CH, Morisse S, Trost P, Lemaire SD. 2012c. Redox regulation in photosynthetic organisms: focus on glutathionylation. *Antioxid Redox Signal* 16, 567-586.

TABLE 1. DIFFERENTIAL ALKYLATION-BASED INDIRECT PROTEOMICS APPLIED IN PLANTS FOR REVERSIBLE CYS OX-PTMS



Table 1. Differential alkylation-based indirect proteomics applied in plants for reversible Cys Ox-PTMs

PTMs	Targeting			Isolation	Identification	Examples in plants
	Blocking	Reduction	Labeling			
All reversible PTMs (-SOH, -S-S-,SSG)	mBBr		IAM	2-DE gel	MS	(Bykova <i>et al.</i> , 2011a)
			mBBr			(Alvarez <i>et al.</i> , 2009b)
	IAM		cysTMT	Enrichment by anti-TMT resin		(Parker <i>et al.</i> , 2012)
		DTT/TCEP	Biotin-IAM & IAF	BIAM-IP/IAF 2-DE		(Wang <i>et al.</i> , 2012)
			IAF	2-DE gel		(Galant <i>et al.</i> , 2012)
		NEM	Biotin-maleimide	2-DE/Streptavidin enrichment		(Muthuramalingam <i>et al.</i> , 2013)
		Biotin-HDPD	Avidin affinity purification >TRAQ	(Liu <i>et al.</i> , 2014)		
Sulfenylation (-SOH)	IAM/NEM	Arsenite	Biotin-NEM	Streptavidin affinity purification > 2-DE gel		—
Disulfide bond (S-S)	IAM/ ¹²⁵ I		IAM based-ICAT	2-DE gel		—
	IAM	Trx	ICAT			
	—		mBBr	2-DE (IEF/SDS), 2-DE	Amino acid	(Alkhalifioui <i>et al.</i> , 2007; Juarez-



			/cyanine 5 maleimide	(Non-reducing/reducing)	sequencing /MS	Diaz <i>et al.</i> , 2006; Wong <i>et al.</i> , 2003; Wong <i>et al.</i> , 2004)	Table 1.
	IAM	-Trx /+ Trx	TCEP >Heavy (¹³ C) ICAT & light (¹² C) ICAT labeling	Avidin affinity purification		(Hagglund <i>et al.</i> , 2008)	
S-glutathionylation (RSSG)	NEM	Grx	BNEM	Avidin affinity purification, 2-DE gel	MS	—	

Table 2

Table 2. Direct proteomics applied in plants for Cys Ox-PTMs

Cys-PTMs	Method	Targeting	Isolation	Identification	Examples in plants
Sulfenylation (-SOH)	Probe	DCP-Bio1 (<i>in vitro</i>)	Streptavidin affinity	MS/ Amino acid sequencing	(Oger <i>et al.</i> , 2012)
		DAz-2 (<i>in vivo</i>)	Biotinylation by click reaction following		
		DYn-2 (<i>in vivo</i>)	Streptavidin affinity		Akter <i>et al.</i> Article submitted
		YAP1 based genetic (<i>in vivo</i>)	Tandem affinity purification		(Oger <i>et al.</i> , 2012; Waszczak <i>et al.</i> , 2014)
		β -ketoesters (<i>in vivo</i>)	Biotinylation by click reaction following		
	BCN (<i>in vivo</i>)	Streptavidin -HRP			
Disulfide bonds (S-S)	Redox				
	2D-PAGE		2-DE gel		(Anderson and Manabe, 1979; Winger <i>et al.</i> , 2007)
	<i>Grx</i> affinity	<i>Grx</i> (CXXA)	<i>Grx</i> affinity purification >SDS-PAGE, 2-DE (IEF/SDS), 2-DE (Non-		For all examples we refer to (Montrichard <i>et al.</i> , 2009)
	trapping		reducing/reducing)		
S-glutathionylation (SSG)	Direct labeling	³⁵ S radiolabeling	Fluorography, 2-DE (Reducing/non-reducing)		(Dixon <i>et al.</i> , 2005; Michelet <i>et al.</i> , 2008)
		GSSG-biotin labeling	Streptavidin affinity enrichment, 2-DE gel		(Dixon <i>et al.</i> , 2005; Zaffagnini <i>et al.</i> , 2012a)
	BioGEE labeling	Anion exchange chromatography, Hydrophobic interaction chromatography			Ito <i>et al.</i> , 2003a
	<i>Grx</i> affinity trapping	<i>Grx</i> (CXXA)?	<i>Grx</i> affinity purification		(Rouhier <i>et al.</i> , 2005)

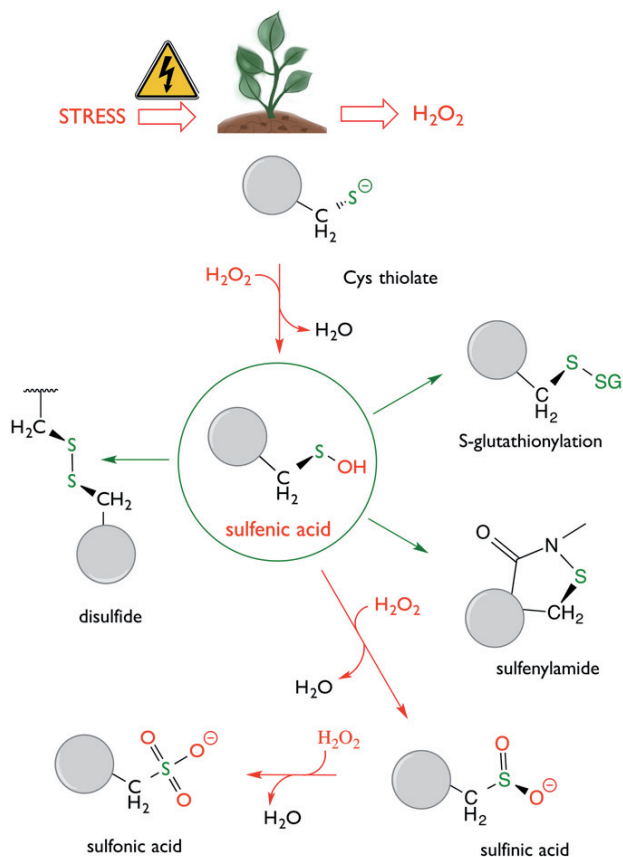


Fig. 1. Plants under ROS attack. Exposure of redox-sensitive cysteine thiolates to H_2O_2 leads to the reversible sulfenic acid formation. The highly reactive sulfenic acids are protected (green arrow) by forming disulfide bonds with nearby thiols or by forming mixed disulfide bonds by S-glutathionylation or by forming sulfenylamide with the backbone nitrogen of the adjacent residue. In the presence of high levels of ROS, overoxidation to irreversible sulfinic acid and sulfonic acid can occur (red arrow). The green arrow represents the protection of the sulfenic acid and the red arrow represents the oxidation of the thiolate or overoxidation of the sulfenic acid.

Curriculum

Silke Jacques

Address: Brechtstraat 43
1790 Affligem
Belgium

Phone Number: +32 479 938506

E-mail: jacques.silke@gmail.com

Date of Birth: 6 October 1987

Nationality: Belgian

RESEARCH EXPERIENCE

2010 – 2015

PhD fellowship in Plant Biotechnology & Genetics

Joint PhD between Faculty of Sciences and Faculty of Medicine, Ghent University

"A multi-angled view on oxidative stress in *A. thaliana*: filling the gaps"

Promoters: Prof. Dr. Kris Gevaert VIB department of Medical Protein Research, UGent Proteome Analysis

Prof. Dr. Frank Van Breusegem - VIB department of Plant Systems Biology, Oxidative Stress Signaling Laboratory

- **Proteomics experience:**
 - Gel-free proteomics: COFRADIC, shotgun-analysis, post-metabolic labeling
 - Chromatography experience: reversed phase HPLC, Agilent 1200, SCX
 - Large scale data analysis: Mascot, MS-Lims, XCalibur, Knime, MaxQuant
 - Production and purification of recombinant proteins: enzymatic assays
 - Designing specific extraction procedures for PTM studies of stressed plants

- **Molecular Biology skills:**
 - General DNA and RNA techniques: Gateway cloning, site-directed mutagenesis, expression vector construction, PCR, transformation, DNA and RNA isolation
 - Complete omics-characterization of oxidative stress related experiments: phenotyping, ribosome profiling -fully optimized and transcriptome analysis via RNA-seq, metabolomics

- **Coaching:**
 - Student supervisor of 3rd Bachelor-students and Master-students
 - Oral examiner practical courses / Jury member student dissertation

Contact: +32 479938506 jacques.silke@gmail.com

- 2009 – 2010** **Thesis 2nd Master of Biochemistry and Biotechnology**
Faculty of Bioscience Engineering, Ghent University
- “Toxicity and working mechanism of *Arabidopsis thaliana* serpin-1 against pea aphid (*Acyrtosiphon pisum*), the model sap-feeding insect”**
Promoters: Prof. Dr. Guy Smagghe – *Laboratory of Agrozoology*
Prof. Dr. Frank Van Breusegem – *Oxidative Stress Signaling Laboratory*
- 2008 – 2009** **Project 1st Master of Biochemistry and Biotechnology**
Faculty of Sciences, Ghent University
- “Automation of plant cell transformation”**
Promoter: Prof. Dr. Pierre Hilson – *Functional Genomics Laboratory*

EDUCATION

- 2010 – 2015** **PhD in Plant Biotechnology** **to be defended**
Faculty of Sciences, Ghent University
- 2005 – 2010** **Master of Biochemistry and Biotechnology** **magna cum laude**
Faculty of Sciences, Ghent University
- 1999 – 2005** **Mathematics - Sciences** **summa cum laude**
Dames Van Maria, Aalst Humaniora

SCIENTIFIC CONTRIBUTIONS

- Publications** **Plant proteins under oxidative attack.**
Jacques S., Ghesquière B., Van Breusegem F., Gevaert K. (2013) *Proteomics*
- Oxidative post-translational modifications of cysteine residues in plant signal transduction.**
Waszczak C., Akter M.S., Jacques S., Huang J., Gevaert K., Messens J. and Van Breusegem F. (2014). *Journal of Experimental Botany*
- Cysteines under ROS attack in plants: a proteomics view.**
Akter M.S., Waszczak C., Huang J., Jacques S., Gevaert K., Messens J. and Van Breusegem F. (2014). *Journal of Experimental Botany*

Contact: +32 479938506 jacques.silke@gmail.com

VARIA

- Languages**
- Dutch > native tongue
 - English > excellent
 - French > very good
- Hobby's**
- adventurous travels
 - sports: rugby in competition, survival runs, mountaineering
 - monitor for French youth kayaking and winter camps in Sweden
- Other**
- driving license B

Contact: +32 479938506 jacques.silke@gmail.com

